



MONASH University

Synthetic surfaces for long-term maintenance of hPSC cultures

Jack William Lambshead

BBmedSc (Hons)

A thesis submitted for the degree of Doctor of Philosophy at

Monash University in 2016

Faculty of Medicine, Nursing and Health Sciences

Table of contents

Copyright Notice	vii
Summary	viii
General Declaration.....	ix
Acknowledgements	x

CHAPTER 1

Introduction and literature review

List of Abbreviations.....	xi
1.1 Introduction	1
1.2 Human pluripotent stem cells (hPSCs).....	3
1.3 hPSC characterisation methods	4
1.4 The evolution of hPSC culture conditions.....	6
1.5 CAMs and the maintenance of pluripotency.....	8
1.5.1 Integrins.....	8
1.5.2 Cadherins.....	9
1.6 Extracellular matrix proteins (ECMPs) as ligands for hPSC culture surfaces.....	9
1.6.1 Collagens	9
1.6.2 Laminins.....	10
1.6.3 Fibronectin	11
1.6.4 Vitronectin.....	12
1.6.5 Combinations of ECMPs as hPSC culture surfaces	13
1.7 Surfaces that interact with hPSCs through non-specific adsorbed media proteins	13
1.8 Two-dimensional substrates for hPSC culture surfaces	14
1.8.1 Characterisation methods for hPSC culture surfaces.....	15
1.8.2 Modifications to plastic and glass culture surfaces.....	15
1.8.3 Self Assembled Monolayers (SAMs)	15
1.8.4 Heparan Sulphate Proteoglycans (HSPGs)	18
1.8.5 Polymer scaffolds.....	19

1.9 Three dimensional (3D) hPSC culture systems.....	22
1.9.1 Hydrogels.....	22
1.9.2 Suspension culture systems.....	23
1.10 Comparisons of hPSCs cultured on different surfaces	23
1.11 Conclusions.....	24
1.12 Hypothesis and Project Aims.....	26

CHAPTER 2

General materials and methods

2.1 Introduction.....	28
2.2 Human pluripotent stem cell lines	28
2.3 Methods for hPSC culture.....	28
2.3.1 Working with Geltrex™	29
2.3.2 EDTA harvesting method for hPSCs.....	29
2.3.3 Cryopreservation of hPSCs.....	30
2.3.4 Thawing cryopreserved hPSCs.....	30
2.4 Monitoring cellular proliferation.....	30
2.4.1 Cell counting with a hemocytometer	30
2.4.2 Colony counting approach to cell quantification	31
2.4.3 MTS cell proliferation assay	31
2.5 Methods for production of polymer brush coatings	33
2.5.1 UV-initiated polymer-coating of tissue culture vessels	33
2.5.2 EDC/NHS-mediated peptide modification of PAAA-coated surfaces.....	34
2.5.3 Copper-catalysed peptide modification of PAPA-coated surfaces	36

CHAPTER 3

Optimising peptide-modified polymer brush coatings for hPSC culture

3.1 Introduction.....	38
3.2 Chapter specific methods	40
3.2.1 Cell quantification.....	40
3.2.2 Sample preparation for surface analysis.....	40

3.2.3 X-ray photoelectron spectroscopy surface analysis.....	40
3.2.3.1 Conversion of XPS data to surface thickness	41
3.2.4 Atomic Force Microscopy (AFM) surface analysis.....	42
3.2.5 Europium (Eu)-tagged peptide assay for quantifying surface peptide density	44
3.2.5.1 Europium tagging of the peptide.....	44
3.2.5.2 Quantifying the density of cRGDfK peptide on cRGDfK-PAPA-coated surfaces.....	45
3.2.6 Cytotoxicity assessment of cell culture surfaces	46
3.2.7 L929 adhesion assays	46
3.3 Results	47
3.3.1 Preliminary optimisation of cRGDfK-PAAA coatings for hPSC adhesion.....	47
3.3.2 Optimising cRGDfK-PAPA coatings for hPSC adhesion and peptide screening	49
3.3.3 The effects of peptide density and number of UV exposures on hPSC adhesion to cRGDfK-PAAA and cRGDfK-PAPA.....	56
3.3.4 The physicochemical effects of additional UV exposures on PAAA and PAPA coatings.....	59
3.3.5 Physical and mechanical characterisation of PAAA and PAPA coatings	73
3.3.6 Assessing the peptide density required to mediated hPSC adhesion.....	79
3.3.7 Cytotoxicity testing of PAAA and PAPA.....	79
3.3.8 hPSCs adhesion to and shelf life testing of cRGDfK-PAPA coated flasks	82
3.4 Discussion.....	84
3.5 Chapter summary	92

CHAPTER 4

Identification of peptides able to mediate hPSC adhesion to polymer coatings

4.1 Introduction	94
4.2 Chapter specific methods	96
4.2.1 Preparation of polymer surfaces for peptide screening	96
4.2.2 Peptide library for screening.....	96
4.2.3 Approach for dissolving peptides	99
4.2.4 Peptide screening approach	102
4.2.5 Cell culture methods for MDA-MB-435 melanocytes	102
4.2.6 Flow cytometric staining for detection of $\alpha\text{v}\beta\text{3}$ integrin	104

4.3 Results	104
4.3.1 Peptide solubility results	104
4.3.2 Results of peptide screening on PAAA with H9-OCT4-mCherry hPSCs	106
4.3.2.1 Validation of lead peptides on PAAA with cultures of H9 and NHF-1-3 hPSCs	110
4.3.3 Peptide screening results on PAPA	114
4.3.4 Further optimisation of pep31-PAPA did not improve hPSC adhesion	114
4.3.5 Peptide screening results summary	119
4.3.6 Flow cytometric assessment of hPSCs for integrin $\alpha\beta 3$	121
4.4 Discussion	121
4.5 Chapter Summary	130

CHAPTER 5

Characterisation of long-term hPSC cultures maintained on synthetic surfaces

5.1 Introduction	133
5.2 Chapter specific methods	135
5.2.1 Preparation of coated flasks for hPSC culture	135
5.2.1.1 Preparation of Geltrex™-coated flasks	135
5.2.1.2 Preparation of cRGDfK-PAPA-coated flasks	135
5.2.1.3 Preparation of Synthemax™-coated flasks	135
5.2.1.4 Preparation of StemAdhere™-coated flasks	136
5.2.2 Cell culture methods	136
5.2.3 hPSC characterisation	137
5.2.3.1 Observations of hPSC cultures	137
5.2.3.2 Flow cytometry	137
5.2.3.3 Cell pellet collection	138
5.2.3.4 Isolation and characterisation of total RNA	139
5.2.3.5 Microarray analysis of total RNA and PluriTest™	139
5.2.3.6 G-banding karyotype analysis	139
5.2.3.7 Teratoma assay	140
5.3 Results	141
5.3.1 Quality control of hPSC lines and culture surfaces	141

5.3.2 Gross observations of morphology and proliferation rates of hPSC cultures on defined surfaces.....	145
5.3.3 Flow cytometric analysis of hPSC cultures maintained on defined culture surfaces.....	156
5.3.4 Teratoma formation with hPSC cultures maintained on defined culture surfaces	156
5.3.5 G-banding karyotyping of hPSC cultures maintained on defined culture surfaces	156
5.3.6 PluriTest™ assessment of hPSC cultures maintained on defined culture surfaces.....	162
5.4 Discussion.....	166
5.5 Chapter Summary.....	172

CHAPTER 6

Conclusions and future directions

6.1 Conclusions	174
6.2 Future directions	176

BIBLIOGRAPHY

Bibliography	184
--------------------	-----

APPENDICES

Appendix 1: Validation of the H9-OCT4-mCherry reporter cell line	208
Appendix 2: Common laboratory reagents.....	209
Appendix 3: Peptide library characterisation details	211
Appendix 4: Inelastic mean free paths for interpretation of XPS results	234
Appendix 5: Information about Eu-tagged peptides.....	235
Appendix 6: hPSC characterisation results	237
Reference list for appendices	241

Copyright Notice

© Jack Lamshead (2016). Except as provided in the Copyright Act 1968, this thesis may not be reproduced in any form without the written permission of the author.

I certify that I have made all reasonable efforts to secure copyright permissions for third-party content included in this thesis and have not knowingly added copyright content to my work without the owner's permission.

Summary

The self-renewal and multilineage differentiation potential of human pluripotent stem cells (hPSC) has inspired a range of potential applications, the most exciting of which are cell replacement therapies using hPSC-derived cells. Many such therapies are under development, and therapies using various hPSC-derived cells to treat four diseases have reached phase one clinical trials. The widespread use of standardised, chemically-defined xeno-free hPSC culture conditions, including culture surfaces, are very important. The use of a global standard for hPSC culture conditions would simplify regulation, prevent xenogeneic contamination and improve consistency of not only the therapeutic product but also of all hPSC-based research and products.

This thesis presents the optimisation of two peptide-presenting co-polymer brush coatings as chemically defined xeno-free hPSC culture surfaces, namely poly(acrylamide-*co*-acrylic acid) (PAAA) and poly(acrylamide-*co*-propargyl acrylamide) (PAPA). Both coatings were synthesised from mixed monomer solutions by repeated exposure to ultraviolet (UV) light. The peptide density and surface stiffness of these coatings could be controlled and were each observed to affect the efficiency of hPSC adhesion. Peptide-modified PAAA coatings (cRGDfK-PAAA) that had been synthesised with higher numbers of UV exposures were observed to increase in thickness and to bind hPSCs less efficiently. On the other hand, PAPA coatings were observed to increase in stiffness rather than thickness; hPSCs were observed to consistently adhere to PAPA coatings that were synthesised with up to 60 UV exposures and modified with reaction solutions containing ~500-fold less peptide than has been reported in similar studies, which resulted in a surface peptide density of 3.6 pmol/cm². This was the first report of the efficacy of chemically-defined hPSC culture surfaces presenting only cRGDfK.

The optimised polymer coatings were individually modified with a library of 35 other peptides reported to bind cells, but the hPSC-binding efficiency of cRGDfK-modified coatings could not be equalled. Although hPSCs adhered to surfaces modified with four other peptides, colony numbers were low and/or adhesion was unstable compared to cRGDfK-modified control wells, even when the other peptides were applied in excess.

hPSC cultures maintained for ten passages in cRGDfK-PAPA-coated flasks passed a battery of pluripotency tests. Parallel hPSC cultures were maintained for benchmarking on flasks coated with Geltrex™ and with commercially available synthetic hPSC culture surfaces, StemAdhere™ and Synthemax™. Morphological assessment, flow cytometry for the pluripotency marker OCT4, PluriTest analysis of global gene expression, G-banding karyotype and teratoma formation assays produced comparable results regardless of surface type. A low level of karyotypic abnormalities were observed to arise in cultures maintained on each of the target surfaces, but not in cultures maintained on cRGDfK-PAPA. This may indicate that the cRGDfK-PAPA surface is protective of genetic damage.

This thesis presents cRGDfK as an optimal ligand for mediating hPSC adhesion to polymer coatings and cRGDfK-PAPA is presented as a well-characterised, affordable and effective synthetic surface for hPSC culture. Furthermore a discussion is presented of the strengths and weaknesses of commercially available alternative hPSC culture surfaces. The surface used for maintaining hPSC cultures must be selected in any case based on individual requirements, considering parameters such as cost, surface stability and the need for cell scraping.

General Declaration

I hereby declare that this thesis contains no material which has been accepted for the award of any other degree or diploma at any university or equivalent institution and that, to the best of my knowledge and belief, this thesis contains no material previously published or written by another person, except where due reference is made in the text of the thesis.

This thesis includes one original paper published in peer reviewed journals. The core theme of the thesis is the optimisation and benchmarking of novel, synthetic hPSC culture surfaces. The ideas, development and writing up of all the papers in the thesis were the principal responsibility of myself, the candidate, working within the School of Biomedical Sciences under the supervision of Andrew Laslett, Carmel O'Brien and Laurence Meagher.


In the case of Chapter 1 my contribution to the work involved the following:

Thesis chapter	Publication title	Publication status*	Nature and extent (%) of students contribution
1	Defining synthetic surfaces for human pluripotent stem cell culture	Published	Research (95 %) and writing (95 %)

* e.g. 'published' / 'in press' / 'accepted' / 'returned for revision'

I have renumbered sections of submitted or published papers in order to generate a consistent presentation within the thesis.

Student signature:



Date: 24/03/16

The undersigned hereby certify that the above declaration correctly reflects the nature and extent of the student and co-authors' contributions to this work.

Main Supervisor signature:



Date: 24/03/16

Acknowledgements

A PhD project is a great challenge, and one not to be entered into lightly. One morning, about six months into this project, I went into work to say that I was considering quitting. So it is with great pride and relief that I submit this thesis today. Here I thank the people that helped to get me over that hurdle, and over the many others that I encountered along the way.

I would like to thank my supervisors A/Prof. Andrew Laslett, Dr. Carmel O'Brien and Prof. Laurence Meagher for their patience and guidance over the past four years. I have enjoyed the casual nature of our meetings and the relaxed yet attentive approach to my supervision; I always felt better about the whole thing when I was leaving meetings than when I had arrived. I could not have found a group of supervisors with a more suitable ethos. I consider myself to be very fortunate in this regard, and I'm sure our relationships will continue well beyond the completion of this project. I would also like to thank my panel members, Prof. Jane Black, A/Prof. James Bourne, Prof. Claude Bernard and particularly Dr. Mitchell Lawrence, who was the only regular panel member, and whose feedback was always thorough and fair.

To the members of the ASCC/CMHT/CMSE/Manufacturing Flagship/Manufacturing Business Unit/bioInnovation X/ARMI stem cell group, and especially to long-serving members of the Laslett Laboratory: Hun Chy, Qi Zhou ("The A-team" from the good old days of the CIRM project), Bei Xu, Irene Ghobrial, Pegah Jamshidi and Tung-Liang Chung: thank you for an enjoyable entry to the workforce and for providing an environment in which I felt comfortable to pursue this doctorate. I would also like to thank members of the CSIRO polymer chemistry and hMSC cell biology labs who readily took on a fly-by-nighter and let me borrow all of their stuff. Especially to Chris Easton for assisting with the surface characterisation. I would also like to thank my funding sources: the Australian Government, CSIRO and ARMI for their various contributions.

To my fellow long-suffering students: Wouter, Ivan (the FND crew, see you soon for a beer in Europe), Anthony, Adie, Jess, Chew-Li, Eamon, Alexei, Ryan, Phong, Sophie, Patrick, Danni, Bianca and others. Thanks for sharing the experience and the laughs along the way. Best of luck to those who are still at it.

I would also like to thank my friends, particularly Daniel, Nick, Rafah, Nicole, Keov, Christian and Shahine. For keeping things in perspective and then for mostly leaving me alone towards the end except for occasionally dragging me out. I know I haven't been very available to do much lately and I now fully intend on overcompensating for that.

Last and most of all I would like to thank my family: my mother Sandra, my father Gary, my sister Amelia and her new husband Sam. Thanks for putting up with me and for not asking me too many questions about when I was going to finish. I would especially like to thank my parents for housing and feeding me over the duration of this project. As mum once put it "I can't help you with your homework anymore because I no longer have any idea about what you're doing, but I can help this way". So thank you for that.

Thank you all for everything.

List of Abbreviations

°C	Degrees Celsius
2D	Two Dimensional
3D	Three Dimensional
AFM	Atomic Force Microscopy
AT	Alkanethiol
Bcl-xL	B-cell Lymphoma-Extra Large
BSA	Bovine Serum Albumin
CAM	Cell Adhesion Molecule
CM	Conditioned Media
CO ²	Carbon Dioxide
DCM	Dichloromethane
DELFA	Dissociation-Enhanced Lanthanide Fluorescent Immunoassay
DIEA	N,N-diisopropylethylamine
DMEM	Dulbecco's Modified Eagle Medium
DMEM/F12	Dulbecco's Modified Eagle Medium with Ham's F-12 Medium
DMF	N,N-dimethylformamide
DMSO	Dimethylsulphoxide
DNA	Deoxyribonucleic acid
EB	Embryoid Body
ECM	Extracellular Matrix
ECMPs	Extracellular Matrix Proteins
EDAC	1-Ethyl-3-(3-Dimethylaminopropyl) Carbodiimide
EDTA	Ethylenediaminetetraacetic Acid, Hydrochloride
ESC	Embryonic Stem Cell
FACS	Fluorescence-Activated Cell Sorting
FCS	Foetal Calf Serum
FGF-2	Basic Fibroblast Growth Factor
FISH	Fluorescence <i>in situ</i> hybridisation
Fmoc	Fluorenylmethyloxycarbonyl

FPLC	Fast Protein Liquid Chromatography
g (as in x g)	Gravitational Force
GAGs	Glycosaminoglycans
HBTU	2-(1H-benzotriazole-1-yl)-1,1,3,3-tetramethyluronium hexafluorophosphate
HOBt	N-hydroxybenzotriazole
HPLC	High Performance Liquid Chromatography
hPSC	Human Pluripotent Stem Cell
HS	Heparan Sulphate
HSPG	Heparan Sulphate Proteoglycan
IgG	Immunoglobulin G
IgG1	Immunoglobulin G1 Isotype
IgG2b	Immunoglobulin G2b Isotype
iPSC	Induced Pluripotent Stem Cell
Klf4	Kruppel-like factor 4
KOSR	KnockOut Serum Replacement
LIF	Leukaemia Inhibitory Factor
LVDT	Linear Variable Differential Transformer
MALDI-TOF	Matrix-Assisted Laser Desorption Ionisation Time-Of-Flight
MEF	Mouse Embryonic Fibroblast
mPSC	Murine Pluripotent Stem Cell
MQ H ₂ O	Type 1 Water from a Milli-Q® Synthesis Water Purification System
mRNA	Messenger Ribonucleic Acid
MS	Mass Spectrometry
NC-CM	Neonatal Chondrocyte-Conditioned Medium
NGS	Normal Goat Serum
NMR	Nuclear Magnetic Resonance
OCT4	Octamer-4, Homeodomain Transcription Factor of the POU Family
OD	Optical Density
PAAA	Poly(acrylamide-co-acrylic acid)

PAMPS	Poly(acrylamide- <i>co</i> -methyl-propane sulphonate)
PAPA	Poly(acrylamide- <i>co</i> -propargyl acrylamide)
Pbf	Pentamethyl-2,3-dihydrobenzofuran-5-sulfonyl
PBS	Phosphate Buffered Saline
pDA	Polydopamine
PFA	Paraformaldehyde
PID	Proportional-Integral-Differential
PLGA	Poly (lactic- <i>co</i> -glycolic acid)
PMVE- <i>alt</i> -MA	Poly(methyl vinyl ether- <i>alt</i> -maleic anhydride)
PSS(S)	Poly(sodium 4-styrenesulphonate)
PVDF	Poly(vinylidene fluoride)
RNA	Ribonucleic Acid
RT	Room Temperature
SAM	Self-Assembled Monolayer
SNP	Single-Nucleotide Polymorphism
Sox2	SRY-Related HMG Box2 2
SPPS	Solid Phase Peptide Synthesis
TAZ	Transcriptional coactivator with PDZ-binding motif
TBSA	Tris Buffered Sodium Azide
TCPS	Tissue Culture Polystyrene
TFA	Trifluoroacetic Acid
THPTA	3,3',3''-(4,4',4''-(nitriлотris(methylene))tris(1H-1,2,3-triazole-4,1-diyl))tris(propan-1-ol)
TIS	Triisopropylsilane
Trt	Trityl
UV	Ultraviolet
XPS	X-ray Photoelectron Spectroscopy
YAP	Yes-Associated Protein

Chapter 1:

Introduction and literature review

1.1 Introduction

Human pluripotent stem cells (hPSCs) include embryonic stem cells (ESCs) and induced pluripotent stem cells (iPSCs) and have enormous potential for applications to drug screening, disease modelling and cellular therapies (Thomson et al., 1998, Takahashi et al., 2007). These applications will necessitate the use of cell culture conditions that are consistent, chemically-defined and/or non-xenogeneic for reasons of scale, reproducibility and safety (Hisamatsu-Sakamoto et al., 2008, Martin et al., 2005). hPSCs are adherent cells and have long been cultured on poorly-defined, complex surfaces of xenogeneic origin. Such surfaces present a wide range of ligands and interact with hPSCs via poorly understood mechanisms through many different cell adhesion molecules (CAMs) on the cell surface. CAM-ligand interactions are restricted by the types of CAMs and ligands available and are governed by the physical properties of the culture surface such as charge and elastic modulus. Specific CAM-ligand interactions mediate various intracellular signalling pathways, some of which are thought to be involved in maintaining the homeostasis and self-renewal of hPSCs. CAM-mediated intracellular signalling pathways are very complex; their details are beyond the scope of this thesis and are addressed in the following reviews (Kim et al., 2011, Li et al., 2012, Shen et al., 2012). A detailed understanding of the effects of CAM-surface interactions on hPSC phenotype and behaviour in culture should facilitate the optimisation of defined culture conditions to support both hPSC self-renewal and somatic differentiation pathways. A wide variety of chemically-defined surfaces that engage different CAM subtypes have been reported to support the long-term self-renewal of hPSCs (for examples see Lu et al., 2006, Braam et al., 2008, Klim et al., 2010, Melkoumian et al., 2010, Nagaoka et al., 2010, Rodin et al., 2010, Saha et al., 2011, Miyazaki et al., 2012). It is challenging to elucidate the importance of specific CAM-ligand interactions from these reports due to the diverse physicochemical properties of the culture surfaces as well as the inter-laboratory variation in cell culture protocols and in the cell and surface characterisation methods utilised. Non-specific protein adsorption to many “defined” surfaces can also confound results (Irwin et al., 2011). Direct comparisons between culture surfaces and the hPSCs cultured thereon are limited and have been focussed on identifying systems able to support culture of hPSCs as defined by minimal criteria including gene expression and qualitative differentiation assays (Brafman et al., 2009, Hakala et al., 2009, Akopian et al., 2010). Detailed characterisation and direct comparison of hPSCs cultured on chemically defined surfaces that specifically engage different CAMs is required to elucidate the roles of CAMs in maintaining pluripotency. The following literature review describes published reports of defined culture surfaces for hPSC self-renewal with a focus on the CAMs and extracellular matrix proteins (ECMPs) thought to be involved in mediating cell-surface interactions and maintaining pluripotency (Figure 1.1). The thesis proceeds to describe the optimisation of novel peptide-presenting polymer coatings as hPSC culture surfaces including a screen to identify optimal peptide ligands and ends with a study benchmarking cultures of hPSCs that have been maintained on the herein identified lead novel surface against cultures maintained in parallel on the commercially available surfaces Geltrex™, StemAdhere™ and Synthamax™.

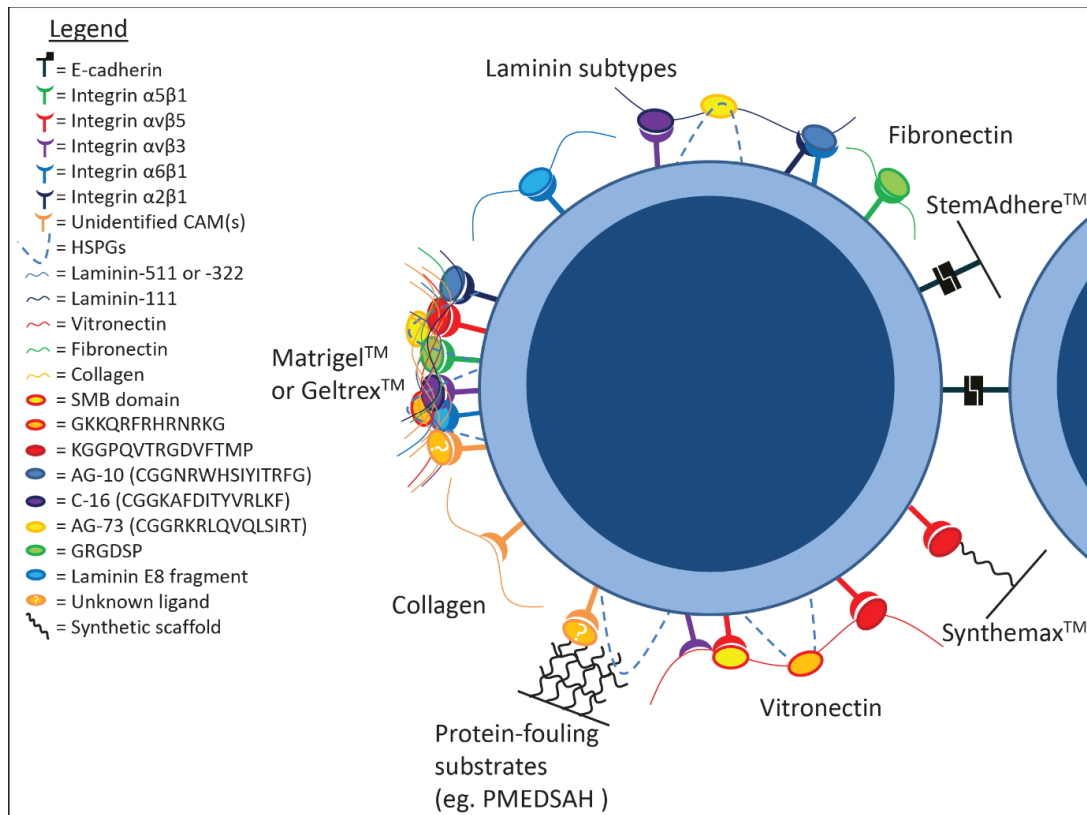


Figure 1.1: A schematic diagram of a single hPSC depicts cell surface binding to a range of culture surfaces. Specific ligands and CAMs are included where they have been reported to be involved in hPSC attachment and/or used in culture studies. CAMs involved in hPSC adhesion include integrin subtypes $\alpha 5 \beta 1$ (green), $\alpha \nu \beta 5$ (red), $\alpha \nu \beta 3$ (purple), $\alpha 6 \beta 1$ (blue) and $\alpha 2 \beta 1$ (dark blue), E-cadherin (black blocks), heparan sulphate proteoglycans (HSPGs; dashed blue lines) and unidentified CAMs (orange). Ligands are depicted by coloured circles and include the SMB domain of vitronectin (yellow/red), GKKQRFRRNRKG (orange/red), KGGPQVTRGDVFTMP (red/dark red), AG-10 (CGGNRWHSIYTRFG; blue/dark blue), C-16 (CGGKAFDITYVRLKF; purple/dark blue), AG-73 (CGGRKRLQVQLSIRT; yellow/orange), GRGDSP (green) and laminin E8 fragments (light blue/blue). The ligands are presented by ECMPs [represented by curved coloured lines: laminin-511 or -322 (blue), laminin-111 (dark blue), vitronectin (red), fibronectin (green) collagen (yellow)] or synthetic surfaces (thick black lines) including Synthemax™, StemAdhere™ and PMEDSAH. On the left of the image complex extracellular matrix extracts (e.g. Matrigel™ and Geltrex™) are illustrated as combinations of ECMPs, and on the right cell-cell adhesion is simplified in the extreme to illustrate homophilic E-cadherin binding. Where specific ECMP ligands are poorly-defined, CAMs are shown to interact with the ECMP line, where CAMs have not been identified the orange CAM is used, and undefined, adsorbed ligands are represented by orange ovals with a white question mark. This figure is a greatly simplified and stylised representation of cell-surface and cell-cell adhesion; actual interactions are assumed to be (and have been shown to be) far more complex. Adapted from (Lamshead et al., 2013).

1.2 Human pluripotent stem cells (hPSCs)

Pluripotency describes the ability of individual cells to differentiate into every cell type in the developing and adult body (Kleinsmith and Pierce, 1964). Pluripotent stem cells are also capable of indefinite self-renewal *in vitro* under appropriate conditions. hPSCs are therefore a potential cell source for myriad regenerative medicine approaches and *in vitro* disease models, for example hPSC-derived cardiomyocytes could be used to repair damaged tissue following a myocardial infarction (Thomson et al., 1998, Takahashi et al., 2007).

A range of hPSC types have been maintained in culture. Initially, karyotypically abnormal embryonal carcinoma (EC) cells (Kleinsmith and Pierce, 1964; Finch and Ephrussi, 1967) were demonstrated to have the potential to self-renew and to differentiate into the three germ layers. Some EC cell lines can be maintained on untreated TCPS in unsupplemented serum-containing medium on untreated TCPS (Przyborski et al., 2004). The subsequent derivation of karyotypically normal mPSCs and hPSCs required more complex surfaces, which are discussed below in Sections 1.5 to 1.9. Human embryonic stem (hES) cells are derived from the inner cell mass of a developing human embryo (Thomson et al., 1998), and human induced pluripotent stem cells (hiPSCs) can be generated by reprogramming somatic cells, following the expression of key pluripotency genes (Takahashi et al., 2007). Other potential sources of pluripotent cell types include epiblast (Brons et al., 2007), cord blood (Harris and Rogers, 2007) and adult spermatogonial stem cells (Guan et al., 2006), however ESCs and iPSCs are the most thoroughly studied lines. Throughout this thesis, “hPSCs” refers to hESC and/or hiPSC, not to hEC cells.

Pluripotency is a complex state that is maintained *in vitro* by large transcriptional networks that are yet to be fully elucidated (reviewed by Greenow and Clarke, 2012). Although many genes are involved in the regulation of pluripotency, cell line variation and population heterogeneity have hampered the identification of reliable molecular markers of pluripotency (Adewumi et al., 2007, Hough et al., 2009). To further complicate matters, murine studies have identified multiple pluripotent states that are maintained by different signalling networks (Nichols and Smith, 2009). It has been suggested that many of the differences between murine pluripotent stem cells (mPSCs) and hPSCs could be attributed to mPSC and hPSC cultures representing different states of pluripotency and it has been reported that hPSCs can move between these states with changes in culture conditions (Nichols and Smith, 2009, Xu et al., 2010, reviewed by Davidson et al., 2015). All of these factors make correct identification and characterisation of hPSCs a challenging task. Adequate characterisation of hPSCs is essential for the unambiguous identification of surfaces capable of supporting hPSC culture.

1.3 hPSC characterisation methods

The quality of ongoing hPSC cultures should be regularly assessed. When developing or implementing novel culture conditions it is important to characterise the cells thoroughly in order to validate the culture system. Daily assessment of hPSC cultures should involve visual observation of characteristic tightly-packed colonies of cuboidal-shaped cells containing prominent nuclei, multiple nucleoli and little cytoplasm, with minimal differentiated cell types present as shown in Figure 1.2 (Thomson et al., 1998). Proliferation rates of ongoing cultures can be monitored over time by recording approximate cell seeding densities and the frequency of passaging. Stronger evidence for pluripotency can be generated by monitoring associated molecular markers. The gold standard genetic marker of pluripotency is POU domain, class 5, transcription factor 1 (Pou5f1) also known as OCT4, a homeodomain transcription factor of the POU family that is essential for the production and maintenance of pluripotent cells (Nichols et al., 1998). Expression of OCT4 and other markers can be assessed in populations of hPSCs using numerous methods, which are listed in Table 1.1 (Martin and Evans, 1975, Solter and Knowles, 1978, Clark et al., 2004, Spencer et al., 2011). A range of more sophisticated *in silico* methods for assessment of pluripotency based on gene expression data are under development (reviewed by Asprer and Lakshmipathy, 2015) and include the microarray-based PluriTest™ assay (Müller et al., 2008). Additional information about the cell state can be obtained by characterising the epigenetic signature. Epigenetic regulation of gene expression is exercised through modifications to the genome that do not affect the genetic sequence. DNA methylation is one of the most-studied epigenetic modifications. Methylation down-regulates expression of local genes and can be detected by sequencing bisulphite-treated DNA (Boyes and Bird, 1992). Signature methylation patterns can be used to identify developmentally regulated cell types and individual hPSC lines and change in response to environmental stimuli (reviewed by Baker-Andresen et al., 2013). DNA methylation patterns have also been linked to the differentiation potential of hPSCs and can therefore be used as molecular markers of pluripotency (Bock et al., 2011). Molecular markers are however not completely specific to pluripotent cells due to the inherent heterogeneity of hPSCs. For example subpopulations with reduced differentiation potential have been identified within OCT4-positive populations of hPSCs (Hough et al., 2009). While combinatorial assessment of marker expression improves the robustness of molecular assays for pluripotency they ultimately remain surrogate assays, whereas functional demonstrations of cell potential provide more stringent tests of pluripotency. The ability of hPSCs to differentiate into cell types of all three embryonic germ layers (endoderm, ectoderm and mesoderm) can be examined both *in vitro* and *in vivo*. *In vitro* differentiation of pluripotent cells is usually associated with the formation of embryoid bodies [complex, non-adherent, three-dimensional structures composed of spontaneously differentiating hPSCs (Doetschman et al., 1985, Keller, 1995)] and can either be spontaneous or directed towards certain cell fates (Martin and Evans, 1975, Jones-Villeneuve et al., 1982). The *in vivo* differentiation potential of hPSCs is typically tested by transplantation into immunodeficient mice. The formation of a teratoma (a benign tumour comprising cell types

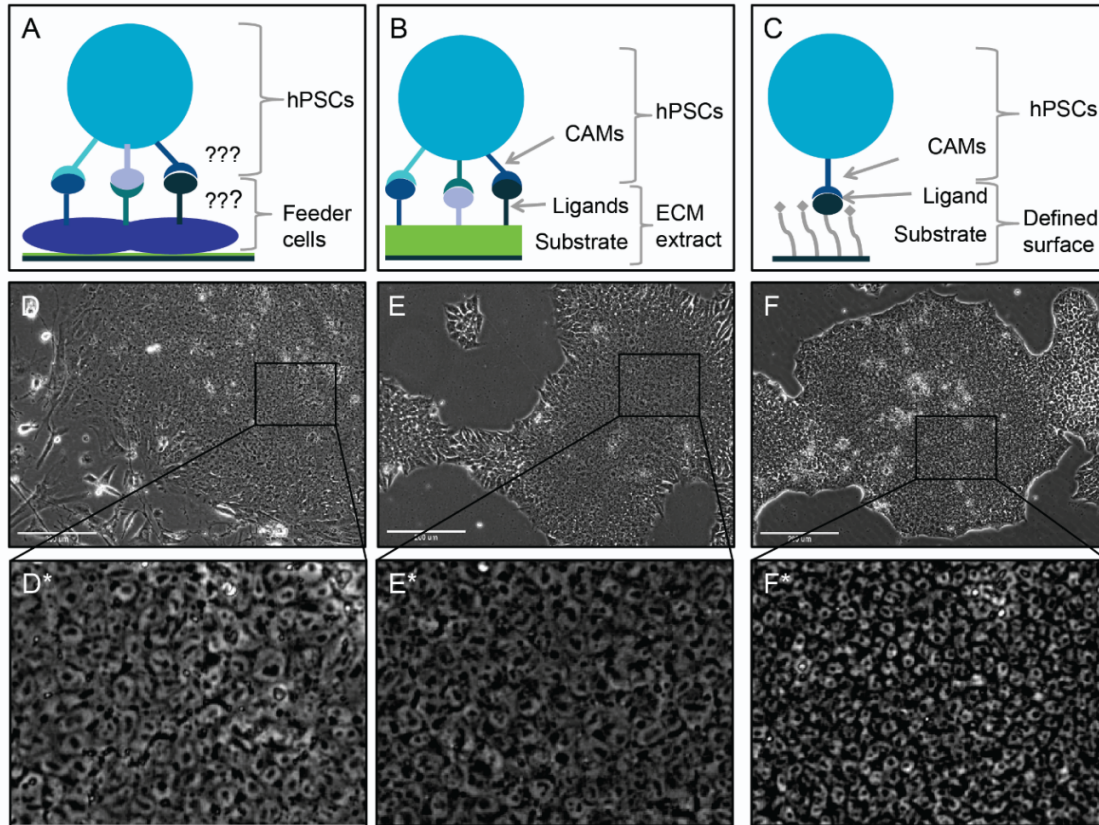


Figure 1.2: HPSCs cultured on different surfaces. Schematic diagrams illustrate the arrangement of cell adhesion molecules (CAMs), ligands and substrates (where appropriate) of the three major types of culture surfaces used for maintenance of human pluripotent stem cells (hPSCs). (A) Feeder cells, (B) extracellular matrix (ECM) extracts and (C) chemically defined culture surfaces. (D-F) Phase contrast images of hPSCs cultured on a surface of each type, murine embryonic fibroblasts, Geltrex™ and Corning Synthemax™ respectively. (D*-F*) Magnified regions of D-F. hPSCs cultured on each surface display a typical morphology with compact colonies of cells with prominent nucleoli and high nuclear-to-cytoplasmic ratio. Adapted from (Lambshead et al., 2013). Scale bars represent 200 μm.

representative of each of the three embryonic germ layers) at the site of implantation is the most stringent validation assay available for the differentiation potential of putative hPSCs (Kleinsmith and Pierce, 1964). However, differentiation assays are laborious, inconsistent in efficiency and difficult to standardise across cell lines and laboratories, so evaluation of molecular markers remains important for assessing the efficacy of hPSC culture systems. Quality control of any long-term cell culture system should also include an assessment of genetic stability using G-banding analysis to detect gross or subchromosomal changes. However, genetic aberrations below the detection limit of G-banding have been identified in hPSC lines and more detailed genetic analysis should also be considered when testing novel culture systems (Laurent et al., 2011). A detailed characterisation of hPSCs should include the methodologies bolded in Table 1.1.

1.4 The evolution of hPSC culture conditions

It is well known that *in vitro* maintenance of the pluripotent state requires culture in supportive media and a favourable cellular microenvironment. hPSCs are routinely cultured in vessels containing complex media and coated with a complex surface to which hPSCs are anchored by CAMs. When the cells reach confluence (usually after 4-7 days) they are enzymatically dissociated, lifted into suspension and a portion is transferred into freshly coated vessels to which they adhere and continue proliferating indefinitely. The signalling pathways regulated by growth factors in the media and by ligands on the culture surface converge downstream and contribute to the maintenance of pluripotency, so the combination of surface and media is critical.

hPSCs were initially derived and maintained in serum-containing conditioned media (CM) [media imbued with factors secreted by cultured cells, often MEFs (MEF-CM)] on a layer of either mitotically-inactivated mouse embryonic fibroblast (MEF) feeder cells (see Figure 1.2A,D) or complex extracellular matrix (ECM) extracts including Matrigel™ and Geltrex™ (Figure 1.2B,E) (Thomson et al., 1998, Xu et al., 2001). However these pluripotency-supporting systems are not compatible with large scale cultures, risk the introduction of pathogens, show batch-to-batch variability and interact with hPSCs in a poorly-defined way.

Landmark developments in hPSC culture media have included the development of serum-free, chemically-defined, KnockOut Serum Replacement media (KOSR) (Price et al., 1998) and mTeSR1 hPSC culture medium (Ludwig et al., 2006a), which have been widely used but are xenogeneic. mTeSR1 is a modified version of the xeno-free and prohibitively expensive TeSR medium. Subsequently, the removal of pairs of components from TeSR medium led to the development of Essential 8™ (E8) medium (Chen et al., 2011b). The removal of ten (10) of the eighteen (18) components that had been added to basal medium to make TeSR, including serum albumin and β -mercaptoethanol, resulted in a hPSC culture medium that was cheaper and less chemically complex than any other to date. For these reasons E8 medium was used throughout this thesis.

Table 1.1: Parameters of interest for hPSC characterisation and methods for their assessment. Physical characteristics, molecular markers, epigenetic profiling, differentiation potential and genetic stability can be assessed by the range of methods listed (not comprehensive). It is recommended that the methods highlighted in bold, performed at frequencies indicated in the first column, are the minimum requirements for validating novel culture systems. Unbolded methods should also be considered for more thorough characterisation of hPSCs. Adapted from (Lamshead et al., 2013).

Parameters	Method	Strength of evidence of pluripotency
Physical characteristics (daily/weekly)	Daily visual assessment of cell/colony morphology calculate adhesion efficiency, population doubling time	Weak, subjective, but critical as non-invasive and sensitive when performed by an experienced operator
Expression of molecular markers eg. OCT4, NANOG, SOX2, REX1 (following passages 1, 5 and >10)	Immunocytochemical staining , flow cytometry, RT-PCR, microarray assays, other <i>in silico</i> methods	Moderate-strong. Depending on marker(s) assessed
Epigenetic profiling	Bisulphite sequencing, ChIP, microarray assays	Moderate-strong. Depending on marker(s) assessed
Differentiation potential (following >10 passages)	Embryoid body differentiation (<i>in vitro</i>) with RT-PCR analysis for molecular markers of differentiation	Very strong
	Teratoma formation assay (<i>in vivo</i>) with histological determination of cells from the three embryonic germ layers	Gold standard
Genetic stability (following >10 passages)	G-banding , FISH, SNP analysis	Not applicable. Important to identify genetically transformed cultures, not indicative of differentiation potential

Despite the wide uptake of KOSR, mTeSR and now E8 hPSC culture media, and while many exciting practical applications of hPSCs will demand chemically-defined, xeno-free culture conditions, many laboratories persist with hPSC culture surfaces composed of MEFs or ECM extracts. Many approaches to improving hPSC culture surfaces, such as using human or autologous feeders (Fu et al., 2011, Prathalingam et al., 2012, Lai et al., 2015), complex human ECM extracts (Wang et al., 2012, Vuoristo et al., 2013, Ding et al., 2015), defined surfaces in combination with CM (Jones et al., 2010) or even fixed feeder cells (Huang et al., 2015, Yue et al., 2012, Joddar et al., 2015) incompletely address these concerns. A suite of chemically-defined, xeno-free surfaces (see

Figure 1.2C,F) have recently been reported to support hPSC culture in defined media, although many of these surfaces are expensive and none have been widely employed by the stem cell community (Mei et al., 2010, Melkounian et al., 2010, Rodin et al., 2010, Stephenson et al., 2012, Villa-Diaz et al., 2012). Defined surfaces that are thought to specifically interact with different CAM-subtypes have been reported to support hPSC culture (Figure 1.1) but the relative efficiencies of individual ligands in supporting hPSC cultures are poorly understood. hPSC culture surfaces must be identified that are reproducible, stable, xeno-free, affordable and that can be tailored to a range of long-term differentiation protocols. Such surfaces should be based on an understanding of the properties of the surfaces and of the requirements of the cells, including CAM-mediated signalling.

1.5 CAMs and the maintenance of pluripotency

CAMs are cell-surface proteins that mediate interactions with nearby cells and ECMPs through extracellular ligands. When engaged by a ligand, CAMs transfer molecular signals “outside-in” to the nucleus of the cell resulting in modification of gene expression. Signals can also be transferred “inside-out” when cytoplasmic agonists alter the affinity of CAMs for certain ligands (reviewed by Hu and Luo, 2013). A range of CAMs have been considered as potential molecular markers for hPSCs and could be involved in the maintenance of pluripotency (Kolle et al., 2009). The main CAM families thought to be involved in hPSC culture are integrins and cadherins, which have each been shown to modulate self-renewal of hPSCs in culture on different surfaces (Xu et al., 2010).

1.5.1 Integrins

Integrins are a family of transmembrane heterodimeric glycoproteins that are composed of α and β chains. Eighteen α and eight β chains have been identified in humans, combining to form the twenty-four known types of integrin (reviewed by Kim et al., 2011). Different integrin types recognise and bind a range of ligands with various affinities. Bound integrins assemble at the cell surface and interact with numerous cytoplasmic proteins to form focal adhesions, which act as transmembrane signalling conduits regulating intracellular kinases and phosphatases (Kim et al., 2011). The formation of focal adhesions by various integrin types modulates different downstream signalling pathways that mediate a range of cell responses and functions. In particular, roles in inner cell mass formation and cell survival make integrins promising targets for hPSC culture surfaces (Adjaye et al., 2005). Integrins $\alpha 5 \beta 1$ (Baxter et al., 2009), $\alpha 6 \beta 1$ (Rodin et al., 2010), $\alpha v \beta 3$ and $\alpha v \beta 5$ (Mei et al., 2010) have been reported to mediate hPSC interactions with several defined culture surfaces and are thought to be involved in maintaining pluripotency.

1.5.2 Cadherins

Cadherins are transmembrane glycoproteins that form calcium-dependent cell-cell and cell-ECM homophilic binding junctions (reviewed by Li et al., 2012). While the cadherin family comprises more than 100 members, E-cadherin is the primary cadherin expressed by hPSCs and its expression and engagement is important for hPSC function (Eastham et al., 2007). Active E-cadherin interacts with multiple intracellular signalling mechanisms and is involved in tissue morphogenesis, hPSC self-renewal (Li et al., 2012) and hPSC mechanosensing of surface nanotopography (Chen et al., 2012). Conversely, disruption of E-cadherin signalling has been linked to hPSC death following dissociation (Xu et al., 2010). Accordingly, reduction in E-cadherin expression correlates with early differentiation processes *in vitro* (Spencer et al., 2011). E-cadherin clearly plays an important role in pluripotency and is therefore a target CAM for defined hPSC culture surfaces. As a homophilic binding protein E-cadherin not only serves as a CAM for hPSC binding but also as a potential ligand. A recombinant human fusion protein composed of E-cadherin and the Fc region of IgG1 antibodies has been developed as a tissue culture coating for untreated polystyrene (Nagaoka et al., 2010). This fusion protein coating, which mediates adhesion through the E-cadherin component, has been reported to support long-term culture of teratoma-forming hPSCs in combination with a range of chemically defined media and has been commercialised as StemAdhere™ (Nagaoka et al., 2010, Stephenson et al., 2012).

1.6 Extracellular matrix proteins (ECMPs) as ligands for hPSC culture surfaces

Most defined culture surfaces have been developed through a reductive approach. Proteomic analyses of complex culture surfaces like MEFs and Matrigel™ have identified several ECMPs involved in hPSC culture including collagen, laminin, fibronectin, vitronectin and heparan sulphate proteoglycans (HSPGs) (Horák and Fléchon, 1998, Hughes et al., 2010). The ability of these ECMPs and their derivative peptides or molecular mimics, alone or in combination, to maintain hPSC culture is discussed below. Peptides and molecular mimics are of particular interest because they mediate fewer interactions than whole ECMPs, facilitating identification of key interactions.

1.6.1 Collagens

Collagens are large, trimeric proteins that assemble into fibrils and fibres and comprise the primary structural component of the extracellular matrix (reviewed by Kadler et al., 2008). Collagens contain multiple binding sites that interact with a wide range of extracellular and cell surface proteins thought to be linked to pluripotency, including various integrins and HSPGs (reviewed by Heino, 2007). These binding sites and interactions suggest that collagen may be a suitable surface for hPSC culture; however in practice the demonstrated ability of collagen to

support hPSCs has been limited. In a 5-day culture experiment collagen subtypes I, III and IV were able to support adhesion and proliferation of hPSCs in MEF-CM, although proliferation did not occur consistently on all subtypes or with all cell lines (Brafman et al., 2009). In longer-term studies MEF-CM (but not chemically defined medium) has been shown to support OCT4 positive hPSC colonies on collagen IV for at least five passages (Braam et al., 2008), but not on collagen I due to poor attachment (Jones et al., 2010). Medium that was conditioned by cells derived from an embryoid-body culture was able to support OCT4 positive hPSC colonies on collagen I for at least one month (Jones et al., 2010). In the latter study, media conditioned by two other somatic cell types failed to support hPSC culture beyond two passages on Matrigel™, highlighting the considerable effects that undefined components in CM can have on the effectiveness of a culture system and the importance of defined media for achieving reproducible cultures. Inclusion of collagen-derived peptides in cell culture surfaces has not been reported and the CAMs involved in the hPSC-collagen interactions have not been investigated, probably due to the lack of success in maintaining cultures on whole collagen. Curiously, long-term culture of hPSCs has been achieved on gelatin (a derivative of collagen) in heavily-supplemented serum-free medium that was designed to emulate mPSC culture conditions (Xu et al., 2010). These “converted hPSCs” could self-renew for more than 20 passages, were OCT4 positive by immunostaining and demonstrated the ability to differentiate into cell types of the three embryonic germ layers *in vitro*. The morphology and gene expression of converted hPSCs was reported to be more mPSC-like and the CAMs involved in mediating adhesion shifted from predominantly integrins to E-cadherin (Xu et al., 2010). This unique example raises questions about the phenotypic stability and adaptability of hPSCs in various culture conditions and demonstrates the importance of standardisation of culture media.

1.6.2 Laminins

Laminins are cruciform, trimeric ECMPs composed of α , β and γ chains and are major proteins in the basal lamina. There are 5 α , 4 β and 3 γ chains that combine to form the 15 known laminin subtypes. Subtypes are named for their chain composition, for example laminin-511 is composed of $\alpha 5$ $\beta 1$ and $\gamma 1$ chains. Laminin proteins have been proposed as hPSC culture surfaces due to their prominence in more complex surfaces (Hughes et al., 2010) and because they contain multiple cell-binding motifs including RGD, E8, IKVAV, AG-10, C-16 and AG-73 (Graf et al., 1987, Nomizu et al., 1997) that interact with various integrins and proteoglycans expressed by hPSCs (Meng et al., 2010). Mixed-subtype human laminin has maintained self-renewing, teratoma-forming hPSCs in several conditioned and defined media over long-term culture and during the establishment of hESC cell lines (Li et al., 2005, Fletcher et al., 2006). Five of the fifteen laminin subtypes have since been tested as hPSC culture surfaces coupled with the use of MEF-CM. In two independent studies laminins-511, -322 and -111 (all mediated by integrin $\alpha 6 \beta 1$ binding) supported culture of OCT4 positive hPSCs capable of *in vitro* differentiation into the three germ layers for at least 10 passages, while laminins-211 ($\alpha 3 \beta 1$) and -411 ($\alpha 7 \beta 1$) failed to even support

adhesion (Miyazaki et al., 2008, Rodin et al., 2010). Laminins-511 and -521 are the most thoroughly tested subtypes and have been demonstrated to support long-term hPSC culture in three different chemically-defined media and also to support hESC derivation (Rodin et al., 2010, Manton et al., 2010, Rodin et al., 2014). Interestingly, endogenous expression of $\alpha 5$ laminin, which contributes to both of these laminin isoforms, is essential for maintenance of hPSC cultures on Synthemax™-coated vessels (Laperle et al., 2015a).

Several peptides derived from laminin-111 have been incorporated into hPSC culture surfaces with varying results. In adhesion studies a peptide (RNIAEIIKDI) derived from the γ -chain successfully mediated attachment of hPSCs in defined xeno-free media while an IKVAV-containing peptide bound hPSCs poorly (Derda et al., 2007, Melkounian et al., 2010). Other laminin-111-derived peptides (AG-10, C-16 and AG-73) have mediated adhesion of hPSCs in defined media by engaging different integrin subtypes or heparan sulphates (Meng et al., 2010). These small peptides were only able to support hPSCs for a few passages when presented together in specific proportions, with differentiation apparent by the third passage (Meng et al., 2010).

More recently, larger laminin fragments composed of three post-translationally modified polypeptide subunits that form the E8 binding sites (Deutzmann et al., 1990) of laminins-332 and -511 have been reported to support the long-term culture of teratoma-forming hPSCs in a range of defined media (Miyazaki et al., 2012). E8 fragments demonstrated a stronger adhesion affinity to hPSCs than either Matrigel™ or the whole laminins from which they were derived, which is a promising finding for the application of functional subunits to replace whole ECMPs in defined surfaces for hPSC culture (Miyazaki et al., 2012). The mixed reports of hPSC culture on laminin-derived subunits reflect how hPSCs can attach to different binding sites on single ECMPs with different affinities and that the maintenance of pluripotency depends on properties of CAM-mediated interactions with the culture surface beyond simple adherence.

1.6.3 Fibronectin

Fibronectin subunits are large (~250 kDa) extracellular glycoproteins which form disulphide-bonded dimers and much larger fibrils (Keski Oja, 1976). Fibronectin is ubiquitously expressed throughout the developing and adult body and plays an organisational role in assembling other ECMPs (reviewed by Singh et al., 2010). In theory fibronectin is a promising candidate surface for hPSC culture because it contains many binding domains that interact with ECMPs and CAMs associated with the self-renewal of hPSCs including fibrin, collagen, heparan sulphates and integrins (Singh et al., 2010). In practice fibronectin has been favourably compared to laminin for its ability to support hPSC adherence and maintenance of pluripotency (Tsutsui et al., 2011, Brafman et al., 2009). Whole fibronectin has been reported to maintain long-term cultures of OCT4 positive hPSCs capable of *in vitro* differentiation into the three germ layers and/or teratoma formation in MEF-conditioned (Tsutsui et al., 2011) or heavily supplemented serum-free media

(Baxter et al., 2009) and also in several chemically-defined media (Lu et al., 2006, Liu et al., 2012, Hughes et al., 2011).

Fibronectin-cell interactions are predominantly mediated by the GRGDSP motif and its interaction with $\alpha 5\beta 1$ integrins (Hautanen et al., 1989); the key role of $\alpha 5\beta 1$ integrins in hPSC-fibronectin adhesion has been supported by a competitive inhibition study (Baxter et al., 2009). Nevertheless, defined surfaces that presented two fibronectin-derived, GRGDSP-containing, $\alpha 5\beta 1$ -binding peptides gave poor hPSC adhesion, suggesting that the ability of fibronectin to support hPSC culture relies on multiple binding domains (Melkounian et al., 2010).

1.6.4 Vitronectin

Human vitronectin is a relatively small (75 kDa) glycoprotein that can be secreted as either a single chain or a dimer, is abundant in blood and throughout the ECM and promotes cell adhesion and migration (reviewed by Schwartz et al., 1999). Vitronectin contains multiple binding sites that engage integrins or HSPGs, which positions vitronectin as one of the most promising ECMs for hPSC culture (Suzuki et al., 1985). The potential applications of vitronectin to hPSC culture are exemplified by a vitronectin-containing chimeric protein that has been used as a media supplement for hPSC culture on a laminin-coated surface (Manton et al., 2010). Vitronectin-coated tissue culture polystyrene (TCPS) has supported long-term culture of teratoma-forming hPSCs (Braam et al., 2008, Saha et al., 2011, Yap et al., 2011, Meng et al., 2012, Sun et al., 2012) and hiPSC derivation (Chen et al., 2011b, Kim et al., 2013) in a range of conditioned and defined media. Only two groups have reported the failure of vitronectin-based surfaces to maintain the pluripotency of cultured hPSCs in appropriate media and these results were probably due to inadequate deposition of the vitronectin protein (Hakala et al., 2009, Abraham et al., 2010). Hakala et al. (2009) were unable to maintain hPSC culture on vitronectin-coated TCPS and Abraham et al. (2010) on a surface composed of vitronectin and HSPG (vitronectin-alone was not tested). Both studies used lower concentrations of vitronectin (200 ng/cm² and 10 ng/cm² respectively) than the threshold for hPSC culture of 250 ng/cm² that was later determined by Yap et al. (2011). Since neither study reports surface characterisation such as performed by Yap et al. (2011) we must assume that concentrations were calculated based on the vitronectin concentration in solution and assuming 100 % deposition. Thus the actual protein surface concentrations would have been well below the threshold, explaining the inability of these culture systems to maintain hPSCs.

As implied by the binding sites described above, hPSC-vitronectin adhesion is mediated by $\alpha v\beta 3/\beta 5$ integrins and HSPGs (Mei et al., 2010, Klim et al., 2010). Accordingly, two integrin-binding peptides and one HSPG-binding peptide derived from vitronectin have been individually demonstrated to support long-term culture of teratoma-forming hPSCs (Klim et al., 2010, Melkounian et al., 2010, Prowse et al., 2010, Higuchi et al., 2015). The subtype-specificity of the

integrin-binding peptides was not assessed, although anchored small molecules that specifically bind $\alpha v \beta 3$ integrins have failed to support hPSC adhesion (Klim et al., 2012). The latter small-molecule data is difficult to interpret without side-by-side and combinatorial comparisons with other integrin-specific small molecules. The apparent functional redundancy within the vitronectin molecule has demonstrated that small peptides can be sufficient to mimic the hPSC-supporting effects of ECMPs and suggests that the maintenance of pluripotency may not depend entirely on specific CAM-ligand interactions.

1.6.5 Combinations of ECMPs as hPSC culture surfaces

Combinations of collagens, fibronectin, laminins and vitronectin have been reported to support long-term culture of hPSCs in a few studies (Brafman et al., 2009, Ludwig et al., 2006a), although combining ECMPs in this way can be superfluous given the aforementioned abilities of single-ECMPs to support hPSCs, especially vitronectin and laminin-511. In one study, hPSCs cultured on a fibronectin-coated surface differentiated after fewer than five passages while a surface coated with fibronectin and HSPG supported culture of alkaline phosphatase-positive cells without morphological differentiation (Abraham et al., 2010). The initial experiments were conducted in a serum-free medium that had been supplemented with 4 ng/mL basic fibroblast growth factor (FGF-2) and although cells proliferated on fibronectin-HSPG in this medium and expressed alkaline phosphatase they would not differentiate when induced (Abraham et al., 2010). In the same study the culture on the fibronectin- and HSPG-coated surface was repeated using media supplemented with additional FGF-2 (100 ng/mL) and the maintenance of pluripotency was demonstrated by successful embryoid body formation. It is unclear if the fibronectin-alone culture was repeated with the higher concentration of FGF-2 in this study (Abraham et al., 2010). These results contrast with other reports of hPSCs being maintained long-term on fibronectin using defined media and highlight the need for investigation of key signalling pathways involved in the maintenance of pluripotency and the importance of standardisation of defined culture methods (Lu et al., 2012, Baxter et al., 2009, Tsutsui et al., 2011, Hughes et al., 2011).

1.7 Surfaces that interact with hPSCs through non-specific adsorbed media proteins

Some surfaces capable of supporting hPSC culture contain no obvious ligands; these surfaces usually rely on a level of culture medium and/or hPSC-secreted protein adsorption (protein-fouling) to mediate adhesion (Irwin et al., 2011, Mahlstedt et al., 2010). Although protein-fouling surfaces may lack native ligands they often have modifiable physical properties which can be used to control cell behaviour and to optimise the adsorption of protein or peptide ligands (discussed

further below). In one unusual report, Bigdeli et al. (2008) reported the culture of two hPSC lines directly on TCPS in a neonatal chondrocyte-conditioned medium (NC-CM). Media conditioned by several different somatic cell types were trialled, but only NC-CM supported effective adhesion and ongoing culture (Bigdeli et al., 2008). It would be interesting to determine which factor secreted by the neonatal chondrocytes was critical to this result. Adaptation to these culture conditions involved high levels of cell death and required an unusually long (20-day) recovery period. Nevertheless the cells were maintained long-term, thoroughly characterised for gene expression and differentiation potential and no genetic abnormalities were detected in either cell line by G-banding or fluorescence *in situ* hybridisation (FISH) analysis. However, culturing hPSCs directly onto polystyrene has not been reproduced by other groups and the hPSC lines used (SA167 and AS034.1) have not been reported in any other culture surface studies and may behave uniquely (Bigdeli et al., 2008).

While protein-fouling surfaces may adequately support hPSC culture they cannot be used to investigate critical molecular signalling pathways due to their poorly defined cell-surface interactions. Another consideration for these surfaces is that the type and concentration of adsorbing proteins may vary between cell lines and media formulations. A surface that depends on adsorbed proteins to mediate adhesion may be vulnerable to these variations and is likely to vary in its effectiveness at supporting different cell lines (Nandivada et al., 2011).

1.8 Two-dimensional substrates for hPSC culture surfaces

In many of the aforementioned culture systems, the CAM-engaging proteins or peptides are simply applied to TCPS in aqueous solutions from which they adsorb onto the plastic (for example Braam et al., 2008, Meng et al., 2010). However physicochemical modifications to TCPS and more complex substrates including self-assembled monolayers (SAMs), polymer scaffolds and hydrogels are also being developed to optimise surface properties including hardness (Chowdhury et al., 2010a), roughness (Chen et al., 2012), stiffness, wettability (Mei et al., 2010) and ligand density (Klim et al., 2010), distribution (Melkounian et al., 2010) and presentation (Kolhar et al., 2010). Some alterations to the physical properties of culture substrates [e.g. nanoroughness (Chen et al., 2012) and stiffness (Trappmann and Chen, 2013)] are thought to be recognised directly by hPSCs while others such as wettability affect the adsorption and presentation of media and secreted proteins (Tamada and Ikada, 1993), indirectly influencing CAM-mediated cell-surface interactions.

1.8.1 Characterisation methods for hPSC culture surfaces

In order to optimise hPSC culture surfaces the physical characteristics of the surfaces must be tuned to optimise CAM-ligand interactions. Table 1.2 outlines the range of methods available and appropriate for this aspect of developing synthetic culture surfaces for hPSC culture. In particular it remains a challenge to control and characterise the quantity, distribution and orientation of ligands bound to polymer surfaces. Since these properties influence CAM-ligand interactions it is of interest to the field to develop new technologies to evaluate them. Throughout this thesis a “substrate” is defined as the non-ligand parts of a surface, those parts that position and present ligands rather than directly engaging CAMs.

1.8.2 Modifications to plastic and glass culture surfaces

Simple modifications that have been used to make TCPS or glass more biologically relevant for hPSC culture include amine-modifications (Kolhar et al., 2010) and physicochemical damage caused by UV-treatment (Saha et al., 2011), plasma-etching (Mahlstedt et al., 2010) or reactive ion etching (Chen et al., 2012). These modifications increase the hydrophilicity, change the nanoscale topography and/or increase the abundance of functional groups on the surface, which can all modulate cell-surface interactions either through modulation of protein adsorption or by allowing modification with specific ligands.

1.8.3 Self Assembled Monolayers (SAMs)

Biologically-relevant self-assembled monolayers (SAMs) are typically comprised of derivatives of organic alkanethiol (AT) molecules, which spontaneously form a monolayer on gold films (comprehensively reviewed by Love et al., 2005). The thiol head groups bind to the gold film and the distal alkane tails arrange themselves roughly perpendicular to the film. Micropatterning of ATs with modified carboxyl or hydroxyl tail groups (to present ligands) and perfluoro-ATs (to provide a protein low-fouling background) allows presentation of multiple and varied ligands in particular orientations at controlled densities and distributions (Love et al., 2005). These customised AT-SAMs have been used by several groups to culture hPSCs and to investigate the molecular mechanisms involved in adhesion and maintenance of pluripotency. AT-SAMs have been used extensively by the Kiessling laboratory (University of Wisconsin) where laminin- and vitronectin-derived peptides have been identified that can support short- and long-term hPSC culture respectively (Derda et al., 2007, Klim et al., 2010). Micropatterned AT-SAMs have also been used to regionalise adsorption of mixed ECMPs onto carboxyl groups presented in a certain distribution, allowing fine control of hPSC colony size for medium-term (5 passages) culture (Jonas et al., 2013). Culturing hPSCs on these ECMP-islands resulted in colonies that were more homogenous for pluripotency marker expression than MEF-supported control cultures (Jonas et al., 2013).

Table 1.2: Parameters of interest for characterisation of hPSC culture surfaces and analytical methods for their assessment. Surface topography, ligand density, chemical properties, wettability and protein adsorption can be tested by the methods listed. Pros and cons are listed for each method in this non-comprehensive list. Adapted from (Lambhead et al., 2013).

Parameter	Analysis method	Pros	Cons
Surface topography	Atomic force microscopy (tapping mode)	Compatible with an aqueous environment, can view individual proteins that have adsorbed to the surface, modern instruments acquire images at a faster rate	Images are generally of a small area, therefore may not be representative
	Scanning or transmission electron microscopy	Widely available	Resolution is not as high, significant sample preparation is required, unable to quantify topography
Ligand density	ELISA assays	Straightforward assay	Not very sensitive for adsorbed protein, requires antibodies to specific proteins or molecules
	Fluorescence from adsorbed or covalently attached fluorophore	Relatively straightforward assay	Microenvironment and dye-dye quenching effects from surface anchored species introduces artefacts, construction of calibration curve difficult
	Fluorescence from fluorophore released into solution	Quantitative, sensitive, relatively straightforward assay	Cleavable fluorophore needs to be synthesised and chemically attached to ligand/CAM
	Lanthanide (e.g. Eu-chelate) labelling of ligand	Quantitative, sensitive, relatively straightforward assay	Need to carry out chemical coupling of Eu-chelate to ligand

	Radio-labelling of ligand	Quantitative, sensitive, relatively straightforward assay	Complex chemistry required to either radio-label pre-synthesised ligands or synthesise ligand with radioisotope-containing precursors
Chemical properties	Nuclear magnetic resonance (NMR)	Straightforward sample preparation	Solid-state NMR generally not sensitive enough, complex spectra
Wettability	Water contact angle	Simple	Very non-specific - many adsorbed species can modify wettability
Chemical composition (directly detecting protein adsorption)	X-ray photoelectron spectrometry	Elemental composition quantitative, sample preparation is very simple (removal of buffer salts and drying)	Elemental composition is straightforward but high resolution spectra complex, amide bond-containing materials generate false positives, no specificity in relation to protein type, ultra-high vacuum technique (can cause structural rearrangements)
	Time-of-flight secondary ion mass spectrometry	Minimally-destructive, minimal sample preparation, efficient,	Analysis generally not quantitative, produces large data sets often requiring statistical methods, no specificity in relation to protein type, ultra-high vacuum technique (can cause structural rearrangements)
	Fourier transform infrared spectroscopy	Widely available, can be powerful if coupled with synchrotron	Not "surface-sensitive" enough, no specificity in relation to protein type
Indirect assessment of protein adsorption	Embryoid body adhesion assay	Straightforward if embryoid bodies are being generated in house	Expensive, time-consuming
	HeLa or other e.g. L929 cell adhesion assay	Reliable, cheap if cell lines are available in laboratory	Cell attachment for cells other than hPSCs may be mediated by different ligands

Although the customisable nature of SAMs makes them useful for investigating cell adhesion mechanisms, SAMs are physically unstable under biological conditions, which limits their utility for long-term hPSC culture and subsequent differentiation assays (Flynn et al., 2003). The gold coatings on which SAMs assemble can also present a challenge for visual assessment of live cultures (Love et al., 2005). For these reasons SAMs are unsuitable for practical applications as a long-term culture surface and while there is much to be learned from hPSC culture on SAMs it is currently unclear how transferrable results from SAM-based studies will be to other prospective culture surfaces.

1.8.4 Heparan Sulphate Proteoglycans (HSPGs)

Proteoglycans are large, membrane-bound extracellular proteins with covalently attached chains of repeating disaccharide units called glycosaminoglycans (GAGs). Proteoglycans are named according to GAG classes such that HSPGs include all proteins bound to heparan sulphate polysaccharides (reviewed by Kim et al., 2011). Different proteoglycan subtypes are found throughout the mammalian ECM, but HSPGs are the most relevant to hPSCs and can be exploited in hPSC culture systems (Klim et al., 2010, Gasimli et al., 2012, Musah et al., 2012). HSPGs bind to, stabilise and mediate interactions with integrins expressed by hPSCs (Ballut et al., 2013) and with growth factors and their receptors. One such growth factor is FGF-2 (Ford-Perriss et al., 2002), a key component of hPSC media which can mediate hPSC adhesion when immobilised (Brafman et al., 2009). This cooperative role of HSPGs is thought to explain why higher levels of FGF-2 are required to support feeder-free hPSC cultures when using non-conditioned media (Levenstein et al., 2006). Since HSPG-hPSC interactions are often mediated by non-HSPG ligands (e.g. FGF-2), for the purposes of investigating the molecular mechanisms involved in maintaining pluripotency HSPGs can be considered as a complex substrate that optimises presentation of a poorly-defined group of ligands.

Few studies have tested the effects of HSPGs on hPSC maintenance and differentiation. HSPGs have been shown to play a role in the differentiation of mPSCs and are not necessary for maintenance of their pluripotency (Kraushaar et al., 2010). However given mPSCs (unlike hPSCs) do not require FGF-2 signalling to self-renew (Xu et al., 2005) and predominantly interact with surfaces through different CAMs to hPSCs (Xu et al., 2010), this finding is not likely to be relevant to culture of conventional hPSCs. HSPG-mediated binding has not been able to support hPSC attachment on its own, although in combination with fibronectin HSPGs have improved the maintenance of pluripotency in the presence of higher concentrations of FGF-2, as discussed above (Abraham et al., 2010). The need for increased FGF-2 supplementation suggests that the HSPGs were not effectively presenting FGF-2 in this study or that other inadequacies in the culture system need to be compensated for (Abraham et al., 2010).

The ability of heparan sulphate (HS) disaccharides to support hPSC culture has not yet been tested, although HSPG-binding peptides (Klim et al., 2010) and HS-mimicking polymers including poly(sodium 4-styrenesulphonate) (PSS(S)) and poly[2-(methacryloyloxy)ethyl dimethyl-(3-sulphopropyl)ammonium hydroxide] (PMEDSAH) have been used to successfully maintain long-term hPSC culture and are discussed in the following section.

1.8.5 Polymer scaffolds

Polymer scaffolds can be loosely defined as physical networks composed of any polymer (long chains composed of monomer subunits). Polymer scaffolds can be applied to culture surfaces of various dimensions and their physicochemical properties can be tailored to meet the demands of hPSC cultures (Mei et al., 2010). Polymers can interact with hPSCs due to intrinsic bioactivity or because they have been modified to present specific ligands. In the latter case, when investigating cell-surface interactions protein low-fouling polymers are preferred to minimise non-specific interactions with proteins and cells. Polymer scaffolds can also be employed as a base with controllable physical properties and then simply pre-coated with ECMPs (Mei et al., 2010, Sun et al., 2012).

The bioactive polymer on which hPSC culture has been most heavily studied is the zwitterionic PMEDSAH, which has been reported to support long-term hPSC culture in a range of conditions but performs most consistently in combination with various CM (Villa-Diaz et al., 2010, Nandivada et al., 2011, Ross et al., 2012, Villa-Diaz et al., 2012). The carboxyl and sulphonyl groups in PMEDSAH have been suggested to mimic HSPGs and to act as a reservoir for growth factors including FGF-2; however this hypothesis has not been tested by surface characterisation (Brafman et al., 2010). The reported protein low-fouling properties of zwitterionic materials that has led to their application to implantable medical devices only further confounds possible mechanisms for PMEDSAH-hPSC interaction (Zhang et al., 2013a). Reports of PMEDSAH supporting hPSC attachment and culture suggest that PMEDSAH is not protein low-fouling and it will be treated as such for the remainder of this discussion. In serum-free chemically-defined media PMEDSAH can be an unreliable surface for hPSC culture and the ability of culture systems to maintain hPSCs depends on the media and cell-lines (Villa-Diaz et al., 2010). This inconsistency may be due to lower levels of certain proteins in defined media limiting the abundance of adsorbed ligands available for CAM binding. Culture results can be improved with pre-incubation of plates with FGF-2-supplemented (4 ng/mL) "human cell" CM (hCCM, GlobalStem®) and hCCM is also required during adaptation from MEF-based culture (Villa-Diaz et al., 2012). Other sulphonyl-containing polymers trialled as hPSC culture surfaces include PSS(S), poly(methyl vinyl ether-alt-maleic anhydride) (PMVE-alt-MA), poly(acrylamido-methyl-propane sulphonate) (PAMPS) and poly[3-sulphopropyl methacrylate] (Brafman et al., 2010, Villa-Diaz et al., 2010). PMVE-alt-MA has supported medium-term culture of several hPSC lines in a defined medium while PAMPS and PSS(S) enabled attachment but were unable to support hPSC culture beyond a few passages (Brafman et al., 2010). PSS(S) has also been integrated into a hPSC-supportive hydrogel which is discussed below (Chang et al., 2013). Bioactive polymers that do not contain

sulphonyl have been used to support hPSC culture when coated with ECMPs. Poly (lactic-co-glycolic acid) (PLGA) coated with subtype non-specific laminin has been reported to adhere hPSCs (Gao et al., 2010) while other bioactive polymers have been able to maintain teratoma-forming hPSCs in long-term culture when coated with either vitronectin or human serum (Mei et al., 2010, Lib et al., 2010). A recent study has reported a bioactive polymer substrate poly(*N*-(4-hydroxyphenyl)methacrylamide-co-hydroxyethylmethacrylate) that supported hPSC culture for five passages without containing or being coated with any obvious potential ligands (Celiz et al., 2015). Integrin-blocking experiments identified a role for αv and $\beta 1$ integrins in mediating hPSC adhesion and the authors admitted that non-specific protein adsorption was a likely contributor. Although bioactive polymers may provide adequate support for hPSC culture they cannot be used to study cell-surface interactions because the interactions are mediated by adsorbed proteins, which can vary between media-type and cell lines.

Protein low-fouling polymer scaffolds with covalently attached ligands, like the ones presented in this study, have not previously been reported to support hPSC culture. Polymer brushes are promising substrates for investigating cell-surface interactions because they can be used to present specific ligands at a controlled density and in specific orientations. Polymer chains can be terminally-modified with different peptides using a range of simple chemistries including “click” chemistries and the formation of amide bonds. These chemistries can be tailored to specific peptides and performed under biologically-relevant conditions, allowing the peptides to retain functionality (reviewed by Barbey et al., 2009). A low background of protein adsorption can be achieved by adjusting the density and length of the polymer chain “bristles” (Coad et al., 2012) while spacers of different molecular lengths ensure appropriate presentation of peptide ligands (Ameringer et al., 2012). Importantly, polymer scaffolds are optically transparent which allows for facile visual assessment of live cell cultures. Protein low-fouling polymer brushes could be developed into commercially viable culture surfaces for hPSC maintenance and also for novel differentiation protocols because radical polymerisation methods allow them to be inexpensively and consistently produced at scale. Further, polymer brushes can be applied to a range of materials including surfaces with complex geometries, which make them relevant to potential future applications including microcarrier suspension cultures, which are discussed below.

Table 1.3: Culture surface coating requirements and costing for the generation of 1 billion ($\times 10^9$) hPSCs. The surfaces, manufacturers, coating density sources and calculated costs are given. Extracellular matrix (ECM) extracts (Matrigel™ and Geltrex™) are compared to recombinant human ECM proteins (laminin-511, vitronectin, fibronectin) and synthetic surfaces (Corning Synthamax™ II-SC and StemAdhere™). Calculations were based on a typical cell density of 2×10^5 cells/cm². These calculations do not take into account requirements for media or plasticware or the implementation of differentiation protocols. It should also be noted that such protocols are not 100 % efficient, so it is likely that additional hPSCs would be required. Adapted from (Lambhead et al., 2013).

Surface	Manufacturer	Coating density source	Cost per cm ² (\$USD) ¹	Cost per 1 trillion cells (5000 cm ²) (\$USD)
Matrigel™	Becton Dickinson Cat No: 354277	Becton Dickinson handbook	\$0.080	\$400
Geltrex™	Invitrogen Cat No: A1413302	Life Technologies™ handbook	\$0.062	\$310
Recombinant human laminin-511 (whole protein)	Biolamina Cat No: LN511	(Domogatskaya et al., 2008) ²	\$10.7	\$53331
Recombinant human vitronectin (truncated protein)	Gibco™ Cat No: A14701SA	(Yap et al., 2011)	\$0.041 ³	\$205
Recombinant human fibronectin	Abcam Cat No: AB92798	(Kalaskar et al., 2013)	\$0.664	\$3320
Corning Synthemax™ II-SC	Corning Inc. Cat No: 3535XX1	Corning handbook	\$0.205	\$1026
StemAdhere™ (E-cadherin fusion protein)	Primorigen Biosciences™ Cat No: S2112	Primorigen handbook	\$0.081	\$406

¹ Prices were obtained from the websites of Australian suppliers of the manufacturers listed and converted from \$AUD to \$USD on the ninth of April 2013 (\$1AUD = 1.04\$USD).

² Only concentrations of ECMPs in solution were reported so a volume of 50 µl/cm² was used for calculations, based on recommendations for Matrigel™ coatings (Becton Dickinson).

³ At the time of writing recombinant vitronectin was being promoted in combination with the hPSC media E8 and as such was being sold at low cost.

1.9 Three dimensional (3D) hPSC culture systems

3D culture systems include hydrogels and suspension cultures and are of increasing interest to the field due to the economies of scale involved. These culture systems can produce superior expansion rates and yields to traditional two dimensional (2D) culture systems. While the more immediate applications for hPSCs are likely to be drug screening and disease modelling, which require fewer cells and could be approached with conventional 2D culture systems; clinical applications demand higher cell numbers and more stringently defined culture conditions for reasons of safety. Well-optimised 3D culture systems are therefore expected to be indispensable for generating the quality and quantity of cells required for clinical applications of hPSCs. For example, repair of a typical myocardial infarction has been estimated to require 1-2 billion ($\times 10^9$) cells (Jing et al., 2008). Standard two dimensional (2D) culture systems routinely produce cell densities of $\sim 2 \times 10^5$ cells/cm² such that 5 000-10 000 cm² of culture surface would be needed to generate enough cells to treat a single myocardial infarction (Want et al., 2012) (see Table 1.3 for costings). Conversely, suspension culture of hPSCs has been reported at culture densities of 6.1×10^6 cells/mL and producing a 20-fold expansion in 7 days compared to the 11.3-fold expansion for 2D culture (Bardy et al., 2013). In order to generate the requisite number of hPSCs to repair a single myocardial infarction using a multi-stage bioreactor system a much more manageable 200 mL culture volume would be needed (Abbasalizadeh et al., 2012).

1.9.1 Hydrogels

Hydrogels are 3D structures composed of cross-linked, hydrophilic, polymeric scaffolds which expand into an ECM-like gel state when exposed to water. Hydrogels have a wide range of potential uses in tissue engineering (reviewed by Collins and Birkinshaw, 2012). For cell culture thin hydrogels can be used as an effectively 2D culture substrate where the cells are only present on the surface, or thicker hydrogels can be used to encapsulate cells, allowing them to proliferate and migrate within the gel (Collins and Birkinshaw, 2012). Like their constituent polymers, hydrogels can be inherently bioactive or relatively inert. Hydrogels can be composed of multiple polymer chains which modify the physical properties of the gel or incorporate cell-binding motifs (Collins and Birkinshaw, 2012).

Hydrogels demonstrated to support long-term culture of hPSCs include hyaluronic acid- (Gerecht et al., 2007, Liu et al., 2012, Zhang et al., 2016) and polyacrylamide-based hydrogels (Brafman et al., 2009) as well as amino-propylmethacrylamide hydrogels (Irwin et al., 2011). These hydrogels interact with hPSCs through non-specific protein adsorption (Irwin et al., 2011, Gerecht et al., 2007), pre-coated ECMPs or peptide ligands (Brafman et al., 2009, Zhang et al., 2016) or combinations of the two (Liu et al., 2012). Hydrogels incorporating sulphonyl-containing polymer chains like PSS(S) and vinyl sulphone-modified PEG hydrogels (Jang et al., 2013) have been shown to support long-term culture of hPSCs, presumably by mimicking HSPGs (Chang et al., 2013).

Interestingly, hydrogels incorporating PMEDSAH failed to support hPSC adhesion, as did several other sulphonyl-containing hydrogels (Chang et al., 2013). With respect to hydrogels presenting specific cell-binding ligands, semi-interpenetrating polymer network hydrogels presenting an RGD-motif have been shown to enable hPSC-binding (Li et al., 2006). However these gels were also protein-fouling, used with MEF-CM and were not tested in longer-term culture (Li et al., 2006). A (meth)acrylate-based hydrogel modified to present vitronectin-derived RGD-containing peptides has become commercially available as the hPSC culture surface Corning Synthemax™ although the protein fouling properties of this hydrogel have not been published. A study using a polyacrylamide hydrogel modified with a vitronectin-derived HSPG-binding peptide demonstrated the first example of long-term self-renewal of hPSCs capable of *in vitro* differentiation into the three germ layers, cultured on protein low-fouling, peptide-presenting hydrogels with modifiable physical properties in defined medium (Musah et al., 2012). This provides an interesting tool for controlling self-renewal of hPSCs in a chemically-defined hydrogel culture system.

1.9.2 Suspension culture systems

Suspension culture systems involve either cell-adherent microcarriers (Chen et al., 2011a) or free-floating clumps of hPSCs (Abbasalizadeh et al., 2012) that are held in suspension by either shaking or stirred suspension bioreactors. The details of this area are beyond the scope of this review and have been well-reviewed elsewhere (Serra et al., 2012, O'Brien and Laslett, 2012) but the potential applications of these culture systems cannot be ignored. Briefly, current challenges for hPSC suspension culture systems include reducing shear forces, maintaining even cell distribution across microcarriers and passaging expanding cell aggregates (Serra et al., 2012). Due to the potential gains and economies of scale involved, all work on hPSC culture surfaces and CAM/ECMP interactions should be undertaken with fully-defined microcarrier-based suspension culture systems in mind. Protein coatings and polymer scaffolds can also be readily adapted to microcarrier-based suspension culture systems (Heng et al., 2012).

1.10 Comparisons of hPSCs cultured on different surfaces

Studies comparing defined surfaces have so far been focused on identifying culture conditions that were equally effective as MEF- or Matrigel™-based systems at reaching the fundamental goals of hPSC culture such as promoting cell adhesion and proliferation and expression of key pluripotency markers (Hakala et al., 2009, Brafman et al., 2009, Meng et al., 2012). These studies used different combinations of surfaces and media without performing comprehensive cross-comparisons (Hakala et al., 2009), were more focused on optimising culture media (Akopian et al., 2010) and/or did not characterise and compare the cells at a high level of detail. Many of these studies also used whole ECMPs with multiple binding sites so they were unable to investigate the

role of CAMs in maintaining pluripotency, and little characterisation of surface properties was performed. Recent studies have included more detailed characterisation of hPSCs as they are cultured in various complex, undefined culture systems and have identified genetic and epigenetic changes that take place during adaptation to changes in culture conditions (Ramos-Mejia et al., 2012, Tompkins et al., 2012, Garitaonandia et al., 2015). While the phenotypic changes were fairly minor and their causes and/or effects unclear, greater molecular variation could be expected between the products of chemically-defined culture systems. It is therefore important that both cell and surface are characterised thoroughly during development of culture systems. Now that a range of defined culture surfaces have been reported to support maintenance of hPSCs to a level equivalent to Matrigel™ by the minimum criteria and that the ligands involved have been identified, this thesis has aimed to compare the resulting cells in more detail and to optimise surfaces for hPSC culture systems by taking into consideration the importance of CAM-mediated interactions, of physicochemical surface properties and of cost.

1.11 Conclusions

Pluripotency is a complex state maintained *in vitro* by molecular signals received from the cellular microenvironment, including the cell culture surface. The most commonly used hPSC culture surfaces are composed of complex animal products presenting poorly-defined ligands that interact with many CAMs on the cell surface and transmit pluripotency-supporting molecular signals to the nucleus (Kim et al., 2011, Li et al., 2012, Shen et al., 2012). hPSC culture surfaces have evolved from xenogeneic feeder cell layers with complex cell-surface interactions and no potential for use at scale to purified human recombinant ECMPs including laminin, fibronectin, vitronectin and HSPGs. Such ECMP-coated surfaces are xeno-free and interact with hPSCs through smaller sets of CAM/ligand interactions that are ECMP-specific, however production of recombinant proteins is expensive. Furthermore, synthetic surfaces based on the functional subunits of ECMPs are under development and these surfaces have been reported to maintain pluripotency through more specific interactions (Table 1.4). Defined surfaces thought to specifically interact with hPSCs through different ligands appear to be equally supportive of culture, although direct and detailed comparisons between hPSCs maintained on synthetic surfaces have not been performed. Identifying the importance of specific ligands in maintaining hPSC cultures and benchmarking against existing synthetic culture surfaces are important steps towards developing defined, affordable, xeno-free culture conditions that are suitable for clinically relevant large scale hPSC culture.

Table 1.4: Ligand-CAM interactions reported to support long-term hPSC culture. Surfaces are arranged according to their substrate. The ligands or extracellular matrix proteins (ECMPs) that are presented from those substrates and the CAMs with which they have been shown to interact (if any) are also listed. Whole ECMPs, ECMP fragments, fusion proteins, and peptides presented by amine-modified or acrylate monomer coated TCPS, protein-fouling hydrogels and polymers have all demonstrated the capacity to support hPSC culture by interacting with various integrins, E-cadherins and/or heparan sulphate proteoglycans. The surfaces listed have all been reported to support hPSC culture subject to at least the minimum cell characterisation requirements outlined in Table 1.1. Key references have been provided for each surface. Adapted from (Lambshead et al., 2013).

Substrates	Ligands or ECMPs	CAM(s)	References
Tissue culture polystyrene (TCPS)	Vitronectin Laminin-511 Laminin E8 fragments Fibronectin Collagen+fibronectin+laminin +vitronectin poly(L-lysine) E-cadherin-IgG1Fc (StemAdhere™)	α V β 3/5 integrins, GAGs α 6 β 1 integrin - α 5 β 1 integrin - - E-cadherin)	(Braam et al., 2008) (Rodin et al., 2010) (Miyazaki et al., 2012) (Baxter et al., 2009) (Ludwig et al., 2006b) (Harb et al., 2008) (Nagaoka et al., 2010)
Amine-modified TCPS	Cyclic-CRGDC	-	(Kolhar et al., 2010)
UV-treated TCPS	Adsorbed serum proteins, vitronectin	-	(Saha et al., 2011)
Acrylate monomer-coated TCPS	KGGNGEPRGDTYRAY (Corning Synthemax™) KGGPQVTRGDTVFTMP Vitronectin	α V β 5 integrins - α V β 3/5 integrins, GAGs	(Melkounian et al., 2010) (Melkounian et al., 2010) (Mei et al., 2010)
Self-assembled monolayers	GKKQRFHRNRKG LTTAPKLPKVTR	HSPGs GAGs	(Klim et al., 2012) (Derda et al., 2010)
Amino-propylmethacrylamide hydrogels	BSA + non-specific proteins (adsorbed from media)	-	(Irwin et al., 2011)
Polyacrylamide hydrogel	GKKQRFHRNRKG	HSPGs	(Musah et al., 2012)
PMEDSAH	Unknown. Adsorbed growth factors?	-	(Ross et al., 2012)

1.12 Hypothesis and Project Aims

Hypothesis: That novel, peptide-modified acrylamide-based polymer brush coatings can be optimised into cost-effective and efficient hPSC culture surfaces

Aim 1: Identify and optimise affordable, scalable peptide-presenting polymer coatings for hPSC culture

Aim 2: Assess the response of hPSCs to surfaces modified with peptide ligands that interact with different CAMs

Aim 3: Benchmark novel hPSC culture coatings against commercially available alternatives

Chapter 2:

General materials and methods

2.1 Introduction

This chapter presents general methods relevant to the work presented in at least two of the three results chapters in this thesis. The methods described herein are focused on cell culture and quantification, and on the synthesis of peptide-modified polymer brush coatings. Additionally, chapter-specific methods sections are included in Chapters 3, 4 and 5. Unless otherwise stated, cell culture reagents were supplied by Life Technologies (Carlsbad, CA), laboratory reagents were of analytical grade and supplied by Sigma Aldrich (St Louis, MO). Solutions were sterilised as required, either by autoclaving or by filtration through a Stericup™ 0.22 µm filter unit (Millipore, Bedford, MA, Cat No.: SCGPU10RE). Supplier locations are provided with the first reference made to each company.

2.2 Human pluripotent stem cell lines

The hESC-WA09 (H9) (Thomson et al., 1998), hESC-GENEA-02 (Briggs et al., 2013) and NHF-iPSC-1-3 (Bradley et al., 2010) cell lines were respectively provided under materials transfer agreements by the Wisconsin Alumni Research Foundation (WARF) and Genea, and kindly by Prof. Ernst Wolvetang (Australian Institute for Bioengineering & Nanotechnology).

The H9-OCT4-mCherry cell line was kindly provided by Profs. Edouard Stanley and Andrew Elefanty (Murdoch Children's Research Institute, Melbourne, Australia) to streamline the assessment of novel hPSC culture surfaces. This cell line enabled rapid assessment of live hPSC cultures for the classical pluripotency marker OCT4 without any need for staining. Flow cytometric validation of the H9-OCT4-mCherry reported cell line was performed by Joshua Kie (Appendix 1.1).

All work using human pluripotent stem cells was carried out in accordance with approvals from Monash University and the CSIRO Human Research Ethics Offices.

2.3 Methods for hPSC culture

Cell cultures were maintained at 37 °C in an atmosphere containing 5 % CO₂ in either a SANYO CO₂ incubator (VWR International, Radnor, PA, Cat No: MCO-19AIC) or a Steri-cycle™ CO₂ incubator (Thermo Fisher Scientific, Waltham, MA, Cat No: 371). Cultures were handled under aseptic conditions in Aura-2000 M.A.C. Class II Biosafety cabinets (LAF technologies, Bayswater North, Australia, Cat No: LD50100). Unless otherwise specified, all solutions were prepared in Dulbecco's phosphate buffered saline that was prepared in house without calcium or magnesium (DPBS-; see Appendix 2.1 for details), and were centrifuged in a 5810 centrifuge (Eppendorf, North Ryde, Australia). E8 medium (Cat No: A15170-01) is the first serum albumin-free hPSC culture medium (Chen et al., 2011b). As the most chemically complex of the recommended surfaces for hPSC culture with E8, Geltrex™ (Cat No: A1413302) coatings were chosen as the positive control surface, and EDTA was used for cell dissociation as recommended for use with E8 medium by the manufacturer.

2.3.1 Working with Geltrex™

Geltrex™ is a complex derivative of Engelbreth-Holm-Swarm sarcoma that contains a mixture of ECMs. As Geltrex™ thaws it passes through a liquid phase and then gels at 37 °C.

1. Geltrex™ was thawed on ice, diluted 1:1 in DMEM/F12 medium (Cat No: 10565) and split into aliquots that were stored in Axygen® 1.7 mL MaxyClear™ Snaplock Microcentrifuge Tubes (Corning Inc., NY, Cat No: MCT-175-C) at -20 °C.
2. Geltrex™ : DMEM/F12 (1:1) aliquots were thawed at 4 °C and further diluted 1:100 in pre-chilled DMEM/F12, for a final dilution of 1:200.
3. Nunclon™ 24-well cell culture plates (Thermo Fisher Scientific, Cat No: 142475) or Corning 25 cm² cell culture flasks with Plug Seal Cap (Sigma Aldrich: CLS430168) were respectively coated with 0.4 mL/well or 4 mL/flask of diluted Geltrex™ and incubated at 37 °C in 5 % CO₂ for no less than one hour. Vessels were used immediately or sealed in parafilm® (Sigma Aldrich, Cat No: P7543) and stored at 4 °C for less than two weeks.
4. Upon removal from storage, vessels were incubated at 37 °C in 5 % CO₂ for no less than 30 minutes prior to use. Excess Geltrex™ was carefully aspirated before culture medium was added to each vessel (24-well plate, 800 µL/well; 25 cm² flask, 5 mL).

2.3.2 EDTA harvesting method for hPSCs

hPSCs were passaged according to the method described in the Life Technologies Handbook “Culturing Pluripotent Stem Cells (PSCs) in Essential 8™ Medium (Prototype)” (Publication Part Number: MAN0007035, Revision Date: 22 August 2012), which is summarised below. All solutions were added to the flask at room temperature.

1. hPSC cultures were washed twice in DPBS- and then incubated for up to 3 minutes in UltraPure™ EDTA (Cat No: 15575-020), which had been diluted to 0.5 mM in DPBS-.
2. The EDTA solution was aspirated and E8 medium was pipetted across the surface to gather the cells into a suspension of small clumps. When hPSCs did not lift during this pipetting they were gently removed from the surface with a cell scraper (Interpath Services, Heidelberg West, Australia, Cat No: 541070).
3. If a high proportion of cells dissociated from the surface before the EDTA solution was removed, then E8 medium was added to the vessel and cells were pelleted in the EDTA/E8 solution at 453 g for 2 minutes and then resuspended in E8 medium.
4. If required, cell counts were performed as described in Section 2.4.1.
5. New vessels containing fresh E8 medium (96-well plate, 100 µL/well; 24-well plate, 400 µL/well; 25 cm² flask, 4 mL) were seeded with hPSCs suspended in E8 to the density required (5000-25 000 cells/cm²).

2.3.3 Cryopreservation of hPSCs

hPSCs were harvested with EDTA as described in Section 2.3.2. Harvested cells were spun down at 453 g for 3 minutes, resuspended in ice-cold cryopreservation medium [(E8 medium containing 10 % Dimethyl sulphoxide Hybri-Max™ (DMSO; Sigma Aldrich, Cat No: D2650)], transferred to a 2 mL cryovial (Interpath Services, Cat No: 121263) and slow-frozen in a Mr Frosty™ Freezing Container (Thermo Fisher Scientific, Cat No: 5100-0001) at -80 °C before transfer to liquid nitrogen storage.

2.3.4 Thawing cryopreserved hPSCs

Vials of cryopreserved hPSCs were removed from liquid nitrogen storage and transferred directly to a water bath maintained at 37 °C. When only a sliver of ice remained, the thawing tube was removed from the water bath and the contents were transferred to a sterile 15 mL tube (In Vitro Technology, Cat No: FAL352096) containing 9 mL of E8 medium at room temperature (RT). Cells were pelleted at 200 g for 3 minutes, resuspended in 1 mL of E8 medium and seeded into a 25 cm² flask that was coated with a hPSC culture surface and contained an additional 4 mL of E8 medium at RT. Flasks were gently shaken in 2D to distribute the cells evenly and then transferred to an incubator and left undisturbed for at least 24 hours.

2.4 Monitoring cellular proliferation

hPSCs that had been harvested as single cells or small clumps were counted using a hemocytometer. When hPSCs were expected to seed at a low density or a non-destructive assay was required, quantification was performed by counting colonies. Cell quantification for higher density hPSC cultures was performed using a colorimetric MTS cell proliferation assay (Section 2.4.3), which is considered to be more accurate but required termination of the assayed cultures.

2.4.1 Cell counting with a hemocytometer

Aliquots of resuspended cells were added to an equal volume of filtered 0.4 % Trypan Blue (Sigma Aldrich, Cat No: T8154). Stained cells were transferred to the counting chambers of a Neubauer Improved Hemocytometer (GrayMed, Melbourne Australia, Cat No: CTL-HEMM-GLDR). Live (L, white) and dead (D, blue) cell numbers were counted up to a total (T, L+D=T) of at least 100 cells from at least two 1 mm² hemocytometer grids (x). The number (n) of live cells per mL was calculated with the following equation $[n = (L \cdot 10^5)/x]$ and % viability was calculated as $L/T \cdot 100$. Although this method is more reliable when working with single cells, individual cells were counted from small cell clumps.

2.4.2 Colony counting approach to cell quantification

Whole-well images were captured by scanning wells at 40x magnification with a Nikon Ti Eclipse microscope equipped with a CoolSnap HQ2 camera (Photometrics, Tuscon, AZ) and attached to a motorised stage and a computer running Metamorph® image analysis software Version 7.7.8.0. Images were captured using both phase contrast and mCherry fluorescence imaging. The mCherry fluorescence was filtered through a Brightline® single-band filter set (excitation: ~540 nm – 590 nm; emission: ~600 nm – 680 nm; Semrock, Inc., Rochester, NY, Cat No: mCherry-B-000). Sixty-three (7x9) images were sufficient to scan each well of a 24-well plate using the “Scan Slide” module on Metamorph®, however colonies were only counted from the central 31 images to avoid edge effects (See Figure 2.1). Colony counting was facilitated by the “Manually Count Objects” module in the Metamorph® software.

2.4.3 MTS cell proliferation assay

The MTS cell proliferation assay is a colourimetric assay based on the reduction of 3-(4,5-dimethylthiazol-2-yl)-5(3-carboxymethoxyphenyl)-2-(4-sulphophenyl)-2H-tetrazolium (MTS) by metabolically active cells to a fluorescent formazan product. The fluorescence intensity of the formazan product is quantified and correlates with the cell density.

Stock solutions containing 2 mg/mL MTS (Promega, Madison, WI, Cat No: G111) or 0.92 mg/mL phenazine methosulphate (PMS) (Sigma, Cat No: P9625) in DPBS-were filter-sterilised, stored at -20 °C and handled in the dark wherever possible.

MTS reaction solution was prepared by adding 2 mL of MTS stock and 100 µL of PMS stock to 10 mL of E8 medium. Cells cultured in 24-well plates were incubated in 300 µL/well MTS reaction solution for 2-4 hours. The resultant formazan product was detected at 490 nm by a BioTek™ PowerWave™ HT Microplate Spectrophotometer (Fisher Scientific, Cat No: BT-RPRWI) connected to a PC running BioTek™ KC4™ Software v3.2. Means and standard deviations were calculated for each sample and control.

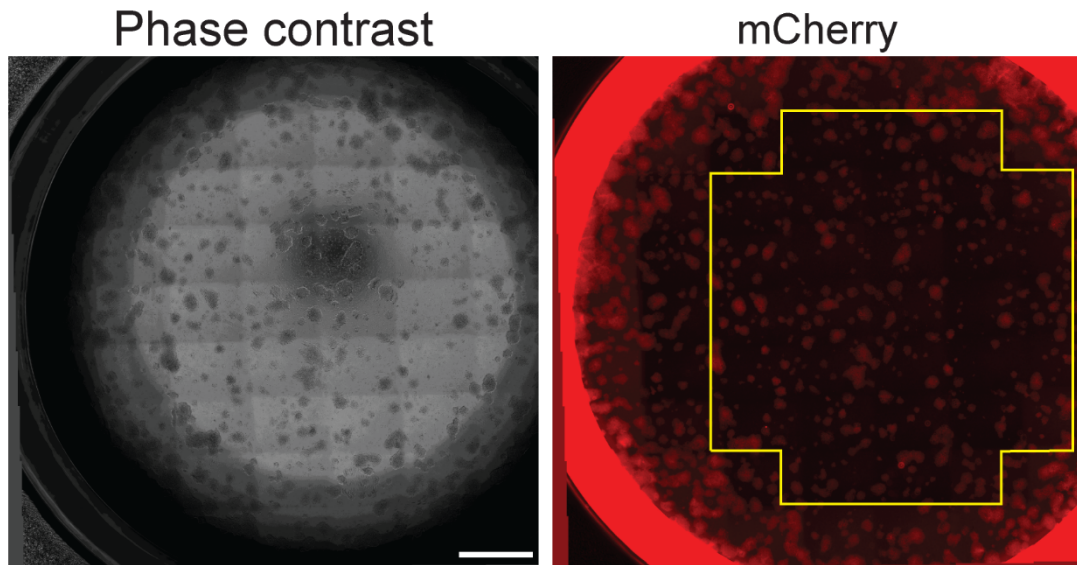


Figure 2.1: This figure presents a typical well scan from a 24-well plate, which was used for colony counting. A series of 40x images were captured, and then stitched together using Metamorph software. The connections between adjacent images can be seen as a faint grid across the well. The region from which colonies were counted is outlined in yellow on the mCherry scan and contains the 31 central fields of view, forming a 5x6 square with three additional fields of view in the centre along the top and bottom. This image is of a cRGDfK-PAPA-coated well four days post seeding with H9-OCT4-mCherry hPSCs at a density of 15 000 cells/cm². Scale bar represents 2 mm.

2.5 Methods for production of polymer brush coatings

All reactions were performed at room temperature in aqueous solutions prepared with Type 1 water from a Milli-Q® Synthesis Water Purification System (MQ H₂O, Merck Millipore, Bayswater, Australia, Cat No: ZMQS6VFT1) unless otherwise stated.

2.5.1 UV-initiated polymer-coating of tissue culture vessels

Protein low-fouling acrylamide (Cat No: 675415)-based brush polymer coatings were grafted from tissue culture-treated 25 cm² flasks or 24-well plates in a process involving repeated exposure to high intensity UV light under oxygen-free conditions. This process can be applied to surfaces of various geometries and using a range of monomers, as long as at least one ethylenically unsaturated monomer is included. Acrylic acid and propargyl acrylamide were used as co-monomers. Acrylic acid (Cat No: 147230) was purified by short-path distillation to remove dimers and inhibitors, and then stored at -20°C until use. Propargyl acrylamide was prepared at the Manufacturing Business Unit of CSIRO (Clayton, Australia) by Dr. Andrew Riches according to a published approach (Malkoch et al., 2005). The nomenclature “peptide-polymer abbreviation-number of exposures to UV light that were used to generate coating” is used throughout this document to describe peptide-modified polymer coatings. For example poly(acrylamide-co-acrylic acid) (PAAA) coatings that were generated with 25 exposures to UV light and then modified with cRGDfK peptide (Appendix 3.1, Peptides International, Louisville, KY, Cat No: PCI-3661-PI) are referred to as “cRGDfK-PAAA-25UV”, and poly(acrylamide-co-propargyl acrylamide) (PAPA) coatings that were generated with 40 exposures to UV light and then modified with cRGDfK-N3 (Peptides International, Cat No: RGD-3749-PI) peptide are referred to as “cRGDfK-PAPA-40UV”.

1. Monomers were weighed out and transferred along with all required consumables into a nitrogen-purged glove-box [constructed at the Manufacturing Business Unit of CSIRO (Clayton, Australia)].
2. Acrylamide and either acrylic acid or propargyl acrylamide were dissolved in nitrogen-purged MQ H₂O to final concentrations of 75 g/L when preparing PAAA coatings, or 100 g/L when preparing PAPA coatings. Monomer solutions were mixed at the desired molar ratios and transferred to vessels for coating (24-well plate, 272 µL/well; 25 cm² flask, 4 mL/flask). To protect the monomer solutions from atmospheric oxygen, tissue culture plates with lids removed were vacuum-sealed into Sunbeam FoodSaver bags (Cat No: VS0420) and flasks were tightly sealed with plug caps. Bagged plates should have an evacuated appearance.
3. To induce polymerisation, airtight vessels containing mixed monomer solutions were placed on a Fusion UV DRS10/12 Conveyor System (Alpha UV Systems, Pymble, Australia) set at speed level 8, and carried through the beam of a Light Hammer® 6 D-bulb lamp (Alpha UV Systems, Model I6B, Part LH6, serial no 21159) running at 70 % power. The lamp-to-belt distance was 63 mm. After each exposure, vessels were

manually transported back to the start of the belt and rotated 180° to ensure even exposure. Plates were placed directly on the conveyor belt, while flasks were placed onto steel trays, which were pre-wrapped in aluminium foil (Officeworks, Bentleigh East, Australia, Cat No DA510182) to prevent over-heating. This made it possible to handle large numbers of flasks.

4. Following UV treatment, polymer-coated vessels were opened or unwrapped and were washed immediately and vigorously in MQ H₂O until clean to the eye. At this stage, vessels were discarded if there was any evidence of atmospheric contamination. The heat imparted by exposure to UV light generated pressure that slightly inflated the FoodSaver bags in which plates were held, and resulted in a “hiss” sound when flasks were opened. If these phenomena were not observed then the monomer-containing vessels were discarded.
5. Vessels were soaked for three days in a large volume of MQ H₂O that was changed daily, dried overnight in a fume hood and then sterilised either by exposure to 15 kGy of gamma irradiation (Steritech, Dandenong, Australia) or by treatment with Antibiotic-Antimycotic solution (Cat No: 15240-062) diluted 1:50 in DPBS-.

2.5.2 EDC/NHS-mediated peptide modification of PAAA-coated surfaces

Exposure to a solution of 1-Ethyl-3-(3-dimethylaminopropyl)carbodiimide (EDC; Cat No: E7750) activates the carboxyl groups of acrylic acid residues, and the addition of N-Hydroxysuccinimide (NHS; Cat No: 56480) improves the reaction efficiency (Wang et al., 2011) (Figure 2.2). Activated plates react with peptide-containing solutions, creating a bond between peptide amine moieties and the activated carboxyl groups in the PAAA coating. N-terminal anchoring of most peptides to PAAA-coated surfaces is therefore possible without any prior chemical modification of the peptides. However EDC/NHS-coupling is unsuitable for ligation of lysine-containing peptides, since lysine side chains contain amine groups, which compete with the N-terminal amine for binding (Figure 2.2).

1. A freshly-prepared aqueous solution containing 125 mM EDC and 125 mM NHS was immediately filter-sterilised and was applied to polymer-coated surfaces for 30-minutes (24-well plate, 272 µL/well; 25 cm² flask, 4 mL/flask).
2. Activated polymer coatings were washed twice with DPBS- and incubated for 20 hours under 200 µL/cm² of sterile peptide solutions in DPBS-.
3. Peptide-conjugated surfaces were washed twice with DPBS-, deactivated with an equal volume of 1 M NaOH (Merck Millipore, Cat No: 7231578) for 30 minutes at 37 °C and washed 10 times in DPBS- for 10 minutes per wash. If vessels were not used immediately, they were stored in DPBS- + 1 % penicillin and streptomycin (Cat No: 15070-063) at 4 °C until use. Vessels were stored for no more than one month.

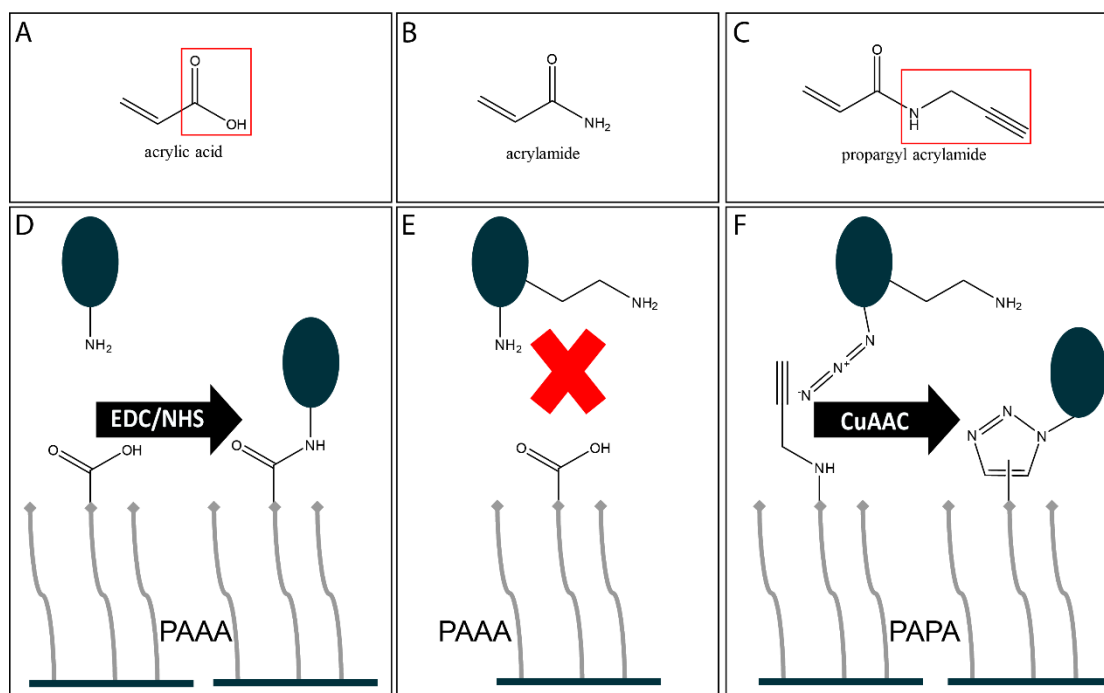


Figure 2.2 Schematic diagrams of the chemistries involved in peptide modification of PAAA and PAPA-coated TCPS. Molecular structures are presented for the monomers (A) acrylic acid, (B) acrylamide and (C) propargyl acrylamide. The functional groups available for peptide binding to acrylic acid (carboxyl group) and propargyl acrylamide (alkyne) are surrounded by red rectangles. (D) A schematic diagram illustrating NHS/EDC-mediated carbodiimide attachment of peptide (navy blue ovals) via N-terminal amines to the carboxyl groups contributed from acrylic acid residues in PAAA coatings. (E) Lysine containing peptides present additional carboxyl groups which can form undesired side-reactions when coupled to PAAA coatings. (F) PAPA coatings are specifically modified with azide-conjugated lysine-containing peptides by Cu(I)-catalysed azide/alkyne Huisgen cycloaddition (CuAAC) reactions.

2.5.3 Copper-catalysed peptide modification of PAPA-coated surfaces

Since EDC/NHS conjugation was inappropriate for lysine-containing peptides, these peptides were N-terminally azide-functionalised (Figure 2.2). Azide-coupled peptides could be anchored to PAPA-coated surfaces by a copper-catalysed “click” azide-alkyne Huisgen cycloaddition (CuAAC) reaction (Figure 2.2) (Meldal, 2008). CuAAC reaction conditions were based on a highly cited review by Hong et al. (2009).

1. The CuAAC reaction solution was prepared in atmospheric conditions and typically comprised 100 μM copper sulphate pentahydrate (VWR International, 10091.4Q), 272 μM sodium ascorbate (Cat No: A4034) and 0.25 μM – 300 μM azide-conjugated peptide in 1 M HEPES buffer (Thermo Fisher Scientific, Cat No: 15630080). The optimisation of these reaction conditions is discussed in Chapters 3 and 4.
2. Filter-sterilised CuAAC reaction solution was added to each vessel (24-well plate, 400 μL /well; 25 cm^2 flask, 4 mL/flask). Culture plates were wrapped in parafilm and sealed in airtight plastic. For flasks, the plug seal caps were tightly sealed to restrict oxygen exposure and minimise oxidation of the catalytic Cu(I). The reaction proceeded for 24 hours on a rocker at 20 rpm (for 25 cm^2 flasks) or on an orbital shaker at 100 rpm (for 24-well plates).
3. Peptide-modified surfaces were washed thoroughly in sterile MQ H_2O , incubated overnight in 0.1 M Na_2EDTA (VWR International, Cat No: 10093.5V) and again thoroughly washed in DPBS-. Peptide modified surfaces were stored until use at 4 $^\circ\text{C}$ under DPBS- + 1 % penicillin and streptomycin, typically for no longer than three months.

Chapter 3:

Optimising peptide-modified polymer brush coatings for hPSC culture

3.1 Introduction

The development and regulation of therapeutic applications of hPSCs will benefit directly from the widespread use of affordable, chemically-defined, xeno-free hPSC culture systems. Despite the potential benefits associated with using synthetic culture surfaces, hPSC cultures are typically maintained on coatings of animal-derived materials such as Matrigel™, Geltrex™ or vitronectin. Although several chemically defined, xeno-free hPSC culture surfaces have been reported to maintain hPSC cultures in various media (Melkounian and Brandenberger, 2011, Nagaoka et al., 2010) and are commercially available, they have not been adopted by the broader stem cell community. The reasons behind this lack of uptake are unclear, but include expense, inertia and lot-to-lot variation. A novel approach has been developed at CSIRO for synthesising polymer brush coatings, which can be used as cell culture surfaces after modification with small peptide ligands (Ameringer et al., 2014). Polymer brushes graft from the surface of the vessel when mixed monomer solutions are repeatedly exposed to high intensity UV light in the absence of any photoinitiator compounds or contaminating atmospheric oxygen. The polymer brush coatings are cheap to produce and easily scalable, they can be applied to both 2D and 3D substrates and are stably, covalently bonded to the underlying TCPS. The coatings can be synthesised from a wide range of monomers, as long as at least one ethylenically unsaturated monomer is included. For the present study, acrylamide was copolymerised with either acrylic acid or propargyl acrylamide co-monomers to produce PAAA and PAPA coatings respectively. High molar proportions of acrylamide in the monomer feed solution resulted in low non-specific protein adsorbing surfaces in which cell-surface interactions were restricted and the inclusion of acrylic acid or propargyl acrylamide residues contributed functional groups that enabled chemical modification of the surface with peptide ligands for cell adhesion. Prior to the current study, human mesenchymal stem cell (hMSC) cultures had been maintained on PAAA coatings modified with the integrin-binding cRGDFK peptide (unpublished results; WO2014000052-A1), but the ability of peptide-presenting PAAA and PAPA coatings to support hPSC cultures had not been tested. As illustrated in Figure 3.1, this chapter outlines the optimisation and characterisation of cRGDFK-presenting PAAA (cRGDFK-PAAA) and PAPA (cRGDFK-PAPA) coatings for hPSC adhesion in E8 medium. Optimisation included altering the monomer ratio and the number of UV exposures used to generate the coatings as well as altering the concentration of peptide in modification reaction solutions. Chapter 4 reports on the use of PAAA and PAPA coatings to screen a library of peptides for their ability to support adhesion and short-term maintenance of hPSCs. In Chapter 5 an experiment is then described in which hPSC cultures were maintained long-term in E8 medium on lead polymer coatings and were benchmarked against cultures maintained in parallel on commercially available alternative surfaces.

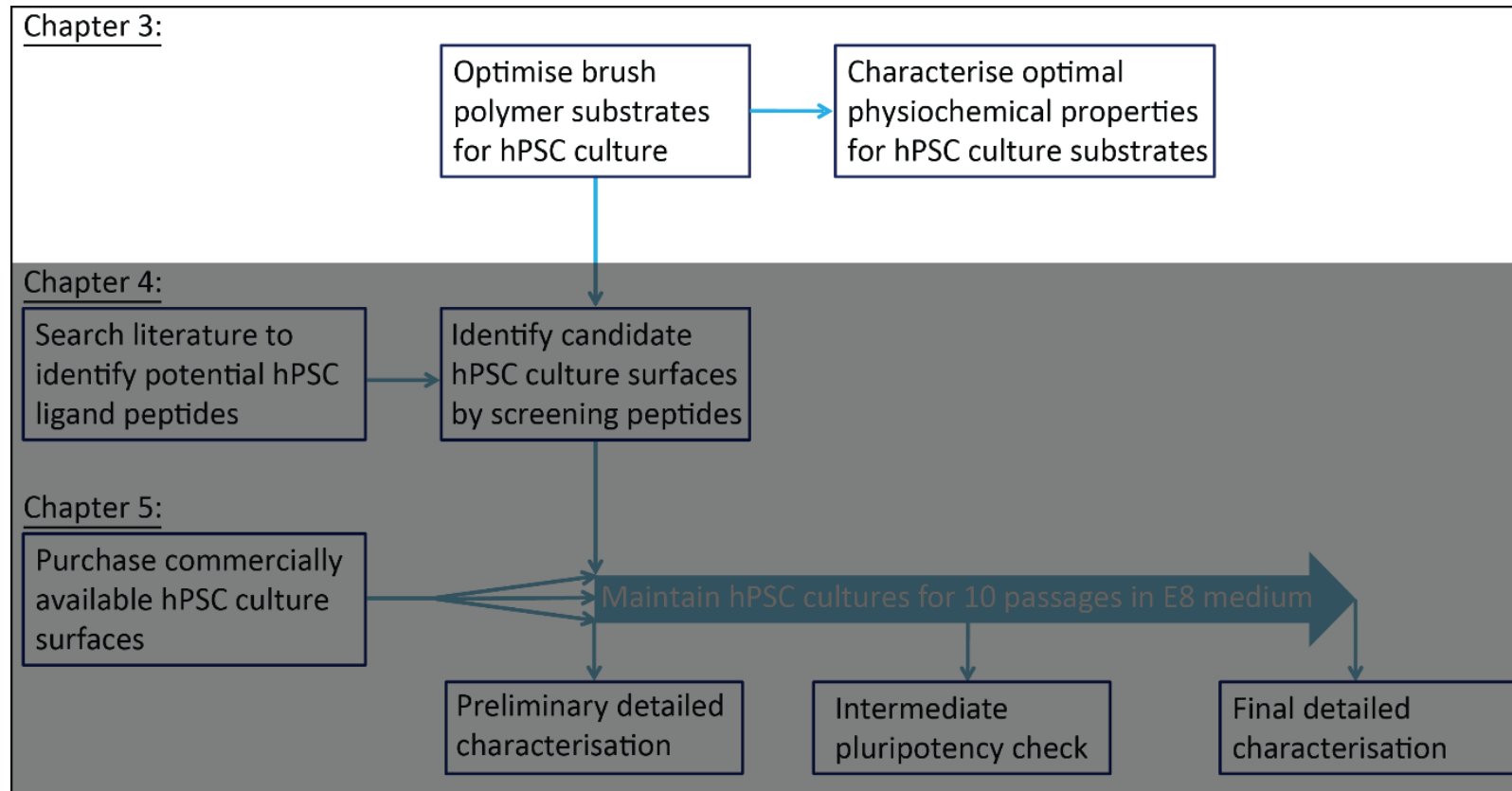


Figure 3.1: The overall project outline is presented and the outline of the present chapter is highlighted. In this chapter the characterisation and optimisation of peptide-presenting polymer brush coatings as hPSC culture surfaces was performed. The coatings were here optimised for hPSC adhesion so that lead peptide ligand(s) could be identified from a screening process (Chapter 4) from which a culture surface could be generated on which hPSC cultures could be maintained long-term and benchmarked against commercially available surfaces (Chapter 5).

3.2 Chapter specific methods

3.2.1 Cell quantification

During early optimisation experiments, the colony counting approach outlined in Section 2.4.2 was used to roughly quantify adherent hPSCs. When greater numbers of bound hPSCs were observed, the colony counting approach became inaccurate and MTS assays (Section 2.4.3) were used to more accurately quantify the higher cell numbers.

3.2.2 Sample preparation for surface analysis

PAAA and PAPA coatings were prepared as described in Section 2.5.1. To prepare polymer-coated TCPS surfaces for physicochemical analyses, circular samples were cut out of the floor of vessels. A bench drilling machine Model HM10, motor type 95 D-1 (Hafco, Northmead, Australia) fitted with an 8 mm hollow tool was used to cut samples for X-ray photoelectron spectroscopy (XPS) analysis, and a 12 mm hollow tool was used to cut samples for AFM analysis. The perimeters of newly cut samples were carefully trimmed of excess burrs and then samples were blown dry with a stream of sterile nitrogen gas. Care was taken to not touch the sample surface at any point during this process.

3.2.3 X-ray photoelectron spectroscopy surface analysis

XPS is a surface-sensitive method that is commonly used to quantify the elemental composition of materials. The sample material is irradiated under ultra-high vacuum conditions by a focused, monochromated X-ray beam, and the binding energy is recorded for each core electron ejected from atoms near the material surface (Hollander and Jolly, 1970). Binding energies are empirically determined values that are specific for each chemical species, and electrons are exponentially less likely to escape from deeper into the material. So quantifying the binding energies of released electrons produces chemical “fingerprints” for each species and this information permits qualitative and quantitative elemental analysis of materials, with sampling weighted exponentially towards the surface. Any hydrogen atom involved in a covalent bond does not possess a free core electron and is therefore undetectable by XPS.

XPS analysis was performed by Prof. Laurence Meagher and Dr. Christopher Easton at the Manufacturing Business Unit of CSIRO (Clayton, Australia) using either an AXIS Ultra DLD spectrometer or an AXIS Nova spectrometer (Kratos Analytical Inc., Manchester, UK). Both instruments use a monochromated Al K α source at a power of 180 W (15 kV \times 12 mA), a hemispherical analyser operating in the fixed analyser transmission mode, and the standard aperture (analysis area: 0.3 mm \times 0.7 mm). The total pressure in the main vacuum chamber during analysis was typically between 10⁻⁹ and 10⁻⁸ mbar. Survey spectra were acquired at a pass energy of 160 eV.

To obtain more detailed information about chemical structure, oxidation states *etc.*, high resolution spectra were recorded in a binding energy window corresponding to the position of carbon peaks at 40 eV pass energy (yielding a peak width that is typical for polymers of ~1.0 eV).

Each specimen was analysed at an emission angle of 0° as measured from the surface normal. Assuming typical values for the electron attenuation length of relevant photoelectrons the XPS analysis depth (from which 95 % of the detected signal originates) ranges between 5 nm and 10 nm for a flat surface.

Data processing was performed using CasaXPS processing software version 2.3.16 (Casa Software Ltd., Teignmouth, UK). All elements present were identified from survey spectra. Binding energies were referenced to the aliphatic hydrocarbon peak at 285.0 eV or to the aromatic hydrocarbon peak at 284.7 eV. The atomic concentrations of the elements detected were calculated using integral peak intensities and the sensitivity factors supplied by the instrument manufacturer.

C 1s spectra were fitted using a Gaussian (70 %) - Lorentzian (30 %) model with residuals for curve fits minimised with multiple iterations using simplex algorithms. C1 was assigned to C-C and C-H (binding energy = 285 eV for PAAA- and PAPA-coated surfaces and 284.7 eV for TCPS), C2 was assigned to secondary shifted aliphatic carbons including from C4 and C5 (binding energy = C1 + 0.5 eV), C3 was assigned to C-N and C-O (unconstrained), C4 was assigned to N-C=O and O-C-O (unconstrained) and C5 to carboxyls O-C=O. For PAAA and PAPA coated flasks, C6 was assigned to aromatic carbons. For the TCPS control surfaces C6, C7 and C8 were all assigned to aromatic carbons.

The accuracy associated with quantitative XPS is approximately 10 % - 15 %. Precision (i.e. reproducibility) depends on the signal/noise ratio but is usually much better than 5 %. The latter is relevant when comparing similar samples.

3.2.3.1 Conversion of XPS data to surface thickness

The approximate thickness of polymer coatings was calculated by applying equation [1] (Tielsch and Fulghum, 1994) to the atomic concentrations of nitrogen of each coating detected via XPS analysis.

$$d_o = -\lambda_o \times \ln\left(1 - \frac{I_o}{I_o^\infty}\right) \quad : [1]$$

The use of equation [1] allows the thickness (d_o , nm) of a coating to be derived from the atomic concentration of specific elements detected in XPS spectra (I_o). The equation was applied to nitrogen atomic % data in this case, because N was expected to be unique to the polymer coating and not present in the underlying TCPS. Data were also obtained using O atomic % data but the results of calculations carried out using this data would be expected to be less informative on polymer coating thickness since O was also present in the underlying TCPS. The theoretical maximal atomic concentrations from infinitely thick coatings (I_o^∞) were calculated using theoretical polymer chain composition, based on the relative molar percentages of each monomer in the monomer feed solution of the coating. For these calculations, the assumption was made that the monomers were present in the coatings at molar percentages identical to those present in the monomer feed solution. Detailed analysis of similar coatings (unpublished data) has shown this to be a reasonable assumption. Equation [1] compares the detected atomic concentrations to the theoretical maxima and accounts for the

attenuation length (λ_e , aka. inelastic mean free path; IMFP) of ejected photoelectrons (Appendix 4.1). Attenuation lengths are empirical constants that are specific to each element and represent the depth from which electrons ejected from atoms of that element are able to escape from the surface of a solid material and be detected (Tanuma et al., 1993). These constants dictate the detection limit of the XPS method for each element and therefore restrict the power of XPS and equation [1] to coating thicknesses less than the analysis depth.

3.2.4 Atomic Force Microscopy (AFM) surface analysis

AFM enables nanoscale resolution detection of the topographical features (topography, roughness) of surfaces and their mechanical properties, such as stiffness (Binnig et al., 1986). Such high resolution is achieved by using a light lever to measure the deflection of a microfabricated cantilever as the cantilever interacts with a surface of interest (Martin et al., 1987). For imaging purposes, the cantilever deflection or vibrational amplitude is coupled in a feedback loop with a proportional-integral-differential (PID) controller to map the topographical or other (stiffness, magnetic or electrical) properties of a surface as the surface is moved relative to the position of the cantilever, usually using piezoelectric devices. In some cases, the XY scanning of the sample is turned off and the interaction of either a scanning tip or spherical particle is measured as a function of distance normal to the surface. This type of experiment produces what is normally known as a force curve and can be used either to measure long- or short-range surface forces or the “surface” mechanical properties of a material.

In the experiments described here, spherical silica particles were glued onto the end of silicon nitride, V-shaped micro-fabricated cantilevers to produce a probe of known mechanical properties and geometry. This allows ready comparison to theory; in this case the Hertz theory for a spherical indenter was used (Vinckier and Semenza, 1998). The spring constant of the cantilever was calibrated by well-known techniques. For the current study, “contact” mode AFM was used to measure surface stiffness. In this mode, the silica particle probe was repeatedly pressed against the sample surface and the deflection of the spring, and known travel distance was transformed into force as a function of separation distance utilising the calibration of the photodetector. This was achieved by measuring the deflection of the spring when the silica particle was in contact with a hard surface (TCPS or silica wafer), which was moved towards and away from the particle. Thus the force (nN) as a function of the indentation of the surface of the material could be evaluated and compared to theoretical expectations, allowing evaluation of the Young’s modulus of the surface of the material through fitting of the data with theoretical indentation curves of defined Young’s modulus. Knowledge of the size of the sphere and the stiffness of the spring allow precise calculations of normalised forces and the elastic moduli of surfaces.

1. The interactions between spherical silica colloid probes and PAAA or PAPA-coated TCPS or control samples (uncoated silicon wafer) were measured using an MFP-3D atomic force microscope (Asylum Research, Santa Barbara, CA) in phosphate buffered saline (PBS; pH 7.2, 0.15 M NaCl, Life Technologies, Cat No: 70011-044). The probes were prepared by attaching a spherical silica particle ($R = \sim 2.2 \mu\text{m}$; Bangs Laboratories, Fishers, IN, Cat No: SS04N) onto Au-coated triangular Si_3N_4 cantilevers (Asylum Research, Cat No: PNP-TR) using epoxy resin

(Shell Chemicals, Cat No: EPON 1004) and an xyz translation stage. The spring constant of these cantilevers was determined to be 0.219 ± 0.019 N/m using the resonance frequency method (Cleveland et al., 1993), and the radius of the sphere was determined using optical microscopy either prior to or immediately after an experiment.

2. All surfaces that came into contact with the PBS solution were first cleaned in a 2 v/v % RBS-35® surfactant solution (Thermo Scientific, Cat No: PI27952) in dH₂O, copiously rinsed with MQ H₂O, and blown dry with purified N₂ gas. The sample was held in a custom designed “clip” arrangement on the base of the fluid cell, the base being constructed of poly(vinylidene fluoride) (PVDF). Silicon wafer control surfaces and the colloid probes were cleaned immediately prior to an experiment by UV/ozone treatment for one hour. Samples for analysis were quickly mounted on the PVDF fluid cell base and fitted into the fluid cell where they equilibrated in PBS solution for at least 20 minutes prior to force curve acquisition.
3. Data were collected as cantilever deflection versus linear variable differential transformer (LVDT) signal and converted to F/R (force scaled by the radius of the attached sphere) using the MFP-3D software. In all cases, the data was converted using an average inverse optical lever sensitivity (InvOLS) factor obtained from repeated measurements of the voltage associated with tip deflection against a hard control surface (e.g. uncoated silicon in PBS). The approach velocities used were always below 1 $\mu\text{m/s}$ and data were collected using a relative trigger of 2 V.
4. At least ten data sets, plotted against the apparent separation distance, were collected per substrate. Large deviations were not observed, suggesting good surface homogeneity. An “average response” representative force curve for each substrate was selected from each data set for comparison to other substrates.

When assessing the thickness of the coatings it was assumed that the range of the repulsive force is equivalent to the hydrated thickness. In reality, since the polymer graft layer is chemically attached to the TCPS substrate, there will always be a thin, highly compressed film present. The thickness of the coatings serves as a measure of the reproducibility of the manufacturing process and is a critical parameter required for fitting of the material properties (see below) and in fact determines the net material properties of the coating plus TCPS substrate, as would be relevant to a cell growing on the cell culture surface. Finally comparison of the force profiles obtained gives a measure of the precision of the force measurement and allows for ready comparison of coatings synthesised under different conditions (e.g. number of UV exposures) within a single batch. The process that was used to analyse the forces and determine the hydrated coating thickness is as follows:

- The raw AFM cantilever deflection versus piezo travel was converted to force versus separation distance using the Asylum Research AFM software data analysis tools. The inputs for this process are the spring constant (measured independently) and the photodetector sensitivity measured using a stiff silicon wafer substrate. The Asylum Research term for this value is the deflection InvOLS, which is in effect the inverse of the slope of the deflection versus piezo travel at high loads (units nm/V).
- The data for all coated samples was scaled using these two input values.
- The highest force value obtained in the experiment was used to offset the data in the X axis, which is henceforth referred to as zero separation distance. In an analogous manner, the force

data at larger separation distance averaged over a range of at least 30 nm and the average number obtained was used to offset the Y axis data to zero force.

- The separation distance where the force started to increase from the baseline value was then used as the thickness of the coating. Identification of this point is critical for fitting of the modulus of the coating using Hertz theory. Generally this value is obtained from the intersection of the baseline data and the initial portion of the repulsive force measured.
- This procedure was carried out for five individual force curves for each sample or condition.
- Values of the thickness of each coating were obtained from coatings synthesised in three different batches.

Determining the material properties of polymer brush coatings required manipulation of the data in the aforementioned manner, and fitting of the data with theoretical expectations based on the Hertz theory (Vinckier and Semenza, 1998) of deformation and the thin film correction to this model (Dimitriadis et al., 2002). Use of the thin film model allows the modulus of the polymer coating alone to be determined. Fitting of the data at higher loads involves larger % strain (compression) in this case and is not valid with the Hertz theory, which only considers low % strains.

3.2.5 Europium (Eu)-tagged peptide assay for quantifying surface peptide density

Europium is strongly fluorescent and can be used to sensitively and quantitatively tag peptide molecules (reviewed by Hagan and Zuchner, 2011). The Dissociation-Enhanced Lanthanide Fluorescent Immunoassay (DELFI) N1 system (Perkin Elmer, Waltham, MA, Cat No: 1244-301) allows reversible tagging of biomolecules with a stably chelated form of Europium whose fluorescence is suppressed. After tagged peptides have been coupled to the surface, exposure to Enhancement Solution (Perkin Elmer, Cat No: 1244-105) releases the Europium molecules into solution where they become re-chelated in micelles, which are highly fluorescent. By quantifying the fluorescence of the Eu-containing solution, comparing the time resolved fluorescence readings against a calibration curve, and accounting for dilution factors (solution and tagged/un-tagged peptide) and sample surface area, it is possible to calculate the absolute amount of bound peptide at the femtogram ($g \cdot 10^{-15}$) level.

3.2.5.1 Europium tagging of the peptide

Tagging of the aspartate (D) residue of cRGDFK-N3 peptide with N¹-(p-aminobenzyl) diethylenetriamine-N¹,N²,N³,N³-tetra acetic acid (DELFI Eu-N1-Amino chelate) was performed by Mr. John Bentley at the Manufacturing Business Unit CSIRO (Parkville, Australia).

Briefly, a 10 mg/mL solution of 1-ethyl-3-(3-dimethylaminopropyl) carbodiimide, hydrochloride (EDAC, Thermo Fisher Scientific, Cat No: 22980) in 18 Ω /cm H₂O (Sartorius Arium 611UV system, Thermo Fisher Scientific, Cat No: 14-555-502) was prepared and 6.3 μ L of this solution was added to a solution of 0.1 mg of cRGDFK-N3 peptide dissolved in 50 μ L of 0.1 M MES buffer (pH 5.5, Sigma Aldrich, Cat No: 8250). The solutions were combined by stirring for 15 minutes at RT.

A 10 mM solution of DELFIA Eu-N1-Amino chelate was prepared in 18 Ω /cm H₂O and 33.6 μ L of this solution was added to the cRGDFK-N3/EDAC solution, resulting in a 1:2 ratio of peptide : Eu-amino chelate. The reaction solution was then stirred overnight in the dark at 4 °C.

The reaction was quenched with 100 μ L of Tris Buffered Saline Azide (TBSA, prepared in house as 10x stock, see Appendix 2.2), spun at 18 g and subjected to gel filtration on a Superdex peptide HR 10/30 column (GE Healthcare) in Gel Filtration Chromatography Buffer (Appendix 2.3) on a fast protein liquid chromatography (FPLC) BioLogic DuoFlow™ 10 system (BioRad, Gladesville, Australia) and collected in 250 μ L fractions. Finally the tagged peptide was eluted into TBSA. Fractions containing the main peak (Appendix 5.1) were pooled and analysed on a Nanodrop ND-1000 spectrophotometer (Thermo Scientific), recording an OD₂₈₀ of 0.06. Aliquots of tagged peptide were stored in Axygen low-binding 1.7 mL tubes at -80 °C.

Eu-tagged peptide was sent to the Australian Proteome Analysis Facility (Macquarie Park, Australia) for amino acid analysis, the results of which are also presented in Appendix 5.1.

3.2.5.2 Quantifying the density of cRGDFK peptide on cRGDFK-PAPA-coated surfaces

1. PAPA-coated 24-well plates were modified with peptide solutions spiked with 1 mol % of Eu-tagged peptide. Peptide modification was performed as described in Section 2.5.2 however the overnight incubation in Na₂EDTA and the subsequent washes (step 2) of plates modified with Eu-tagged peptide were replaced with HEPES buffer due to the potential for buffering incompatibility. However, the Na₂EDTA incubation was retained to ensure elimination of copper from control plates that were modified in parallel with untagged peptide for cell-binding assays. Plates modified with Eu-tagged peptide were air-dried and stored in the dark at 4 °C for no more than three days before the Eu content was assessed.
2. Europium was liberated from the surface-peptide-bound DELFIA complexes during a 45 minute incubation at RT in 250 μ L/well of Enhancement Solution. The Eu-containing Enhancement solution was transferred (100 μ L/well) into two replicate wells of a white LUMITRAC™ 96-well plate (Greiner bio-one, Cat No: 655074). Six negative control wells containing only Enhancement Solution were included on each plate to establish a baseline. A calibration curve was constructed from a Europium standard (Perkin Elmer, Cat No: B119-100) diluted to 0.2 nM, 0.1 nM, 0.05 nM, 0.02 nM, 0.01 nM and 0.005 nM was also included on each plate. The Eu-containing Enhancement solutions extracted from Eu-peptide-modified wells were further diluted immediately prior to analysis. Plates were analysed in a PHERAstar FS plate reader (BMG Labtech) attached to a PC running PHERAstar Software Installation Package Version 1.50.
3. To convert the Eu counts recorded from solutions extracted from wells modified with Eu-tagged peptide into the absolute amount of Europium liberated from the peptide-modified wells (fmol/cm²), the mean counts from Enhancement Solution control wells were subtracted from the experimental means and the results were compared to the inbuilt calibration curve. The difference between the volume of enhancement solution used to liberate the peptide and the volume of the aliquots analysed were also accounted for, as was the relevant surface area of the plate (including the side of the well) and the dilutions performed immediately prior to analysis.

4. The surface Europium density for each well (pmol/cm²) was calculated by dividing the Eu counts/cm² by the slope of the calibration curve (Appendix 5.2) and then multiplying by the spiking ratio (Eu-tagged peptide : untagged peptide, 1:100).

3.2.6 Cytotoxicity assessment of cell culture surfaces

Determining cytotoxicity is a routine and important quality control assessment for all biomaterials. The following methodology was developed to meet the requirements for cytotoxicity assays stated in ISO10993-5 (ISO, 2009).

1. On experimental day 1, PAAA- and PAPA-coated 24-well plates were treated as described in Sections 2.5.2 and 2.5.3 respectively, except the reaction solutions contained no peptide. An extraction solution was then prepared by adding 720 µL of E8 basal medium to each well and incubating the plates at 37 °C, 5 % CO₂, whilst rocking at 30 rpm for 66 hours. A vessel control extraction solution was prepared in parallel with 720 µL of E8 basal medium in three wells of a clean 24-well plate.
2. On experimental day 2, H9 hPSCs were harvested from Geltrex™-coated maintenance flasks (Section 2.3.2) and seeded at a density of 50 000 cells/cm² onto a Geltrex™-coated 96-well plate.
3. The 66-hour incubation of polymer-coated and control wells concluded on the fourth experimental day, which coincided with day 2 post-seeding for the H9-OCT4-mCherry culture. After 66 hours the extraction media and vessel control solutions were collected and E8 supplement (1:50) was added. Supplemented extraction solutions were aliquoted into six wells of a clean 96-well plate (120 µL/well) and serially diluted two-fold through 8 wells containing E8 medium, for a final dilution of 1:128. Control solutions included the undiluted TCPS vessel control, E8 + 5 µL/mL DMSO to assess the robustness of the cell culture, E8 + 5 µL/mL DPBS- as a vehicle control for the DMSO control, and also an E8 medium control.
4. Culture medium was aspirated from the 96-well plate containing day 2 post-seeding H9 cultures and was replaced with 100 µL of diluted extraction solution or one of the control solutions. Cultures were then returned to the incubator for a further 20 hours.
5. The following day, all wells were visually assessed for morphological changes and cell numbers were assessed with an MTS assay (Section 2.4.3).

3.2.7 L929 adhesion assays

Cultures of L929 fibroblasts were maintained at the Manufacturing Business Unit of CSIRO by Ms. Jess Andrade, Mr. Cheang Ly Be and Ms. Jacinta White. L929 cultures were maintained in 25 cm² flasks (Interpath Services, Cat No: 690175V) under L929 medium (Appendix 2.4) and dissociated with TrypLE™ Express (Life Technologies, Cat No: 12604-013) for harvesting.

1. Cultures of L929 fibroblasts in 25 cm² flasks were washed twice in 5 mL DPBS- and then incubated in 1 mL TrypLE™ Express for 5 minutes.

2. Dissociated cells were harvested with TrypLE™ Express in 2 x 5 mL L929 medium by pipetting across the surface.
3. Cells were pelleted at 805 g for 2 minutes, resuspended in 3 mL L929 medium and a 20 µL aliquot was taken for counting as described in Section 2.4.1. The tube was then topped up with L929 medium to 10 mL and cells were pelleted again.

To test the low protein adsorption properties of surfaces, L929 fibroblasts were seeded in L929 medium at a density of 30 000 cells/cm². After 24 hours, surfaces were visually assessed for adherent L929 fibroblasts. Images were captured using an IX71 microscope (Olympus, Notting Hill, Australia) equipped with a TH4-200 lamp (Olympus) and a DP70 camera (Olympus) and attached to a computer running analySISB image analysis software Version 5.0. The absence of elongated fibroblasts adhering to the surface was indicative of a surface with low non-specific protein adsorption properties. TCPS wells were included in each assay as a positive control for L929 adhesion.

3.3 Results

3.3.1 Preliminary optimisation of cRGDfK-PAAA coatings for hPSC adhesion

Prior to this report, cRGDfK-PAAA coatings had been used for culture of L929 fibroblasts in L929 medium and of human mesenchymal stem cells (hMSCs) in a serum-containing medium (Ameringer et al., 2014). Fibroblasts and hMSCs were found to adhere efficiently to PAAA-40UV coatings that were synthesised from a solution containing 10 mol % acrylic acid and 90 mol % acrylamide (total monomer concentration = 75 mg/mL) and modified with a solution that contained 75 µM cRGDfK peptide (unpublished observations). A pilot experiment performed by Mr. Qi (George) Zhou had shown that a low number of collagenase-harvested H9 hPSCs seeded onto cRGDfK-PAAA coatings prepared under the aforementioned conditions. hPSCs seeded in either KOSR-based medium (with or without MEF conditioning) or mTeSR were able to adhere to the surface and form proliferative, morphologically normal colonies; these conditions therefore provided a starting point for optimisation of peptide-presenting PAAA coatings for hPSC culture.

It was hypothesised that the surface peptide density was inadequate for high levels of hPSC adhesion, so the concentration of peptide in the reaction solution was increased to 200 µM. Cultures were observed over the course of a week to ensure that hPSC colony adhesion was stable. The number of adherent hPSC colonies was observed to weakly correlate with input peptide concentration, but colony numbers were still extremely low with fewer than 10 colonies per well by day 7 post-seeding (Figure 3.2, left). Increasing the proportion of acrylic acid in the monomer feed solution was anticipated to further improve surface peptide density by improving the availability of carboxyl functional groups for chemically coupling of peptides via water-soluble carbodiimide-chemistry. It had been observed that PAAA coatings generated with as little as 60 mol % of acrylamide retained protein low-fouling properties, assessed using an L929 fibroblast adhesion assay (unpublished observations). PAAA coatings were therefore synthesised from a monomer feed solution containing 40 mol % acrylic acid and 60 mol % acrylamide and were modified with reaction solutions that contained between 50 µM and 200 µM cRGDfK peptide. A significantly greater number of adherent mCherry-positive colonies of H9-OCT4-mCherry cells were observed on coatings prepared with 40 mol % acrylic acid than on

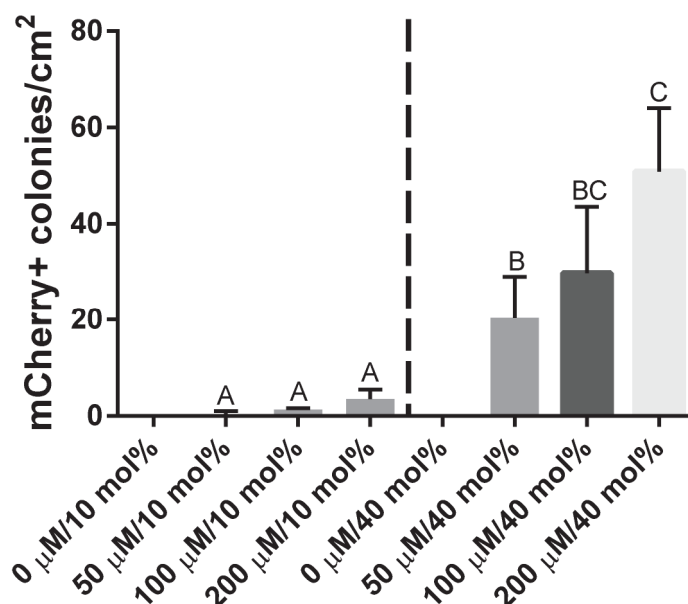


Figure 3.2 This figure shows preliminary optimisation of cRGDfK-PAAA coatings for adhesion of H9-OCT4-mCherry cells. PAAA-40UV coatings were synthesised from monomer feed solutions containing 10 mol % (left) or 40 mol % (right) acrylic acid in acrylamide and were each modified with reaction solutions containing 50 µM, 100 µM and 200 µM cRGDfK peptide. H9-OCT4-mCherry cells were seeded in E8 medium onto the cRGDfK-PAAA-40UV surfaces at a density of 15 000 cells/cm². The number of adherent, mCherry-positive H9-OCT4-mCherry colonies/cm² that were observed on day 7 are plotted. The results of two separate experiments are separated by a dotted line. Mean counts from three replicate wells are presented and error bars represent standard deviations from the mean. Different letters indicate statistically significantly different samples (unpaired Student's t-test, $p < 0.05$). Geltrex™-coated control wells were included in all experiments and were observed to be 80 % confluent by day 4 (data not shown).

coatings prepared with 10 mol % acrylic acid, regardless of peptide concentrations (Figure 3.2). A significant increase in colony number was also observed between the 40 mol % surfaces modified with 50 μ M and 200 μ M solutions of cRGDfK on day 7 post-seeding (Figure 3.2, right). All adherent colonies in this experiment were observed to contain levels of mCherry that were detectable by fluorescence microscopy and this was consistent in H9-OCT4-mCherry cultures on all cRGDfK-modified surfaces over the duration of the work presented in this thesis. At this stage, the peptide screening experiment presented in Chapter 4 of this thesis was commenced using PAAA-UV40 coatings that were modified with reaction solutions containing 200 μ M concentrations of each peptide, with cRGDfK-modified surfaces included as the first hit candidate and as a positive control. PAAA coatings were henceforth synthesised from mixed monomer solutions containing 60 mol % acrylamide and 40 mol % acrylic acid.

Despite the incremental improvements, H9-OCT4-mCherry cells were observed to be much less confluent in PAAA-40UV-coated wells modified with 200 μ M solutions of cRGDfK peptide than in Geltrex™-coated wells, on which the cells were over-confluent within four days of seeding (data not shown). The adhesion of H9-OCT4-mCherry cells to PAAA coatings modified with up to 400 μ M was therefore tested, as was the use of coatings that had been synthesised using fewer UV exposures. H9-OCT4-mCherry hPSCs were seeded onto 24-well plates that had been coated with PAAA-25UV, PAAA-30UV, PAAA-35UV and PAAA-40UV and in which triplicate wells had been modified with reaction solutions containing 50 μ M – 400 μ M cRGDfK peptide. Colony counts (Section 2.4.2) performed 2 days after seeding identified trends of higher colony numbers on coatings that had been generated with fewer UV exposures and that were modified with solutions containing higher concentrations of cRGDfK peptide up to 200 μ M (Figure 3.3). H9-OCT4-mCherry colonies were observed to continue to grow and to remain mCherry-positive in all cRGDfK-PAAA-coated wells out to day 5 post-seeding, by which point morphologically normal hPSCs were observed to cover 60 % of the plate. This result was comparable to control cultures maintained on Geltrex™-coated wells.

To assess whether the observed improvements in hPSC adhesion could be attributed to non-specific protein adsorption onto the coatings (either from the E8 medium or expressed by the hPSCs), an L929 fibroblast adhesion assay (Section 3.2.7) was performed on the PAAA coatings. Elongated L929 fibroblasts were not observed to bind to any of the surfaces tested (Figure 3.4), indicating that it was unlikely that the observed increase H9-OCT4-mCherry colony numbers was due to protein adsorption onto these surfaces and that other physicochemical properties of the substrate may have been influencing hPSC adhesion. Furthermore, no adherent H9-OCT4-mCherry cells were observed on peptide-free control surfaces. This phenomenon was consistently observed for the duration of this project, not a single hPSC was observed to adhere to PAAA-coated surfaces without peptide modification.

3.3.2 Optimising cRGDfK-PAPA coatings for hPSC adhesion and peptide screening

The carbodiimide chemistry used for peptide modification of PAAA-coated surfaces results in a chemical reaction between the carboxylic acid functional groups present in the acrylic acid residues of PAAA coatings and the amine side chain of N-terminal lysine residues that were included in all peptides in this study. Peptides that contained additional lysine residues were expected to undergo side reactions with PAAA-coated surfaces resulting in a non-preferred, uncontrolled peptide

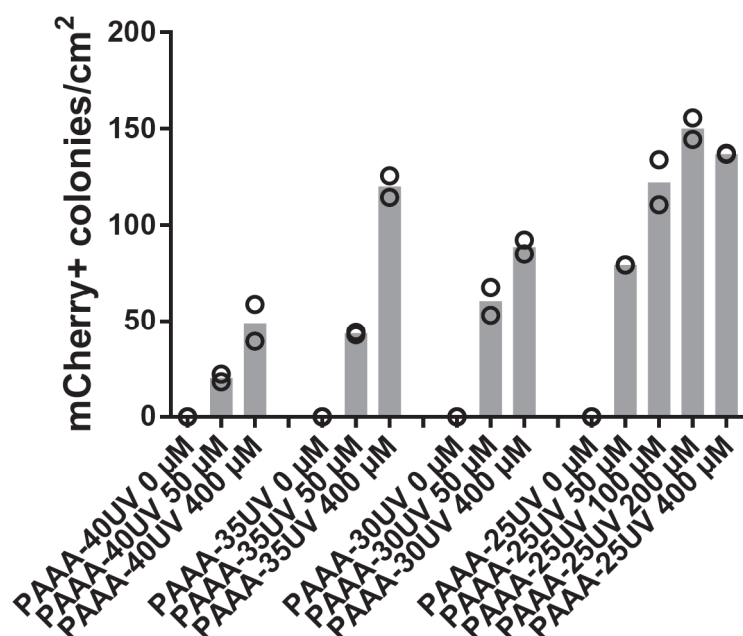


Figure 3.3: Results are presented from a preliminary experiment optimising hPSC adhesion to cRGDfK-PAAA coatings. PAAA coatings were synthesised from monomer feed solutions containing 40 mol % acrylic acid and 60 mol % acrylamide using 25, 30, 35 or 40 exposures to UV light and then modified with solutions containing 50 μM, 100 μM, 200 μM or 400 μM cRGDfK peptide and seeded with H9-OCT4-mCherry cells at a density of 15 000 cells/cm². This graph plots the number of adherent, mCherry-positive H9-OCT4-mCherry colonies that were observed on day 2 post-seeding. The mean (bars) and individual (hollow circles) colony counts are presented from duplicate wells. Geltrex™-coated control wells were observed to reach 80 % confluence by day 4 of culture.

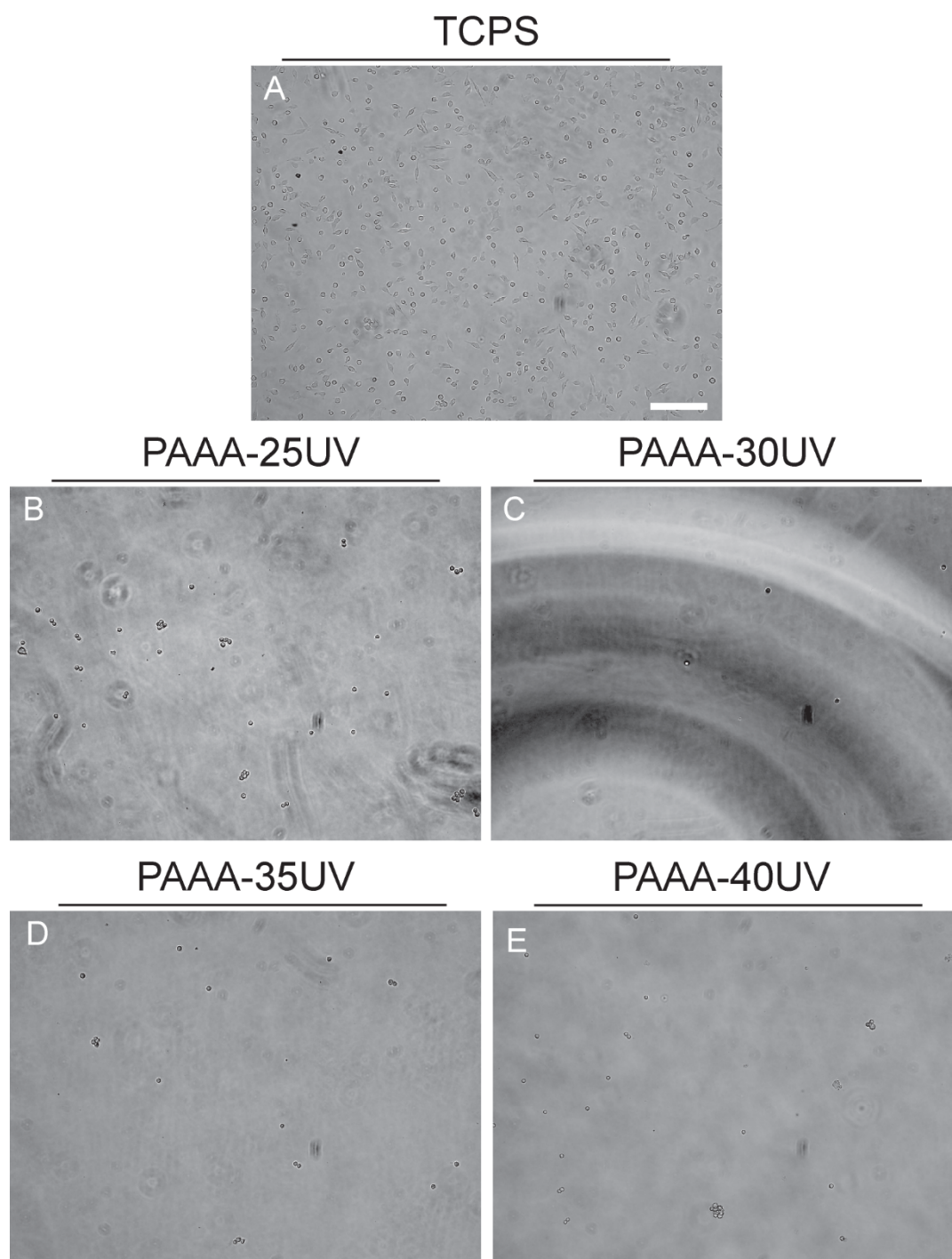


Figure 3.4: This figure presents the results of an L929 adhesion assay for assessing the non-specific protein adsorbing nature of PAAA coatings. An image of L929 fibroblasts bound to (A) TCPS is presented alongside images of L929s seeded into wells coated with PAAA coatings synthesised with (B) 25, (C) 30, (D) 35, or (E) 40 UV exposures. Scale bar represents 100 μm .

orientation, and were therefore deemed unsuitable for modification of PAAA-coated surfaces. In order to screen peptides that contained additional lysine residues, a second polymer coating (PAPA) was synthesised from acrylamide and propargyl acrylamide monomers and optimised for hPSC culture. Azide-modified peptides can react with PAPA via the propargyl functional groups in a CuAAC reaction.

Very low L929 attachment had previously been observed when cells were seeded onto PAPA coatings that had been synthesised from monomer feed solutions containing up to 30 % propargyl acrylamide and using greater than 30 UV exposures (unpublished data). Adhesion of L929 fibroblasts and hMSCs had also been observed following modification of such coatings with cRGDfK-N3 peptide. It had been observed that compared to cultures of L929 fibroblasts or hMSCs, H9-OCT4-mCherry hPSCs had bound more efficiently to PAAA coatings that had been synthesised using fewer UV exposures and modified with reaction solutions containing higher concentrations of cRGDfK peptide (Figures 3.2 and 3.3). Identification of optimal conditions for PAPA plates for hPSC culture therefore commenced with coatings synthesised from monomer feed solutions containing 30 mol % propargyl acrylamide and 70 mol % acrylamide using 10, 20, 30 or 40 UV exposures (as described in Section 2.5.1) to develop a baseline response to hPSC culture.

As noted above, peptide modification of PAPA coatings was carried out by CuAAC reactions with azide-conjugated peptides. A surface-based CuAAC peptide conjugation method was developed based on previous work (Hong et al., 2009) and is described in Section 2.5.3. Test reaction conditions included a range of concentrations of peptide (200 μ M, 400 μ M and 600 μ M) and of CuSO₄ (100 μ M, 400 μ M and 800 μ M). The molar concentration of sodium ascorbate was consistently five-fold higher than the concentration of CuSO₄ and the use of 3,3',3''-(4,4',4''-(nitrilotris(methylene)))tris(1H-1,2,3-triazole-4,1-diyl))tris(propan-1-ol) (THPTA; Sigma Aldrich, Cat No: 762342) equimolar to sodium ascorbate was also tested. High numbers of hPSCs were observed to consistently bind to cRGDfK-PAPA coatings regardless of the peptide modification. This result indicated that the reaction chemistry was robustly efficient, which was consistent with the principles of “click” chemical reactions such as CuAAC. As with cRGDfK-PAAA surfaces, H9-OCT4-mCherry cells were able to efficiently adhere to cRGDfK-PAPA coatings and formed proliferative, mCherry-positive colonies that morphologically resembled control cultures maintained on Geltrex™ (Figure 3.5).

Since greater numbers of H9-OCT4-mCherry colonies had been observed attached to peptide-modified PAAA coatings synthesised from monomer feed solutions containing higher molar proportions of acrylic acid and using fewer UV exposures, PAPA coatings were synthesised from 70 mol % acrylamide and 30 mol % propargyl acrylamide monomer feed solutions using 10, 20, 30 or 40 UV exposures. In an adhesion assay, large numbers of elongated L929 fibroblasts bound onto PAPA-10UV and PAPA-20UV coatings, while cells on PAPA-30UV coatings appeared to be more rounded, and no cell attachment was observed on PAPA-40UV coatings prepared under these conditions (Figure 3.6). Meanwhile consistent numbers of adherent, mCherry-positive colonies were observed to be attached to all test coatings (Figure 3.7). Based on the results presented in Figures 3.6 and 3.7, screening of lysine-containing peptides commenced on PAPA-30UV coated plates modified with reaction solutions containing 200 μ M of peptide, with cRGDfK-N3 peptide again included as the positive control and first hit candidate. As with the PAAA-coated surface, without peptide modification, zero hPSCs were observed to adhere to any PAPA-coated surfaces that had been generated with at least 10 UV exposures at any time over the duration of this project.

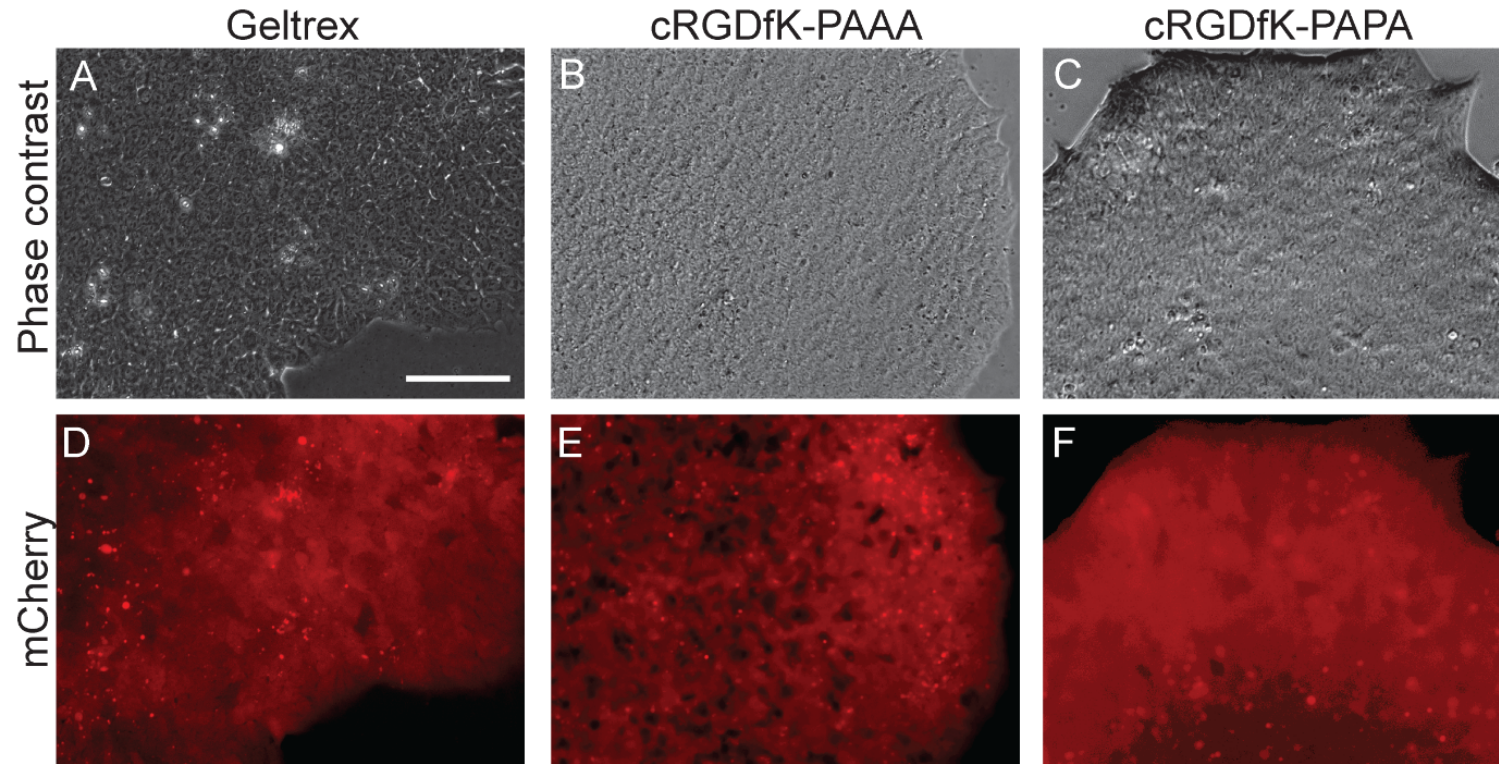


Figure 3.5: cRGDfK-modified polymer coatings were able to support adhesion and short term maintenance of hPSC cultures. Pluripotent H9-OCT4-mCherry reporter cells maintained on (A,D) Geltrex™, (B,E) cRGDfK-PAAA-40UV and (C,F) cRGDfK-PAPA-30UV were (A-C) morphologically similar and (D-F) remained mCherry-positive. Images were captured at culture day 3 under phase contrast and mCherry fluorescence. Scale bar, 100 μm.

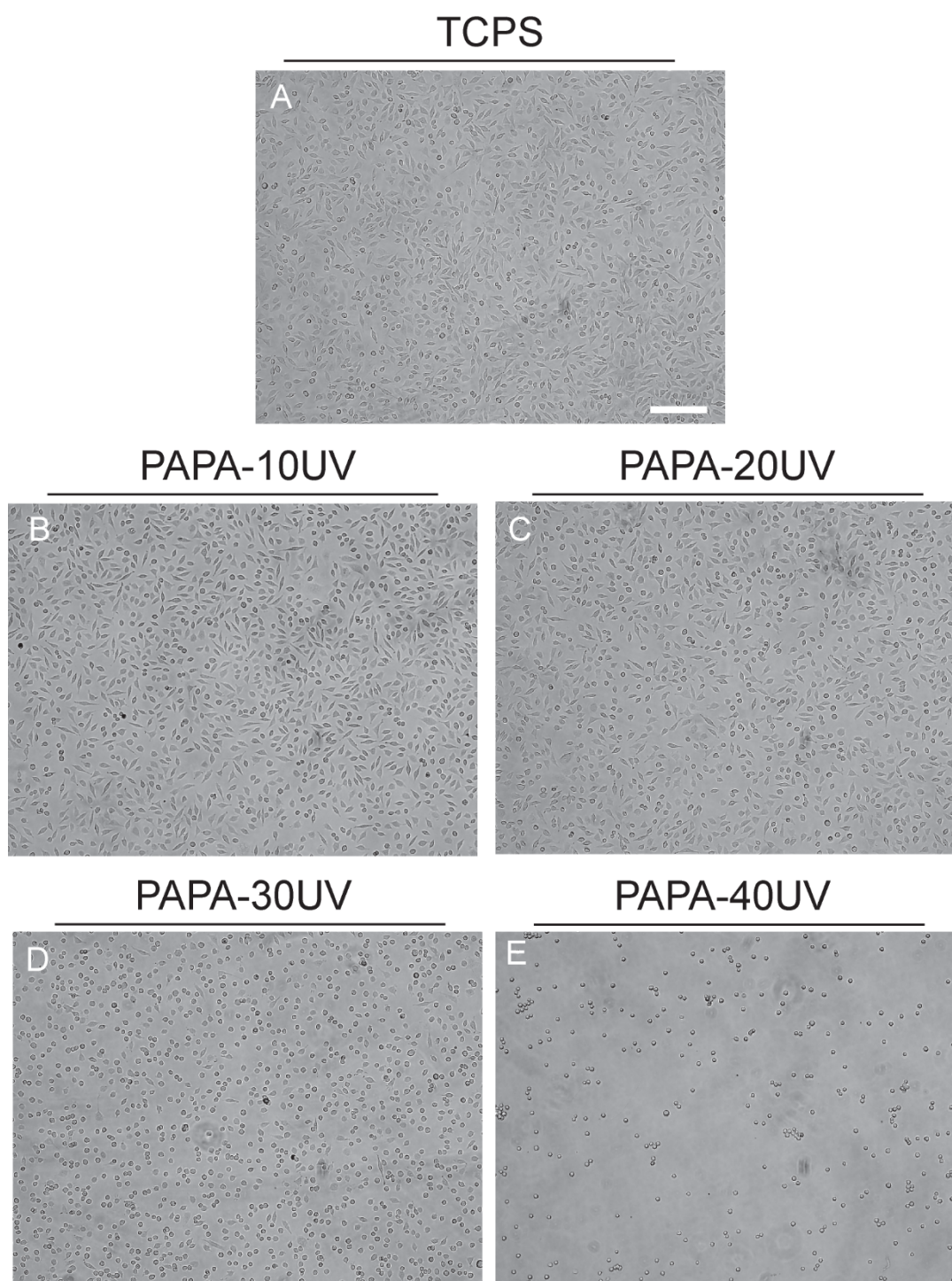


Figure 3.6: This figure presents the results of an L929 adhesion assay for assessing the level of non-specific protein adsorption to PAAA coatings. A control image of L929 cells bound to (A) TCPS is presented alongside images of L929s seeded into wells coated with PAPA coatings that were synthesised from a feed monomer solution containing 30 % propargyl acrylamide and 70 % acrylamide using (B) 10, (C) 20, (D) 30 or (E) 40 exposures to high intensity UV light. Scale bar represents 100 μm .

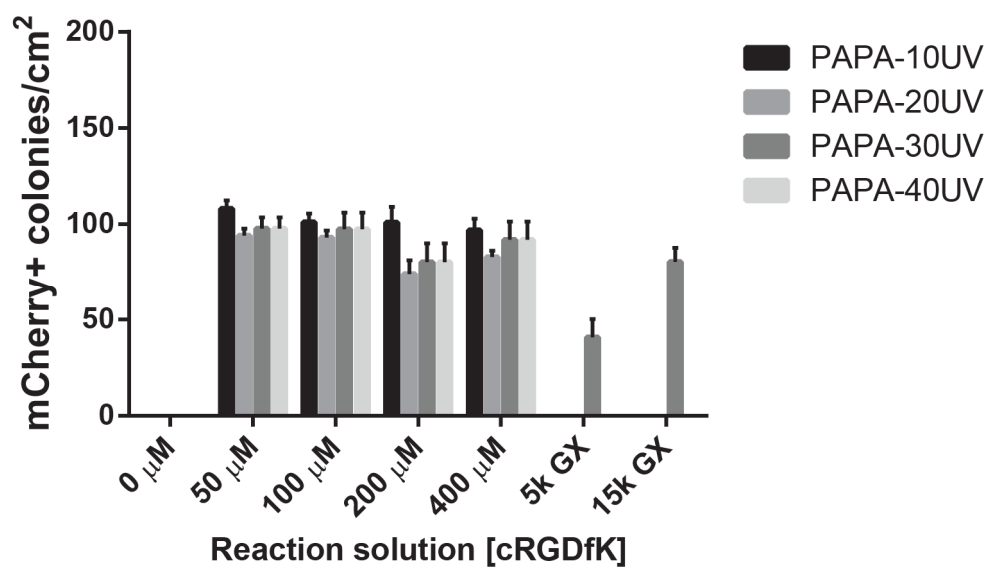


Figure 3.7: This figure presents the results of a preliminary experiment optimising cRGDfK-PAPA-coated 24-well plates for hPSC adhesion. PAPA-coated 24-well plates were synthesised with 10, 20, 30 or 40 UV exposures, modified with reaction solutions containing 50 μM , 100 μM , 200 μM or 400 μM cRGDfK-N3 peptide and then seeded with H9-OCT4-mCherry cells at a density of 15 000 cells/cm². Geltrex™-coated wells were seeded in parallel at equal (15k GX) or one-third (5k GX) cell density. Wells were scanned at culture day 2. The mean colony counts from three wells are presented. Error bars represent standard deviations.

3.3.3 The effects of peptide density and number of UV exposures on hPSC adhesion to cRGDfK-PAAA and cRGDfK-PAPA

During the early optimisation of cRGDfK-PAAA surfaces, it was observed that the number of bound colonies of H9-OCT4-mCherry hPSCs appeared to correlate inversely with the number of UV exposures involved in surface production (Figure 3.3). It was hypothesised that this difference was related to UV-induced changes in the thickness of the polymer brush coating modulating the stiffness of the substrate (coating plus polystyrene), and that coatings synthesised using more UV exposures resulted in softer surfaces that were sub-optimal for hPSC adhesion. A matching correlation was not observed in the number of adherent hPSC colonies on PAPA-10UV and PAPA-40UV coatings (Figure 3.7). The absence of a matching trend on PAPA coatings was hypothesised to indicate that PAPA coatings required a larger number of UV exposures than PAAA coatings in order to be thick enough to sufficiently mask the hard underlying polystyrene to inhibit hPSC adhesion. Correlations between stiffer substrates and improved hPSC adhesion had previously been reported (Musah et al., 2012, Keung et al., 2012, Jang et al., 2013). A study was therefore designed to assess the combinatorial effects on hPSC adhesion to cRGDfK-PAAA and cRGDfK-PAPA coatings of the number of UV exposures used to generate PAAA and PAPA coatings and the concentrations of peptide used to modify the coatings.

Three batches of PAAA and PAPA coatings were to be synthesised using a range of UV exposures across which hPSCs adherence to the coatings was expected to be impaired, and modified with a range of concentrations of cRGDfK peptides, resulting in surfaces to which low-to-high numbers of hPSCs would adhere. For PAAA coatings, the concentration range (50 μ M, 100 μ M, 200 μ M, 400 μ M) and the number of UV exposures (25, 30, 35 and 40) were selected based on the results presented in Figure 3.3. However, parameters that produced similar hPSC adhesion results were yet to be established for PAPA coatings. PAPA coatings were therefore synthesised with 30, 40, 50 and 60 exposures to provide a greater chance for low hPSC attachment properties to arise. An L929 adhesion assay found that the cells stretched out onto PAPA-30UV, but rounded on PAPA-40UV and did not bind to PAPA-50UV or PAPA-60UV (Figure 3.8). A slight yellowing of the TCPS plates was observed at greater than 60 exposures to high intensity UV light, suggesting that some oxidative degradation was occurring. Therefore the plates were not treated with greater than 60 UV exposures.

The peptide-conjugation reaction conditions were also further optimised for this study in order to determine the minimal concentration of peptide solution required to produce a surface to which hPSCs could adhere. hPSCs were observed to bind to PAPA-30UV coated surfaces that were modified with reaction solutions containing as little as 3 μ M cRGDfK without a reduction in colony numbers (Figure 3.9). There appeared to be a slight reduction in colony numbers on surfaces modified with reaction solutions containing 0.3 μ M cRGDfK-N3 peptide, and no colonies were observed on surfaces modified with 0.03 μ M reaction solutions. Peptide concentrations of 0.125 μ M, 0.25 μ M, 0.5 μ M, and 1 μ M were therefore used to modify PAPA coatings for the cross-comparison study.

The colony counting approach is a simple and effective method for easy comparison of hPSC culture surfaces that bind low-to-moderate numbers of colonies, however when the colony numbers increase to ~100 colonies/cm², the colonies begin to fuse and become much more difficult to meaningfully count. A colorimetric MTS assay (Section 2.4.3) was therefore used to more accurately compare cell numbers at high densities.

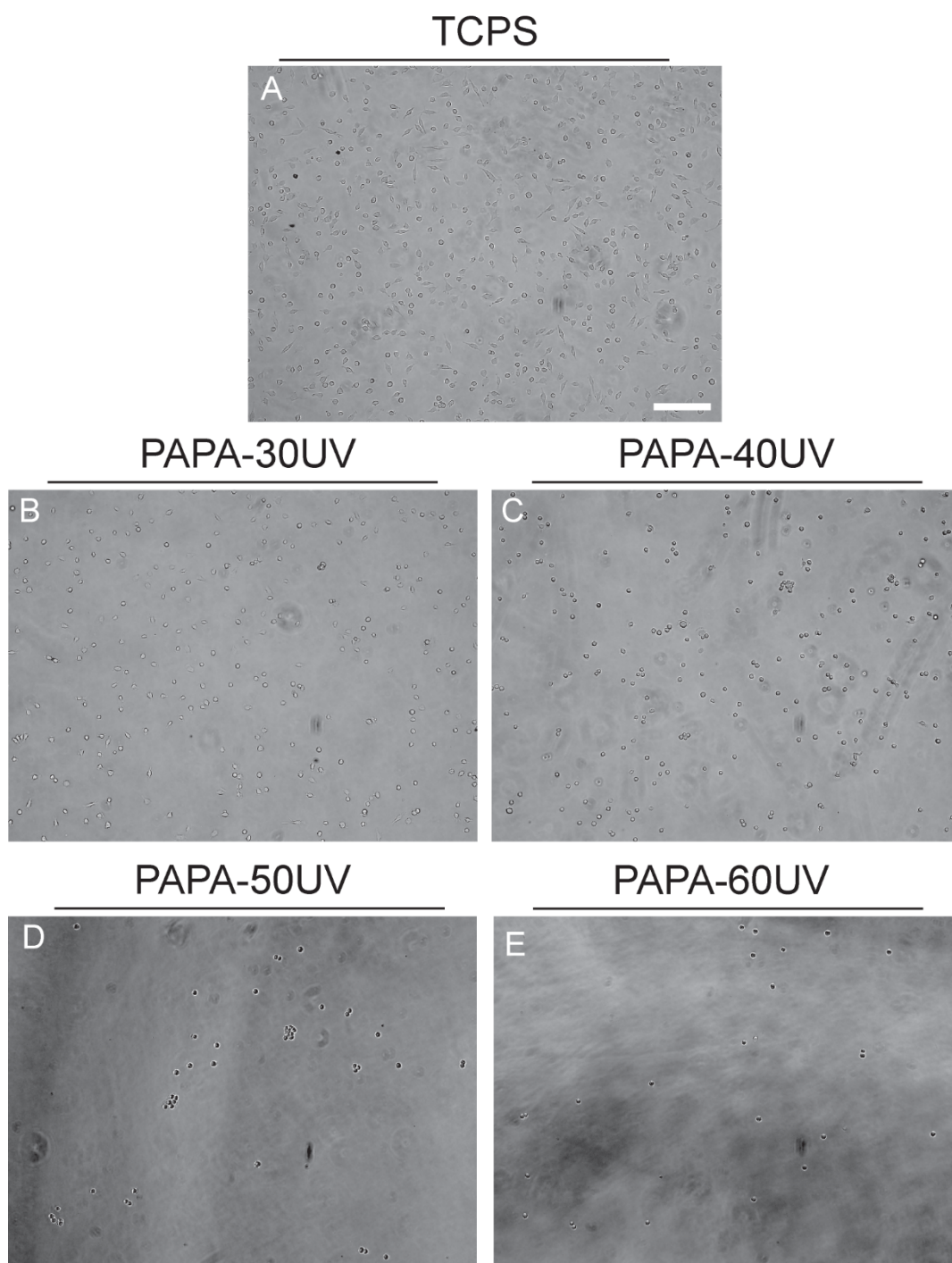


Figure 3.8: This figure presents the results of an L929 adhesion assay for assessing the level of non-specific protein adsorption to PAAA coatings. (A) An image of L929 cells bound to a clean TCPS control well is presented alongside images of L929s seeded into wells coated with PAPA coatings generated with (B) 30, (C) 40, (D) 50 or (E) 60 UV exposures. Scale bar represents 100 μm .

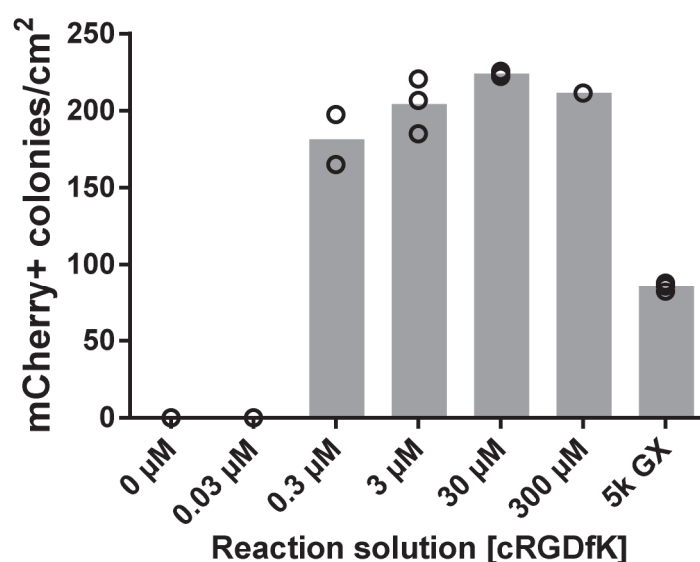


Figure 3.9: hPSC adhesion to cRGDfK-PAPA coatings that were modified with low peptide concentrations. PAPA-30UV-coated 24-well plates were modified with CuAAC reaction solutions containing between 0.03 μM and 300 μM cRGDfK peptide. cRGDfK-PAPA-30UV-coated wells were seeded with H9-OCT4-mCherry cells at a density of 15 000 cells/cm², alongside control PAPA surfaces exposed to peptide-free (0 μM) reaction solutions as well as Geltrex™-coated wells that were seeded at equal (15k GX) or one-third (5k GX) density. Wells were scanned at culture day 2. The mean colony counts are presented for *n* wells that had been modified with reaction solutions containing the following concentrations of cRGDfK peptide: three wells with 0.03 μM , 3 μM and 30 μM , two wells with 0.3 μM and one well with 300 μM . Error bars represent standard deviations.

In three independent experiments, cells from three different hPSC lines (H9-OCT4-mCherry, H9 and NHF-1-3) were seeded at a density of 15 000 cells/cm² into triplicate wells that had been coated with PAAA and PAPA in three different batches and modified to present different concentrations of cRGDfK peptide. On day 2 post-seeding, a MTS colorimetric assay was used to compare the adherent cell numbers on each polymer coating to each other and to Geltrex™-coated control wells that had been seeded in parallel at equal and one-third (5000 cells/cm²) density. Three independent experiments were performed. Wells coated with cRGDfK-PAAA-25UV were observed to consistently bind significantly greater numbers of cells than cRGDfK-PAAA-35UV or cRGDfK-PAAA-40UV wells, regardless of the peptide concentration that had been used for modification (Figure 3.10A). On the other hand when PAPA coatings were modified with equal peptide concentrations, hPSC adhesion did not change as a function of the number of UV exposures used to synthesise the coatings (Figure 3.10B).

However, a clear correlation was observed between modifying peptide concentration and the number of adherent hPSCs on PAPA coatings, while the number of cells attached to cRGDfK-PAAA coatings was not observed to vary as a function of the peptide concentration in the modification reaction solutions. This was inconsistent with the colony counting results presented in Figure 3.2 and 3.3, for which a correlation was observed between hPSC adhesion and peptide concentration in PAAA plates modified with reaction solutions containing 50 µM and 200 µM cRGDfK peptide. This difference may be related to differences in the two cell quantification approaches used. The MTS assay is a measure of metabolism, and depends on the assumption that individual cells are not becoming more or less metabolically active, while the colony counting approach assumes that the colonies on each surface contain similar numbers of cells. The contradictory trends may also be a result of increased operator experience in coating production.

3.3.4 The physicochemical effects of additional UV exposures on PAAA and PAPA coatings

It was consistently observed that fewer hPSCs adhered to cRGDfK-PAAA-40UV coatings compared to cRGDfK-PAAA-25UV coatings when both surfaces had been modified with solutions containing equimolar concentrations of peptide (Figure 3.10). This result suggested that physicochemical properties of PAAA coatings related to hPSC adhesion efficiency changed as the number of UV exposures was increased from 25 to 40. However, reduced hPSC adhesion was not observed as a function of the number of UV exposures used to synthesise the PAPA coatings. The observed difference in cellular responses to the two coatings that were synthesised using a similar method, positioned cRGDfK-PAPA as a good negative control surface, affording comparison of the key changes in properties that occurred in PAAA but not in PAPA as the number of UV exposures was increased. In this way, the key parameters that led to the observed cellular response could be investigated.

In order to compare the elemental composition of PAAA and PAPA coatings as a function of UV exposures and to assess the thickness of dry coatings, XPS analysis was performed (Section 3.2.3). XPS is a surface sensitive method that quantitates the number and binding energies of core photoelectrons that have been ejected from the surface of a sample material during exposure to a high intensity beam of monochromatic X-rays.

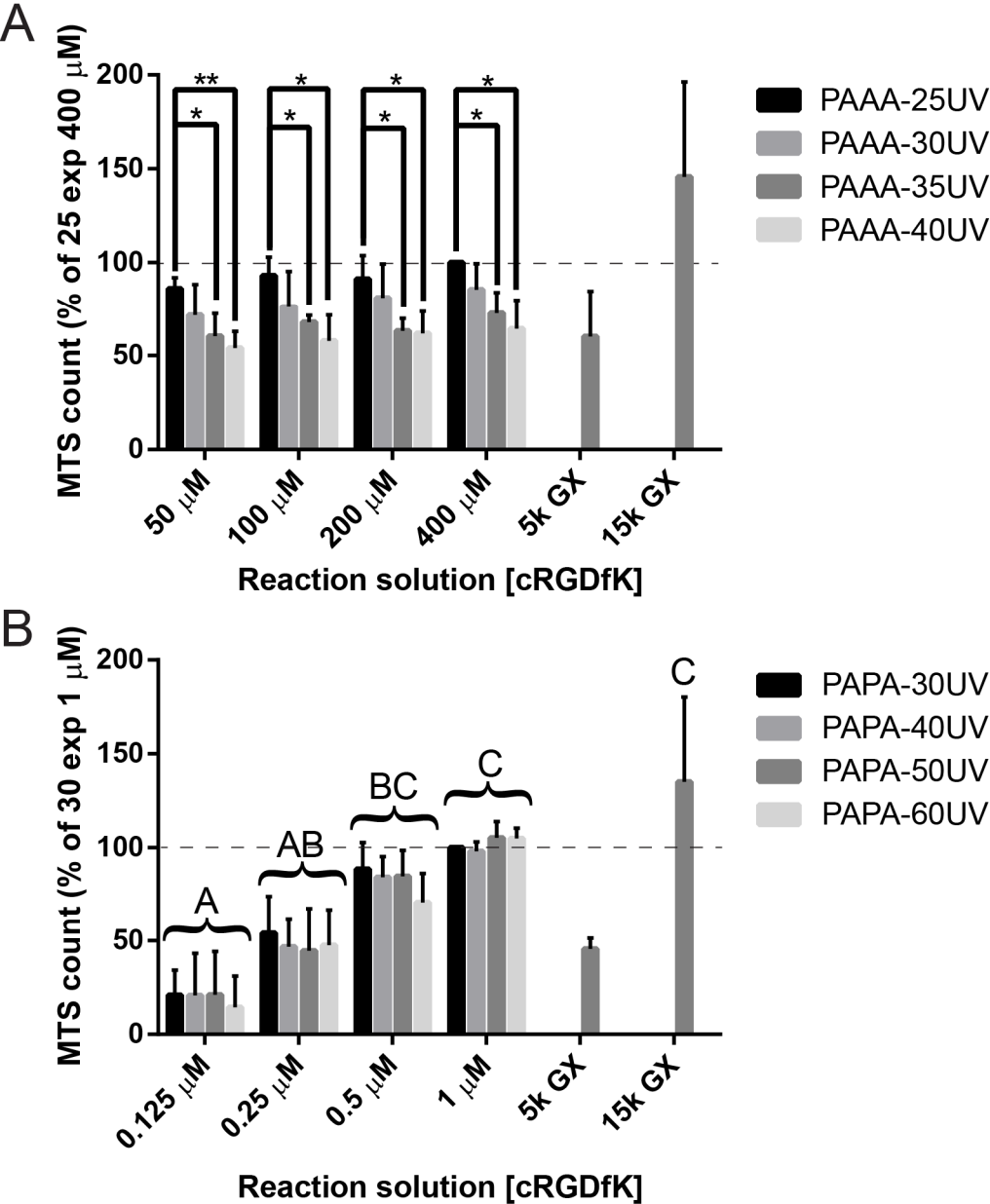


Figure 3.10: Caption on subsequent page.

Figure 3.10: Figure is on the previous page. This figure presents the combinatorial influence on hPSC adhesion of the number of UV exposures used to generate (A) PAAA and (B) PAPA coatings and the concentration of cRGDfK peptide included in surface modification reaction solutions. PAAA coatings were synthesised with 25, 30, 35 and 40 UV exposures and modified with reaction solutions containing 50 μM , 100 μM , 200 μM and 400 μM of cRGDfK peptide. PAPA coatings were synthesised with 30, 40, 50 and 60 UV exposures and modified with reaction solutions containing 0.125 μM , 0.25 μM , 0.5 μM and 1 μM cRGDfK-N3 peptide. Wells coated with cRGDfK-PAAA or cRGDfK-PAPA were seeded with hPSCs at a density of 15 000 cells/cm², alongside Geltrex™-coated wells seeded at equal (15k GX) or one-third (5k GX) density. On culture day 2, cell numbers were quantified using an MTS assay. Means are presented from three independent experiments in which polymer coatings were generated and peptide modified in different batches, triplicate wells were modified with each concentration of peptide and then seeded with a different cell line (H9-OCT4-mCherry, H9 and NHF-1-3). Error bars represent standard deviations. Results for surfaces coated with each co-polymer were normalised to the coatings synthesised with the lowest number of exposures and modified with the highest peptide concentration (PAAA-25UV 400 μM cRGDfK and PAPA-30UV 1 μM cRGDfK-N3; dotted lines). An asterisk (*) indicates a statistically significant difference (unpaired Student's t-test, $p < 0.05$). ** indicates a highly significant difference ($p < 0.01$). Different letters indicate statistically significantly different samples (unpaired, two-tailed Student's t-test, $p < 0.05$). Samples that are grouped by curly brackets each individually follow the statistical similarities and differences attributed to the group. The 5k GX control was not included in statistical analyses.

Since the binding energy of each photoelectron is specific to the type of atom from which it was ejected (see Table 3.1), and because only photoelectrons ejected from a certain depth (see Appendix 4.1) can escape from the surface of a material, the spectra acquired via XPS (see Figure 3.11 for examples) can provide information about the elemental composition and chemical structure of surface coatings (see Figure 3.12 for the relevant monomer structures).

Table 3.1: Binding energy information is presented to facilitate the interpretation of XPS data. XPS analysis measures the number and binding energies of photoelectrons ejected during exposure of a surface to monochromatic X-rays. The approximate ranges of binding energies that can be attributed to photoelectrons ejected from the 1s shell of each detectable element in TCPS, PAAA and PAPA (oxygen, nitrogen and carbon) are presented in this table alongside the range of binding energies for each element (Naumkin et al., 2016).

Electron origin	Binding energies (eV)	Binding energy range (eV)
O 1s	527-534	7
N 1s	395-409	14
C 1s	281-297	16

Representative spectra acquired via XPS from TCPS coated with PAAA and PAPA coatings generated with high numbers (40 and 60, respectively) of UV exposures are presented in Figure 3.12 to facilitate comprehension of the XPS data. The plotted peaks represent detection of atoms, about which information can be inferred based on the detected binding energies (Table 3.1). The wide spectra (A,C,E) contain peaks that represent different elements and immediately indicate that high levels of C have been detected in all three surfaces. It is also clear that very low levels of N were detected in the TCPS sample, as would be expected. The C 1s spectra are plotted on the right (B,D,F) and can be considered to be magnified, higher resolution versions of the C 1s peaks that can be observed in the wide spectra. The original spectral data (thick line) have been divided into six or eight components that are depicted by thinner lines and which represent carbon atoms that are engaged in different binding configurations. Analysis and interpretation of these components is discussed in detail later.

In the following discussion of XPS analyses of PAAA and PAPA coatings, the assessment of individual parameters will initially be presented for each surface type and then correlations between results from multiple parameters will be interpreted.

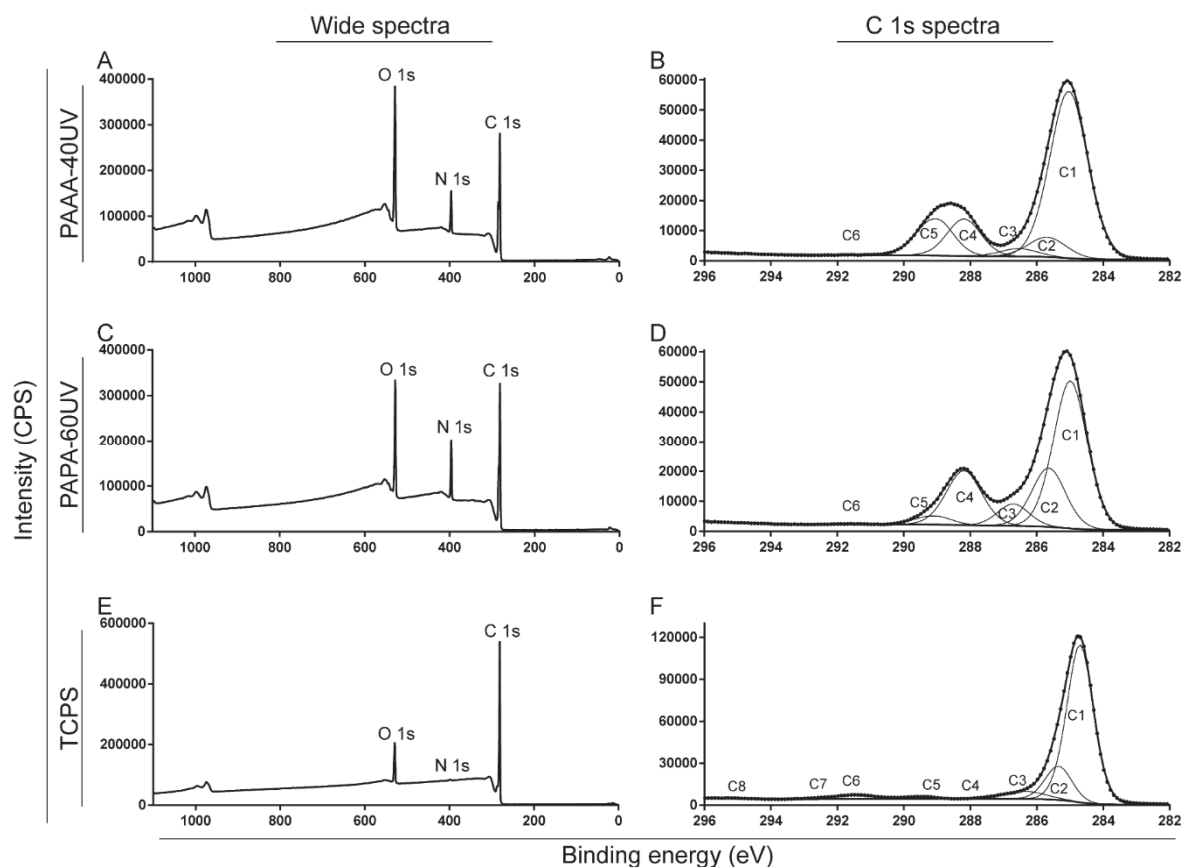


Figure 3.11: This figure presents representative spectra obtained via XPS analysis of TCPS with or without polymer coatings. Wide scan spectra of (A) PAAA-40UV and (C) PAPA-60UV coatings, and of (E) clean TCPS are presented with C 1s, N 1s and O 1s peaks labelled. Magnified, curve-fitted spectra of the carbon (C 1s) peaks are also presented for each surface, with the components C1-C6 highlighted in (B and D) the polymer brush coating spectra and components C1-C8 highlighted in (F) the TCPS spectra. The spectral components (fine lines) were modelled from the original spectral data (thick line). The sum of the spectral components (dotted line, aka the “spectral envelope”) is also presented. A close correlation between the original data and the spectral envelope is required for well-fitted data.

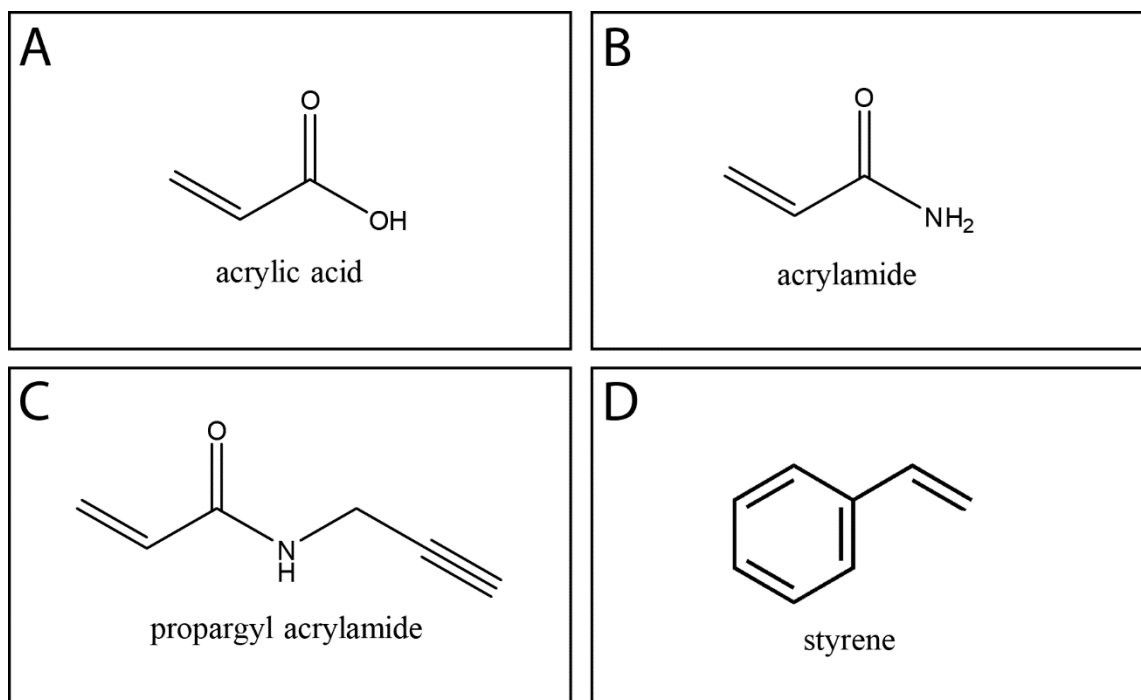


Figure 3.12: In this figure the structures of the monomers that comprise PAAA and PAPA coated TCPS are presented as an aid to interpretation of data acquired via XPS. Structures are presented for (A) acrylamide, (B) acrylic acid, (C) propargyl acrylamide and (D) styrene. When present in coatings, carbon-carbon double bonds are replaced with single bonds.

The underlying TCPS is carbon-rich and essentially nitrogen-free. While nitrogen is present in the acrylamide that comprises the bulk of both coatings and in the propargyl acrylamide co-monomer in PAPA, the acrylic acid co-monomer in PAAA does not contain nitrogen (Figure 3.2). Since the sampling depth is a constant for each element under consideration, when the concentration of an element is compared across a series of samples, the atomic percentage of N found in the surface can be correlated with the coating thickness. For a number of reasons, it is convenient to carry out comparisons between the ratio of the nitrogen atomic % to the carbon atomic % (N/C), instead of the O/C ratio, which can also be correlated with coating thickness. For thicker coatings, a greater volume of the nitrogen-containing polymer contributes to the analysis result and the surface of the essentially nitrogen-free underlying TCPS will be sampled to a lesser degree than for thinner coatings. As the coating continues to increase in thickness, the contribution of TCPS to the spectra continues to decrease until the coating reaches a thickness greater than the analysis depth of the technique. At this point the nitrogen component of the spectra will no longer increase and the result obtained should represent the actual elemental composition of the coating. The theoretical elemental composition of infinitely thick coatings of PAAA and PAPA were calculated from the atomic and molar proportions of the input monomers by assuming equal and consistent contributions of input monomers. The relationships between the composition of the acquired spectra and the theoretical composition of each coating provided insights into the actual composition of the polymer coatings and their thickness. The N/C atomic ratios of spectra acquired from PAAA and PAPA coatings generated with different numbers of UV exposures are compared to the theoretical compositions of each surface (dashed red lines) in Figure 3.13A.

A statistically significant increase was observed between the N/C atomic ratios of PAAA-25UV and PAAA-40UV surfaces. A significant difference in N/C atomic ratios was also observed between PAPA coatings generated with the lowest (30) and highest (60) number of UV exposures (Figure 3.13A). The experimental N/C atomic ratios were observed to increase between PAAA-25UV and PAAA-30UV before plateauing at ~80 % of the theoretical maxima from PAAA-30UV to PAAA-40UV. Meanwhile the experimental N/C atomic ratios in spectra acquired from PAPA coatings demonstrated minor incremental increases with increasing numbers of UV exposures, which only reached statistical significance when comparing PAPA-30UV to PAPA-60UV, the latter being approximately equal to 75 % of the theoretical maxima. The ~20 % difference between the theoretical N/C maxima for PAAA coatings, and the experimental results for PAAA-30UV, PAAA-35UV and PAAA-40UV is likely due to the presence of adventitious carbon, which is ubiquitous in XPS analysis. Assuming the amount of adventitious carbon was constant on all surfaces, it is possible that the ~25 % difference between experimental and theoretical N/C ratios suggests that thickness of the PAPA-60 samples was approaching but may not have reached the maximum sampling depth.

The O/C ratios (Figure 3.13B) can be slightly more difficult to interpret, as there are potentially three sources of O to consider. As well as each monomer containing a single oxygen atom, oxidation of polystyrene as a result of the tissue culture treatment of TCPS, and potentially as a result of the UV treatment used to initiate polymerisation, means that oxygen will be detected in both the substrate and the coating, depending on the thickness of the coating. As the theoretical O atomic %s present in the polymer coatings (PAAA, 28 %; PAPA, 17 %) are expected to be higher than the O atomic % observed in the clean TCPS substrate (10 %), an increase in O surface concentration is expected to occur as a result of the presence of a coating. Nevertheless, for PAAA-coated wells, the trends observed for O/C atomic ratios mirrored those observed for N/C atomic ratios, with an increase

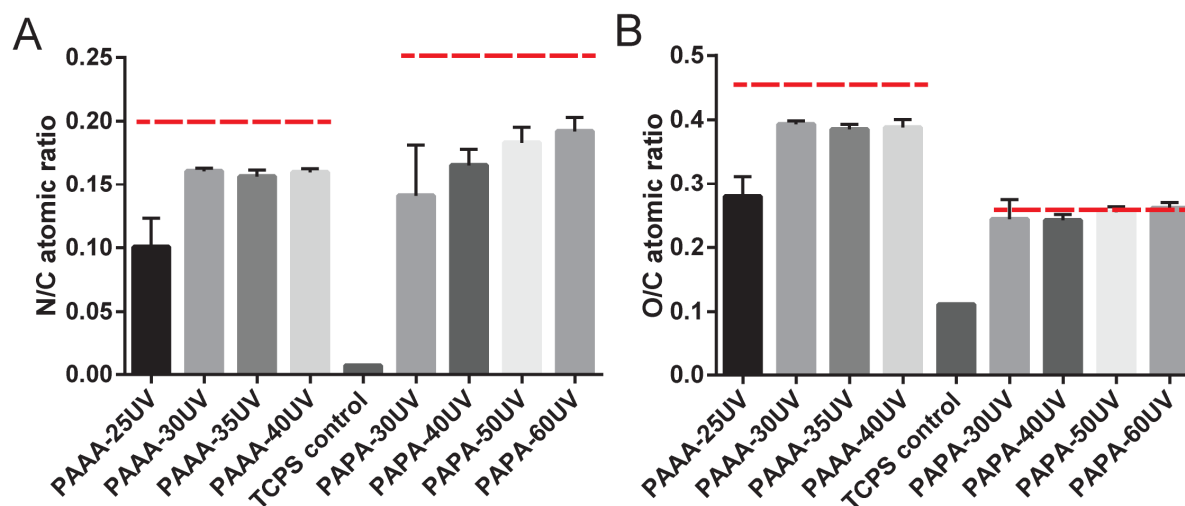


Figure 3.13: Atomic ratios are presented from XPS analysis of TCPS coated with PAAA coatings generated with 25, 30, 35 and 40 UV exposures and with PAPA coatings generated with 30, 40, 50 or 60 UV exposures and of clean TCPS. The (A) N/C and (B) O/C atomic ratios from spectra acquired from each surface are compared to the calculated theoretical maxima of each coating (dotted red lines). Means and standard deviations are presented for each polymer coating from spectra acquired from three wells that were each assessed at three different locations. The mean result is also presented from spectra collected from three different locations in one clean TCPS well.

between PAAA-25UV and PAAA-30UV followed by a plateau at ~83 % of the theoretical maxima. However, no significant differences were observed in the O/C data acquired from PAPA coatings, which were approximately equal to the theoretical maxima regardless of the number of UV exposures used to generate the coatings. In the case of changing coating thickness, the observed O/C atomic ratio may plateau if the O/C ratio observed in analysis of the substrate surface and the coating were the same. This result therefore indicates that oxidation (an increase in O content) in the acquisition regions of both the TCPS and the polymer coating produced equivalent oxygen contents in both coating and underlying substrate, which masked any changes to polymer coating thickness.

As mentioned previously, additional information about the chemical properties of surfaces can be elucidated from detailed analyses of components of the C 1s portion of the spectrum, which is highlighted in Figure 3.12B,D,F. The ranges of binding energy values outlined for each element in Table 3.1 are related to the range of local binding environments that each element can occupy. With four valence electrons, carbon atoms can be involved in a wide variety of chemical bonds with various elements, and these binding environments affect the specific binding energy of individual carbon atoms (Table 3.2). The C 1s spectra can therefore be separated into a series of components that quantitatively represent the acquisition of specific types of carbon. The spectral resolution of XPS is poor compared to other spectroscopic techniques and as such an assigned component may represent a number of chemical bonds; this is particularly the case in materials with a variety of functional groups. The components for spectra recorded from uncoated TCPS and TCPS coated with PAAA or PAPA are described in Table 3.2.

As indicated in Table 3.2, bonding configurations contributing to components C1 and C2 can be detected in every monomer in both the polymer coatings and the underlying TCPS. As such, analysis of these components cannot be used to identify the contribution of any individual material.

Component C3 represents carbon atoms that are singly bound to either nitrogen (C-N) or oxygen (C-O). Of the constituent molecules of PAAA and PAPA coatings on TCPS, only propargyl acrylamide would be expected to contribute to the C3 component as it contains one C-N bond per monomer unit. However, increased oxidation (C-O) of TCPS in combination with thinner coatings could also contribute to component C3.

The spectra acquired from the TCPS control well contained a 5 % contribution of component C3 to total C (C3/C), which is likely to have resulted from the oxidising tissue culture treatment. The peak C3/C were observed in PAAA and PAPA coatings generated with the lowest number of UV exposures (25 and 30, respectively) and are probably evidence of increased oxidation of TCPS during the coating process. Additional UV exposures resulted in a reduction in the C3/C acquired from PAAA coatings to a baseline of 2.5 % as a result of greater coating thickness. This residual C3 component could represent a low level of TCPS substrate sampling or possibly an artefact of the curve-fitting routine used (peak widths, positions and shapes *etc.*). The C3/C obtained for PAPA was considerably higher than PAAA surfaces, which was probably due to the cumulative effect of the contribution of the propargyl acrylamide in PAPA and that of the increasingly oxidised TCPS. Meanwhile, the C3/C of PAPA coatings gradually decreased with every additional ten UV exposures, as the coating thickness increased and less of the UV-oxidised TCPS was detected. The C3/C of PAPA coatings generated with 60 UV exposures was slightly below the theoretical maxima, which is consistent with the thickness of these coatings being close to the analysis depth of the XPS technique.

Table 3.2: Sample spectra are provided for components C1 from C8 as detected from uncoated TCPS and TCPS coated with PAAA or PAPA. The binding energy range for each component is listed alongside the chemical bonds that may contribute to each spectral component and the likely sources of those bonds in the PAAA or PAPA systems. C7 and C8 were required for the TCPS fit, but are suppressed by the addition of an overlayer. X represents nitrogen or oxygen.

Component	Binding energy (eV)	Chemical bonds represented	Potential sources
C1	284.7 (TCPS) or 285 (PAAA/PAPA)	$\underline{\text{C}} - \text{C} / \underline{\text{C}} - \text{H}$	TCPS, acrylamide, acrylic acid, propargyl acrylamide
C2	C1 + 0.65	$\underline{\text{C}} - \text{C} - \text{X}$	TCPS, acrylamide, acrylic acid, propargyl acrylamide
C3	286.9 – 286.1	$\underline{\text{C}} - \text{N} / \underline{\text{C}} - \text{O}$	Propargyl acrylamide, oxidised materials (low)
C4	288.3 – 287.7	$\underline{\text{C}} = \text{O} / \text{O} - \underline{\text{C}} - \text{O} / \text{N} - \underline{\text{C}} = \text{O}$	Acrylamide, propargyl acrylamide, highly oxidised materials (very low)
C5	289.5 – 288.9	$\text{O} - \underline{\text{C}} = \text{O}$	Acrylic acid, highly oxidised materials (very low)
C6	293 – 291	Aromatic carbon ring, unsaturated hydrocarbon	TCPS
C7	~292	Aromatic carbon ring	TCPS
C8	~295	Aromatic carbon ring	TCPS

Component C4 represents C=O or N-C=O. Acrylamide and propargyl acrylamide molecules both contain a single C bonded singly to N and double-bonded to O (i.e. N-C=O). Based on theoretical considerations, we expect that the contribution of C4 to total carbon (C4/C) obtained for the PAPA coating should be 7.8 % higher than those obtained for PAAA, since the PAPA coatings in this study were synthesised from solutions containing more acrylamide than the PAAA coatings. The C4/C of PAAA coatings was observed to increase between PAAA-25UV and PAAA-30UV samples, and to plateau between PAAA-30UV and PAAA-40UV. Meanwhile minor, incremental increases were observed in the C4/C of the PAPA coatings, consistent with an increasing coating thickness composed entirely of acrylamide species.

Component C5 represents O-C=O, which should only be present in the spectra as a result of the presence of acrylic acid residues in PAAA and should theoretically be absent from PAPA coatings. The low C5/C calculated from quantification of high resolution spectra acquired from PAPA coatings may be a due to the detection of oxidised carbon of the underlying TCPS as highlighted previously and are within the accuracy error range of the XPS method. The increase in C5/C between PAAA-25UV and PAAA-30UV represents a higher acrylic acid contribution to the spectra due to a reduced sampling of the underlying TCPS substrate.

Since aromatic hydrocarbon atoms should only be present in the underlying TCPS and not in the polymer brush coatings, the presence of C6 in spectra acquired from PAAA-25UV and PAPA-30UV samples indicated that these coatings were thinner than the sampling depth of XPS (Figure 3.14D). The lack of intensity in the region defined for C6 for PAAA coatings generated greater than 30 UV exposures indicates that these coatings were thicker than the sampling depth of XPS for this element.

In order to calculate the approximate dry thickness of each coating, equation [1] was applied to the nitrogen atomic % data acquired from each coating (Figure 3.15A). The results from applying equation [1] indicated that PAAA-25 UV and PAPA-30UV were each ~3 nm thick (*in vacuo*). PAAA coatings that had been synthesised using 30-40 UV exposures were determined to be ~6 nm thick (Figure 3.15A, left). With increased numbers of UV exposures, PAPA coatings were calculated to incrementally grow up to a thickness of 4-5 nm for PAPA-60UV coatings. As expected, these results correlated directly with C4/C (representing the nitrogen component of the coating), and inversely with C6/C (representing detection of the underlying TCPS) for both coating types (Figure 3.15B-C). These three parameters independently corroborate the growth profiles of the two polymer coatings within the analysis depth restrictions inherent in XPS.

In order to determine the contribution of each monomer to PAAA and PAPA coatings, comparisons were made between the experimental data acquired from the presumably thickest coatings of each type (PAAA-40UV and PAPA-60UV) and calculations based on the atomic and molecular ratios of theoretical polymers composed of different monomer ratios. The theoretical polymer compositions were based on the molecular composition of the monomer feed solutions from which PAAA and PAPA coatings were synthesised and for polymers containing of +/- 10 % of each monomer. So whereas PAAA polymers were prepared from monomer feed solutions containing a 60:40 molar ratio of acrylamide : acrylic acid, the experimental results from the PAAA-40UV coatings were compared to theoretical results of polymers containing 70:30, 60:40 and 50:50 molar ratios. Likewise, theoretical results were calculated for PAPA polymers containing 80:20, 80:20 and 60:40 ratios of propargyl acrylamide and acrylamide. The experimental and theoretical ratios of N/C, O/C, as well as percentages of C3-C5/C are presented in Figure 3.16. The key parameters for PAAA coatings are the contributions of N from acrylamides, and of O from acrylic acid. Most experimental values for PAPA are lower than the theoretical equivalents because this coating is thin, and the contribution from the TCPS (mostly C1 and C2) would bring down the percentages of the other carbon components and of other atoms relative to carbon.

As discussed above, XPS analysis is effective at assessing the surface elemental composition of materials. Although XPS data can be used to determine the thickness of a coating, this approach is restricted by the attenuation lengths of ejected electrons and can be confounded by an inability to exclusively connect the emission of electrons of particular binding energies to sampling of the substrate or the coating. The apparent abrupt cessation of growth in PAAA coatings generated with greater than 30 UV exposures, and the proximity of these results to the maximal theoretical limits, indicates that these coatings were possibly still increasing in thickness as a function of increased UV exposure but that the increases were not able to be detected by XPS due to the surface-sensitive nature of the measurements. Atomic force microscopy was therefore used to complement the XPS data by more reliably and accurately determining the hydrated thickness of these coatings, and their associated elastic moduli.

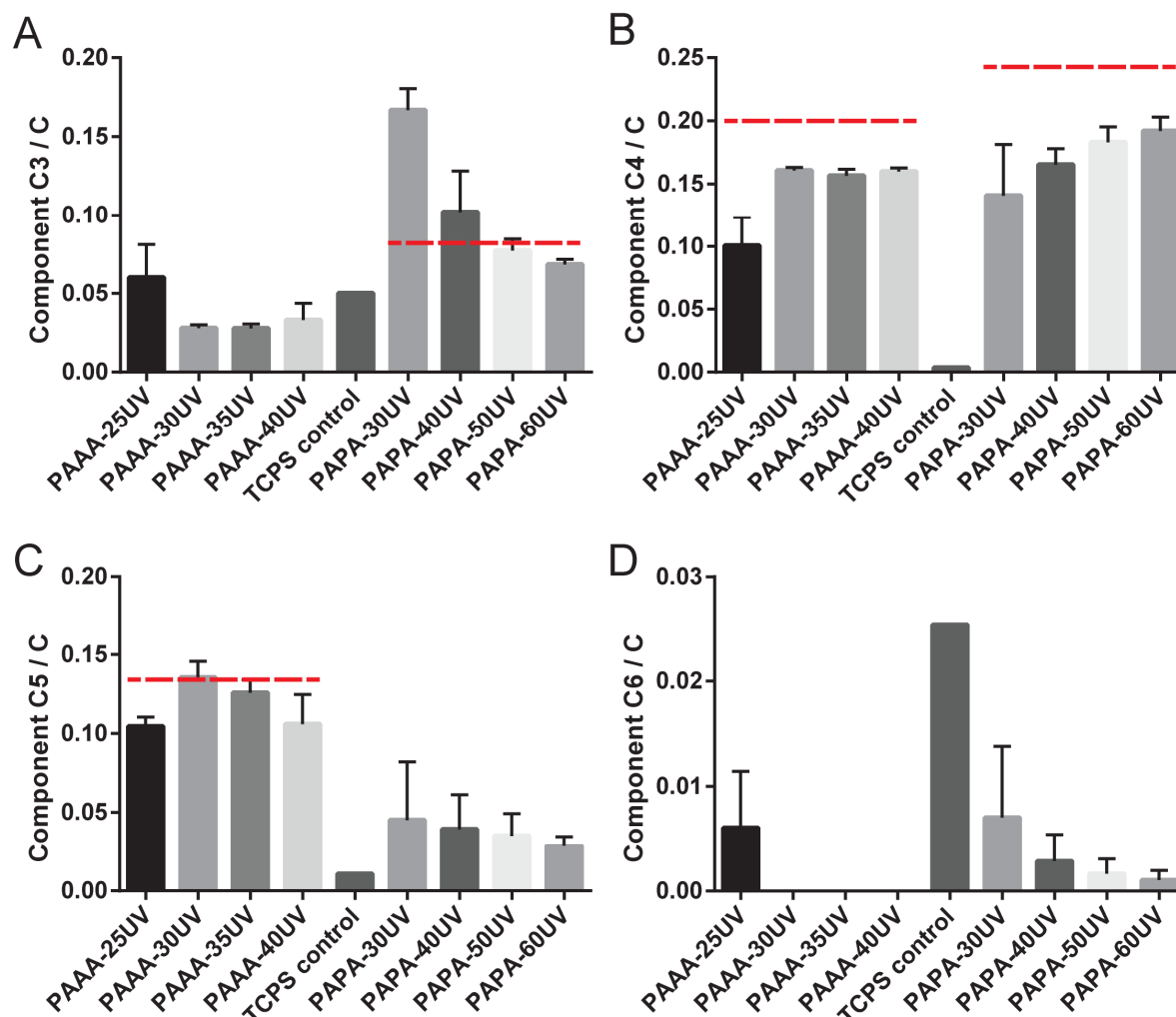


Figure 3.14: Component fitting results for high resolution C 1s spectra are presented from XPS analysis of polymer coatings. PAAA coatings generated with 25, 30, 35 and 40 UV exposures and with PAPA coatings generated with 30, 40, 50 or 60 UV exposures were analysed alongside a TCPS control. Percentage values of total carbon are presented for components (A) C3, (B) C4, (C) C5 and (D) C6 for each surface. Means and standard deviations are presented for each polymer coating from spectra acquired from three wells that were each assessed at three different locations. The mean result is also presented from spectra collected from three different locations in one clean TCPS well.

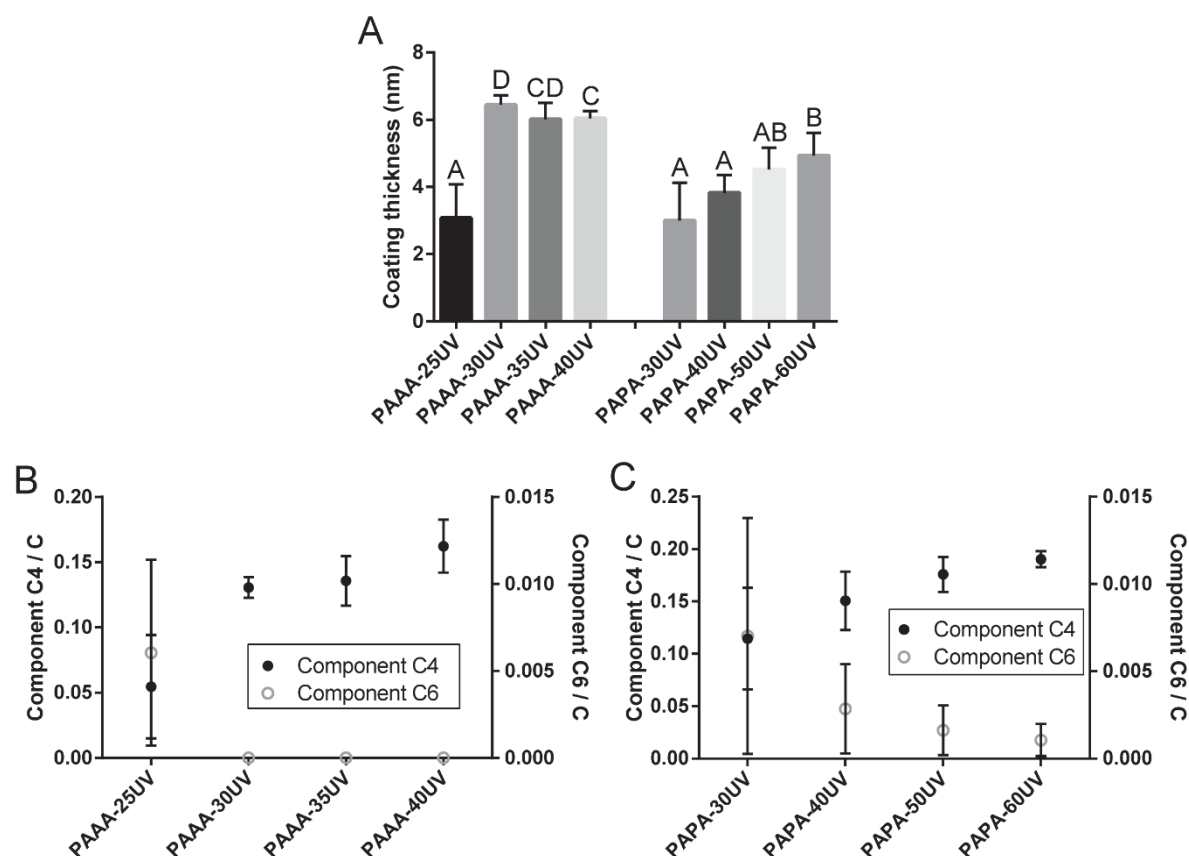


Figure 3.15: This figure presents XPS results that are indicative of coating thickness. (A) The thickness of PAAA coatings synthesised using 25, 30, 35 or 40 UV exposures and PAPA coatings synthesised using 30, 40, 50 or 60 UV coatings were calculated by applying the over-layer equation [1] to nitrogen atomic % data collected via XPS analysis. Different letters indicate statistically significantly different samples (unpaired Student's t-test, $p < 0.05$). Analyses of C 1s data is also presented for the same (B) PAAA and (C) PAPA coatings. Component C4/C (left y-axis) and C6/C ratios (right y-axis) are each plotted against the number of UV exposures used to generate the coatings. For each coating type, mean \pm SD is presented for spectra acquired from $n = 3$ wells that were each analysed at 3 different points.

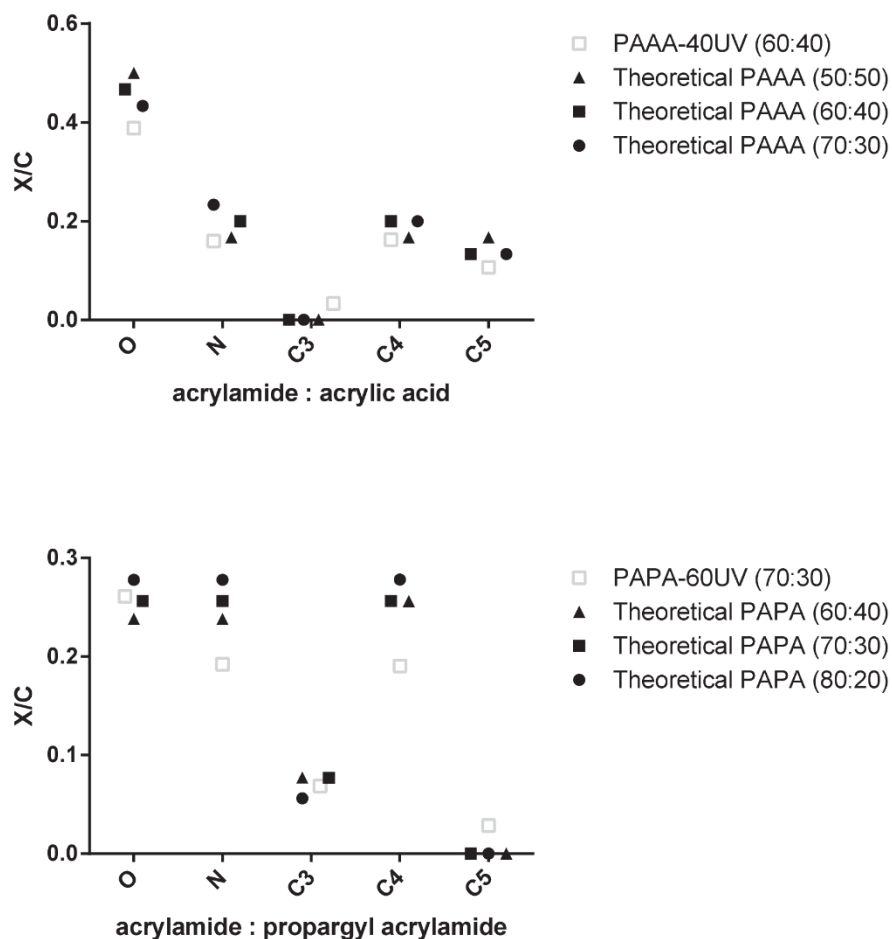


Figure 3.16: The scatterplots presented in this figure compare experimental XPS results from PAAA-40UV and PAPA-60UV coatings to theoretical results from polymers composed of a range of monomer ratios. (A) The theoretical elemental compositions of PAAA coatings containing 70:30, 60:40 and 50:50 molar ratios of acrylamide : acrylic acid are presented alongside the experimental elemental compositions of PAAA-40UV coatings that were synthesised from a 60:40 monomer feed solution. (B) The theoretical elemental compositions of PAPA coatings containing 80:20, 70:30 and 60:40 molar ratios of acrylamide : propargyl acrylamide are presented alongside the acquired elemental compositions of PAPA-60UV coatings that were synthesised from a 70:30 monomer feed solution. O/C, N/C, C³/C, C⁴/C and C⁵/C values are presented. The experimental results presented are the mean result of spectra acquired from $n = 3$ wells that were each analysed at 3 different points.

3.3.5 Physical and mechanical characterisation of PAAA and PAPA coatings

Atomic force microscopy (AFM) is able to sensitively assess the hydrated thickness and stiffness (elastic modulus) of surfaces by measuring the interaction between a spherical silica particle and the coating of interest. The measurements are carried out in aqueous media, allowing direct assessment of the thickness and stiffness of polymer coatings under conditions relevant to hPSC culture. However, this technique cannot determine the absolute hydrated thickness of coatings, since an independent measure of surface separation is not possible. Nonetheless, in most cases, this error is relatively small. AFM is a scanning probe microscopy that is typically used in imaging mode, which involves rastering a sharp tip attached to a cantilever spring over a surface and monitoring the force of interaction. In the experiments undertaken in this thesis, the sample was not scanned, but was simply moved towards a cantilever spring onto which a spherical silica particle was glued. A force curve is generated by measuring the bending of the spring (Figure 3.17) relative to motion of the piezoelectric crystal in the direction normal to the surface of the sample. The amount of force required to deform the materials, and therefore the material stiffness, was then assessed by comparison to model predictions as described in Section 3.2.4.

As illustrated in Figure 3.17, as the distance between probe and surface decreased (reading plots from right-to-left) the force remained zero and was represented by a horizontal line at a force of zero. At the point of first interaction with the surface (arrows) the line began to curve upwards as compression of the surface coating exerted force on the probe. After the initial kick-off, the force increased at a variable rate, which is related to the stiffness of the coating as detected by the probe as it is pushed further into the surface. Finally the surface reached a point of full compression, which has been assigned a zero separation distance value, after which the probe was retracted.

Careful assignment of the kick-off point and the point of full compression allowed assessment of coating thickness (Figure 3.18). It was observed that PAAA-40UV coatings were consistently ~90 nm thicker than batch-paired PAAA-25UV coatings, while little or no difference in thickness was observed between PAPA-30UV and PAPA-60UV coatings. Although batch-to-batch variation obscured statistical analysis, the PAAA-25UV, PAPA-30UV and PAPA-60UV coatings appeared to each be approximately 150 nm thick, and the PAAA-40UV coatings were approximately 300 nm thick.

In order to assess the intrinsic stiffness of the polymer coatings, force data that had been acquired by AFM was interpreted using the Hertz theory with thin film correction applied (Dimitriadis et al., 2002). The force profiles of PAAA-25UV and PAAA-40UV coatings were similar in form and could be fitted using theoretical curves of deformation calculated using a modulus of less than 250 Pa (Figure 3.19). PAPA-30UV and PAPA-60UV coatings were each observed to be intrinsically stiffer than both of the PAAA coatings. Data acquired from PAPA-30UV coatings could be fitted with theoretical data generated using moduli between 250 Pa and 500 Pa, and data acquired from PAPA-60UV coatings

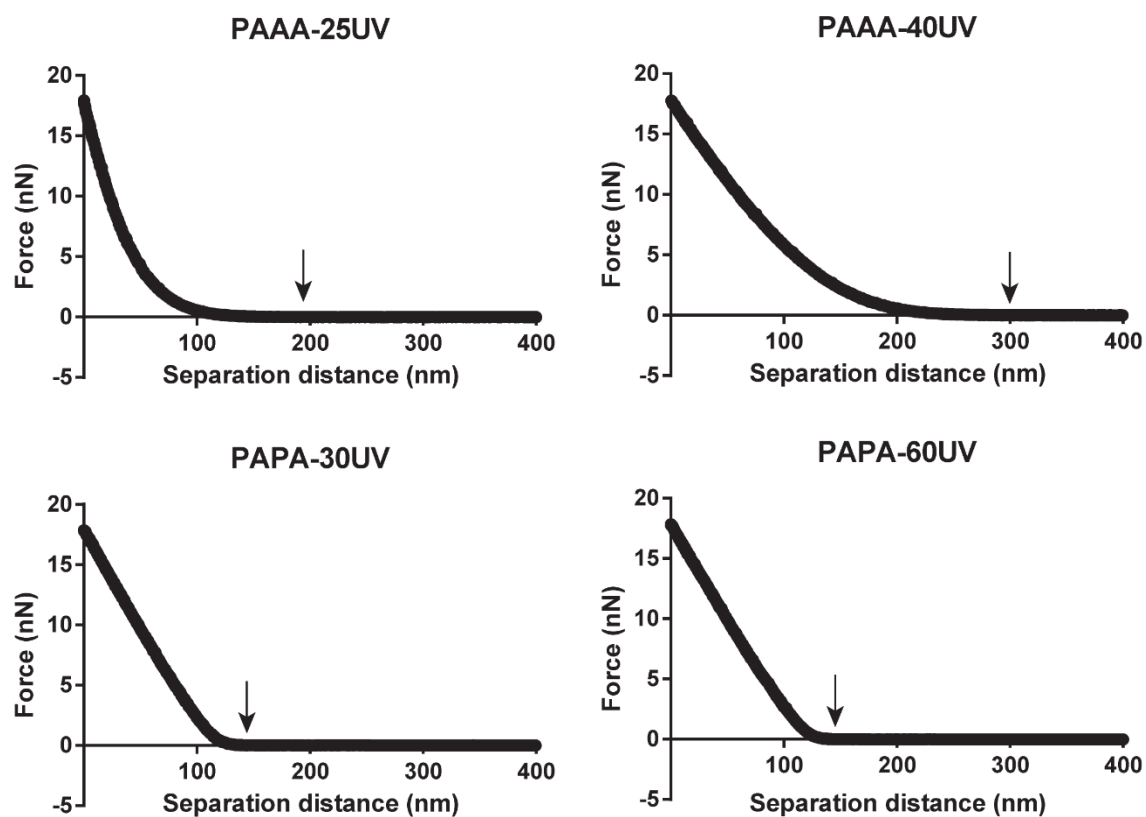


Figure 3.17: Representative force curves are presented for PAAA-25UV, PAAA-40UV, PAPA-30UV and PAPA-60UV coatings. The force (y-axis) experienced by the probe as it is approached by and presses into the coating is plotted against the separation distance (x-axis) of the probe from the point of greatest surface compression ($x=0$). Arrows indicate “kick-off” points at which the probe first interacts with each surface. It can be observed from these plots that the force curves acquired from PAAA (top) surfaces were broader than those acquired from PAPA (bottom). The curves acquired from PAAA-40UV coatings (top-right) appeared to be the broadest.

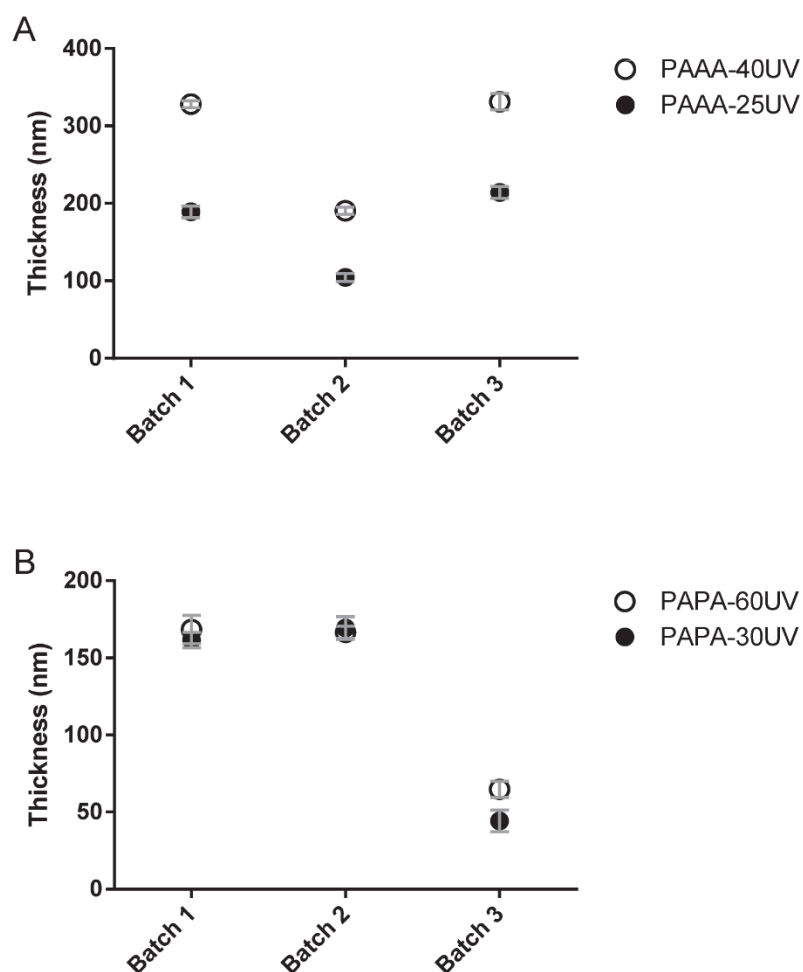


Figure 3.18: The hydrated thicknesses of polymer coatings were assessed by AFM analysis. Three batches of (A) PAAA and (B) PAPA coatings were assessed. Each batch included low-exposure (PAAA-25UV, PAPA-30UV, full circles) and high-exposure (PAAA-40UV, PAPA-60UV, hollow circles) coatings. Mean and standard deviations are presented from five replicate curves acquired from each surface. Results are grouped by batch to account for batch-to-batch variation.

could be fitted using theoretical data generated using moduli between 500 Pa and 1000 Pa (Figure 3.19). This increase is probably a result of cross-linking caused by additional UV exposures. However, thin film corrected analysis only assesses the stiffness of the outer portion of the coating, independent of the underlying substrate. In reality, when two otherwise identical coatings are applied to a stiff surface, the thinner coating will appear to be stiffer due to contribution from the underlying substrate in the same way that short hair is stiffer than a long hair. Only after a certain thickness has been reached will the stiffness of the underlying substrate be undetectable. Representative force curves acquired from each coating (from Figure 3.17) are overlaid in Figure 3.20 and magnified plots of the kick-off points are also included to illustrate the region of the curve that is assessed by the Hertz thin film correction model (inset).

It was observed that the kick-off profiles (Figure 3.20, inset) for coatings of either type were very similar in form regardless of the number of UV exposures that had been involved in synthesis. Force profiles acquired from the two PAAA surface coatings were observed to have a gentler slope than the force profiles obtained from the PAPA surface coatings, which varied very quickly over the same range of piezo travel. This low force (low indentation) region at the surface of the coating is the region that was assessed by the Hertz thin film corrected analysis presented in Figure 3.19. Whilst this region is accessible for fitting to theoretical expectations, the most evident differences in stiffness (slope) between force curves acquired from PAAA-25UV and PAAA-40UV coatings were observed deeper into the coatings, where the resistant force of the coating reached 1-10 nN. The slope of the curve acquired from PAAA-40UV appeared to differ from the slope acquired from PAAA-25UV and the PAPA coatings, by more across this range than in the lower compression force data range. The higher compression force data range is therefore likely to be of more relevance to hPSC behaviour, however this region cannot be reliably assessed using Hertz theory, which requires low degrees of strain. It is clear that the PAPA coatings were thinner and stiffer than the PAAA coatings and that the compression distance over which the stiffness increases is much smaller for the PAPA surfaces than the PAAA surfaces. Determining the exact mechanical structure of the coatings and how they change with separation distance would require a detailed analysis that is outside the scope of this thesis. Such constraints are not present for studies that have used thick hydrogel samples to test the influence of surface modulus on cell behaviour since such thick samples have a more consistent modulus through the depth of the hydrogel. However, an intention of this thesis was to produce surface-coated materials that were useful from a real world cell culture point of view, in materials used routinely by cell biologists and that could potentially be translated to a manufacturing process. Whilst it was not possible to give exact quantitative numbers for the “effective modulus”, i.e. that of the combined coating and underlying substrate, we have undoubtedly verified that hPSCs prefer to grow on stiffer PAAA and PAPA coatings, and that hPSC adhesion efficiency is reduced on thicker PAAA coatings which can mask the stiffness of the underlying substrate.

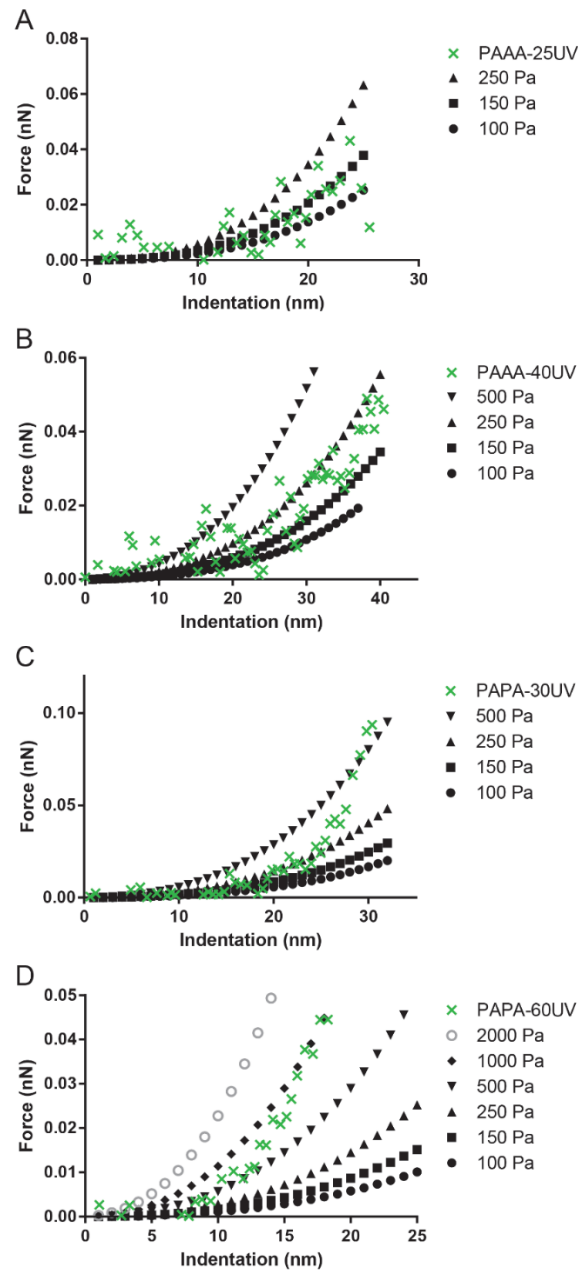


Figure 3.19: The intrinsic stiffness of polymer coatings was assessed by applying the Hertz thin film correction model to representative force curves collected via AFM (see Figure 3.17). Representative force curves acquired from the four polymer coatings were modelled against theoretical curves from surfaces of defined stiffness. (A) A representative force curve acquired from PAAA-25UV is plotted against theoretical curves from surfaces with Young's moduli of 100 Pa, 150 Pa and 250 Pa. (B) A representative force curve acquired from PAAA-40UV is plotted against theoretical curves from surfaces with Young's moduli of 100 Pa, 150 Pa, 250 Pa and 500 Pa. (C) A representative force curve acquired from PAPA-30UV is plotted against theoretical curves from surfaces at 100 Pa, 150 Pa, 250 Pa and 500 Pa. (D) A representative force curve acquired from PAPA-60UV coatings were also modelled against theoretical surfaces of defined stiffness at 100 Pa, 150 Pa, 250 Pa, 500 Pa, 1000 Pa and 2000 Pa.

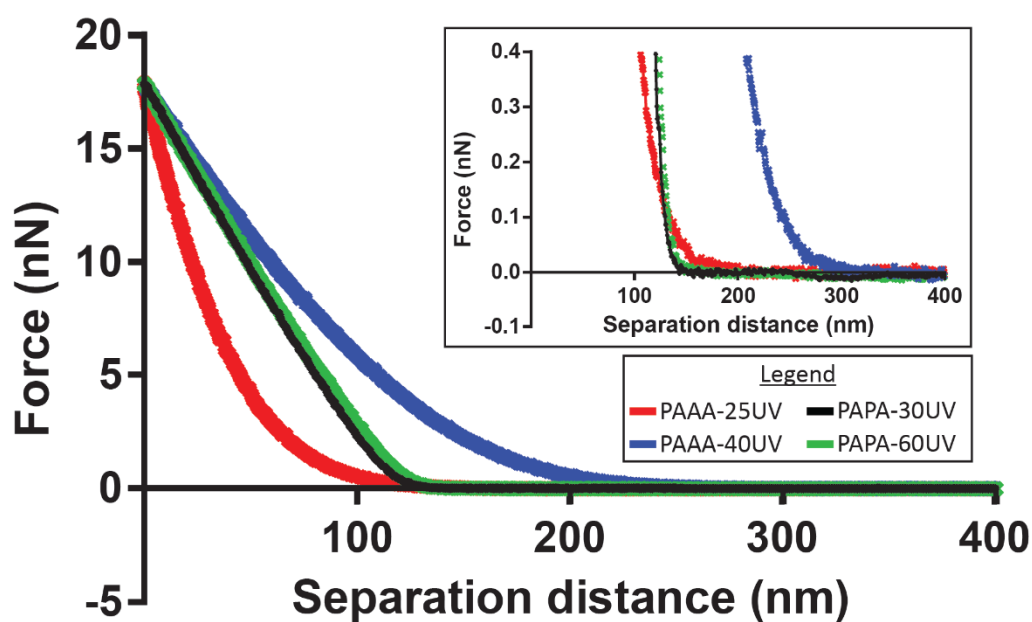


Figure 3.20: Typical force curves acquired from PAAA and PAPA coatings generated with high and low numbers of UV exposures are overlaid and magnified. The curves from PAAA-25UV (red), PAAA-40UV (blue), PAPA-30UV (black) and PAPA-60UV (green), that are also presented in Figure 3.17. The magnified base of the curve is also presented (inset).

3.3.6 Assessing the peptide density required to mediated hPSC adhesion

In order to assess the minimum surface peptide concentration required to support hPSC adhesion, a DELFIA Eu-tagging assay was performed. For this assay, cRGDfK-N3 peptide was tagged with a complex that contained reversibly chelated Europium (Eu^{3+}) (see Section 3.2.5 for details).

In three independent experiments, diluted Eu-tagged peptide was coupled to triplicate wells of PAPA-30UV coated 24-well plates that had been synthesised in three different batches. Plates modified in parallel with non-tagged peptide served as inbuilt controls for adhesion of H9-OCT4-mCherry, H9 and NHF-1-3 hPSCs respectively, and were assessed by MTS assay. The reaction conditions and cell quantification methods were performed exactly as in previous experiments (Figure 3.9) except for the use of buffers as described in Section 3.2.5.3. As observed in the previous experiment, no adherent hPSCs were observed on cRGDfK-PAPA coatings that had been modified with solutions containing 0.125 μM or 0.25 μM cRGDfK-N3 peptide, which corresponded to surface peptide densities of >0.5 pmol/cm² (Figure 3.21). Wells modified with solutions containing 1 μM cRGDfK-N3 peptide were observed to contain significantly higher surface peptide densities (~ 3.6 pmol/cm²) and the control wells consistently bound ~ 70 % as many cells as GeltrexTM-coated control wells (Appendix 5.3). Surfaces modified with solutions containing 0.5 μM cRGDfK were calculated to contain a low surface peptide density (~ 0.5 pmol/cm²) that was not significantly higher than wells modified with 0.125 μM or 0.25 μM peptide reaction solutions. High cell numbers were occasionally observed to bind to these surfaces, but not as consistently as in the earlier experiment (compare Appendix 5.3 to Figure 3.9). Unfortunately it is unclear whether this difference was due to inconsistent surface peptide density between the two surfaces or due to variation between the hPSC cultures, although H9 cells used in this adhesion assay were also observed to bind poorly to GeltrexTM-coated surfaces. The total absence of bound cells observed in the Cu-free control wells highlighted the specificity of the CuAAC reaction. These wells contained background levels of Eu that were statistically inseparable from the wells modified with solutions of 0.5 μM cRGDfK-N3, yet bound fewer cells than any other and it was interesting to note that a similar level of fluorescence was detected in these wells to the wells modified with solutions containing 0.5 μM . It is likely that Eu detected in the Cu-free control wells was liberated from peptide that had simply adsorbed to the well. It's possible that a greater amount of peptide was non-specifically adsorbed to the 1 μM Cu-free control wells than was chemically bound to the 0.5 μM wells, yet this did not result in any observable hPSC adhesion. These results highlight the importance of ligand orientation and stability, and indicate that the threshold density of cRGDfK peptide for hPSC adhesion is between 0.5 pmol/cm² and 3.6 pmol/cm² and is likely to be at the lower end of this range.

3.3.7 Cytotoxicity testing of PAAA and PAPA

In order to assess the suitability of PAAA and PAPA coatings for hPSC culture, and to ensure that any differences in cell culture results between the two coatings could not be attributed to the presence of cytotoxic chemicals, an MTS-based cytotoxicity assay was performed as described in Section 3.2.6. No cytotoxic effect was observed in cultures treated with extraction solutions derived from wells coated with either PAAA or PAPA (Figure 3.22).

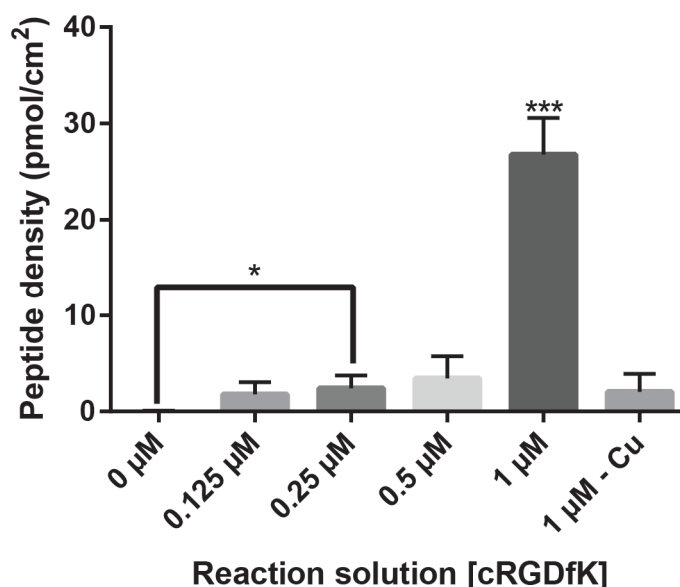


Figure 3.21: This figure compares (x-axis) the concentration of cRGDfK peptide included in CuAAC reaction solutions to (y-axis) the surface peptide density in cRGDfK-PAPA coatings. PAPA coatings were modified with reaction solutions containing 0.125 µM, 0.25 µM, 0.5 µM and 1 µM of Eu-tagged peptide or with control reaction solutions in which either peptide (0 µM) or copper catalyst (1 µM - Cu) was omitted. Surface peptide density was assessed by a DELFIA Eu-N1 ITC chelate assay. The means of three independent experiments are presented. Error bars represent standard deviation from the mean. An asterisk (*) indicates a statistically significant difference ($p < 0.05$) identified by an unpaired Student's t-test, *** indicates data that are extremely significantly ($p < 0.001$) different to all other data points.

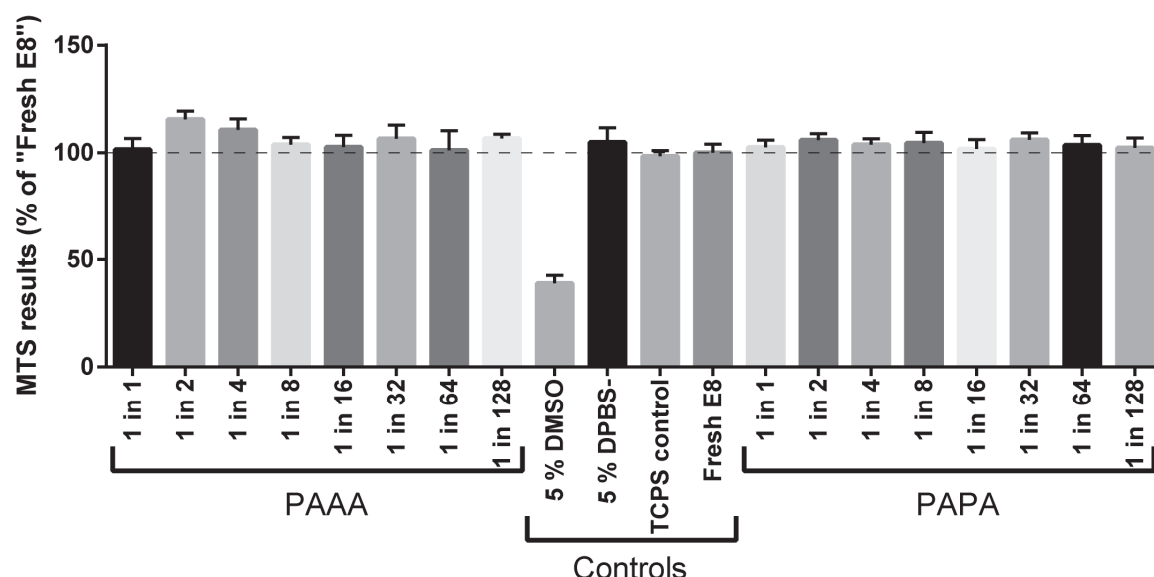


Figure 3.22: The results of an MTS-based cytotoxicity assay (Section 3.2.6) are presented for PAAA (left) and PAPA (right) coatings. Wells of PAAA- and PAPA-coated 24-well plates were put through their respective peptide modification processes (Sections 2.5.2 and 2.5.3, respectively) in the absence of peptide. Extraction solutions of E8 basal medium were incubated in the faux-modified wells for 66 hours to extract any potential cytotoxic chemicals. A control extraction was also performed on clean TCPS wells (TCPS control) to account for any breakdown in essential medium components over time. Day 2 cultures of H9-OCT4-mCherry cells on Geltrex™-coated 96-well plates were maintained for 24 hours in extraction solutions that had been serially diluted through E8 medium. Control cultures were exposed to E8 medium that had been properly stored (Fresh E8), a negative control solution of 5 % DMSO in E8 medium and a vehicle control containing 5 % DPBS-. An MTS assay was used to quantify H9-OCT4-mCherry cell numbers after exposure to control or serially diluted test solutions, and the results of that assay are presented in this figure. Mean \pm SD of $n = 6$ replicate wells are presented for each condition as a proportion of the mean result for "Fresh E8" control (dotted line).

3.3.8 hPSCs adhesion to and shelf life testing of cRGDfK-PAPA coated flasks

Due to the low amounts of peptide required to produce cRGDfK-PAPA coatings, the associated cost reduction, the preference of hPSCs for stiffer substrates and the ability to modify these surfaces with any azide-functionalised molecules, PAPA PAPA-30UV coatings were selected for scale up and applied to 25 cm² flasks as described in Section 2.5.1. cRGDfK-N3 modification of these coatings was performed using CuAAC chemistry as described in Section 2.5.3. PAPA coatings were modified with reaction solutions containing an excess (36 µM) of cRGDfK-N3 to ensure reliable hPSC attachment.

To establish the shelf-life of this prospective commercial product, 25 cm² flasks coated with cRGDfK-PAPA-30UV were stored under DPBS- at 4 °C. After 6 months of storage, three cRGDfK-PAPA flasks were seeded with H9 hPSCs at a density of 15 000 cells/cm². The cells seeded at a high density and formed morphologically normal colonies and exhibited a typically low amount of cell death. The cultures reached 60 % confluence and were ready to harvest 4 days after seeding as had been observed with newly-modified flasks. cRGDfK-PAPA-coated flasks have been stored for up to 12 months with no noticeable effect on adhesion of morphologically normal cultures of hPSCs (Figure 3.23).

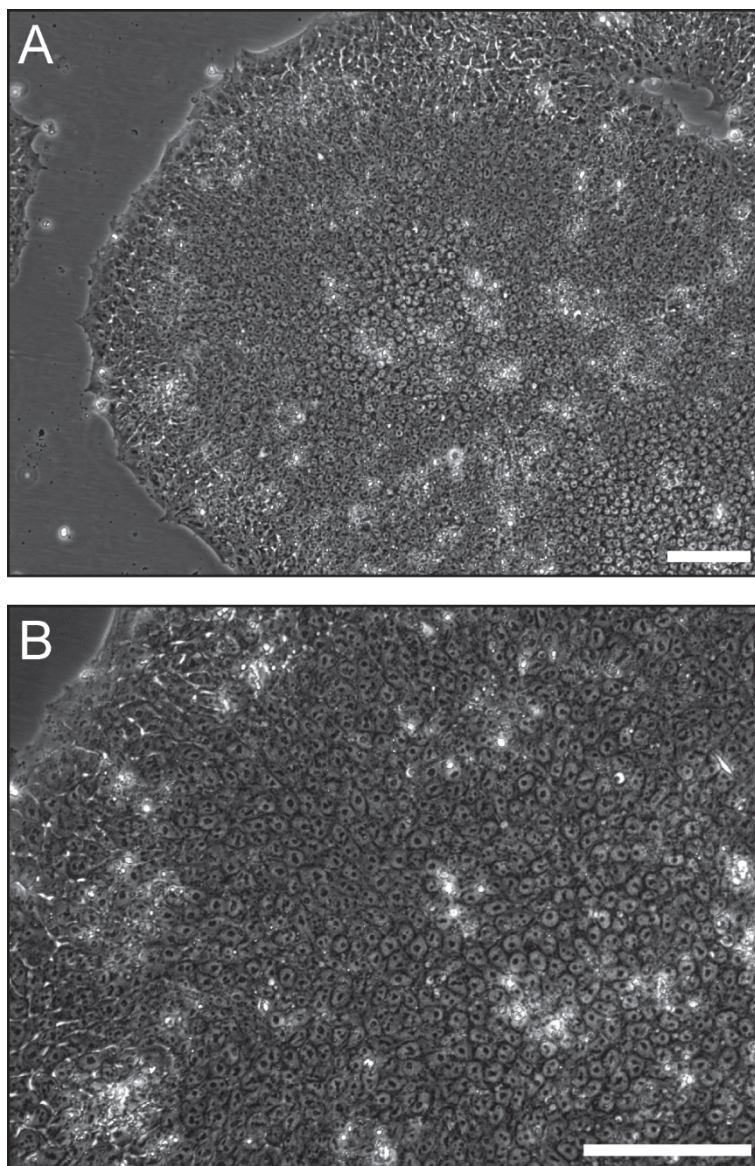


Figure 3.23: Phase contrast photomicrographs are presented of H9 cells attached to a 12-month-old cRGDfK-PAPA culture surface. Flasks were coated with PAPA, modified with cRGDfK peptide and then stored at 4 °C under DPBS- + 1 % antibiotic-antimycotic. After up to 12 months of storage, flasks were rinsed twice with DPBS- and seeded with H9 cells that had been harvested with EDTA from cultures maintained in E8 medium on Geltrex™-coated flasks. Phase microphotographs of a H9 colony in a 12-month-old cRGDfK-PAPA flask were captured at (A) 100x and (B) 200x magnification. Scale bars represent 100 μm.

3.4 Discussion

Defined, xeno-free culture conditions will contribute to the development of therapeutic applications of hPSC, and understanding the minimum environmental requirements for maintaining hPSCs will contribute to the optimisation of such conditions. The optimisation and characterisation of cRGDfK-PAAA and cRGDfK-PAPA coatings as hPSC culture surfaces was described in this chapter. These coatings are chemically defined, xeno-free, synthesised using a scalable manufacturing process and were able to adhere and maintain short-term culture of hPSCs in combination with E8 medium, the most chemically simple hPSC medium available. Furthermore, harvesting of hPSCs only required the use of EDTA (i.e. enzymes were not required).

PAAA and PAPA coatings were each synthesised by repeated exposure of mixed monomer solutions to high intensity UV light, which resulted in grafting of polymer brush coatings from the underlying TCPS surface. Each UV exposure is thought to initiate the covalent addition of monomer subunits to polymer chains that graft from the underlying TCPS in a loosely controlled manner. The expected result is a complex structure of soft and flexible polymer chains that becomes thicker with each exposure to UV light as it grows away from the underlying TCPS.

TCPS coated with PAAA and PAPA coatings that had been generated with increasing numbers of UV exposures were subjected to physicochemical analysis by XPS and AFM. According to these analyses, PAAA and PAPA coatings each reached a dry thickness of ~3 nm (Figure 3.15) after a similar number of exposures (25 and 30, respectively) (Figures 3.15). These coatings swelled to a hydrated thickness of ~150 nm (Figure 3.18). Additional UV exposures resulted in further growth of PAAA coatings, such that PAAA-40UV coatings had a dry thickness that exceeded the sampling depth of XPS analysis, and a hydrated thickness of approximately 300 nm (Figure 3.18). On the other hand, considerably less growth was observed in PAPA coatings, with the thickness of PAPA-60UV coatings only reaching a dry thickness of ~5 nm (Figure 3.15), and a hydrated thickness that was indistinguishable from PAPA-30UV coatings by analysis of AFM force curve (Figure 3.18), despite polymerisation of this coating being activated by 20 additional UV exposures. The slow (if any) growth of PAPA coatings and the increase to the intrinsic stiffness (Figure 3.18) of PAPA coatings could be due to the unprotected alkynes in propargyl acrylamide monomers failing to polymerise and forming crosslinks instead.

The changes to surface thickness were consistent across three batches of plates, however batch-to-batch variation was observed in the absolute thickness of polymer-coatings, which obscured statistical analysis of these trends. This batch-to-batch variation could be attributed to difficulties in standardising steps of the coating procedure using the current workflow since the duration of the UV exposures and the time between each exposure has been observed to influence polymer formation (Ameringer et al., 2014). Potential sources of variation in the workflow used to synthesise these surfaces included the time involved in manual transportation of vessels that contained mixed monomer solutions from the glove box on the first floor to the UV lamp set up on the second floor, and repeated manual transfer of vessels back to the start of the conveyor belt. The timing of these steps could be readily standardised in an automated manufacturing plant and would reduce batch-to-batch variation.

Increasing the number of UV exposures that were used to generate cRGDfK-PAAA coatings from 25 to 40 was observed to result in reduced hPSC adhesion efficiency (Figure 3.10A), a correlation that was not observed for cRGDfK-PAPA coatings (Figure 3.10B). It was hypothesised that this difference in cellular response was related to the growth profiles of each coating and the corresponding variation in stiffness resulting from combinations of coatings and the stiff underlying TCPS (Section 3.3.5).

A large body of work has been directed at the effects of substrate stiffness on cultured cells using a wide range of cell types and culture surfaces, which can make direct comparisons between studies difficult to interpret. Reports of cellular responses to increasing substrate stiffness have included increased spreading of smooth muscle cells (Engler et al., 2004), the activation of integrin-ligand complexes (Du et al., 2011), increased formation of focal adhesions (Fu et al., 2010) and the induction of differentiation bias of hMSCs towards stiffer cell types (Engler et al., 2006). The results of these studies and more have been summarised in a number of reviews (Murphy et al., 2014, Trappmann and Chen, 2013, Di Cio and Gautrot, 2016). Responses to substrate stiffness have been observed to vary between cell types, so the present discussion will focus on the reported responses of pluripotent stem cells to substrate stiffness.

By applying mechanical stress to mPSC colonies cultured on collagen-coated TCPS, and quantifying the resulting strain, Chowdhury et al. (2010b) determined that the cells are intrinsically soft (0.5 kPa to 2 kPa). When cultured on surfaces of equivalent stiffness, mPSCs were observed to spread out more (Chowdhury et al., 2010b) and to remain pluripotent in the absence of key growth factor LIF (Chowdhury et al., 2010a). A similar intrinsic stiffness (0.4 kPa to 1.0 kPa) has been assigned to hPSC colonies cultured on Matrigel™-coated TCPS (Hammerick et al., 2011). However, despite a range of publications reporting that cells “prefer” substrates of matching stiffness, the results presented in this chapter and in other publications (summarised in Table 3.3) indicate that hPSCs adhere more efficiently to stiffer surfaces.

Briefly, approaches for altering surface stiffness have included cross-linking by altering the composition of the monomer feed solution (Li et al., 2006) glutaraldehyde-induced crosslinking (Keung et al., 2012) and changing the length of flexible microposts (Sun et al., 2012), although none of these approaches can modify the stiffness of a surface in isolation from all other physiochemical changes (Trappmann and Chen, 2013).

It has been reported that hPSCs bind with a reduced efficiency to softer (0.1 kPa) acrylamide-based hydrogels than stiffer (73 kPa) surfaces (Keung et al., 2012) and that culturing hPSCs on 3D PEG-based hydrogels of reduced stiffness can result in increased apoptosis compared to stiffer hydrogels (Jang et al., 2013). Downregulation of OCT4 has also been observed in hPSCs after 24 hours on soft (1.92 kPa) compared to stiff (1218.4 kPa) vitronectin-coated PDMS micropost substrates. Furthermore, since soft (0.7 kPa), Matrigel™-coated hydrogels have failed to adhere as many cells as stiff (10 kPa) Matrigel™-coated hydrogels, the effect of stiffness appears to be ligand independent, assuming the same amount of Matrigel™ adsorbed onto each surface (Musah et al., 2012).

Table 3.3: Summary of studies in which the stiffness of hPSC culture surfaces have been assessed. The types of surfaces used, cell lines screened and moduli tested (“soft”, “moderate” and “stiff”; kPa) are presented along with cellular responses that were observed in hPSCs in response to surfaces of different stiffness, if a direct comparison was made. N/A indicates either that a surface of intermediate stiffness was not produced or that mechanical stiffness was not tested. HDF, human dermal fibroblasts; PDMS, polydimethylsiloxane; PEG, polyethylene glycol; PEGNB, poly(PEG norbornene-*co*-PEG dithiol); PVA-IA, poly(vinyl alcohol-*co*-itaconic acid).

Reference	Surface type	hPSC line(s)	“Soft” (kPa)	“Moderate” (kPa)	“Stiff” (kPa)	Response to increase in stiffness
Current study	cRGDfK-PAAA	H9-OCT4-mCherry, H9, NHF-1-3	0.1-0.25	N/A	0.15-0.25	More cells bound to stiffer surfaces
Current study	cRGDfK-PAPA	H9-OCT4-mCherry, H9, NHF-1-3	0.25-0.5	N/A	0.5-1	No response, also no difference in stiffness
(Sun et al., 2012)	PDMS microposts coated with vitronectin	H1 and H9	1.92	14.22	1218.4	More cells stained positive for OCT4 by immunostaining after 24 hours without supplementation with FGF-2
(Keung et al., 2012)	Polyacrylamide- <i>co</i> -bisacrylamide hydrogels	WA01, hMSC-iPS hiPSCs	0.1	0.7	73	Colony area correlated with surface stiffness. Soft surfaces promoted early neurogenesis. No difference in cell numbers was observed.

(Musah et al., 2012)	Polyacrylamide-co-bisacrylamide hydrogels	H1, H7, H9, H14, SA02	0.7	3	10	Cells detached from the soft surface by 7 days post-seeding. Cells remained attached to stiffer surfaces.
(Musah et al., 2014)	Polyacrylamide-co-bisacrylamide hydrogels OR (PEGNB hydrogels)	SA02, H1, H7, H9	0.7	3	10	YAP/TAZ localised to the nucleus. Neurogenesis was impaired.
(Jang et al., 2013)	3D PEG hydrogels	H9, H1, Novo	N/A	N/A	N/A	Cell adhesion improved, hPSCs did not bind to softer hydrogels.
(Park et al., 2015)	Polydopamine coating	H9, CCALD-hiPSCs	N/A	3×10^5	N/A	Only one stiffness was tested. hPSCs attached efficiently to this surface.
(Higuchi et al., 2014)	Polyacrylamide hydrogels coated with gelatin	New iPSCs from HDF	0.5	N/A	4	HDFa cells reprogrammed less efficiently into iPSCs on TCPS compared to soft hydrogels.
(Higuchi et al., 2015)	Glutaraldehyde cross-linked PVA-IA	WA09, HPS0077 (hiPSC)	10.3	25	30.4	25 kPa was deemed optimal for cell adhesion. Differentiation was observed after 5 days culture on 30.4 kPa surface.
(Oral et al., 2011, Alderighi et al., 2009)	Polystyrene				$>3 \times 10^6$	This measurement is included for comparison

An interesting application of the cellular response to surface stiffness is in the development of thermoresponsive hydrogels based on 2-(diethylamino)ethyl acrylate, that allow harvesting of hPSCs by simply transferring the culture to room temperature for 15 minutes (Zhang et al., 2013b). At the cooler temperature the hydrogels become more hydrated and cellular dissociation occurs. This effect is likely to be associated with changes in elastic modulus, although this was not assessed directly.

A substrate stiffness of 25 kPa has recently been reported to be optimal for hPSC attachment to glutaraldehyde-crosslinked acrylamide-based hydrogels (Higuchi et al., 2015). Attachment of two hPSC lines was reported to be significantly higher on coatings with an elastic modulus of 25.3 kPa coatings than on coatings with moduli of 15.8 kPa or 30.4 kPa. However, other studies have observed maintenance of hPSC cultures on far stiffer surfaces (Sun et al., 2012). Whilst the approach of grafting a soft coating from a stiff TCPS substrate does not allow us to quantify the effective modulus easily, it is reasonable to expect that the bulk modulus of PAAA and PAPA coatings would be in the low-to-moderate kPa range, intermediate between the 100's of Pa value of the coating itself and that of TCPS (2-3 GPa) (Alderighi et al., 2009) and that the actual value will vary based on the coating thickness and degree of crosslinking *etc.* of the coating. One important point to make here is that people have been maintaining hPSC cultures successfully for over a decade on thin coatings of Matrigel™. The other point is that a substrate composed of MEF feeder cells would have a wide variation in stiffness, between the soft MEFs and the ECM that they generate, whose stiffness would also be dependent on the amount of ECM that is deposited, but would likely be quite stiff. Similar adsorbed layers of fibronectin, vitronectin, Synthamax™ and StemAdhere™ are also thin and therefore the “effective moduli” of these coatings will be quite high.

A potential confounding factor for investigating the optimal stiffness of a cell culture substrate, aside from the use of different cell lines and of surfaces whose physicochemical properties differ by more than just stiffness (Trappmann and Chen, 2013), is in the difference between how cells and analytical methods each determine surface stiffness.

As intrinsically soft polymer brush coatings like PAAA and PAPA grow thicker, the stiffness of the underlying TCPS has a reduced contribution to the apparent stiffness at the surface of the coating, where interactions occur with a cell or a spherical indenter. For AFM analysis, a spherical indenter is pressed into the coating, while dissociated cells simply rest on the surface, probably compressing it slightly due to gravity. The cells then interact with the surface via CAM-ligand interactions, which transmit forces generated by fluid flow and by the actin-myosin cytoskeleton (Di Cio and Gautrot, 2016). Through these interactions, cells are thought to sense coating stiffness to a certain depth, and there is some evidence that hMSCs are able to sense the stiffness of an underlying glass substrate through collagen-coated polyacrylamide hydrogels with a modulus of 1 kPa to a depth of 5-10 μm (Buxboim et al., 2010), which is ~15 times thicker than any of the coatings reported in this study. This depth may vary between cell types and between the co-polymers, but the moduli measured by AFM or by other approaches, like rheology, may not accurately represent the physical environment experienced by the cells. It would be interesting

to model the forces through the depth of the coating, to assess how they change throughout the depth of the coating, although such models are unavailable to us at this time. Although the 20 nN force imparted onto a surface by an AFM probe could be assumed to be similar to the amount of force imparted by a cell settling, the cells attach to specific parts of the surface via CAM-ligand interactions, and forces are transferred to those interactions by the actin-myosin cytoskeleton, so any response to the surface stiffness by the cell will be different to the response of an AFM probe.

The effects of the underlying substrate stiffness on that of the overlying thin coatings, and the potential differences between stiffness as detected analytical approaches and stiffness as experienced by cells is rarely discussed, yet these effects may confound comparisons of cell responses to the stiffness of cell culture surfaces. It is therefore important to optimise the stiffness of hPSC culture surfaces by directly assessing the cellular response to a surface that can be manufactured at scale. Nevertheless, the present results correspond with the findings of a range of other studies by indicating that stiffer surfaces are preferred by hPSCs (Table 3.3).

The adhesion of hPSCs to PAAA and PAPA coatings was observed to vary not only as a function of surface stiffness, but also as a function of surface peptide density. The initial optimisation of polymer brush coatings (Figures 3.2 and 3.3) indicated that reaction solutions containing higher concentrations of peptide were required to mediate adhesion of hPSCs than was required to mediate adhesion of L929 fibroblasts or hMSCs. The input peptide concentrations at which hPSC adhesion to cRGDfK-PAPA surfaces failed was subsequently identified in the multivariate study (Figure 3.10) and the threshold surface density of cRGDfK peptide required to mediate hPSC adhesion to PAPA coated TCPS was subsequently assessed by a Eu-tagging assay (Figure 3.21).

Due to the range of characterisation methods that have been used to calculate surface ligand density in various studies, it is difficult to make direct comparisons. As discussed in Sections 1.6 and 1.8 of this thesis, peptide ligands and ECMPs have been variously adsorbed onto TCPS or used to modify a range of substrates using different chemistries, and often little attempt is made to quantify the surface ligand density. Input peptide/ECMP concentrations are usually reported, but this fails to account for adsorption or reaction efficiencies or for the orientation and bioavailability of the ligands.

Assessments of ligand density thresholds required for hPSC adhesion have included measuring the fluorescence intensity of gels that had been modified with fluorescently tagged peptides (Musah et al., 2012) (which allows relative but not absolute quantification) and calculating density based on the input molar concentration of peptide-presenting ATs to generate SAMs (Derda et al., 2007, Klim et al., 2010) (which assumes that both types of AT contribute equally and stably to the surface). XPS analysis has also been used for relative quantification of surface peptide density, but could not be used for absolute quantification (Higuchi et al., 2015).

In the current study, the threshold surface peptide density for hPSC adhesion to PAPA coatings was determined by a Eu-tagging assay to be between 0.5 pmol/cm² and 3.6 pmol/cm² (Figure 3.21). The threshold surface vitronectin density for hPSC adhesion has been reported to be 3.33

pmol/cm² by Ponceau S staining (where bound peptide is reversibly stained and the stain is then liberated and compared to standards of known concentration) and also by a Bradford protein assay (which quantifies the leftover peptide that remained in the post-reaction modifying solution) (Yap et al., 2011). Although this study by Yap et al. produced results consistent with the current study, the comparison comes with some caveats. While cRGDfK molecules constitute single ligands that interact with single ECMPs, vitronectin contains at least two binding motifs. So one mole of vitronectin contains at least twice as many potential ligands as one mole of cRGDfK. However, adsorbed vitronectin will also be deposited randomly, so each molecule would not be ideally orientated to present these binding sites, reducing the effective ligand density. It's also possible that the Europium assay, the Ponceau S staining and the Bradford assay could all be measuring ligand molecules that are on the surfaces but inaccessible to the cells. Regardless, the concentration of cRGDfK that was required to deposit sufficient cRGDfK peptide onto the surface to support hPSC adhesion was lower than was initially required for cRGDfK-PAAA coatings and far lower than the concentrations of RGD-containing peptides that have been reported in other studies.

The development of the Corning Synthemax™ hPSC culture substrate was reported in a study in which only surfaces modified with carbodiimide reaction solutions containing high (at least 500 µM) concentrations of peptide were able to support adhesion of hPSCs at a similar level to Matrigel™-coated surfaces (Melkounian et al., 2010). Although the amount of peptide actually used in the generation of Synthemax™ products has not been reported, a recent study from another laboratory reported that carbodiimide reaction solutions containing between 314 µM and 943 µM of peptide were required to produce surfaces that efficiently supported hPSC adhesion (Higuchi et al., 2015). This constitutes greater than a three-fold difference in the input peptide concentrations required to modify these surfaces and cRGDfK-PAAA with enough peptide ligand to mediate hPSC adhesion. Furthermore cRGDfK-PAPA coatings only require modification with solutions of peptide that are ~300-fold more dilute than the surfaces reported by Melkounian et al. (2010) and by Higuchi et al. (2015). This constitutes a considerable potential cost-reduction.

The ligand density of StemAdhere™ has not been assessed. StemAdhere™ is a fusion protein that adsorbs to the surface by a murine IgG1Fc domain, and presents an E-cadherin binding region. StemAdhere™ molecules are smaller than antibody molecules. Mouse and human IgG molecules are highly homologous. Coatings of human IgG antibodies adsorbed to TCPS have been measured density of 1.8 pmol/cm² and 14 nm thick, which equated to a monolayer of antibody molecules (Svensson and Arnebrant, 2012). Since StemAdhere™ molecules are smaller than antibodies and also form monolayers, the coatings would be expected to be slightly thinner and to have a slightly higher molecular density. The properties of StemAdhere™ are discussed further in Section 5.4.

hPSC adhesion has also been reported on SAMs that present the peptide GKKQRFHRNRKG (peptide 31 in the screen presented in Chapter 4) at a surface density as low as 3 pmol/mm² (Klim et al., 2010). Surface peptide density was calculated based on the proportion of input ATs that

were peptide-presenting, and this is a 1000-fold greater density than the threshold peptide density required for hPSC adhesion to cRGDfK-PAPA coatings.

The difference between the threshold concentration of cRGDfK peptide for hPSC adhesion to cRGDfK-PAPA coatings (1 μ M, Figure 3.10) and that was initially required to improve adhesion of H9-OCT4-mCherry cells to cRGDfK-PAAA (100 μ M, Figures 3.2 and 3.3) may have been due to a requirement for excess ligand density to compensate for suboptimal surface stiffness or to the greater efficiency of the CuAAC reaction compared to the carbodiimide chemistry. Generally speaking, it is expected that the Cu-mediated “click” reaction between an azide and an alkyne will be more efficient than an amide coupling between an amine and carboxylic acid, mediated by carbodiimide chemistry in aqueous media. However the chemistry used to couple cRGDfK peptide to PAAA was very similar to those used in the other studies with RGD-containing peptides, so reaction efficiency cannot explain the three-fold difference between cRGDfK-PAAA and those other surfaces.

The absence of a trend correlating hPSC adhesion to the concentrations of cRGDfK peptide used to modify PAAA surfaces in Figure 3.10A is most likely due to the surface peptide concentration being consistently higher than necessary for maximum attachment of H9-OCT4-mCherry cells. This result is inconsistent with the colony counting results presented in Figures 3.2 and 3.3. The apparent improvement in cell adhesion over time could be due to differences in the sensitivity of colony counting and MTS assays, where the decrease in colony numbers presented in Figures 3.2 and 3.3 could be offset by cells forming larger colonies on surfaces that were modified with reaction solutions containing 50 μ M cRGDfK peptide. Improved reaction efficiency and surface production with increased operator experience could also explain this difference.

At no stage throughout this study were any hPSCs observed to bind to polymer brush coatings unless they were modified with an appropriate peptide. The resistance of these coatings to background hPSC adhesion and the specificity of the catalytic peptide modification reaction was highlighted by the total absence of bound cells observed in the copper-free control PAPA-coated wells (Appendix 5.3). These wells contained background levels of Eu that were statistically inseparable from the wells modified with solutions containing less than or equal to 0.5 μ M cRGDfK-N3, yet cells often bound to those wells. Every single PAAA or PAPA coating that was modified with cRGDfK peptides over the course of this study, after the preliminary optimisation (Figures 3.2 and 3.3), was observed to consistently bind high numbers of hPSCs.

One of the most interesting findings presented in this chapter was that polymer brush coatings modified with cRGDfK-alone were suitable for adhering and maintaining short-term culture of hPSCs. The only previous study that reported adhesion of hPSCs to a cRGDfK-presenting surface observed that the cells would not adhere in the absence of a Rho-ROCK pathway inhibitor (Y-27632) and that differentiation occurred after three passages (Melkounian et al., 2010). This finding will be discussed further in the following chapter, which reports a screening experiment where PAAA and PAPA coatings modified with cRGDfK were compared to coatings modified with a library of known cell-binding peptides.

3.5 Chapter summary

In this chapter, two chemically defined polymer brush coatings were optimised for the maintenance of hPSC culture and characterised. The effect on hPSC adhesion of changing the number of UV exposures used to synthesise PAAA and PAPA coatings and of changing the concentration of cRGDfK peptide used to modify these surfaces was assessed. Furthermore the physicochemical effects of additional UV exposures on PAAA and PAPA coatings were characterised with XPS and AFM analysis and the threshold surface cRGDfK density required for hPSC adhesion was assessed with a Eu-tagging assay. It was observed that the elemental composition of the coatings reflected the molar ratio of the monomer feed solution, which indicated that the coating methodology produced predictable and consistent results. It was also observed that a surface density of at least 0.5-3.6 pmol/cm² of cRGDfK peptide ligand and an elastic modulus greater than 0.2 kPa were ideal conditions for hPSC adhesion. The chemical simplicity of these culture surfaces also made them ideal for investigating the ability hPSCs to adhere to specific peptide ligands (Chapter 4) and their scalability and simplicity make them a potential commercial hPSC culture surface, so the results of long-term maintenance of hPSC cultures on polymer brush coatings were also benchmarked against cultures maintained on Geltrex™, StemAdhere™ and Synthemax™ (Chapter 5).

Chapter 4:

Identification of peptides able
to mediate hPSC adhesion
to polymer coatings

4.1 Introduction

Maintenance of hPSC cultures has been reported in various media on a diverse range of surfaces, to which hPSC adhesion is mediated by different ligands {Nagaoka, 2010 #243;Melkounian, 2010 #244;Klim, 2010 #358;reviewed by \Lamshead, 2013 #454}. A wide range of peptide ligands reported to mediate hPSC adhesion have been identified by isolating the binding regions of ECMPs {Klim, 2010 #358;Melkounian, 2010 #244}, by screening randomly generated peptides using phage display {Derda, 2010 #135} or, as in the case of cRGDfK, by mimicking the binding sites of specific CAMs {Pierschbacher, 1987 #476}. As illustrated in Figure 4.1, the previous chapter described characterisation of the physicochemical properties of two cRGDfK peptide-presenting polymer coatings (PAAA and PAPA) and optimisation of PAAA and PAPA to support the short-term maintenance of H9-OCT4-mCherry cultures. This optimisation was performed using cRGDfK-modified coatings because they had previously supported adhesion and growth of other cell types (e.g. hMSCs) and hPSC attachment had been observed in preliminary studies using cRDfK-modified coatings. However, assessment of hPSC adhesion to cRGDfK-presenting surfaces had only been previously reported in one study {Klim, 2010 #358}, in which OCT4-expression was not observed to be maintained in hPSCs cultured on a streptavidin-coated TCPS surface modified with biotinylated cRGDfK-alone. The study by Klim et al. {, 2010 #358} compared hPSC adhesion to SAMs modified with nine different peptides and found that hPSC adhesion to SAMs modified with any of several HSPG-binding peptides was consistent when the surface peptide density was reduced, compared to SAMs modified with KGRGDS, to which a reduction in hPSC attachment was observed at a higher peptide density. cRGDfK-presenting SAMs were not assessed in the study by Klim et al. Furthermore, SAMs modified with the HSPG-binding peptide sequence GKKQRFHRNRKG (peptide 31 in the present study) were demonstrated to support the adhesion, proliferation and long-term maintenance of OCT4-expressing hPSC cultures. Another study {Melkounian, 2010 #244} compared hPSC adhesion to “peptide acrylate surfaces” that were modified with one of six RGD-containing peptides. The study by Melkounian et al. {, 2010 #244} reported that acrylate surfaces modified with either KGGNGEPRGDTYRAY or KGGPQVTRGDVFTM (peptides 34 and 35 in the current study) resulted in the adhesion of similar numbers of hPSCs to Matrigel™-coated control surfaces, although surfaces modified with cRGDfK or peptide 31 were not tested in the Melkounian study. In order to identify the most suitable peptide ligand(s) for PAAA and PAPA coatings as hPSC culture surfaces, a recent literature search performed in the Meagher laboratory identified all peptides with reported roles in cell adhesion. In the present chapter, 36 of these peptides were screened in the context of PAAA and PAPA coatings for their ability to support the adhesion, proliferation and maintenance of mCherry of H9-OCT4-mCherry hPSCs. The screen was conducted to complete optimisation of a lead hPSC culture surface from the brush polymer coatings optimised in Chapter 3 of this thesis. Chapter 5 describes an experiment in which long-term maintenance of hPSC cultures is performed on the lead surface and benchmarked against cultures maintained on commercially available culture surfaces.

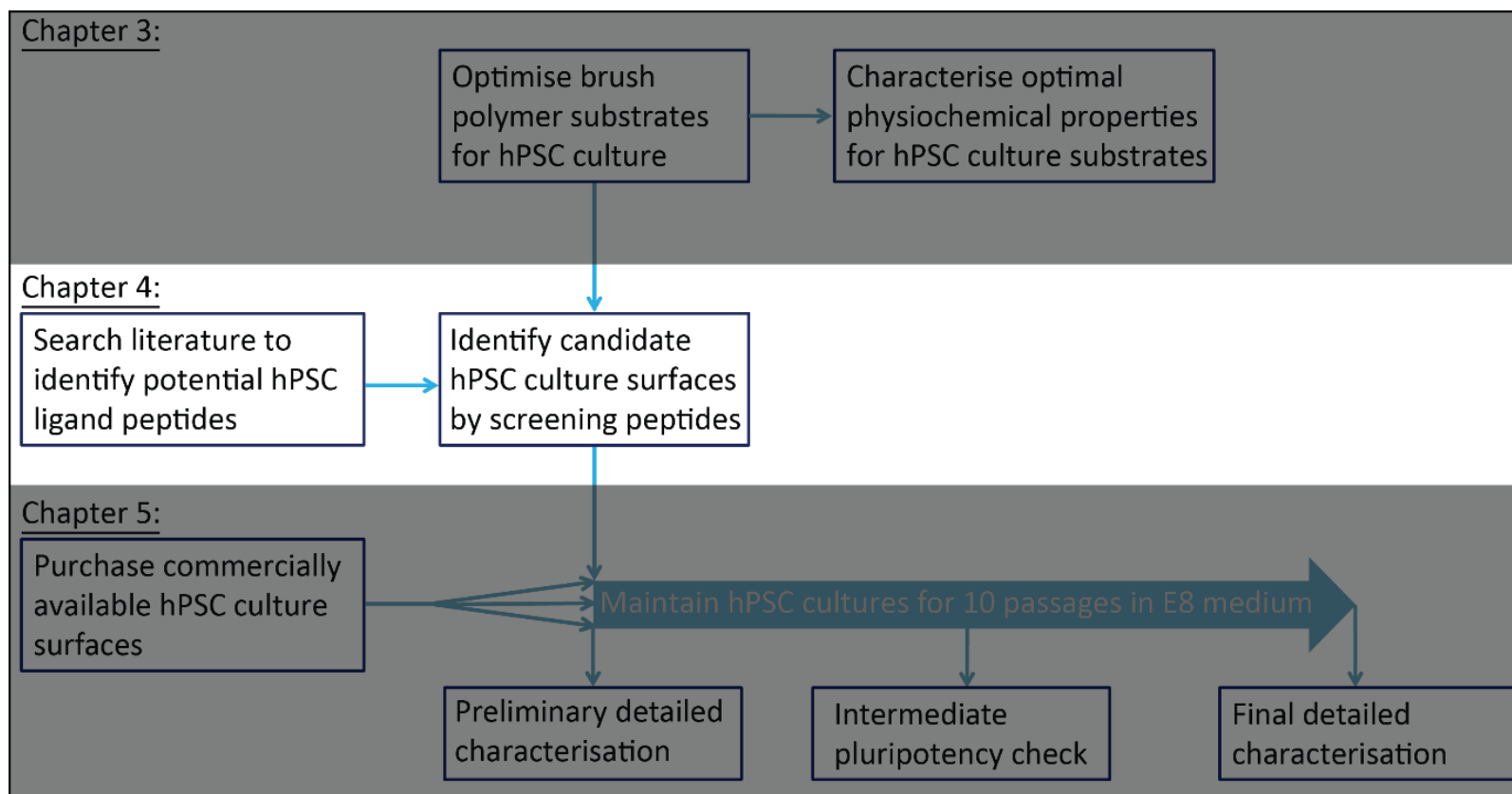


Figure 4.1: The overall project outline is presented and the outline of Chapter 4 is highlighted. In this chapter, the polymer brush coatings optimised for hPSC culture in Chapter 3 (PAAA and PAPA) were modified with a library of short peptide ligands that had been identified as cell-binding by a literature search. These surfaces were screened to identify the most suitable ligands for hPSC culture.

4.2 Chapter specific methods

4.2.1 Preparation of polymer surfaces for peptide screening

Production and peptide modification of polymer coatings for peptide screening were performed under the following conditions unless stated otherwise.

PAAA coatings were synthesised onto 24-well plates from a monomer solution comprising 60 mol % acrylamide and 40 mol % acrylic acid at a total monomer concentration of 0.75 g/mL. The coatings were prepared as described in Section 2.5.1. Plates were activated with an aqueous solution containing 125 mM EDC and 125 mM NHS, incubated overnight in a 200 μ M solution of test peptide in DPBS- and washed as described in Section 2.5.2.

PAPA coatings were synthesised onto 24-well plates from a monomer solution comprising 70 mol % acrylamide and 30 mol % propargyl acrylamide at a total monomer concentration of 1 g/mL. The coatings were prepared as described in Section 2.5.1 using 30 UV exposures. Surfaces were chemically modified with reaction solutions containing 200 μ M of azide-functionalised peptide in 100 μ M CuSO₄ and 227 μ M sodium ascorbate dissolved in DPBS- and washed as described in Section 2.5.3.

Further optimisation of CuAAC reaction conditions included the use of HEPES buffer (Life Technologies, Cat No: 15630-080), THPTA and L-Histidine (Sigma Aldrich, Cat No: H8000).

4.2.2 Peptide library for screening

Wells coated with PAAA or PAPA were modified with one of the peptides listed in Table 4.1. An N-terminal lysine residue was included in all peptides to serve as a spacer, to standardise the ligation sites of each peptide at the N-terminus and to reduce any effects of proximal residues on the efficiency of surface modification reactions. The N-terminal primary amines of peptides screened on PAAA substrates were acetylated (i.e. reacted with acetyl groups during synthesis) so that the only available amine groups for specific carbodiimide coupling reactions were found on the lysine side chains. Peptide sequences that contained additional lysine residues could form unwanted side-reactions with the PAAA coatings that may result in suboptimal peptide orientation. Lysine-containing peptides were therefore N-terminally azide-functionalised and screened on PAPA-coatings.

Table 4.1: This table lists the peptides that were used to modify test hPSC culture surfaces in this screening study. The sequence and biological origin of each peptide is listed along with the polymer coating they were screened on and the cell receptors with which they've been reported to interact. Ac refers to acetylation of the N-terminal amine, kDa; kilodaltons, K(N3); azide-conjugated lysine, PAAA; poly(acrylamide-co-acrylic acid), PAPA; poly(acrylamide-co-propargyl acrylamide). Additional details can be found in Appendix 3.

#	Sequence	Surface	Peptide origin	Cell receptor
1	K(N3)GTTVKYIFR	PAPA	Laminin γ 1-chain	Unknown
2	K(N3)GRNIAEIIKDI	PAPA	Murine laminin β 2 chain	Unknown
3	Ac-KGRYVVLPR	PAAA	Laminin β 1 chain	Glycosaminoglycan
4	K(N3)LTTAPKLPKVTR	PAPA	Phage display library	Unknown
5	K(N3)TVKHRPDALHPQ	PAPA	Phage display library	Unknown
6	Ac-KPHSRN	PAAA	Fibronectin	Integrin $\alpha_5\beta_1$
7	Ac-KYIGSRY	PAAA	Laminin β 1 chain	76 kDa Laminin binding protein (Glycosaminoglycan) $\alpha_3\beta_1$, $\alpha_4\beta_1$, $\alpha_6\beta_1$
8	Ac-KGACRRETAWACGA	PAAA	Phage display library	Integrin $\alpha_5\beta_1$
9	Ac-KGCWLDVCGY	PAAA	Fibronectin CS-1 domain	Integrin $\alpha_4\beta_1$
10	Ac-KSVVYGLR	PAAA	Osteopontin	Integrin $\alpha_4\beta_1$, $\alpha_4\beta_7$, $\alpha_9\beta_1$, $\alpha_v\beta_3$
11	Ac-KVDTYDGRGDSVVYGLR	PAAA	Osteopontin	Integrin $\alpha_4\beta_1$, $\alpha_4\beta_7$, $\alpha_9\beta_1$, $\alpha_v\beta_3$
12	Ac-KYGYGDALR	PAAA	Laminin-1	Integrin $\alpha_2\beta_1$
13	Ac-KFYFDLR	PAAA	Collagen IV	Integrin $\alpha_2\beta_1$
14	K(N3)-IKVAV	PAPA	Laminin α -1 chain	Integrin $\alpha_3\beta_1$, $\alpha_6\beta_1$, $\alpha_4\beta_1$
15	Ac-KDGEA	PAAA	Collagen I	Integrin $\alpha_2\beta_1$
16	K(N3)GDITYVRLKF	PAPA	Laminin γ 1-chain	Integrin $\alpha_v\beta_3$
#	Sequence	Surface	Peptide origin	Cell receptor
17	Ac-KGDIRVTLNRL	PAAA	Laminin γ 1-chain	Unknown/not integrin
18	K(N3)GFQVAYIIKA	PAPA	Laminin α 1 chain	Heparan sulphate proteoglycan/ β 1 Integrins

19	Ac-KGSIYITRF	PAAA	Laminin α 1 chain	Heparan sulphate proteoglycan
20	K(N3)GLSIELVRGRVKV	PAPA	Laminin α 1 chain G	Heparan sulphate proteoglycan
21	Ac-KGLOVQLSIR	PAAA	Laminin α 1 chain	Syndecans
22	Ac-KGHQNMMDYATLQLO	PAAA	Laminin α 1 chain	Integrin α 2 β 1
23	K(N3)GSYNGIIFFLK	PAPA	Laminin α 5 chain G	Heparan sulphate proteoglycan
24	Ac-KGHQMNGSVNVSVG	PAAA	Laminin α 5 chain G	Heparan sulphate proteoglycan
25	Ac-KGSYLQFVGI	PAAA	Laminin α 5 chain G	Heparan sulphate proteoglycan
26	Ac-KGAPVNVTSVQIQ	PAAA	Laminin α 5 chain G	Heparan sulphate proteoglycan
27	Ac-KGAFGLALWGTR	PAAA	Laminin β 1 chain	Heparan sulphate proteoglycan/Integrins
28	K(N3)GDSITKYFQMSL	PAPA	Laminin β 1 chain	Heparan sulphate proteoglycan
29	Ac-KGILQQAADIAR	PAAA	Laminin β 1 chain	Heparan sulphate proteoglycan/Integrins
30	K(N3)GTSIKIRGTYS	PAPA	Laminin γ 1 chain	Integrin α 2 β 1
31	K(N3)GGKKQRFHRNRKG	PAPA	Vitronectin	Heparin binding site
32	K(N3)GFHRIKA	PAPA	Bone Sialoprotein	Heparin binding site
33	Ac-KGGWQPPRARI	PAAA	Fibronectin HBS	Heparan sulphate proteoglycan
34	Ac-KGGNGEPRGDTYRAY	PAAA	Bone Sialoprotein	Integrins
35	Ac-KGGPQVTRGDVFTM-OH	PAAA	Vitronectin	Integrins
36	cRGDFK	PAAA/ PAPA	Synthetic	Integrins

Peptides were either produced by Genscript Inc. (Piscataway, NJ), Peptides International Inc. (Louisville, KY), Mimotopes Pty (Notting Hill, Australia), or at the Manufacturing Business Unit of CSIRO (Clayton, Australia) by Wioleta Kowalczyk and James Gardiner at the Manufacturing Business Unit of CSIRO (Clayton, Australia). The peptides from CSIRO were synthesised by solid state synthesis.

Briefly, all peptides were synthesised manually on fluorenylmethyloxycarbonyl (Fmoc)-Ala-Wang (loading: 0.72 mmol/g; Mimotopes, Cat No: 47644), Fmoc-Arg(Pbf)-Wang (loading: 0.38 mmol/g; Mimotopes, Cat No: 47362), Fmoc-Gln(Trt)-Wang (loading: 0.61 mmol/g; Mimotopes, Cat No: 47402) or Fmoc-Gly-Wang (loading: 0.8 mmol/g; Mimotopes, Cat No: 47659) resin at 0.1 mmol scale. For manual synthesis operations, the peptide resin was placed in a syringe reactor fitted with a porous polyethylene frit (Sigma Aldrich, Cat No: 57181). The resin was pre-swollen in N,N-dimethylformamide

(DMF; Merck, Cat No: 103053) for 30 minutes and then filtered. The following deprotection and coupling steps were carried out until the desired sequences were synthesised.

Fmoc-Deprotection: a mixture of piperidine (Sigma Aldrich, Cat No: 104094) and DMF (20:80, v/v) was added to the resin. The resin was shaken for 5 minutes and filtered and the fresh portion of the mixture of piperidine and DMF (20:80, v/v) was added to the resin. The resin was shaken for 15 minutes and filtered and washed with DMF (3×5 minutes), Dichloromethane (DCM; Sigma Aldrich, Cat No: 270997; 3×5 minutes) and DMF (3×5 minutes).

Coupling step: Three-fold excesses of Fmoc-L-amino acids; 2-(1H-benzotriazole-1-yl)-1,1,3,3-tetramethyluronium hexafluorophosphate (HBTU; Mimotopes, Cat No: 00702) and N-hydroxybenzotriazole (HOBt; Sigma Aldrich, Cat No: 54802), in the presence of double the molar amount relative to Fmoc-L-amino acid of N,N-diisopropylethylamine (DIEA; Sigma Aldrich, Cat No: 387649), were used for the coupling steps, with DMF as solvent. The resin was shaken for 1 hour at RT. The resin was filtered and washed with DMF (3×5 minutes), DCM (3×5 minutes) and DMF (3×5 minutes).

Cleavage protocol: Peptide resin was treated with 5 mL of cleavage mixture: Trifluoroacetic Acid (TFA; Sigma Aldrich Cat No: T6508)/ Triisopropylsilane (TIS; Sigma Aldrich Cat No: 233781)/H₂O (95/2.5/2.5, v/v/v); 90 minutes, RT. The cleavage solution was separated from the resin by filtration and peptides were precipitated by addition of chilled diethyl ether (Sigma Aldrich, Cat No: 346136), centrifuged, and decanted. The product peptides were washed twice with the same solvent. Samples were then left under vacuum for 30 minutes. Peptides were dissolved in MQ H₂O and lyophilised.

Analysis and Purification: Analytical reversed-phase high performance liquid chromatography (HPLC) was performed as described above. Preparative HPLC was performed on C18 column (21.2 × 250 mm, 10 µm, Phenomenex, Torrance, CA) in a model Agilent 1260 Infinity system (Agilent Technologies, Santa Clara, CA). Solvents A and B were 0.1 % TFA (v/v) in MQ H₂O and acetonitrile, respectively, and elution was with 5–70 % linear gradients of solvent B into A over 25 minutes, at 15 mL/minute flow rate, with UV detection at 210 nm. Preparative fractions of satisfactory purity (≥95 %) by analytical HPLC were pooled and lyophilised.

All peptides were characterised for identity by HPLC analysis and mass spectrometry. Mass spectrometry on peptides generated at CSIRO was performed by Lindsay Sparrow at the Manufacturing Business Unit of CSIRO (Parkville, Australia). See Appendix 3 for peptide characterisation.

4.2.3 Approach for dissolving peptides

Peptide solubility is a multifactorial property that is affected by properties of the peptide including charge, size and polarity. Table 4.2 outlines these properties for each peptide screening in this chapter (Table 4.1). The general guidelines for dissolving peptides are well established and readily accessible, but the process involves trial and error. The primary approach in the current study was to dissolve peptides in MQ H₂O. Peptides that remained insoluble in MQ H₂O following vortexing and sonication were snap frozen, freeze-dried and dissolved in DMSO. Peptides that dissolved in DMSO were then

diluted to 100 $\mu\text{L/mL}$ DMSO in MQ H_2O . In the event that peptides were insoluble in 100 $\mu\text{L/mL}$ DMSO, a new aliquot of peptide was dissolved in formic acid and acetonitrile. A final solution of 100 $\mu\text{L/mL}$ formic acid, 200 $\mu\text{L/mL}$ acetonitrile was prepared in MQ H_2O with vortexing and sonication if required. If peptides remained insoluble at this point, then the incompletely dissolved peptide solutions were nevertheless included in the assay. Since high peptide concentrations (200 μM) were used for the screen, it was anticipated that even surfaces modified with partially dissolved peptides would present enough peptide to elicit a cellular response.

Table 4.2: This table describes the chemical properties that are related to each solubility of each peptide listed in Table 4.1. The number of residues, isoelectric point, charge, and hydrophobicity is included for each peptide. Isoelectric point, charge and hydrophobicity were calculated using the tool at <http://www.lifetein.com/peptide-analysis-tool.html>. This tool was unable to account for the presence of azide groups or peptide cyclisation so these factors were not included in this analysis. The peptides highlighted in bold dissolved incompletely.

Peptide #	# of residues	Isoelectric point	Charge	Hydrophobicity at pH 2.0	Hydrophobicity at pH 6.8
1	10	10.72	+3 Basic	24.6	30.1
2	12	10.02	+1 Basic	24.67	20.83
3	9	11.4	+3 Basic	19.11	24.22
4	13	11.86	+4 Basic	10.46	13.92
5	13	10.7	+4 Basic	1.08	8.92
6	6	11.51	+3 Basic	-33.17	-20.17
7	7	9.85	+2 Basic	18.29	26.14
8	14	8	+2 Basic	22	20.71
9	10	3.1	Neutral	36.1	35.6
10	8	10.32	+2 Basic	39.62	34.12
11	17	4.27	Neutral	17.53	14.47
12	10	6.78	+1 Basic	21.3	23.8
13	7	6.95	+1 Basic	36	37.86
14	7	10.72	+2 Basic	32	34.43
15	5	2.98	-1 Acidic	0	-13.6

16	11	10.3	+2 Basic	28.64	30.27
17	11	11.29	+2 Basic	22.18	21.91
18	12	10.31	+2 Basic	43.5	46.58
19	9	10.32	+2 Basic	31.56	36.56
20	14	11.56	+3 Basic	29.43	29.79
21	10	11.51	+2 Basic	27.3	31.3
22	15	5	+1 Basic	11.53	16
23	12	10.31	+2 Basic	34.25	38.58
24	14	10.28	+2 Basic	8.43	13.21
25	10	6.09	+1 Basic	35.8	39.7
26	14	6.41	+1 Basic	19.79	20.5
27	13	11.51	+2 Basic	38.38	40.62
28	13	9.64	+1 Basic	23.28	25
29	13	7.13	+1 Basic	24.38	23.38
30	12	10.83	+3 Basic	13.42	18.08
31	15	12.98	+9 Basic	-17.4	-6.27
32	9	12.53	+5 Basic	7.89	19
33	11	12.51	+3 Basic	2.91	7.64
34	15	7	+1 Basic	-1.87	-2.93
35	14	7.13	+1 Basic	14.64	14.36
36/RGDfK	5	10.27	+1 Basic	2.2	1
RADfK	5	10.27	+1 Basic	11.6	9.2

4.2.4 Peptide screening approach

The PAAA and PAPA coatings were used to screen a library of peptides (Table 4.1) for their ability to support adhesion, proliferation and maintenance of mCherry as a surrogate marker for pluripotency of the H9-OCT4-mCherry reporter cell line. The screening approach is outlined in Figure 4.2.

1. Polymer-coated 24-well plates were prepared and modified as described in Section 4.2.1. Each plate included triplicate wells in randomised locations that were modified with either the lead cRGDfK peptide, the non-binding control cRADfK peptide (for screening on PAAA only) or one of six test peptides. Experiments were repeated three times using polymer coatings synthesised in different batches that were also modified in different batches and seeded with cells harvested from different passages to account for intra-plate and intra-passage variation. If no hPSCs were observed to bind to any of the wells modified with a peptide in either of the first two experiments, then the peptide was excluded from further experiments.
2. H9-OCT4-mCherry cells were harvested from Geltrex™-coated maintenance flasks using EDTA as described in Section 2.3.2, and seeded in all polymer-coated wells at a density of 15 000 cells/cm² in 400 µl of E8 media. Geltrex™-coated control wells seeded at 5000 cells/cm² and 15 000 cells/cm² were included in triplicate on a separate 24-well plate. The lower-density control was included because cells seeded on Geltrex™ at 15 000 cells/cm² would reach 100 % confluence by day 2 or 3, and a control was needed against which to compare test wells out to day 4 and beyond. Freshly seeded cells were left undisturbed for 48 hours.
3. Forty-eight hours after cell seeding, cultures were visually assessed under phase contrast microscopy and wells were scanned at 40x magnification under both phase contrast and mCherry fluorescence so that colony numbers could be counted as described in Section 2.4.2. Colony counts from surfaces modified with each peptide were compared to counts from the inbuilt cRGDfK-modified controls. Geltrex™-coated control wells were not included in any colony counting analyses because it was difficult to count the large numbers of colonies that spread out more than on the polymer surfaces.
4. Daily media changes were gently performed from day 2 and the cultures were observed daily.
5. Colony growth was roughly assessed four days after cell seeding by scanning wells as described in Section 2.4.2. This was a simple binary observation, with colonies categorised as either “growing” or “not growing”. The proportion of colonies in which mCherry could be observed under fluorescence microscopy was also assigned into quartiles (0-25 %, 25-50 %, 50-75 % or 75-100 %).

4.2.5 Cell culture methods for MDA-MB-435 melanocytes

The melanocyte cell line MDA-MB-435 was kindly provided by A/Prof John Price (Victoria University, Melbourne, Australia) as a positive control for flow cytometric staining of $\alpha v \beta 3$ integrins. MDA-MB-435 cells were maintained in high glucose DMEM (Life Technologies) supplemented with 10 v/v % HyClone™ Foetal Bovine Serum (GE Healthcare, Parramatta, Australia, Cat No: SH30071.03, Lot#: AXK49952) and dissociated for harvesting with TrypLE™ Express.

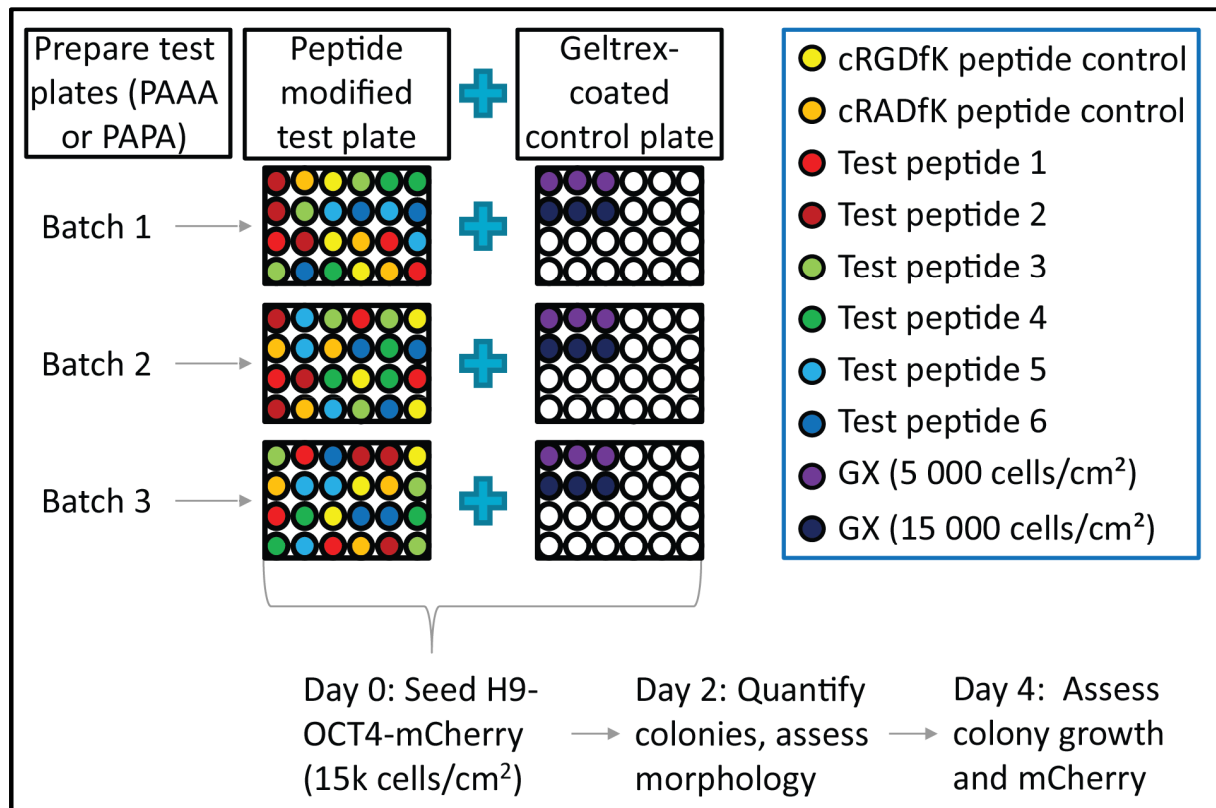


Figure 4.2: A schematic diagram illustrates the screening process that was used in this chapter to identify peptides that, when chemically bound to PAAA or PAPA coatings, produced a surface able to bind and maintain short-term culture of hPSCs. (A) Three batches of peptide-coated plates were prepared and triplicate wells in randomised locations of each plate were modified with either the cRGDfK peptide, the non-binding negative control cRADfK peptide or one of six test peptides. Plates were seeded with H9-OCT4-mCherry hPSCs at a density of 15 000 cells/cm². Geltrex™ (GX)-coated control wells were also seeded at equal and one-third (5000 cells/cm²) density. Colony number and morphology was assessed at 48 hours post-seeding and growth and maintenance of mCherry were assessed at day 4 post-seeding.

4.2.6 Flow cytometric staining for detection of $\alpha\beta3$ integrin

Flow cytometric analysis can be used to quantify the presence of cell surface proteins on live cells. Flow cytometry assessment of $\alpha\beta3$ integrins was performed on H9 hPSCs and the positive control melanocyte cell line MDA-MB-435.

1. Cultures of H9 and MDA-MB-435 cells in 25 cm² flasks were washed twice in 5 mL DPBS- and then incubated in 1 mL TrypLE™ Express for 5 min.
2. Single cells were harvested in 2 x 5 mL DMEM/F12 medium by pipetting across the surface.
3. Cells were pelleted at 800 g for 2 min and resuspended in 3 mL DMEM/F12. Aliquots were taken for counting as described in Section 2.4.1. The cells were then topped up to 10 mL with DMEM/F12 and pelleted again.
4. H9 cells were aliquoted at 500 000 cells/tube into three tubes and were pelleted and resuspended in 100 μ L of DMEM/F12 that was unsupplemented or contained either anti- $\alpha\beta3$ integrin antibody (Abcam) or IgG1 isotype control antibody (see Table 4.3 for antibody details). An additional tube containing 5x10⁵ MDA-MB-435 cells was also resuspended in anti- $\alpha\beta3$ integrin antibody. Cells were incubated for 20 minutes on ice and washed twice in DPBS-
5. Cells were then resuspended in 100 μ L of diluted secondary antibody, stained for 20 minutes on ice and washed twice.
6. Stained cells were analysed on an LSR II flow cytometer (Becton Dickinson). Ten thousand events were collected and data were exported as .fcs3 files. Post-analysis was performed on a PC with FlowJo Software Version 10 (FlowJo, LLC, Ashland, OR). Single-cells were isolated based on forward vs side scatter and $\alpha\beta3$ integrin-stained cells were gated against isotype control-stained cells.

Table 4.3: This table describes the primary antibodies used for staining hPSCs for $\alpha\beta3$ integrin by flow cytometry, including the target, animal-of-origin, source, and dilution factors.

Antibody	Source	Dilution
Mouse monoclonal IgG1 anti-integrin alpha V beta 3	Abcam, Cambridge, UK Cat No: ab78289	1:100
IgG1 isotype control	Becton Dickinson, Cat No: 557273	1:250
Alexa Fluor® 488 conjugated goat anti-mouse IgG1	Life Technologies, Cat No: A-21121	1:500

4.3 Results

4.3.1 Peptide solubility results

Twenty-one (21/38, 70 %) peptides were observed to dissolve readily in MQ H₂O, but the other peptides required stronger solvents (summarised in Table 4.4). Of the twelve remaining, peptides 19, 22 and 29 dissolved completely in DMSO, while peptides 24 and 26 had a faint grainy appearance in

100 $\mu\text{L/mL}$ DMSO. Peptides 16, 18, 20, 23, 28 and 30 failed to dissolve in DMSO. When transferred to formic acid and acetonitrile peptides 23 and 30 dissolved poorly. Peptides 20 and 28 stayed in solution when diluted to 100 $\mu\text{L/mL}$ formic acid, 200 $\mu\text{L/mL}$ acetonitrile while peptides 16 and 18 remained mostly dissolved. As there were no clear differences in residue number, isoelectric point, charge or hydrophobicity between the peptides that dissolved readily and those that were insoluble (see Table 4.2), it is difficult to explain the differences in solubility.

Table 4.4 A summary of the peptide solubility results is presented. Three different approaches were adopted taken to dissolve peptides. Six peptides remained incompletely dissolved under all conditions tested. ACN, acetonitrile; DMSO, dimethyl sulphoxide; FA, formic acid.

Solvents tested	Peptide solubility (peptide # given as per Table 4.1)
1. MQ H ₂ O ↓ Vortexing for 3 min ↓ Sonication for 5 min	1, 2, 3, 4, 5, 6, 7, 8, 9, 10, 12, 14, 15, 21, 27, 31, 32, 34, 35, cRGDfK, cRADfK and cRGDfK-N3 dissolved 17, 29 and 33 dissolved 11 and 13 dissolved Undissolved peptides were freeze-dried and progressed to step 2
2. DMSO ↓ 100 $\mu\text{L/mL}$ DMSO in MQ H ₂ O	19, 22 and 29 remained in solution. 24 and 26 were mostly dissolved, but a small amount of precipitate could be seen. Undissolved peptide was discarded. Fresh peptide was used for step 3
3. Formic acid ↓ 330 $\mu\text{L/mL}$ FA, 660 $\mu\text{L/mL}$ ACN ↓ 100 $\mu\text{L/mL}$ FA, 200 $\mu\text{L/mL}$ ACN in MQ H ₂ O	16, 18, 20, 23 and 28 went into solution No change observed 20 and 28 stayed in solution 16 and 18 came partly out of solution 23 formed a gel
4. Incompletely dissolved peptides	16, 18, 23, 24, 26, 30

4.3.2 Results of peptide screening on PAAA with H9-OCT4-mCherry hPSCs

Twenty-three peptides (cRGDfK, cRADfK, 3, 6, 7, 8, 9, 10, 11, 12, 13, 15, 17, 19, 21, 22, 24, 26, 27, 29, 33, 34 and 35) were screened on PAAA-40UV, as described in Sections 4.2.1 and 4.2.4. H9-OCT4-mCherry cells were observed to adhere to surfaces modified with the cRGDfK peptide (cRGDfK-PAAA) or peptide 34 (pep34-PAAA) or 35 (pep35-PAAA), which constitute a total of 13 % of all peptides (3/23). Observations of H9-OCT4-mCherry cells cultured on Geltrex™, cRGDfK-PAAA, pep34-PAAA and pep35-PAAA are outlined in Table 4.5 and images of these cells are presented in Figure 4.3. Briefly, more colonies were observed in Geltrex™- or cRGDfK-PAAA-coated wells than pep34-PAAA- or pep35-PAAA-coated wells, and colonies on the latter surfaces often formed rounded clumps that appeared to be only loosely tethered to the surface (Figure 4.3).

Table 4.5: Observations of H9-OCT4-mCherry cultures on PAAA coatings modified with hit peptides cRGDfK, peptide 34 and peptide 35 compared to control cultures in Geltrex™-coated wells.

	Confluence	Colony appearance	mCherry
Geltrex™	High	Flat, thin	Observed in almost all colonies
cRGDfK-PAAA	Moderate	Flat, thicker than Geltrex™	Observed in almost all colonies
Pep34-PAAA	Low	Some flat, thick colonies, several round clumps that were barely attached	Observed in almost all colonies
Pep35-PAAA	Low	Mostly rounded clumps that were barely attached. A few flatter colonies surrounded by morphological differentiation	Observed in all colonies, not observed in morphologically differentiated cells

Approximately 10-fold more colonies were counted in cRGDfK-PAAA wells than pep34-PAAA or pep35-PAAA (Figure 4.4 I). The mCherry protein was detectable by fluorescence microscopy in the vast majority of cell colonies on all surfaces (Figure 4.4 E-H). Prior to conducting the screen, cRGDfK-PAAA surfaces had been optimised for hPSC culture by increasing the molar percentage of acrylic acid and the concentrations of peptide solutions (Section 3.3.1). To optimise the pep34-PAAA and pep35-PAAA surfaces for hPSC culture, the concentration of peptide solutions was further increased to 400 µM and 600 µM. Pep34-PAAA and pep35-PAAA surfaces modified with solutions containing higher peptide

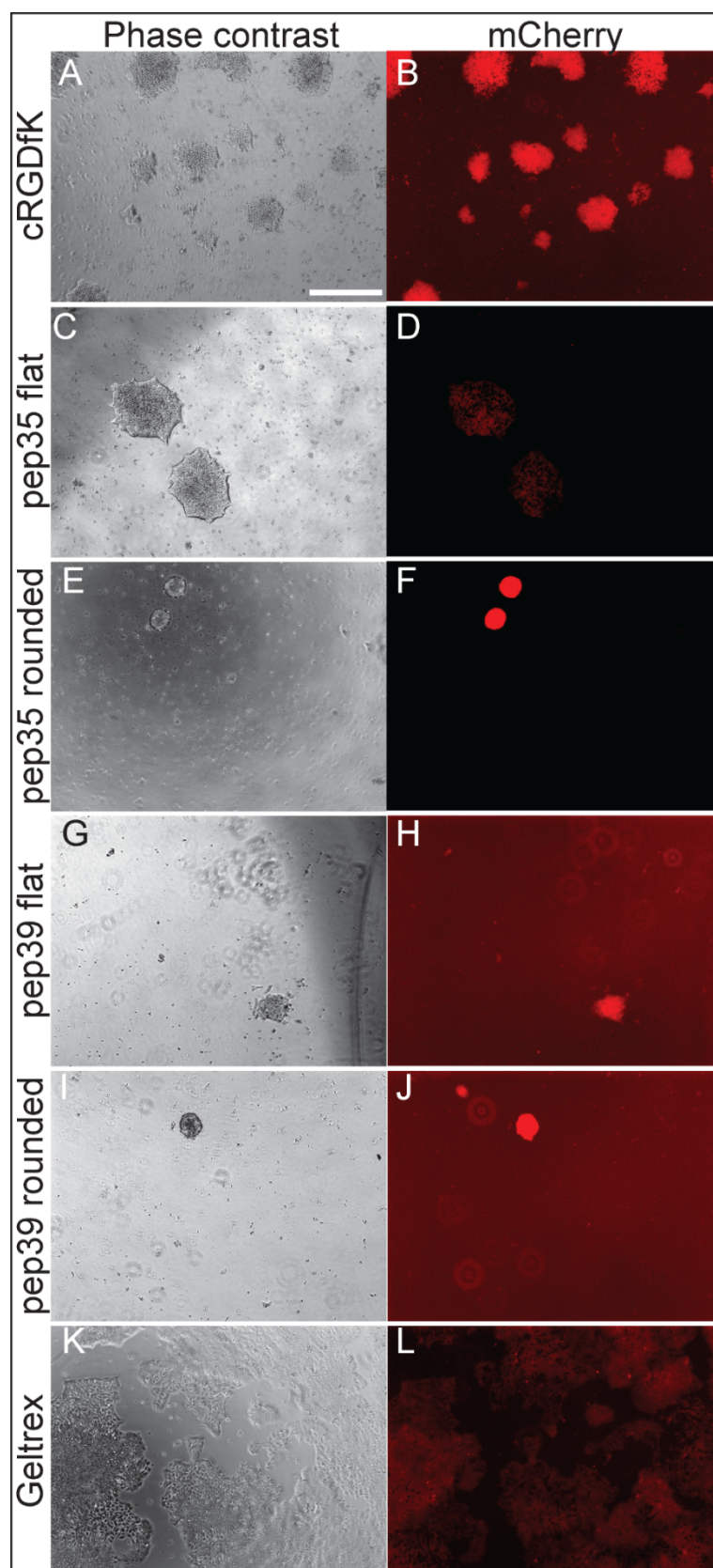


Figure 4.3: Caption is on the following page.

Figure 4.3: Figure is on the previous page. This figure presents (A, C, E, G, I, K) phase contrast and (B, D, F, H, J, L) mCherry fluorescence microphotographs of H9-OCT4-mCherry hPSCs growing in E8 medium on PAAA-coated surfaces modified with hit peptides as well as Geltrex™-coated control surfaces. (A,B) H9-OCT4-mCherry cells growing on cRGDfK-PAAA were observed to spread across the surface and form thick colonies in which mCherry was detectable by fluorescence microscopy. Some cells grown on pep34-PAAA formed (C,D) colonies similar to those observed on cRGDfK-PAAA but most formed (E,F) rounded clumps of cells that were tethered to the surface. (G,H) Rare flatter colonies of H9-OCT4-mCherry cells observed on pep35-PAAA were associated with differentiated cells, (I,J) while most of the colonies observed on pep35-PAAA were rounded and barely attached to the surface. (K,L) Control H9-OCT4-mCherry cells growing on Geltrex™ were flatter and more confluent than on any of the PAAA coatings. Images were captured on day 4 after cell seeding. Scale bar represents 300 µm on all images.

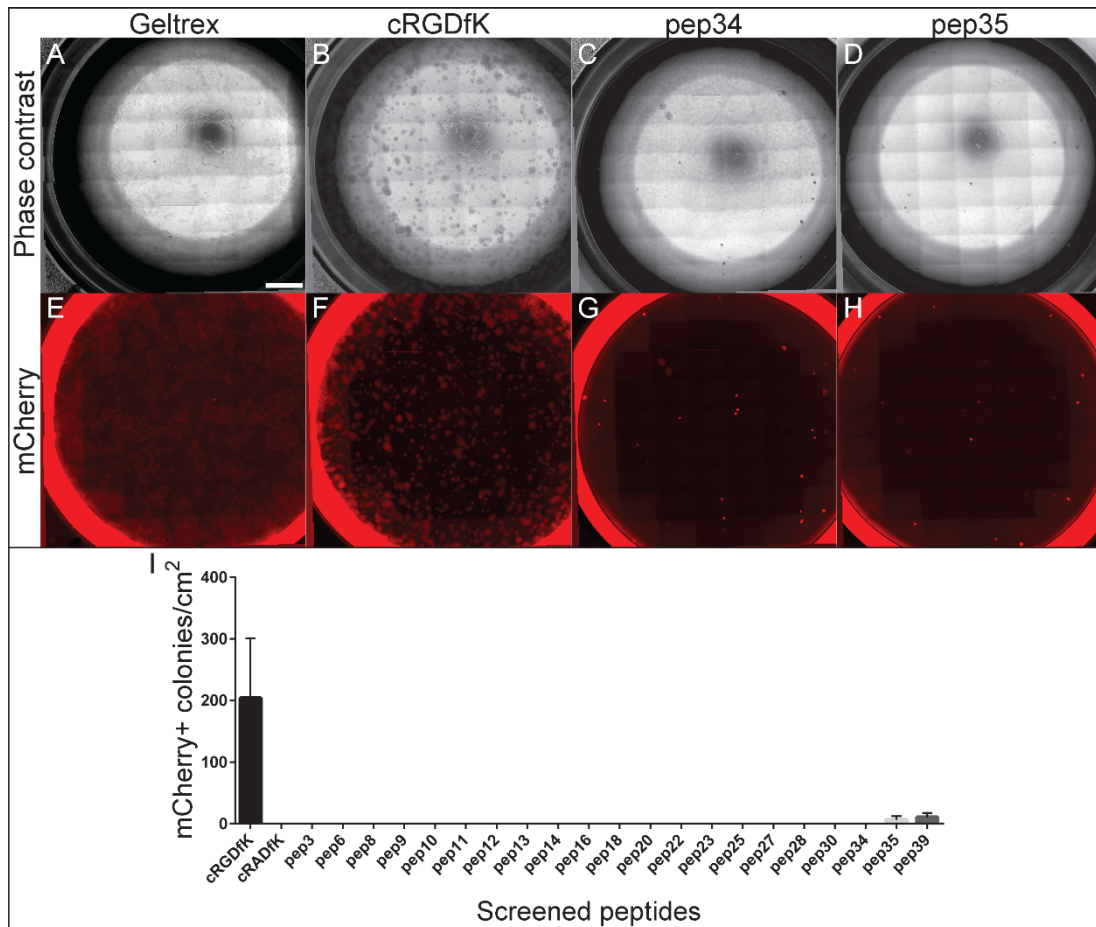


Figure 4.4: This figure presents the results of H9-OCT4-mCherry adhesion assays that were used to identify peptides that enable hPSC adhesion when chemically coupled to PAAA-40UV coatings. The images presented in A-H are representative scans of whole wells of 24-well plates that were produced by stitching together a series of images captured at 40x magnification using (A-D) phase contrast and (E-H) mCherry fluorescence microscopy. H9-OCT4-mCherry cells were seeded at a density of 15 000 cells/cm² in E8 medium in wells that had been coated with (A,E) Geltrex™ or PAAA coatings modified with solutions containing 200 μM of a peptide selected from a library (Table 4.1) that included (B,F) cRGDfK, (C,G) peptide 34 or (D,H) peptide 35. Wells were scanned 48 hours after seeding. Scale bar represents 2 mm in all images. (I) The number of colonies visible in the mCherry fluorescence scans of PAAA-coated wells (E-H for examples) modified with cRGDfK, cRADfK and test peptides from the library presented in Table 4.1 were counted. The mean number of colonies/cm² are presented from three independent experiments. Error bars represent standard deviations from the mean.

concentrations bound far fewer colonies than cRGDfK-PAAA surfaces modified with 200 μ M peptide solutions (Figure 4.5). This indicated that the reduced affinity of peptides 34 and 35 compared to cRGDfK may not be compensated for by increased peptide concentration.

All screening to this point was completed on PAAA-40UV coated plates, which had bound large numbers of hPSC colonies when modified with the peptide cRGDfK (see Figure 4.4B,F and Figure 4.5). However the subsequent findings on the effects of number of UV exposures on cell adhesion to PAAA coatings (Section 3.3.3) indicated that more colonies might adhere to pep34-PAAA and pep35-PAAA if PAAA-25UV coatings were used instead of PAAA-40UV coatings. Since in-plate technical replicates were highly consistent across the screen, a final PAAA screening experiment was conducted using single wells modified with each of 17 peptides (3, 6, 7, 8, 9, 10, 11, 12, 13, 15, 17, 19, 21, 22, 24, 29, 33) and triplicate wells modified with the hit peptides cRGDfK, 34 and 35. This was a final assessment of the 17 peptides that to this point had not resulted in the adhesion of a single hPSC colony. The results obtained were very similar to those from the main screen (Figure 4.4). Only cRGDfK-PAAA, pep34-PAAA and pep35-PAAA surfaces were able to bind any colonies of H9-OCT4-mCherry cells (Figure 4.6) and adherent cells were observed in all wells modified with these peptides. There appeared to be a slight increase in colony numbers bound to pep34-PAAA and pep35-PAAA surfaces in this experiment compared to experiments performed with 40-exposure plates (Figure 4.6), but significantly more colonies were still observed to attach to cRGDfK-PAAA surfaces, a difference of approximately 4-fold (Figure 4.6). More colonies of cRGDfK-PAAA H9-OCT4-mCherry cells consistently bound to cRGDfK-PAAA surfaces than to pep34-PAAA or pep35-PAAA surfaces.

4.3.2.1 Validation of lead peptides on PAAA with cultures of H9 and NHF-1-3 hPSCs

To determine if the ability of H9-OCT4-mCherry cells hPSCs to adhere to cRGDfK-PAAA, pep34-PAAA and pep35-PAAA modified surfaces was cell line dependant, the surfaces were validated with H9 and NHF-1-3 hPSCs. The screening approach described in Section 4.2.4 was followed with hit peptides cRGDfK, 34 and 35 used to modify a PAAA-40UV coated 24-well plate. In this experiment, more colonies of H9 cells than of NHF-1-3 attached to each surface (Figure 4.7), which could be due to errors in counting clumps of cells with a hemocytometer, improved survival of H9 cells or the H9 colonies being dissociated into smaller clumps that formed a larger number of colonies despite cell numbers remaining equal. Colony counts for both cell lines produced a clear trend of more hPSC colonies being observed on cRGDfK-PAAA than on pep34-PAAA, which in turn bound more cells than pep35-PAAA (Figure 4.7). This result correlated with earlier observations that hPSCs adhered to and could be maintained for at least four days on surfaces coated with cRGDfK-PAAA, while far fewer cells bound to surfaces coated with pep34-PAAA and pep35-PAAA.

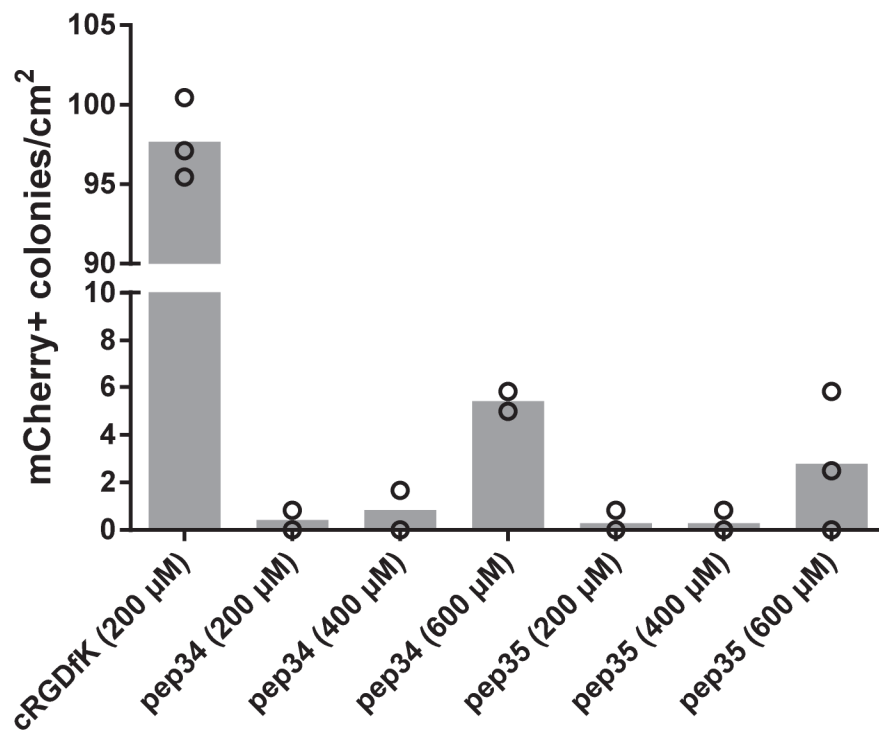


Figure 4.5: This figure presents the results of an H9-OCT4-mCherry adhesion assay on PAAA surfaces modified with high concentrations of the hit peptides 34 (pep34) and 35 (pep35). PAAA-coated wells were modified with solutions containing 200 µM, 400 µM or 600 µM of pep34 or pep35 and were seeded with 15 000 H9-OCT4-mCherry cells/cm² in E8 medium. Control wells were modified with solutions containing 200 µM of cRGDfK peptide. Scanned images were captured of all wells 48 hours after seeding and mCherry-positive colonies were counted as described in Section 2.4.2. Means of colony counts are presented from two or three technical replicates and individual data points are marked with hollow circles.

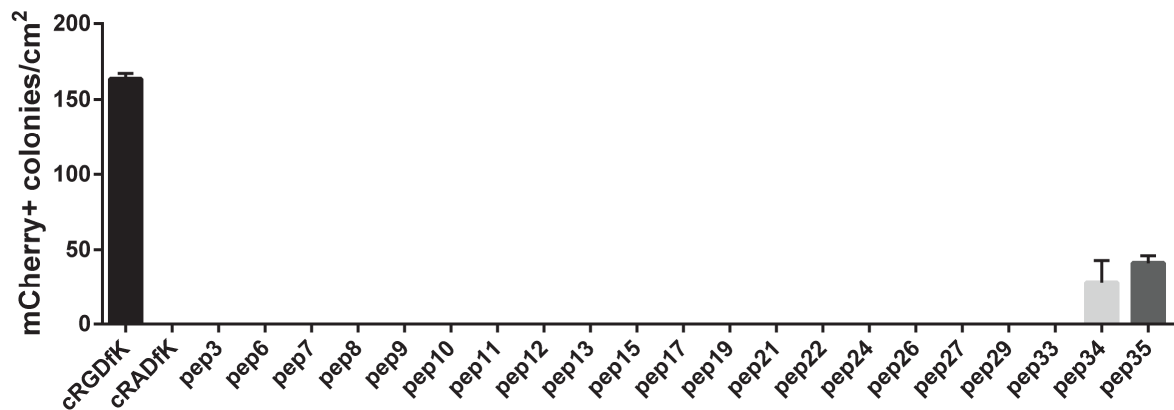


Figure 4.6: This figure presents the results of an H9-OCT4-mCherry adhesion assay in a single experiment that re-screened peptide-modified PAAA coatings using the thinner PAPA-25UV surfaces. PAAA-25UV-coated wells were modified with solutions containing 200 μ M of each peptide and were seeded with 15 000 H9-OCT4-mCherry cells/cm² in E8 medium. Negative control wells were modified with solutions containing 200 μ M of the no-binding cRADfK peptide. Scanned images were captured of all wells 48 hours after seeding and mCherry-positive colonies were counted as described in Section 2.4.2. Means of three technical replicates are presented. Error bars represent standard deviations from the mean.

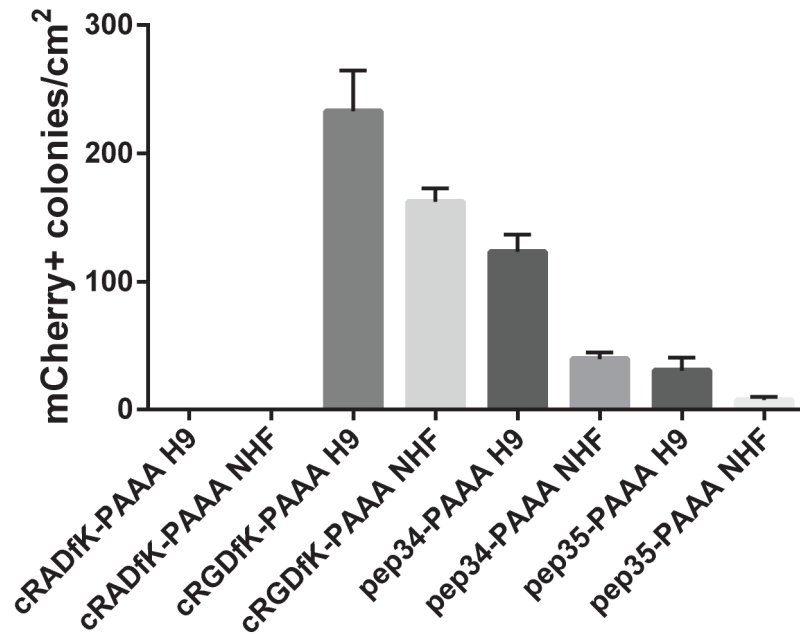


Figure 4.7: The hPSC response to PAAA coatings modified with cRGDfK, peptide 34 (pep34) and peptide 35 (pep35) was validated using H9 and NHF-1-3 (NHF) hPSCs. PAAA-40UV coated surfaces were modified with solutions containing 200 μ M of cRGDfK, pep34 or pep35. Wells were seeded with H9 or NHF-1-3 (NHF) hPSCs at a density of 15 000 cells/cm². Colony counts are presented from phase contrast scans of these wells as described in Section 2.4.2. Non-binding cRADfK-modified control wells were included. Means of three technical replicates are presented. Error bars represent standard deviation.

4.3.3 Peptide screening results on PAPA

PAPA coatings were modified with fourteen peptides (cRGDfK 1, 2, 4, 5, 14, 16, 18, 20, 23, 28, 30, 31 and 32) and screened for adhesion and maintenance of H9-OCT4-mCherry cells as described in Section 4.2.4. In the first experiment, H9-OCT4-mCherry cells were observed to bind to the surfaces modified with peptides cRGDfK (cRGDfK-PAPA), 20 (pep20-PAPA) and 31 (pep31-PAPA) (3/14, 17 % of peptides). Twenty-four hours after seeding, large numbers of flat colonies that contained mCherry levels detectable by fluorescent microscopy were observed bound to Geltrex™-coated control wells and to cRGDfK-PAPA-coated wells, while moderate numbers of very small and rounded colonies were observed on pep20-PAPA (approximately 20 colonies/well) and pep31-PAPA (approximately 50 colonies/well). No signs of cell attachment were observed in wells modified with the remaining 11 peptides. By the second post-seeding day many colonies had lifted; one pep20-PAPA well contained three colonies while the other two showed no signs of cell attachment. Meanwhile pep31-PAPA wells retained an average of 23 bound colonies per well (Figure 4.8).

By day 3 post-seeding, all colonies that had adhered to pep20-PAPA wells had lifted from the surface and most colonies had lifted from the pep31-PAPA wells, but no sign of colony detachment was observed on cRGDfK-PAPA. Following six (6) days of cultures in maintenance medium, the colonies growing on cRGDfK-PAPA were large and were estimated to cover 80 % of the well (Figure 4.9, A-D), while the colonies on pep31-PAPA modified wells were much smaller (Figure 4.9 E-H). The six colonies in total that remained attached to three pep31-PAPA wells remained adherent and expanded gradually until the experiment was terminated at day 8, by which point the cRGDfK-PAPA wells were over-confluent. This result indicated that hPSCs may be able to adhere to surfaces modified with pep20-PAPA and pep31-PAPA. Each of these peptides had previously been reported to bind HSPGs and were therefore of interest to developing and comparing surfaces that interacted with different CAMs. In order to improve hPSC-binding to surfaces modified with HSPG-binding peptides, the CuAAC peptide modification reaction conditions for PAPA coatings were further optimised, with the intention of repeating the full screen using the optimised reaction conditions. Since PAPA coatings modified with the HSPG-binding peptide 31 resulted in adhesion of more H9-OCT4-mCherry colonies than any other test peptide on PAPA, and because several peptide 31-presenting surfaces had previously been reported to support hPSC adhesion (Klim et al., 2010, Musah et al., 2012, Park et al., 2015), further optimisation of the CuAAC peptide modification protocol was focused on improving adhesion of H9-OCT4-mCherry colonies to pep31-PAPA before the other peptides were reintroduced for the repeated screen.

4.3.4 Further optimisation of pep31-PAPA did not improve hPSC adhesion

To improve adhesion of H9-OCT4-mCherry cells to pep31-PAPA surfaces, the concentrations of reagents were optimised. Concentrations of peptide 31 (3-fold) and copper sulphate (8-fold) were varied, while sodium ascorbate was used at a concentration 5-fold greater than that of copper sulphate (Figure 4.10A). The inclusion of copper ligands THPTA and L-histidine (data not shown), which stabilise copper ions in the catalytic Cu(I) state, were also tested along with the buffers DPBS- and 1mM HEPES. THPTA was used at the recommended five-fold greater concentration than copper (Hong et al., 2010) and 100 mM L-histidine was tested. The conditions and controls for this optimisation are

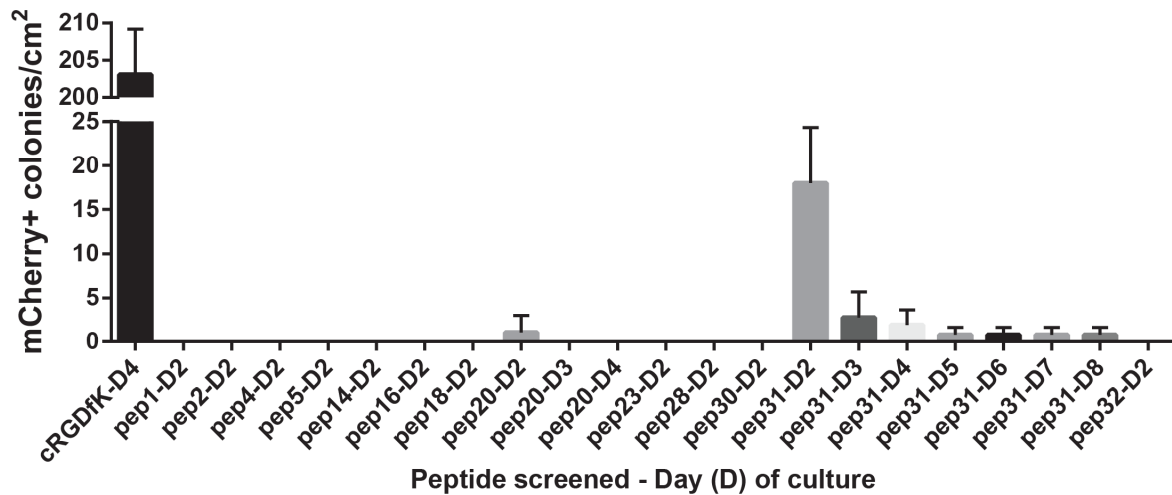


Figure 4.8: This figure presents the results of an H9-OCT4-mCherry adhesion assay on PAPA surfaces modified with the peptides listed in Table 4.1. PAPA-coated wells were modified with solutions containing 200 μ M of each peptide and were seeded with 15 000 H9-OCT4-mCherry cells/cm² in E8 medium. Negative control wells were modified with solutions containing 200 μ M of the non-binding cRADfK-N3 peptide. Scanned images were captured of all wells 48 hours (D2) after seeding and mCherry-positive colonies were counted as described in Section 2.4.2. The low colony numbers in wells modified with peptides 20 and 31 were counted on subsequent days (D3-D8) without scanning the wells. Means of three technical replicates are presented. Error bars represent standard deviations from the mean.

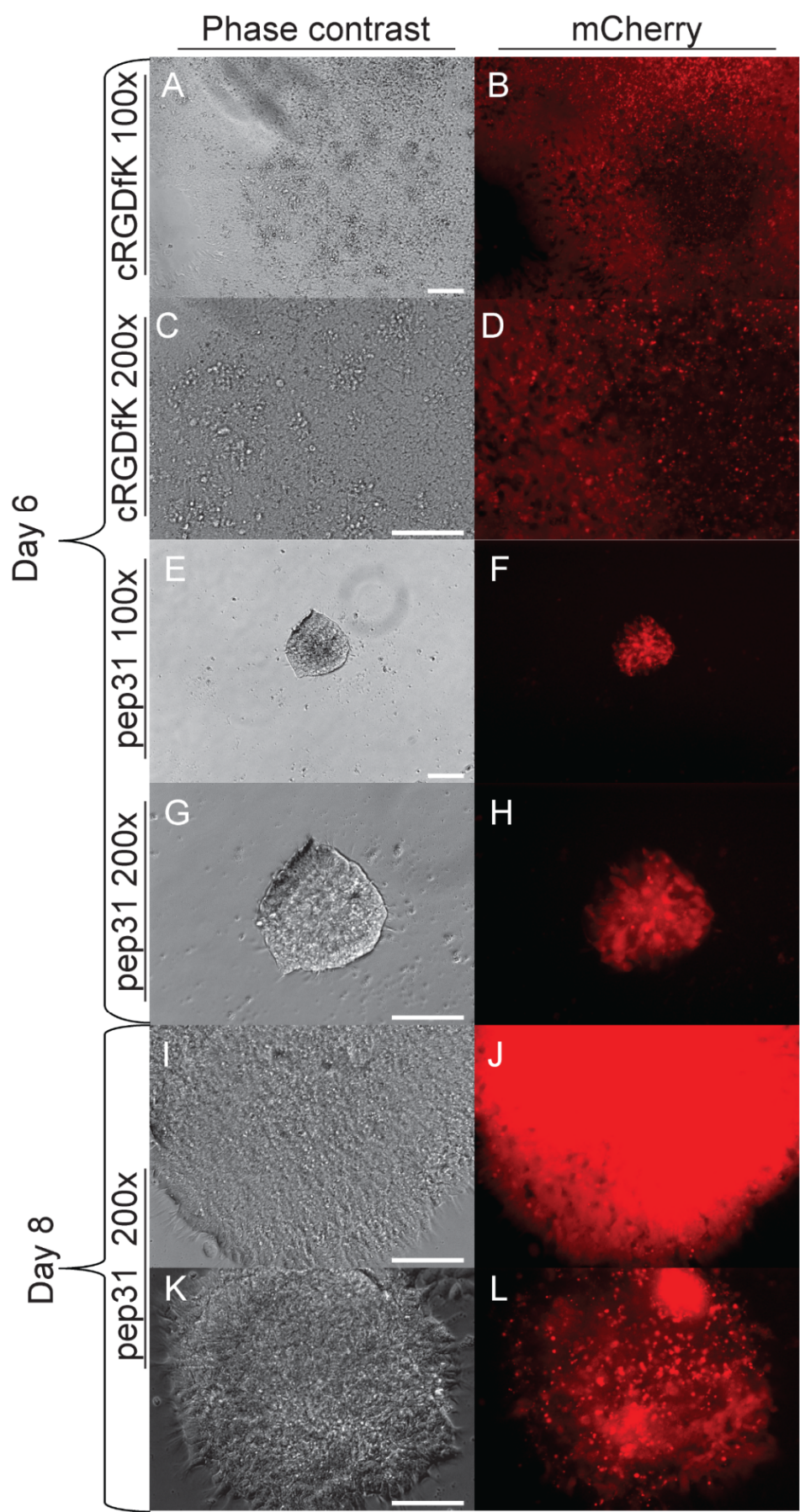


Figure 4.9: Caption is on the following page.

Figure 4.9: Figure is on the previous page. Phase contrast and mCherry photomicrographs are presented of H9-OCT4-mCherry colonies growing on PAPA coatings modified with hit peptides. (A-D) Colonies of H9-OCT4-mCherry cells, six days after seeding onto cRGDfK-PAPA were large and mostly mCherry-positive. (E-H) At the same time point the colonies on pep31-PAAA were considerably smaller and more rounded than those on cRGDfK-PAPA. By the eighth day of culture H9-OCT4-mCherry colonies on pep31-PAPA colonies had grown considerably (G and H are the same colony at the same magnification as I and J) and either (I, J) contained fine neural-like projections while remaining mostly mCherry-positive or (K,L) was mostly mCherry-negative and showed more distinct morphological differentiation. Scale bars represent 100 μm .

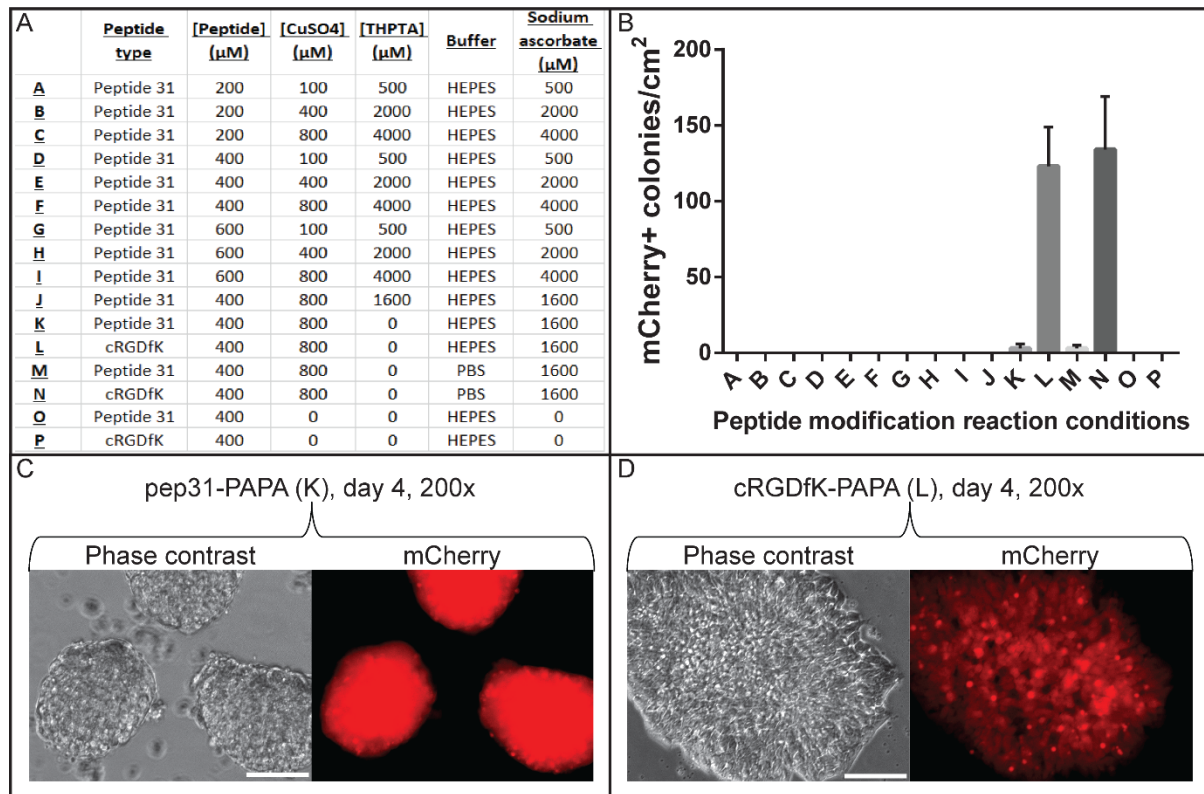


Figure 4.10: Optimisation of CuAAC reaction conditions to improve adhesion of H9-OCT4-mCherry cells to pep31-PAPA surfaces. (A) A table shows the reaction conditions that were trialled to improve cellular adhesion to pep31-PAPA surfaces. (B) Counts of mCherry-positive colony numbers on PAPA wells modified with the conditions presented in A. Means are presented of three technical replicates. Error bars represent standard deviation from the means. Images are also presented from day 4 after seeding when (C) rounded colonies of H9-OCT4-mCherry cells were loosely attached to pep31-PAPA and (D) typical colonies of H9-OCT4-mCherry cells were attached to cRGDfK-PAPA. Scale bar represents 100 μm .

reported in Figure 4.10A. Since colony numbers were expected to be low on pep31-PAPA surfaces, the colony counting approach to cell quantification was used.

Most test conditions resulted in a complete absence of adherent H9-OCT4-mCherry cells on day 2 (Figure 4.10B), while control wells modified with cRGDfK consistently bound large numbers of colonies in which mCherry could be detected by fluorescence microscopy. An average of two colonies per square centimetre bound to pep32-PAPA wells modified with reaction conditions identical to those conditions used in the previous screening experiment (Figures 4.8 and 4.9) except for the buffer (conditions K and M, Figure 4.10). As with the previous experiment, the clumps that bound were very rounded and looked close to detaching (Figure 4.10C). By contrast, cRGDfK-PAPA-coated wells prepared using matching conditions (L and N) each bound >100 colonies/cm² and these colonies appeared to be more typically flat (Figure 4.10D). Optimising the CuAAC reaction conditions failed to improve cell adhesion to pep31-PAPA. Since the PAPA coatings for peptide screening were modified with solutions of test peptides that were 100-fold more concentrated than the minimum required for hPSC-supporting cRGDfK-PAPA (Section 3.3.6), and attempts to optimise the reaction conditions failed to improve colony adhesion to surfaces modified with the most widely-published candidate peptide(pep31-PAPA), while cRGDfK-PAPA surfaces consistently bound large numbers of hPSCs, the screening of the remaining peptides on PAPA was abandoned. The long-term culture experiment (Chapter 5) therefore tested and benchmarked the ability of cRGDfK-PAPA to maintain long-term culture of hPSCs against other commercially available synthetic substrates instead of against brush polymer coatings modified with other short peptides.

4.3.5 Peptide screening results summary

When polymer coatings PAAA and PAPA were individually modified with a library of 36 peptides, five surfaces (14 %) supported a degree of adherence of H9-OCT4-mCherry colonies (Figure 4.11). Both PAAA and PAPA coatings that had been modified with the cRGDfK peptide consistently resulted in the observation of a high number of adherent, mCherry-positive H9-OCT4-mCherry colonies. PAAA coatings modified with two other RGD-containing peptides 34 and 35 reproducibly resulted in adherence and maintenance of a low number of mCherry-positive colonies of H9-OCT4-mCherry cells and morphologically normal colonies of H9 and NHF-1-3 hPSCs. This is the first report of cRGDfK being an effective ligand for the adherence and short-term maintenance of hPSC cultures. Adhesion of a low number of H9-OCT4-mCherry cells was also observed on pep20-PAPA and pep31-PAPA in a single experiment, but most colonies lifted off these coatings within two days of cell seeding, and those that remained showed some morphological differentiation and loss of mCherry. Optimising the CuAAC reaction conditions did not improve adhesion of H9-OCT4-mCherry cells to pep31-PAPA surfaces, so the peptide screen was not repeated on PAPA. Only surfaces modified with cRGDfK bound sufficient colonies to be considered as potential hPSC culture surfaces.

Peptide	Geltrex (+)	cRGDfK (36,+)*	cRADfK (-)	3	6	7	8	9	10	11	12	13	15	17*	19	21	22
Adhesion	4	3	1	1	1	1	1	1	1	1	1	1	1	1	1	1	1
Proliferation	✓	✓	×	×	×	×	×	×	×	×	×	×	×	×	×	×	×
OCT4 score	4	4	1	1	1	1	1	1	1	1	1	1	1	1	1	1	1
n=	N/A	N/A	N/A	2	2	2	2	2	2	2	2	2	2	2	2	2	2

Peptide	24 [#]	25	26 [#]	27	29	33*	34*	35*	1	2	4*	5*	14	16* [#]	18 [#]	20	23 [#]	28	30* [#]	31*	32*
Adhesion	1	1	1	1	1	1	2	2	1	1	1	1	1	1	1	2	1	1	1	2	1
Proliferation	×	×	×	×	×	×	✓	✓	×	×	×	×	×	×	×	×	×	×	×	✓	×
OCT4 score	1	1	1	1	1	1	4	4	1	1	1	1	1	1	1	1	1	1	1	2	1
n=	2	2	2	2	2	2	3	3	1	1	1	1	1	1	1	1	1	1	1	4	1

Figure 4.11: Peptide screening summary results are presented in this figure. The adhesion, proliferation and OCT4 scores are presented for H9-OCT4-mCherry cells cultured on polymer coatings modified with 36 peptides. Controls include surfaces modified with binding (cRGDfK) and non-binding (cRADfK) peptides and Geltrex™-coated wells. For adhesion (assessed at day 2): green (4) = more colonies attached than cRGDfK control; yellow (3) = similar number of colonies to cRGDfK control; orange (2) = fewer colonies than cRGDfK control; red (1) = no attachment. For proliferation (day 4): green (Y) = colony growth was observed; red (N) = colony growth was not observed OR no attachment. For OCT4-expression green (4) = 100-75 % of colonies are mCherry-positive; yellow (3) = 75-50 % positive; orange (2) = 50-25 % positive; red (1) = 25-0 % of colonies are mCherry-positive OR no attachment. *denotes peptides that had previously been reported to bind hPSCs [#]denotes incompletely soluble peptides.

4.3.6 Flow cytometric assessment of hPSCs for integrin $\alpha\beta 3$

It has variously been asserted that cRGDfK specifically interacts with $\alpha\beta 3$ integrins (Mondal et al., 2013), that undifferentiated hPSC cultures attach to but are unable to be maintained on cRGDfK-presenting surfaces (Klim et al., 2010) and that hPSCs are unable to bind to surfaces that only present $\alpha\beta 3$ -specific ligands (Klim et al., 2012). However reports of hPSC integrin expression profiles are inconsistent and the absolute specificity of cRGDfK- $\alpha\beta 3$ integrin interactions has not been demonstrated directly (Xu et al., 2001, Braam et al., 2008, Li et al., 2012). In order to determine whether interactions between hPSCs and cRGDfK-PAAA or cRGDfK-PAPA surfaces could be mediated by $\alpha\beta 3$ integrins, flow cytometry was used to assess the presence of $\alpha\beta 3$ integrins on the surface of H9 hPSCs compared to the positive control MDA-MB-435 cell line. MDA-MB-435 stained positive for $\alpha\beta 3$ integrin, but the protein was undetectable on the surface of H9 hPSCs by flow cytometry (Figure 4.12). This result indicates that hPSC adhesion to cRGDfK-presenting polymer substrates is likely mediated by different cell adhesion molecules, and suggests that hPSC interactions with cRGDfK are not exclusively mediated by $\alpha\beta 3$ integrins.

4.4 Discussion

In this chapter, the library of 36 peptides presented in Table 4.1 (and characterised in Appendix 3) were screened in the context of the polymer coatings optimised in Chapter 3 for their ability to support adhesion, proliferation and the short-term maintenance of hPSCs. Surfaces modified with any one of three peptides (cRGDfK or peptides 34 or 35) resulted in consistent binding of colonies of H9-OCT4-mCherry cells, while cells cultured on surfaces modified with peptides 20 or 31 weakly and/or inconsistently adhered to the surface. Each of the three peptides that contributed to consistent hPSC adhesion contained the integrin-binding motif Arg-Gly-Asp (RGD).

The RGD motif is the smallest functional unit of integrin-binding proteins (Pierschbacher and Ruoslahti, 1984), and can be found in a wide range of integrin-binding ECMPs including fibronectin, vitronectin, laminin, collagen, fibrinogen, osteopontin, bone sialoprotein and entactins (Ruoslahti, 1996). The linear RGD peptide is flexible and is known to interact with complex and multivalent binding sites in eight of the 24 known integrin subtypes including $\alpha\beta 3$, $\alpha\beta 5$ and $\alpha 5\beta 1$ (Xiong et al., 2002, Barczyk et al., 2010). The conformation of the RGD domain in short peptides is dictated by the flanking sequences and related secondary structure, which control the integrin-binding specificity; RGD-containing peptides can be thereby restricted to binding specific integrin subtypes (Haubner et al., 1996) or to lose integrin-binding function altogether (Pierschbacher and Ruoslahti, 1987). The *in vivo* conformation of the RGD motif in proteins is also controlled by tertiary structure and post-translational modifications, but the short, synthetic peptides used in this study lack these contributing factors. The present screen included four RGD-containing peptides: the synthetic cRGDfK peptide and the ECMP-derived peptides 11, 34 and 35, which are respectively derived from osteopontin, bone sialoprotein and vitronectin. Bound hPSC colonies were observed on surfaces that had been modified with three of the four RGD-containing peptides, and the PAAA and PAPA polymer coatings on which the most colonies clearly and consistently bound were modified with the synthetic cRGDfK peptide.

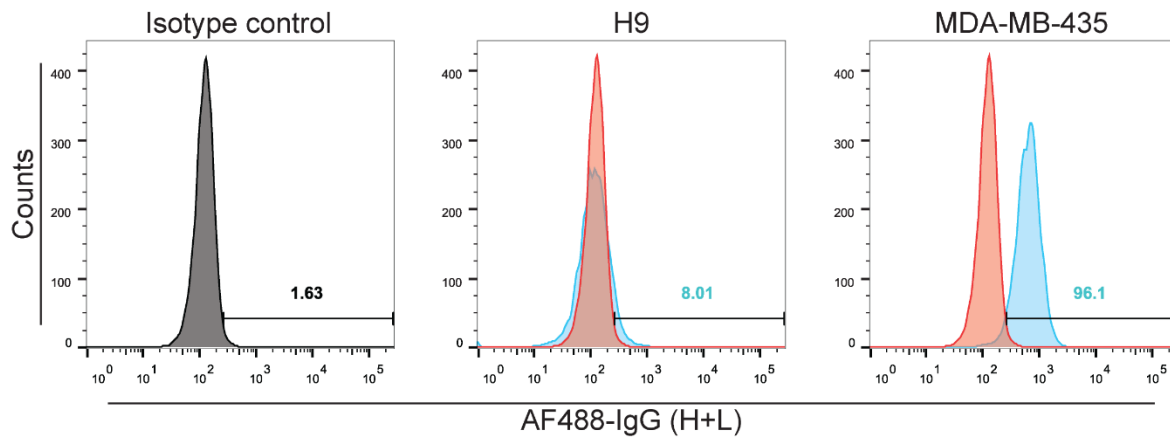


Figure 4.12: Integrin $\alpha\beta3$ was undetectable on the surface of H9 hPSCs by flow cytometry. Populations of the test H9 hPSCs (centre, blue overlay) and MDA-MB-435 cells (right, blue overlay) were each immunostained with an anti $\alpha\beta3$ integrin primary antibody and an anti-IgG(H+L) secondary antibody and assessed by flow cytometry. Gates were set against a population of H9 cells that had been stained with an IgG isotype control antibody (left and red overlays).

Decades of research pertaining to the optimisation of RGD-containing sequences for subtype-specific integrin binding found that cyclisation produced RGD-containing peptides that were proteolytically stable and that bound specifically and with high affinity to certain ECMPs (Pierschbacher and Ruoslahti, 1987). Iterations of cyclic RGD peptides including cRGDEv, cRGDfV (Cilengitide) and cRGDfK were further optimised as anti-cancer drugs that targeted $\alpha\beta3$ integrins (Haubner et al., 1996). Cyclic peptides containing the RGDf sequence were reported to possess optimal affinity for $\alpha\beta3$ integrins and the chemical functionality afforded by a lysine residue resulted in a useful molecular tool in the peptide cRGDfK (Haubner et al., 1996). Although it is often assumed that cRGDfK interacts specifically with $\alpha\beta3$ integrins, a recent study has suggested that the peptide can also interact with $\alpha\beta5$ and $\alpha5\beta1$ integrins (Mondal et al., 2013). Despite widespread use in various applications including *in vitro* adhesion of osteoblasts (Hirschfeld-Warneken et al., 2008), chondrocytes (Jeschke et al., 2002, Kantelehner et al., 2000) and melanoma cells (Klim et al., 2012), and despite the success of $\alpha\beta3$ -binding surfaces including vitronectin, laminin-111 and Corning Synthemax™ in hPSC culture, only one other study to date has reported the use of a hPSC culture surface that presents cRGDfK as a sole ligand (Klim et al., 2010).

The culture surface tested by Klim et al. (2010) presented biotinylated cRGDfK peptides from a streptavidin-coated TCPS surface. Although this surface was able to support adhesion and short-term proliferation of two hPSC lines (WA07 and WA14), a large amount of differentiation was observed. hPSCs were observed to form multilayered aggregates that were loosely attached to the surface, lost OCT4 as detected by flow cytometry and would detach in the absence of the p160ROCK inhibitor Y-27632, a phenomenon that is discussed below. In a subsequent study, Klim et al. (2012) were unable to detect $\alpha\beta3$ integrin on undifferentiated WA07 hESCs by flow cytometry. These results were inconsistent with an earlier study where $\alpha\beta3$ integrins were detected by flow cytometry on WA01 hESCs and where antibody blocking experiments demonstrated the contribution of $\alpha\beta3$ integrins to hESC adhesion to Matrigel™ (Meng et al., 2010). Reports of integrin expression in hPSCs vary between studies, partly due to cell line differences and due to a lack of correlation between transcription and translation of integrin genes (Li et al., 2012, Braam et al., 2008, Xu et al., 2001). For example a study by Lee et al. (2013) detected high expression levels of $\beta5$ and low levels of αv integrin mRNA by Q-PCR in H9 hPSCs, but high levels of $\alpha\beta5$ integrins by flow cytometry. In the study by Lee et al., a very low level of expression of the $\beta3$ subunit was detected by Q-PCR and $\alpha\beta3$ integrin levels were not assessed by flow cytometry. Klim et al. (2012) also found that a surface modified with an $\alpha\beta3$ -specific peptidomimetic small molecule was only able to bind differentiated (OCT4 could not be detected by immunocytochemistry) cells from populations mixed with undifferentiated WA07 hPSCs, while both cell types were able to bind to vitronectin-coated surfaces ($\alpha\beta3$ - and $\alpha\beta5$ -binding). A subsequent study using antibody-blocking experiments demonstrated that hPSC interactions with the Synthemax™ culture surface are predominantly mediated by $\alpha\beta5$ integrins (Jin et al., 2012) and it has also been reported that blocking $\alpha\beta3$ integrins had no observable effect on hPSC adhesion to Matrigel™ (Zhang et al., 2013b). Flow cytometric staining of hPSCs for $\alpha\beta3$ integrins in the present study (Figure 4.12) indicated that $\alpha\beta3$ integrins were not present, which indicates that cRGDfK-hPSC interactions are mediated by other CAMs, probably $\alpha\beta5$ integrins. Regardless,

the present short-term studies found that in the context of PAAA and PAPA-coated surfaces, cRGDfK-modified surfaces more efficiently supported adhesion and proliferation of hPSCs than the other RGD-containing peptides tested.

Surfaces modified with peptides derived from bone sialoprotein [peptide 34, (Oldberg et al., 1988)] or from the hPSC-supporting ECMP vitronectin [peptide 35, (Suzuki et al., 1985, Braam et al., 2008)] were able to support adhesion of low numbers of hPSCs (Figures 4.3 and 4.4). Chemically-defined surfaces that presented these peptides have previously been reported to support hPSC culture (Li et al., 2006, Melkounian et al., 2010) and one of these surfaces has been patented (Fadeev et al., 2009) and sold as Corning Synthemax™-R. It was therefore surprising to observe that so few colonies bound to pep34-PAAA and pep35-PAAA surfaces compared to cRGDfK-PAAA in this study.

In the study by Melkounian et al. (2010), it was reported that surfaces modified with either “BSP peptide” (peptide 34) or “VN peptide” (peptide 35) bound more hPSCs than surfaces modified with the laminin-derived “LM peptide” (which contains the sequence of peptide 14) on which low numbers of abnormal-looking colonies were observed. The low numbers of colonies that were observed on pep34-PAAA and pep35-PAAA surfaces in the present study, and the complete lack of hPSC adhesion observed on pep14-PAPA indicate that the PAAA and PAPA substrates used in the current study may be less permissive than the “peptide acrylate substrates” used in the study by Melkounian et al. In Section 3.3.6 it was reported that a surface peptide density of 0.5 pg/cm^2 – 3.7 pg/cm^2 was sufficient for hPSC adhesion on cRGDfK-PAPA surfaces. It is possible that peptides 34 and 35 are less efficiently coupled to the surface than cRGDfK and/or that hPSCs require higher surface concentrations of these two peptides. The peptide acrylate surfaces in the study by Melkounian et al. (2010) were generated from different monomers [2-hydroxyethyl methacrylate, 2-carboxyethyl acrylate, and tetra(ethylene glycol) dimethacrylate] from feed solutions containing monomer concentrations that were 10-fold lower than the feed solutions used in this study. Polymerisation was initiated with a single exposure to UV light in the presence of a photoinitiator and they did not report any assessment of surface stiffness.

Acrylate surfaces in the Melkounian (2010) study were modified with peptides using a carbodiimide chemistry similar to that used to modify PAAA coatings in the present study. Peptide solutions were applied to the activated surfaces at a range of concentrations ($62.5 \text{ }\mu\text{M}$ - 1 mM) that encompassed those used in the current study ($200 \text{ }\mu\text{M}$ - $600 \text{ }\mu\text{M}$) and while relative ligand density was assessed using a rhodamine-labelled peptide, absolute surface densities were not calculated. As discussed in Section 3.5, it is difficult to compare peptide densities between different studies because of the variety of methods used for surface modification and because if anything, most studies only calculated relative densities. A reduction in the efficiency of hPSC adhesion to peptide acrylate surfaces was observed when the surfaces were modified with solutions containing concentrations of peptide between 500 and $250 \text{ }\mu\text{M}$ (Melkounian et al., 2010). These concentrations are within the range used in the experiment presented in Figure 4.5, in which only a very weak trend of increasing colony numbers was observed between pep34-PAAA and pep35-PAAA surfaces modified with $200 \text{ }\mu\text{M}$ and $600 \text{ }\mu\text{M}$ peptide solutions. A more recent

study modified poly(vinyl alcohol-co-itaconic acid) coatings with “oligoVN” (peptide 34) using the same carbodiimide chemistry and also reported that similar peptide concentrations were required to modify hPSC-supporting surfaces. The authors stated that “it seems high concentration of oligoVN is necessary to keep pluripotency of hPSCs on the surface grafted with oligoVN” (Higuchi et al., 2015). Meanwhile cRGDfK-PAAA surfaces that had been modified with solutions containing 200 μM of peptide clearly bound more colonies than surfaces modified with other peptides that were applied at concentrations up to 600 μM , regardless of the peptide concentration used. Other differences between the 2010 study by Melkounian et al. and the present study include the cell harvesting method and slight variations in peptide sequence; the peptide 35 equivalent had an extra N-terminal proline “P”, but minor changes in distal sequences should have little impact on the affinity of RGD-containing peptides (Haubner et al., 1996). The range of discussion points on this matter highlight the need for the type of direct comparison reported in this study and especially for properly controlled, long-term culture studies as reported in Chapter 5.

Unlike peptides 34 and 35, neither the full osteopontin protein nor surfaces presenting its derivative peptide 11 have been reported to support hPSC cultures. Fibronectin has been reported to support hPSC cultures and contains a GRGDSP motif that is included in peptide 11, but the isolated motif can have a 1000-fold lower affinity for integrins than the post-translationally modified fibronectin fragment (Hautanen et al., 1989). It was therefore unsurprising when hPSC colonies failed to bind to surfaces modified with peptide 11 in the present experiment. The difference in affinity of the GRGDSP motif compared to fibronectin fragments also mirrors the present results with peptide 35, where a peptide segment isolated from a full length, post-translationally modified protein with well-recognised ability to maintain hPSC cultures (vitronectin) did not enable the adherence of large numbers of cells in the context of PAAA. The net result of this screen was that the naturally-derived RGD-containing peptides were outperformed by the synthetically-derived cRGDfK, which has been optimised for integrin-binding *in vitro* in the absence of post-translational modifications or a larger protein structure. These results are supportive of the observation by Melkounian et al. (2010) that “the RGD sequence alone is not sufficient for optimal [cell-surface] interaction” and suggest that the cRGDfK peptide may be more suitable for hPSC culture surfaces than other peptides tested to date. Furthermore an aim of this project was to compare hPSC cultures that had been adapted to culture on surfaces that interacted with different CAMs, and aside from the aforementioned integrin-binding peptides (cRGDfK, peptides 34 and 35), only surfaces modified with HSPG-binding peptides were observed to support adhesion of hPSCs.

As described in Section 1.7.4, HSPGs are long chains of sugar residues that form part of cell-surface syndecans and other proteoglycans, which contribute to the glycocalyx that surrounds and can be used to control the differentiation of hPSCs (Huang et al., 2014). HSPG chains are negatively charged and therefore bind positively charged molecules, including growth factors like FGF-2 (Ibrahimi et al., 2004) and highly basic peptide sequences (Liu et al., 1996). Many HSPG-binding peptides have been identified (Table 4.1) and more continue to be discovered (Dogra et al., 2015).

Of the eleven surfaces modified with HSPG-binding peptides in the current study, only pep20-PAPA and pep31-PAPA were able to bind hPSCs in the pilot screening experiment (Figure 4.8). Peptide 20 is a moderately basic laminin-derived peptide that has not previously been reported to bind hPSCs (Hozumi et al., 2010), while peptide 31 is a highly basic, vitronectin-derived peptide that has been included in several hPSC culture surfaces (Suzuki et al., 1985, Vogel et al., 1993, Klim et al., 2010). Surfaces that have been reported to bind hPSCs when modified with peptide 31 include AT-SAMs, biotin-streptavidin-coated polystyrene, glass coverslips functionalised with bromoacetamide groups (Klim et al., 2010), polyacrylamide hydrogels (Musah et al., 2012) and polydopamine-immobilised peptides (Park et al., 2015). In the pilot screen on PAPA-coated surfaces, more hPSC colonies were observed to bind to pep31-PAPA than all other surfaces modified with HSPG-binding peptides (Figures 4.4, 4.8 and 4.9), but attempts to optimise the peptide coupling chemistry on pep31-PAPA coatings failed to improve hPSC adhesion (Figure 4.10).

The first study that included peptide 31 in an hPSC culture surface used AT-SAMs to present peptides (peptide-AT) from a polyol-AT non-binding background (Klim et al., 2010). Peptide surface density was controlled with the ratio of peptide-ATs to polyol-ATs and absolute surface ligand concentrations were not calculated. Adhesion of hPSCs was observed on AT-SAMs presenting one of nine integrin- and HSPG-binding peptides (including KGRGDS) at high surface density, but when surfaces were modified with lower peptide densities, hPSCs only adhered to surfaces that presented HSPG-binding peptides (including peptides 31, 32 and 33). Surfaces modified with peptide 31 at the lowest peptide density tested (0.5 %) were reported to support hPSC adhesion. As discussed in Section 3.4, this “low” peptide density was still 1000-fold higher than the threshold surface peptide density for hPSC attachment to cRGDfK-PAPA. Like every other report of hPSC culture on surfaces that present peptide 31-presenting or other HSPG-binding peptides, the study by Klim et al. used medium supplemented with Y-27632 or other Rho pathway inhibitors (Harb et al., 2008, Klim et al., 2010, Musah et al., 2012, Musah et al., 2014, Wrighton et al., 2014, Park et al., 2015, Meng et al., 2012).

Supplementing hPSC cultures with Y-27632 inhibits apoptosis by an unknown mechanism and is sometimes able to rescue hPSC cultures from otherwise inadequate culture conditions (Meng et al., 2012, Gharechahi et al., 2014). Y-27632 is often added to hPSC cultures to improve viability during passaging, or can be used throughout culture. However Y-27632 is an animal-derived product, the downstream effects of continued exposure for Y-27632 are unclear (Gharechahi et al., 2014) and there is also some evidence that treatment with Y-27632 can bias cell fate (Chaddah et al., 2012). Krawetz et al. (2009) hypothesised that Y-27632 primarily increases cell-cell interaction and adherence instead of inhibiting apoptosis per se, and concluded by stating a preference for improved defined substrates that eliminate the need for pharmacological inhibitors. For these reasons, and due to the early successes of cRGDfK-presenting polymer coatings in Y-27632-free media (see Chapter 3), Y-27632 was not used to supplement media in the present study.

In the study by Klim et al. (2010) streptavidin-coated TCPS that presented only biotinylated peptide 31 failed to support hPSC culture without constant Y-27632 supplementation, however a combined cRGDfK- and peptide 31-presenting surface did allow withdrawal of Y-27632 after the cells had seeded. An earlier study that used laminin-111-derived peptide ligands also found that hPSC cultures could be maintained in the absence of Y-27632 on surfaces presenting both HSPG-binding and integrin-binding peptides, but not on surfaces that presented the peptides individually (Meng et al., 2010). A recent study found that pre-coating microcarriers with poly-L-lysine (PLL) prior to coating with vitronectin or laminin improved subsequent adhesion of hPSCs, an improvement that was attributed to PLL-HSPG interactions facilitating the formation of hPSC-microcarrier aggregates (Lam et al., 2014). Nevertheless, the present study demonstrates that the cRGDfK-presenting surfaces outperform HSPG-binding peptides in the context of PAAA and PAPA substrates without Y-27632 supplementation, and are capable of maintaining hPSC cultures in the absence of other ligands.

One potential reason for the poor performance of the cRGDfK-presenting surface reported by Klim et al. (2010) is instability of the underlying substrate. With a bond-dissociation energy of -18 kcal/mol, biotin-streptavidin interactions are recognised as one of the strongest non-covalent bonds (Wong et al., 1999). By comparison the free energy of $\alpha v \beta 3$ integrins binding to GRGDSP has been measured at -3.10 kcal/mol (Choi et al., 2010) while carbon-carbon covalent bonds are much stronger, with a bond-dissociation energy of -83 kcal/mol. Despite this, there is some evidence that forces generated by focal adhesions and transmitted through integrin-cRGDfK bonds are able to break biotin-avidin bonds (Jurchenko et al., 2014). Jurchenko et al. (2014) observed the removal of a cRGDfK-fluorophore construct that had been bound to the underlying TCPS by covalent and biotin-streptavidin bonds. The micro-regions from which this construct was lost co-localised with the presence of focal adhesions and progressive loss of the construct was observed over 5 hours. This removal of cRGDfK ligands from biotin-streptavidin surfaces may be further exacerbated over the multi-day timeframe of the study by Klim et al. (2010). Although no loss of cellular attachment was observed in the study by Jurchenko et al., it is conceivable that cell-mediated removal of peptide ligands could affect cell adhesion on surfaces with a lower ligand density, especially if the ligands are anchored by weaker bonds. In the Klim (2010) study, biotinylated cRGDfK peptides were bound to polystyrene plates by reacting with streptavidin that was simply adsorbed to the underlying polystyrene. Ligand removal may also occur on other surfaces that contain non-covalent bonds including AT-SAMs, which form on gold with low-stability bonds (Flynn et al., 2003). Furthermore, a study of focal adhesion formation in fibroblast cells attached to a cRGDfK-presenting substrate found that αv -containing integrins selectively localise with high force regions at the sub-100 nm scale and that blocking of αv integrins rapidly decreases cellular traction force (Morimatsu et al., 2015). These results suggest that integrins that contain αv subunits transmit a large fraction of the cell-generated forces to cRGDfK ligands presented from culture surfaces. The intrinsic mechanics of focal adhesions are currently not well understood (Jurchenko and Salaita, 2015, Morimatsu et al., 2015). However HSPGs form large chains and interact with the cell membrane through a wide range of spatially distributed ligands and through many different proteoglycans and therefore appear to be poor candidates for

exerting forces (Kim et al., 2011). If cell-generated forces are transmitted through the integrin-mediated interactions of focal adhesions, then the streptavidin-biotin-peptide 31 surface developed by Klim et al. (2010) would not be damaged in the same way that is being proposed for the cRGDfK-presenting surface. The fact that hPSCs were able to bind to all surfaces that had been modified with HSPG-binding peptide 31 in the study by Klim et al. (2010) but not to surfaces modified with integrin-binding peptides, may be counter-intuitively due to the weaker HSPG-ligand interactions that generate forces at a “sweet spot” that is strong enough to support cellular adhesion but not does not impart enough force to remove the ligand from the surface. Alternatively, the requirement of Y-27632 supplementation for hPSC culture on the cRGDfK-presenting surface may reflect the role of Y-27632 in inhibiting myosin contractility (Xu et al., 2010), which would prevent the cell-mediated destruction of the surface). Conversely, PAAA and PAPA are covalently bonded from the peptide ligand through to the underlying polystyrene and so physical removal of cRGDfK peptide ligands by cellular forces is highly unlikely.

It is difficult to isolate essential ligand-CAM interactions for maintaining hPSC cultures because interactions between and within the extracellular matrix and CAMs are very complex, and poorly understood and because investigations of receptor cross-talk are in their infancy (Hozumi et al., 2015, Zaba et al., 2015). Antibody-blocking experiments often focus on small subsets of integrin subtypes that are supposed to represent specific and singular receptors for one ECMP, and this is not accurate (reviewed by Lambshead et al., 2013). A few studies have focused on ligand-receptor interactions in hPSCs, however the studies discussed in the following passage illustrate some of the pitfalls involved in assigning specific CAM-ligand interactions to the key peptides that arose from the screen.

A 2015 study assessed hPSC adhesion to peptide 31- and 35-modified polydopamine (pDA)-coated substrates, which were designed to be applied to as wide a range of underlying materials as possible (Park et al., 2015). The broadly adhesive nature of this surface increases the likelihood of high levels of background interactions. Accordingly, a level of hPSC adhesion was observed on peptide-free pDA coatings, whereas no hPSC colonies were observed to form on any unmodified PAAA or PAPA surfaces over the course of this project. Park et al. (2015) also observed that a peptide with an otherwise identical sequence to peptide 31 formed dimers linked by N-terminal cysteines, which were not included in peptide 31 as used in the present study (Table 4.1). Peptide multimerisation can increase integrin-binding activity (Englund et al., 2012). The pep31-pDA mix was also observed to form complexes on the surface, which may have contributed to non-specific cellular adhesion. Park et al. (2015) also reported that peptide 31-mediated binding was completely abrogated by blocking $\alpha v \beta 5$ integrins, which combined with results from the aforementioned study by Mondal et al. (2013) indicates that both cRGDfK and peptide 31 may interact with hPSCs through $\alpha v \beta 5$ integrins. Although Vogel et al. (1993) initially observed that peptide 31 was able to immunoprecipitate αv and $\beta 5$ integrin subunits, peptide 31 is typically discussed as a HSPG-binding peptide. Park et al. have also reported that $\beta 1$ -blocking resulted in disruption of peptide 31-mediated binding, and this subunit was unsuccessfully immunoprecipitated in the study by Vogel et al. (1993). Ultimately, background integrin-pDA

interactions could potentially be responsible for many of the results from the Park study. Furthermore, an older study (Nomizu et al., 1997) found that different substrates can be variously effective at eliciting cell-binding responses to identical peptides, which demonstrates the importance of optimising culture conditions on scalable surfaces that are able to translate directly to therapeutically-relevant hPSC culture systems.

Aside from the synthetically designed cRGDfK peptide and those derived from vitronectin, laminin and bone sialoprotein, there were five peptides in the screening library (Table 4.1) that have previously been reported to feature in hPSC-binding surfaces. Peptides 4 and 5 are randomly generated peptides that were identified from a phage display library (Derda et al., 2010) and the current study is believed to be the first reported follow-up assessment of hPSC adhesion to surfaces that present these peptides. As discussed in Section 1.5.2, surfaces presenting laminin-derived peptides 16, 17 and 30 have only been shown to support hPSC cultures when all three peptides were adsorbed to TCPS at specific relative concentrations and then treated with BSA, which may itself interact with hPSCs (Meng et al., 2010). The screening results of peptides 16, 17 and 30 presented in this chapter support the hypothesis that laminin-derived peptides are individually inadequate for supporting maintenance of undifferentiated hPSC culture. The remaining 27 peptides that were screened had been included in this study due to reported interactions with other cell types. These peptides had never been reported to bind hPSCs and were not observed to do so in the context of PAAA or PAPA substrates in this study.

One CAM that is highly expressed in hPSCs that has not been probed in this study is E-cadherin. The HAV peptide has been reported to block binding to CAMs when it is in solution but has been unable to function as a tethered ligand for cellular adhesion, probably due to the size, complexity and multimeric nature of E-cadherin binding interactions (Blaschuk et al., 1990, Renaud-Young and Gallin, 2002). As discussed in Section 1.4.2, coatings of the E-cadherin fusion protein sold as StemAdhere™ have been demonstrated to maintain hPSC cultures and are included in the long-term culture study in Chapter 5, but any novel synthetic peptides able to bind cells to a surface would be of great interest.

The library of peptides for screening was curated by a literature search to restrict the number of test peptides and ensure a high rate of success compared to screening random peptides. Introducing any pre-selection criteria necessarily includes a risk of excluding potential hits, however a screen of high numbers of randomised peptides for adhesion of hPSCs had already been conducted (Derda et al., 2010) and so the low chance of identifying completely novel peptides was outweighed by the relative ease of this approach. The screen by Derda et al. (2010) may have been hampered by the use of MEF-CM and/or by cross-contamination between adjacent array elements. Conducting the current screen in individual wells instead of on a micro-patterned surface ensured that peptides could not contaminate the surrounding array elements.

Peptide insolubility was a potential source of false negative results in this study. The six peptides that displayed solubility issues (peptides 16, 18, 23, 24, 26 and 30) did not possess exceptional length, charge, isoelectric point or hydrophobicity (Table 4.2) so it is unclear why they were

difficult to dissolve. The research group headed by Prof. Motoyoshi Nomizu (Nomizu et al., 1997) were able to dissolve peptides 18 and 23 in MQ H₂O using sonication (*pers. comm.*), but in the present study this was found to be insufficient. In order to improve the hydrophobicity of these peptides, hydrophilic groups such as a C-terminal Ser-Gly-Ser could be added, but this may subsequently interfere with cell binding activity. The possibility of peptide-based variation in coupling efficiency leading to variable surface peptide density can also not be excluded. Performing Europium-tagging experiments with each peptide would enable optimisation of coupling reaction conditions to achieve maximal peptide densities for optimal screening results from each peptide, although this was not feasible for the current study.

The colony counting assay used in this study is insensitive at high cell numbers, but was sufficient for identifying weak leads that could be optimised. Strong lead peptides were to be separated in the long-term culture study in Chapter 5. Repeating the whole screening process with additional pluripotent cell lines may have identified more hits, but this approach would just have identified extra peptides that only bound to certain cell lines, and consistency and reliability were considered to be important qualities for developing standardised hPSC culture conditions.

The peptide screen presented in this chapter was designed to identify peptides by which hPSCs could be tethered to the PAAA or PAPA coatings, allowing the cells to proliferate and to maintain pluripotency as indicated in real-time by maintenance of detectable levels of mCherry in the H9-OCT4-mCherry line. This screen thus identified cRGDfK-modified coatings as the lead candidates for comparative long-term hPSC maintenance studies.

4.5 Chapter Summary

The experiments described in this chapter were designed to compare the efficiency of various peptide ligands in mediating hPSC adhesion to peptide-modified PAAA and PAPA coatings, optimised in Chapter 3, to identify lead ligands for modification of PAPA-coated flasks for the long-term culture study presented in Chapter 5. A screening experiment assessed the efficiency of adhesion of H9-OCT4-mCherry cells to PAAA and PAPA coatings modified with individual peptides from a library of 36 peptides with previously reported roles in cell adhesion. A greater number of hPSCs were consistently observed to adhere to cRGDfK-PAAA and cRGDfK-PAPA coatings than to coatings modified with any other peptide. Although high peptide concentrations were used to modify surfaces for screening, a low number of colonies were observed on coatings modified with RGD-containing peptides 34 and 35, which are included in the commercially available hPSC culture surface Synthemax™. A likely reason for this difference in hPSC adhesion efficiency is a difference in peptide-ligand binding affinity. The synthetic cRGDfK peptide was optimised *in vitro* to have a high integrin-binding affinity, whereas the other two peptides are not presented in their optimal *in vivo* conformation and may therefore be required at higher concentrations. Surfaces modified with two HSPG-binding peptides (20 and 31) bound a very low number of colonies and colony adhesion was observed to be unstable. Based on the literature hPSC adhesion to surfaces presenting HSPG-binding peptides, and particularly peptide 31 relies on media supplementation

Chapter 4: Identification of peptides able to mediate hPSC adhesion to polymer coatings

with Rho-ROCK inhibitors, which was consciously avoided throughout this study. The results of the peptide screen presented in this chapter and the surface optimisation presented in Chapter 3 resulted in the selection of cRGDfK-PAPA coatings as the lead hPSC culture surface for the long-term culture benchmarking study presented in Chapter 5.

Chapter 5:

Characterisation of long-term
hPSC cultures maintained on
synthetic surfaces

5.1 Introduction

According to Recommendation 6 of the ISSCR Guidelines for the Clinical Translation of Stem Cells (in draft; available at <http://www.isscr.org/home/publications/ClinTransGuide>) “Where possible, components of animal origin used in the culture or preservation of cells should be replaced with human components or with chemically defined components to reduce the risk of accidental transfer to patients of unwanted chemical or biological material or pathogens”. The widespread use of chemically defined hPSC culture surfaces will therefore contribute the clinical translation of hPSCs. At the commencement of this project, StemAdhere™ and Synthemax™ II-SC (Synthemax™) were the only two commercially available chemically defined hPSC culture surfaces. Although it is yet to be seen how the recently released L7™ hPSC Matrix (Lonza) will be received, neither StemAdhere™ nor Synthemax™ have been taken up by the wider scientific community for reasons that include cost and inertia. During the development of StemAdhere™ {Nagaoka, 2010 #243} and Synthemax™ {Melkounian, 2010 #244}, hPSC cultures maintained on each surface were compared to control cultures maintained on Matrigel™ however a direct, side-by-side comparison of hPSC cultures maintained long-term on each surface has not been reported. As depicted in Figure 5.1, the previous chapters of this thesis describe the optimisation of peptide-modified polymer brush coatings PAAA and PAPA as novel synthetic hPSC culture substrates (Chapter 3) and the use of those substrates to screen for hPSC adhesion to surfaces modified with a library of anchored peptide ligands (Chapter 4). hPSCs were observed to bind most effectively to thin coatings that had been modified with low concentrations of the cRGDfK peptide. The associated savings for prospective large scale hPSC cultures were involved in the selection of PAPA-cRGDfK as the lead candidate hPSC culture surface. In the present chapter, cRGDfK-PAPA coatings and E8 medium were used to maintain long-term culture of three hPSC lines and the resulting cells were benchmarked against cultures maintained in parallel on flasks coated with StemAdhere™, Synthemax™ or Geltrex™-coated flasks. Detailed cell characterisation and comparisons of the application and use of each culture surface were performed to facilitate future selection of hPSC culture surfaces for large and small scale cultures.

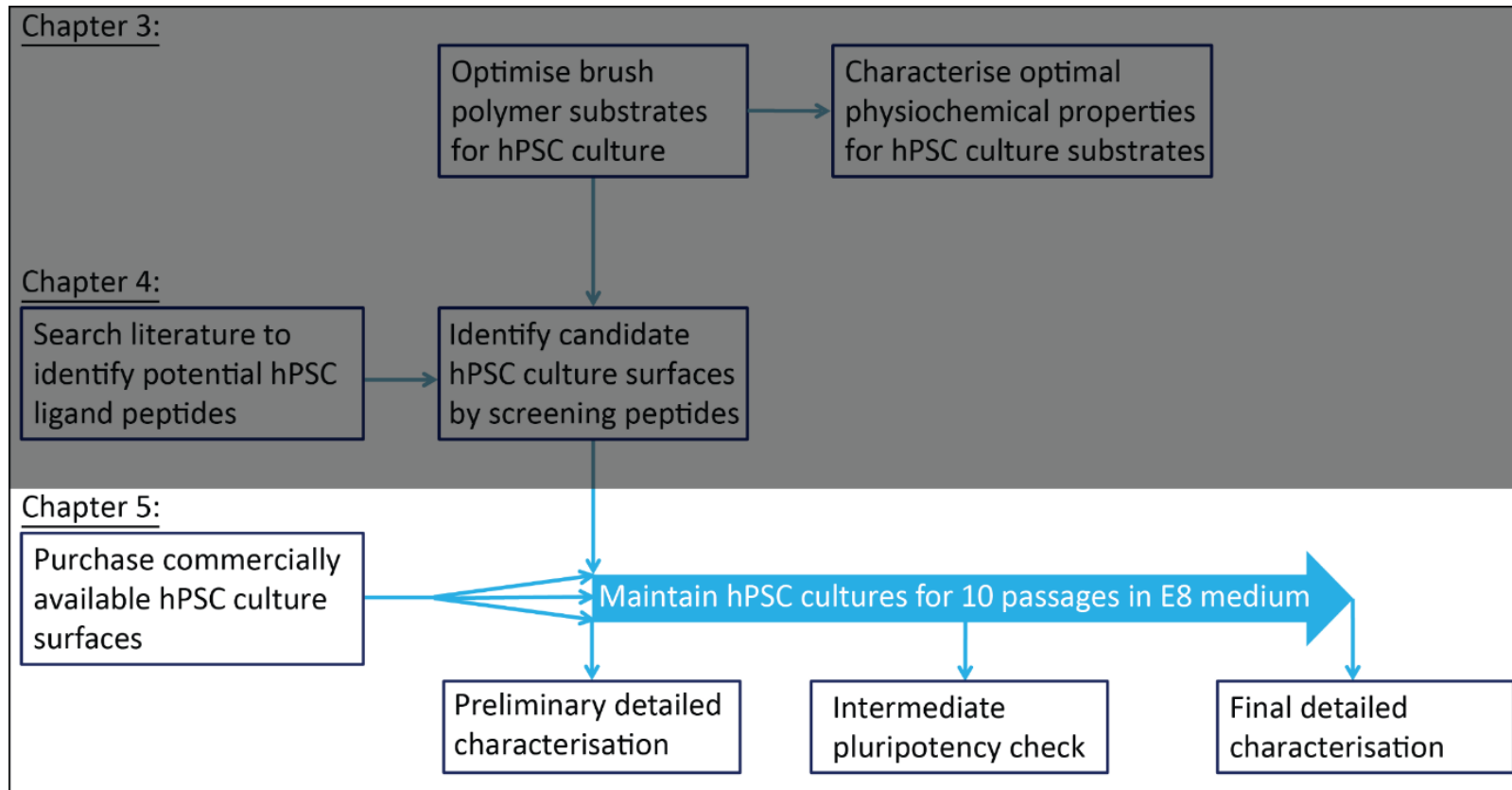


Figure 5.1: Schematic depicting the overall project outline. The experimental approach that yielded the results presented in Chapter 5 is highlighted. hPSC cultures were maintained in E8 medium for ten passages on surfaces coated with the novel candidate hPSC culture surface (PAPA-cRGDfK). hPSCs were characterised before and after ten passages, and comparisons were made to cultures maintained in parallel on commercially available hPSC culture surfaces (Geltrex™, StemAdhere™, Synthamax™).

5.2 Chapter specific methods

5.2.1 Preparation of coated flasks for hPSC culture

In order to minimise variables between the culture conditions, methods for maintaining hPSCs on commercial culture surfaces were standardised as much as possible while following the manufacturers' instructions. This necessitated that each surface coating be applied to specific TCPS cultureware; StemAdhere™ must be applied to non-TC-treated polystyrene (Sigma Aldrich, Cat No: CLS431463) and Synthemax™ to plasma-treated CellBIND® polystyrene (Sigma Aldrich, Cat No: CLS3289), while Geltrex™ and PAPA-cRGDfK were each applied to regular tissue-culture-treated polystyrene (Sigma Aldrich: CLS430168). All coatings were applied to the appropriate Corning-brand 25 cm² flasks in order to standardise flask properties including airflow, size, and shape. Duplicate flasks were maintained at all times the first flask of a new batch was paired with a flask from a previously validated batch, which mitigated the risks of coating failure for individual flasks and for whole batches.

5.2.1.1 Preparation of Geltrex™-coated flasks

Geltrex™-coated flasks were prepared as described in Section 2.3.1.

5.2.1.2 Preparation of cRGDfK-PAPA-coated flasks

Five batches, totalling 136 PAPA-coated flasks were prepared and assessed for quality control as described in Section 2.5.1 of this thesis. Batches of PAPA-coated flasks were subsequently modified with reaction solutions containing 36 µM cRGDfK peptide as described in Section 2.5.3 and stored for no longer than three months. These conditions were in excess of the minimum peptide concentration and well within the shelf life as determined in Sections 3.3.3 and 3.3.8 respectively.

5.2.1.3 Preparation of Synthemax™-coated flasks

The original Synthemax™-R substrate was developed as an acrylate-based UV-activated surface that was cured *in situ* (Melkounian et al., 2010). The Synthemax™ II-SC coating used in the current study appears to interact with the underlying polystyrene by adsorption alone, and the physiochemical properties of this coating have not been reported. Synthemax™-coated flasks were prepared according to the handbook entitled "Corning Synthemax™ II-SC Substrate Self-Coating Protocol" (Corning Inc., 2012, CLS-AN-204 REV4).

1. Synthemax™ II-SC substrate (Sigma Aldrich, Cat No: CLS3535XX1) was dissolved in tissue culture grade water (Life Technologies, Cat No: 15230-162) to 1 g/mL. This stock solution was further diluted in tissue culture grade water to a final concentration of 0.025 g/mL.
2. Plasma-treated CellBIND® 25 cm² flasks were coated with 5 mL of Synthemax™ II-SC solution for 2 hours at room temperature, after which all visible solution was aspirated so that plates appeared dry.
3. Coated flasks were wrapped in parafilm and stored at 4 °C for up to three months.

5.2.1.4 Preparation of StemAdhere™-coated flasks

StemAdhere™-coated plates were prepared according to the STEMCELL Technologies handbook entitled “Maintenance of hPSCs on StemAdhere™ Defined Matrix for hPSC” (Version 1.0.0, Cat No: 28795).

1. StemAdhere™ Defined Matrix for hPSC (STEMCELL Technologies, Vancouver, Canada, Cat No: 07160) was thawed and diluted 1:25 in StemAdhere™ Dilution Buffer (STEMCELL Technologies, Cat No: 07163).
2. Non-tissue culture treated 25 cm² flasks were coated with 2.5 mL of diluted Matrix solution at 37 °C for at least one hour.
3. StemAdhere™-coated flasks were used immediately or sealed with parafilm and stored overnight at 4 °C.
4. Immediately prior to cell seeding, StemAdhere™-coated flasks were rinsed with 2.5 mL of StemAdhere™ Dilution Buffer.

5.2.2 Cell culture methods

Cell culture methods were standardised across all surfaces as much as possible. Human pluripotent cell lines H9, Genea-02 and NHF-1-3 (Section 2.2) were maintained in E8 medium on all coatings and seeded at a density of 15 000 cells/cm² following dissociation with EDTA as described in Section 2.3.2. Cells cultured on Geltrex™, cRGDfK-PAPA and Synthemax™ were exposed to EDTA for ~3 minutes, while cells cultured on StemAdhere™ lifted more rapidly and were therefore exposed to EDTA for ~100 seconds. Cells that did not lift from pipetting with medium after incubation in EDTA were manually removed from the surface using a cell scraper (Interpath Services, Cat No: 541070).

In order to minimise any confounding effects of adaptation from pre-existing culture conditions, and so this study could identify any effects of adaptation from culture on Geltrex™ to culture on defined surfaces, cell banks were prepared of cryopreserved H9, NHF-1-3 and Genea-02 hPSCs that had been adapted to culture in E8 medium on Geltrex™-coated surfaces. Extant cultures of H9, NHF-1-3 and Genea-02 cells in KOSR medium on MEFs were harvested and transferred directly into E8 medium, seeded into Geltrex™-coated flasks and maintained for ten passages before being cryopreserved as described in Section 2.3.3. These cell lines were then used as required for the experiments described herein.

Throughout this chapter, cell passage numbers are reported as “cell line name pa+b+c+de” where “p” represents the word “passage”, “a” represents the number of mechanical passages in KOSR/MEF conditions following initial derivation, “b” represents the number of collagenase-mediated passages in KOSR/MEF conditions, “c” represents the number of EDTA-mediated passages in E8 medium on Geltrex™, “d” represents the test culture surface (GX, Geltrex™; RGD, cRGDfK-PAPA; SA, StemAdhere™; SX, Synthemax™) and “e” represents the number of EDTA-mediated passages in E8 medium on test culture surfaces. Each cell line was adapted to culture in E8 medium on Geltrex™ (“c”) for at least ten passages prior to seeding on test culture surfaces. In the case of control cultures maintained on Geltrex™, the values c and d represent identical conditions but for this report they have been kept separate to indicate the duration of the experiment.

5.2.3 hPSC characterisation

hPSCs thawed from the E8/Geltrex™-adapted banks were subjected to the quality control assays described below, namely flow cytometry for detection of OCT4, G-banding karyotyping and teratoma formation assays. At the commencement of the long-term culture experiment, quality-controlled cultures were thawed from the bank and passaged at least twice in E8 medium on Geltrex™ to establish robust pluripotent cultures prior to parallel adaptation to culture on test surfaces. After ten passages on each surface the quality control assays were repeated and cells were further characterised using the PluriTest™ assay. Frozen stocks were generated at passages 3, 6 and 10 of culture on test surfaces as a contingency for culture failure, and cell pellets were collected at each passage to enable subsequent isolation of RNA for gene expression analyses at intermediate passage numbers.

5.2.3.1 Observations of hPSC cultures

Daily observations were made to assess the confluence of each culture, the amount of cell death in each flask and the amount of morphological differentiation in all ongoing hPSC cultures. Differentiation was arbitrarily classified as “low”, “medium” or “high” level based on the proportion of cells that appeared to be morphologically differentiated. When cell scraping was required to harvest cells, the proportion of cells that had not lifted following treatment with dissociation reagents and pipetting with culture media was estimated and recorded.

5.2.3.2 Flow cytometry

As discussed in Section 1.3, flow cytometric analysis for detection of OCT4 protein is a rapid and effective approach for monitoring the pluripotency of ongoing cell cultures. Flow cytometric assessment of OCT4 was performed at passages 1, 3 and 10 of culture on defined culture surfaces. Cultures that contained less than 50 % OCT4-positive cells at passage 3 were discontinued.

1. hPSC cultures maintained in 25 cm² flasks were washed twice in 5 mL DPBS- and incubated in 1 mL TrypLE™ Express (Life Technologies, Cat No: 12604) for 5 min.
2. Single cells were harvested by pipetting 2 x 5 mL DMEM/F12 medium (Life Technologies, Cat No: 10565) across the surface. When hPSCs did not lift from pipetting the proportion of cells remaining was estimated and then they were gently removed from the surface using a cell scraper.
3. Cells were pelleted by centrifuging at 800 g for 2 min and resuspended in 3 mL DMEM/F12. Aliquots were taken and subjected to hemocytometer-based counting as described in Section 2.4.1. The cell suspensions were then topped up to 10 mL with DMEM/F12 and pelleted again.
4. Pelleted cells were resuspended in 50 µL DMEM/F12 and transferred dropwise into 1 mL of 20 mg/mL paraformaldehyde (Polysciences, Inc., Taipei, Taiwan, Cat No: 04018) and fixed for 30 minutes. After two washes with 1 mL DPBS-, cells were permeabilised for 5 min in 200 µL DPBS- + 0.1 % Triton X-100 (Sigma Aldrich, Cat No: T8787).
5. Fixed, permeabilised cells are very fragile and were henceforth handled very gently. For example pelleted cells were resuspended by flicking the bottom of the tube, instead of with repeated pipetting. Cells were incubated for 30 minutes at RT in 1 mL 10 % normal goat serum (Life Technologies, Cat No: 16210-072) to block non-specific antibody binding sites.

6. 50 µL of blocked cell suspension was transferred to an unstained control tube while <2 million cells per tube were allocated for immunostaining and for the isotype control. Blocked cells were pelleted and resuspended in 200 µL of mouse anti-human OCT4 antibody or IgG2b isotype control antibody diluted in blocking buffer (see Table 5.1), incubated for 20 minutes on ice and washed twice in DPBS-.
7. Cells were then resuspended in 200 µL of goat anti-mouse AF488-conjugated secondary antibody, stained for 20 minutes on ice and washed twice.
8. Stained cells were assessed using one of three different flow cytometers. Data recorded on a Guava easyCyte™ 8HT sampling flow cytometer (Millipore) were analysed on a PC using the InCyte2.6 module of guavaSoft™ software. Data recorded on an LSR II (Becton Dickinson) or a FACSCalibur™ (Becton Dickinson) flow cytometer were analysed on PCs using FACSDiva™ Software v8.0.1. Approximately 10 000 events were collected and data were exported as .fcs3 files. Post-analysis was performed on a PC using FlowJo™ Version 10 (FlowJo, LLC, Ashland, Oregon). Single-cells were isolated based on forward versus side scatter and OCT4-stained cells were gated against isotype control-stained cells.

Table 5.1: This table describes the primary antibodies used for staining hPSCs for OCT4 by flow cytometry, including the target, animal-of-origin, source, and dilution factors.

Antibody	Source	Dilution
Mouse monoclonal IgG2b anti-human Oct-3/4 antibody	Santa Cruz Biotechnology, CA, Cat No: C-10	1:50
IgG2b isotype control	Becton Dickinson, Cat No: 559530	1:250
Alexa Fluor® 488 conjugated goat anti-mouse IgG2b	Life Technologies, Cat No: A-21141	1:500

5.2.3.3 Cell pellet collection

Cells were collected at each passage so that RNA could later be isolated for gene expression analyses.

1. Cells were harvested with EDTA as described in Section 2.3.2.
2. After the new maintenance flasks were seeded, the remaining cells were divided into two 1.7 mL tubes (Corning Inc., Cat No: MCT-175-C) and pelleted at 800 g for 2 min.
3. Supernatant was aspirated from both tubes. Cells collected for RNA isolation were resuspended and lysed in 600 µL of Buffer RLT (Qiagen, Cat No: 79216) + 1 % β-mercaptoethanol (Sigma Aldrich, Cat No: M-3148). Tubes were snap frozen in a bath of dry ice and ethanol and stored at -80 °C.

5.2.3.4 Isolation and characterisation of total RNA

Lysate of undifferentiated hPSCs stored in Buffer RLT was thawed and the RNA was isolated using RNeasy Mini Kits (Qiagen, Cat No: 74106) according to the Qiagen handbook entitled “RNeasy Mini Handbook 04/2006”.

The quality and quantity of RNA was assessed using a Nanodrop ND-1000 spectrophotometer (Thermo Scientific) and by the Micromon facility located at Monash University (Clayton, Australia) on an Agilent 2100 Bioanalyzer, using RNA 6000 Nano (total RNA) microfluidic chips (Agilent Technologies, Cat No: 5067-1511). Thresholds for passing these assays were set at an OD_{260}/OD_{280} ratio greater than 1.8 and an RNA Integrity Number (RIN) greater than 8.

5.2.3.5 Microarray analysis of total RNA and PluriTest™

PluriTest™ is an open access bioinformatic assay that uses gene expression analysis to assess pluripotency (Müller et al., 2011). In the present study, the PluriTest™ assay was applied to all hPSC cultures after their long-term maintenance on defined culture surfaces in order to identify any changes to gene expression related to the use of specific culture surfaces. Furthermore, gene expression analysis is included in the recommendations for determining pluripotency in the Guidelines for the Clinical Translation of Stem Cells established by the International Society for Stem Cell Research (ISSCR) (Hyun et al., 2008). Genome-wide transcriptional results from microarray analyses are compared using a non-negative matrix factorisation approach to over 450 profiles from a wide range of stem and differentiated cell types, including expression profiles from over 250 hPSC lines from multiple laboratories. PluriTest™ generates a “pluripotency score” based on reference data from all cell types, which places data generated from test samples on a spectrum from pluripotent (20 to 75) to differentiated (-125 to -30). The more sensitive “novelty score” represents deviation from a model pluripotent data set. Query data that fits empirically-derived thresholds for pluripotency score (>20) and novelty score (<1.67) indicate that the test RNA was extracted from a population of normal pluripotent cells. The PluriTest™ assay also generates a phylogenetic tree, probe intensity plots for quality control and a translational karyotype feature that is under development and that groups expression data by gene loci and presents the collective expression levels of each cytobands.

1. Quality control tested total RNA samples were sent to the Australian Genome Research Facility (Parkville, Australia) for analysis on HumanHT-12 v4 Expression BeadChip Microarrays (Illumina, San Diego, California).
2. The microarray files (*.idat) were uploaded to www.pluritest.org for post-analysis.

5.2.3.6 G-banding karyotype analysis

G-banding is one of the most common assays used to detect gross karyotypic abnormalities.

1. Flasks that were approximately 40 % confluent with hPSC cultures were sent to Southern Cross Pathology in the Cytogenetics department of Monash Medical Centre (Clayton, Australia) for G-banding karyotype analysis.
2. Following overnight metaphase arrest, 20 or 30 metaphase spreads were prepared and assessed for gross karyotypic abnormalities.

5.2.3.7 Teratoma assay

As described in Section 1.3, the most stringent test of pluripotency available for human cells involves injecting test cells into immunodeficient mice and observing subsequent teratoma formation. The teratoma-forming potential of all hPSC lines was tested at the start of the experiment and after >10 passages on test surfaces. Between the initial characterisation and the experimental end points, the injection method was modified to minimise anaesthetic use and discomfort for the mice. All surgeries were performed with mice on a heat pad. Breeding, surgery and all animal work was performed by Daniela Cardozo (CSIRO) and Jess Hatwell-Humble (CSIRO) at the Monash Animal Research Platform (Clayton, Australia).

Animal care. Protocols and use of animals in this project were undertaken with approval of the Monash University Animal Welfare Committee following the Australian Code for the Care and Use of Animals for Scientific Purposes (8th Edition 2013) and the Victorian Prevention of Cruelty to Animals Act and Regulations legislation.

1. Three 25 cm² flasks containing hPSC cultures at approximately 70 % confluence were harvested with EDTA (see Section 2.3.2), pelleted at 453 g for 3 min and resuspended in DMEM/F12 medium + 30 % Matrigel™ Basement Membrane Matrix (Becton Dickinson, Wembley, WA, Cat No: 354234). Six aliquots of 60 µL volume were prepared from this cell suspension for injection into each testis of three mice, either NOD-SCID C57BL6 or NOD-SCID IL2R gamma chain knockout mice.
2. **Surgical approach 1:** Mice were sedated by inhaling methoxyflurane (Medical Developments International, Melbourne, Australia, Cat No: ME-759046-MK2). Sedated mice were injected with 100 µL per 10 g body mass of 50 mg/mL Tergive (Pfizer, New York City, NY, CAS Number: 53716-49-7) and the testis region was shaved. A small (2-3 mm) incision was made to reveal the underlying testis capsule, into which no more than 30 µL of cell-Matrigel™ suspension was injected. Each incision was sealed with 9 mm stainless steel wound clips.
Surgical approach 2: Mice were restrained and the testis region was shaved and wiped with ethanol. The testis were gently pushed down into the scrotum and injected subcutaneously with 100 µL per 10 g body mass of 50 mg/mL Tergive followed by no more than 20 µL of cell-Matrigel™ suspension.
2. Post-operative mice were observed daily and were euthanised either after no more than 12 weeks, or when lumps were seen to extend beyond 1200 mm³ or when lumps were causing noticeable discomfort.
3. Mice were euthanised by cervical dislocation. The testes and any nearby tumours were dissected, placed under vacuum in animal tissue fixative (Appendix 2.5) and stored in 0.1 M Sorenson's buffer (Appendix 2.5) prior to embedding in paraffin, sectioning and staining with hematoxylin and eosin. All embedding, sectioning and staining was performed by Chad Heazelwood (CSIRO).
4. Tumours were histologically scored for the presence of tissue types representing endoderm, mesoderm and ectoderm. Test populations were deemed pluripotent if the three germ layers were collectively represented in any tumour or tumours derived from that population.

5.3 Results

5.3.1 Quality control of hPSC lines and culture surfaces

An experiment was conducted to test the ability of cRGDFK-PAPA-coated surfaces to maintain long-term hPSC culture in E8 medium, and to benchmark these cultures against cultures maintained in parallel on commercially available chemically defined surfaces StemAdhere™ and Synthemax™, as well as the current commonly used hPSC culture surface Geltrex™. In preparation for this experiment, all culture surfaces and cell lines were subjected to quality control measures. The ability of hPSCs to remain pluripotent in the short term when cultured in E8 medium in 25 cm² flasks coated with chemically defined culture surfaces was tested with the H9-OCT4-mCherry reporter cell line, which allows visual assessment of mCherry as a surrogate measure of pluripotency.

H9-OCT4-mCherry cells seeded at a density of 15 000 cells/cm² in E8 medium were observed to adhere to flasks coated with cRGDFK-PAPA, StemAdhere™ or Synthemax™ with low levels of cell death, and to proliferate and remain mCherry-positive over two serial passages (Figure 5.2). H9-OCT4-mCherry cells cultured on cRGDFK-PAPA contained large nuclei with prominent nucleoli and formed tightly-packed colonies that were remarkably morphologically similar to control cells on Geltrex™. H9-OCT4-mCherry cells cultured in flasks coated with Synthemax™ or StemAdhere™ also displayed similar morphologies, although cells maintained in StemAdhere™-coated flasks were observed to appear flatter, to individually occupy more space and to form colonies that were less tightly-packed than hPSCs on other surfaces (Figure 5.2C). Cultures maintained on all surfaces were observed to reach 60 % confluence in fewer than 4 days for each passage, at which point they were ready to be harvested for subsequent passages. This result is typical for hPSC cultures and indicated that each surface had the potential to maintain long-term hPSC cultures.

Meanwhile, cultures of H9, NHF-1-3 and Genea-02 hPSCs were thawed from cell banks prepared from cultures that had been pre-adapted to E8 medium on Geltrex™-coated flasks (Section 5.2.2). Thawed cultures of each cell line were observed to contain typically high nucleus-to-cytoplasm ratios and prominent nucleoli (Figure 5.3A-C). G-banding karyotype assessment did not detect any abnormalities (Figure 5.3G-I, Appendix 6.1) and each cell line was able to generate teratomas containing tissues representative of all three embryonic germ layers (Figure 5.3J-R). Furthermore, >90 % of H9 and NHF-1-3 cells were detected as OCT4-positive by flow cytometry (Figure 5.3D,E) whereas Genea-02 cells were not subjected to this assay at this stage due to time constraints and low cell numbers. Collectively, the results presented in Figure 5.3 indicate that the hPSC cultures maintained on Geltrex™-coated flasks were of high quality and were suitable for testing novel culture conditions.

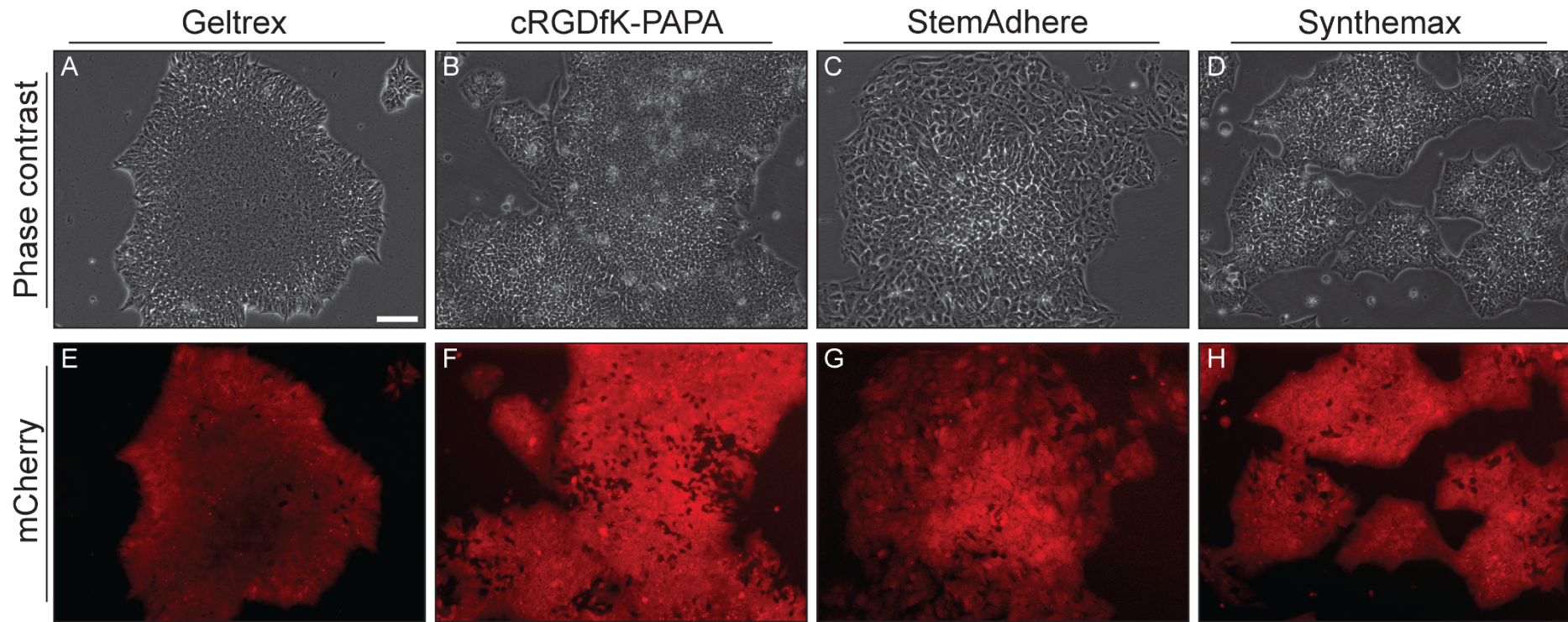


Figure 5.2: Short-term H9-OCT4-mCherry cultures were maintained for 3 days in E8 medium on test surfaces and assessed for morphology and the presence of mCherry. (A-D) Phase contrast and (E-L) mCherry fluorescence photomicrographs are presented of H9-OCT4-mCherry cells three days post-seeding, following two serial passages in flasks coated with (A,E) Geltrex™, (B,F) cRGDfK-PAPA, (C,G) StemAdhere™ and (D,H) Synthemax™. All fluorescence images were acquired with 600 ms exposure times. The mCherry signal in image G was less bright than images E, F and H and was not visible when all images were treated identically. Image G was therefore scaled to a grey level minimum of 370 and maximum of 580 instead of the same grey level range (1000 to 2000) as E, F and H. Scale bar represents 100 μm on all images.

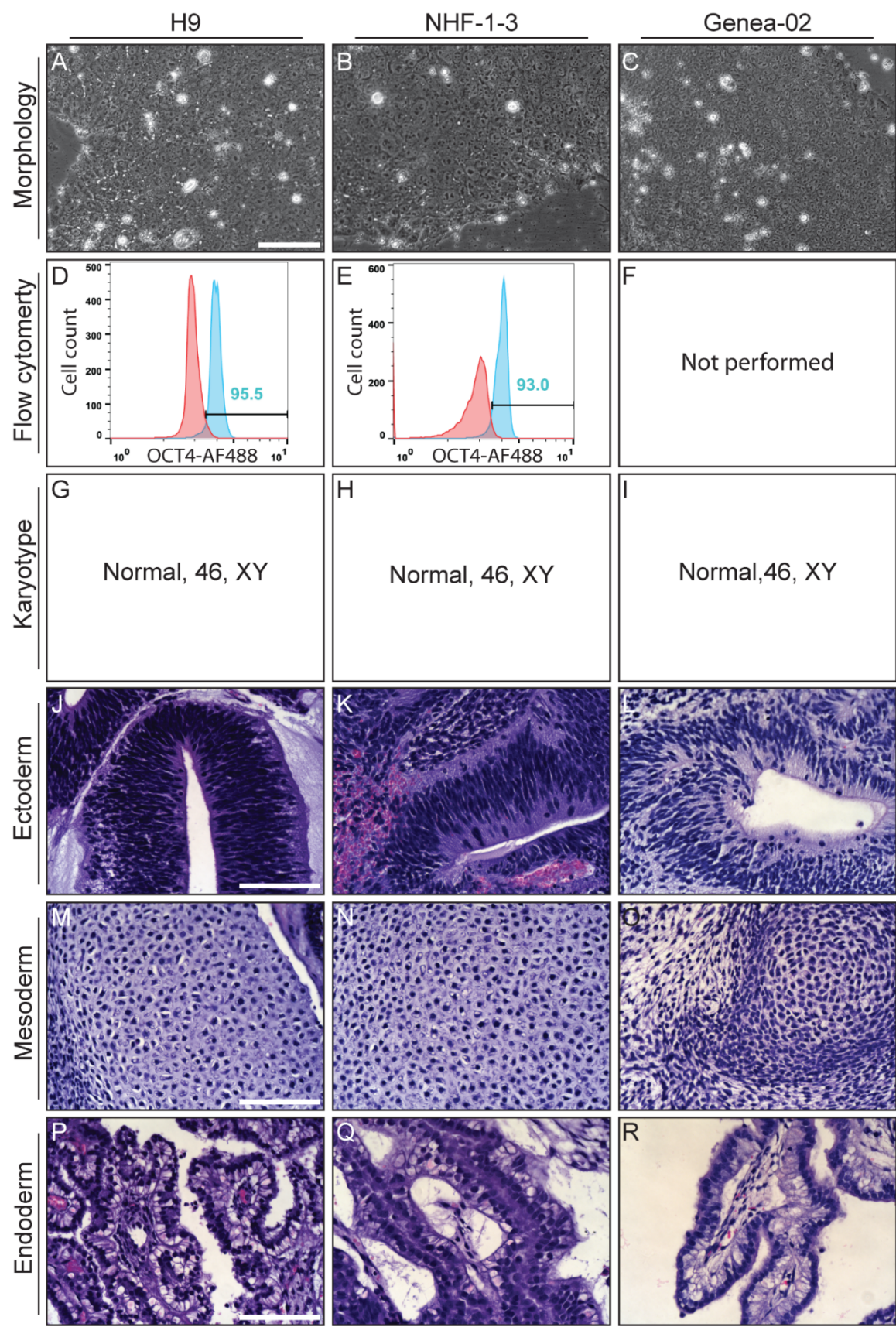


Figure 5.3: Caption on subsequent page.

Figure 5.3: Characterisation of H9, NHF-1-3 and Genea-02 cell lines that had been adapted to culture in E8 medium on Geltrex™-coated surfaces for greater than ten passages. (A-C) Phase contrast images were captured of cultures of H9, NHF-1-3 and Genea-02 cultures maintained on Geltrex™ at day 3 post-seeding. (D-F) Representative histogram plots show flow cytometric detection of OCT4 (AF488) in H9 and NHF-1-3 cells compared to cells stained with an isotype control antibody. The percentage of cells in which OCT4 was detected are included in each plot. (G-I) G-banding karyotype results of H9, NHF-1-3 and Genea-02 hPSC cultures maintained in E8 medium on Geltrex™-coated surfaces. Full karyograms are presented in Appendix 6.1. (J-R) Teratoma formation assay results are also presented for the three adapted hPSC lines, showing formation of (J-L) neural rosettes (ectoderm), (M-O) cartilage (mesoderm) and (P-R) secretory epithelial cells (endoderm). Scale bars, 100 µm.

5.3.2 Gross observations of morphology and proliferation rates of hPSC cultures on defined surfaces

In order to test the ability of cRGDfK-PAPA-coated surfaces to maintain long-term culture of hPSCs, high quality H9, NHF-1-3 and Genea-02 cells were thawed from the validated cell banks described above, passaged twice to allow them to recover from the thawing process and expanded into four Geltrex™-coated flasks. This ensured that enough cells were available to seed duplicate flasks coated with cRGDfK-PAPA, as well as flasks coated with StemAdhere™, Synthemax™ and Geltrex™ for comparison. hPSC cultures were then EDTA-harvested from all four flasks and seeded at 15 000 cells/cm² directly into a total of eight flasks. Ongoing cultures of H9, NHF-1-3 and Genea-02 cells were thereafter maintained independently for at least ten passages as a total of twelve separate cultures in duplicate flasks coated with each test culture surfaces (Figure 5.1). Additional flasks were included for characterisation at passages 3 and 10

Over ten passages of culture in flasks coated with either cRGDfK-PAPA, StemAdhere™, Synthemax™ or Geltrex™, H9, NHF-1-3 and Genea-02 cells consistently formed tightly-packed colonies displaying typical hPSC morphology (Figures 5.4). However, as is typical for hPSC cultures, minor variation was observed in colony morphology and density within individual flasks. Within the normal spectrum of morphology, the majority of cultures maintained on cRGDfK-PAPA or Synthemax™ were morphologically indistinguishable from control cultures maintained in Geltrex™-coated flasks. However cultures maintained in StemAdhere™-coated flasks were observed to plate down as single cells or smaller colonies than on other surfaces, even during the first culture, where they were seeded from the same harvest, which indicates that this difference was not based on differences in EDTA harvesting. As had been observed with the H9-OCT4-mCherry cell line (Figure 5.2C), cells from each hPSC line appeared to be flatter when maintained on StemAdhere™ than the other surfaces, forming colonies that were generally less tightly-packed (Figure 5.4C,G,K). Cultures of hPSCs maintained on StemAdhere™ were also observed to contain regions where cells were over-crowded and appeared to pile up on top of each other (Figure 5.5), such regions were not observed in cultures maintained on the other surfaces.

In order to estimate the proliferation rates of hPSC cultures maintained on defined culture surfaces, it was considered that when cultures are seeded at a consistent density, any meaningful changes in proliferation rate will be reflected in the amount of time taken to reach a suitable confluence (60 %) for harvesting and/or in the cellular yield from each flask at that time. The duration of each passage and the number of cells harvested from each flask were therefore recorded. No significant difference was observed in the number of days required for hPSC cultures to recover from each passage (Figure 5.6A) or the cellular yield (Figure 5.6B) between hPSC cultures maintained on different culture surfaces. Furthermore the trends for passage duration and yield were similar, which also indicates that proliferation rates were relatively consistent for cultures maintained on all surfaces since cellular proliferation is a function of time. The viability of cells harvested from flasks coated with any surface was consistently over 80 % (Figure 5.6C).

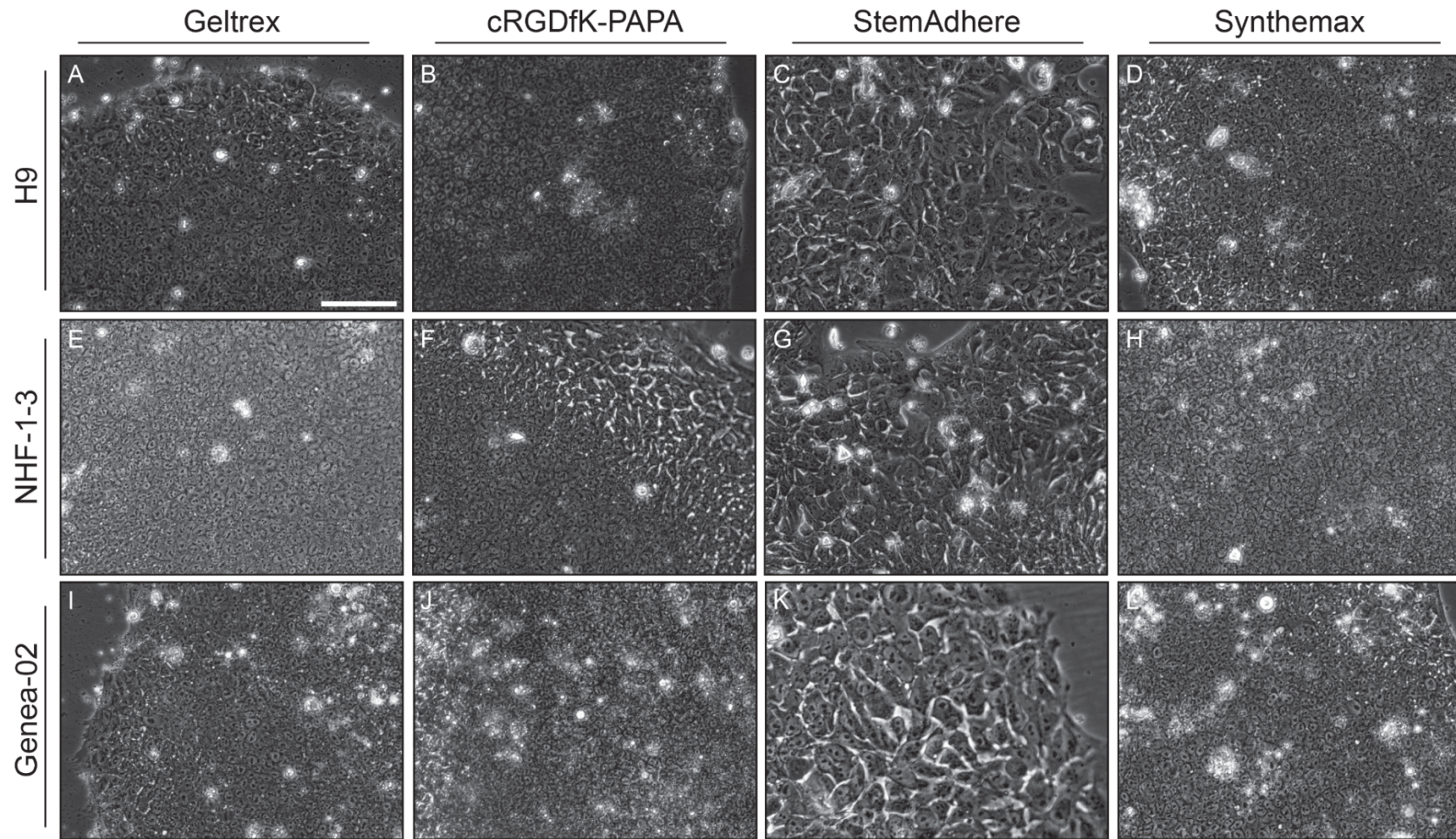


Figure 5.4: This figure illustrates the morphology of hPSC cultures during long-term maintenance on defined culture surfaces and Geltrex™-coated controls. Phase contrast images of (A-D) H9, (E-H) NHF-1-3 and (I-L) Genea-02 hPSCs cultured on (A,E,I) Geltrex™, (B,F,J) cRGDfK-PAPA, (C,G,K) StemAdhere™ and (D,H,L) Synthemax™. The cells maintained on StemAdhere™-coated surfaces appear to be flatter or larger than hPSCs on the other surfaces, which are morphologically indistinguishable from each other. The scale bar (A) represents 100 μ m for all images.

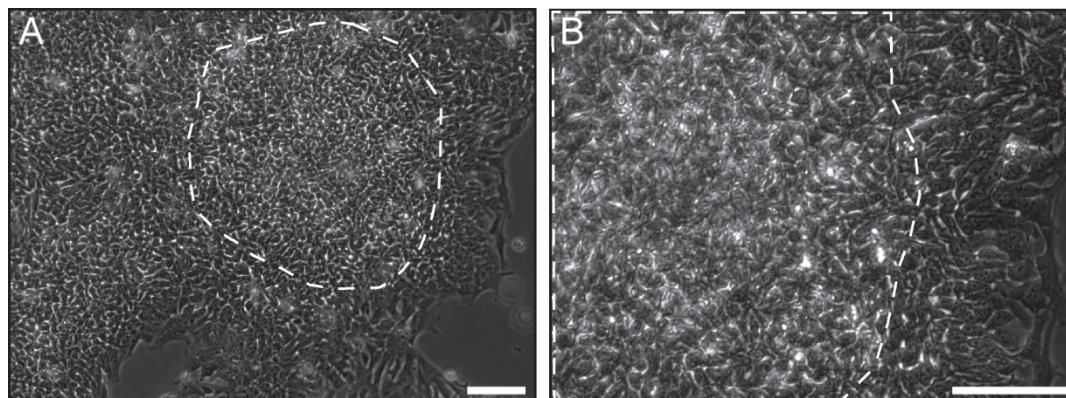


Figure 5.5: Representative images are presented of over-crowded regions (dotted lines) that were observed in hPSC cultures grown for on StemAdhere™ coated flasks. Phase contract images show NHF-1-3 hPSCs forming a representative very tightly-packed packed colony. Images were captured of 5 day post-seeding cultures and taken under (A) 100x and (B) 200x magnification. This phenomenon was observed with all cell lines. Scale bars represent 100 μ m.

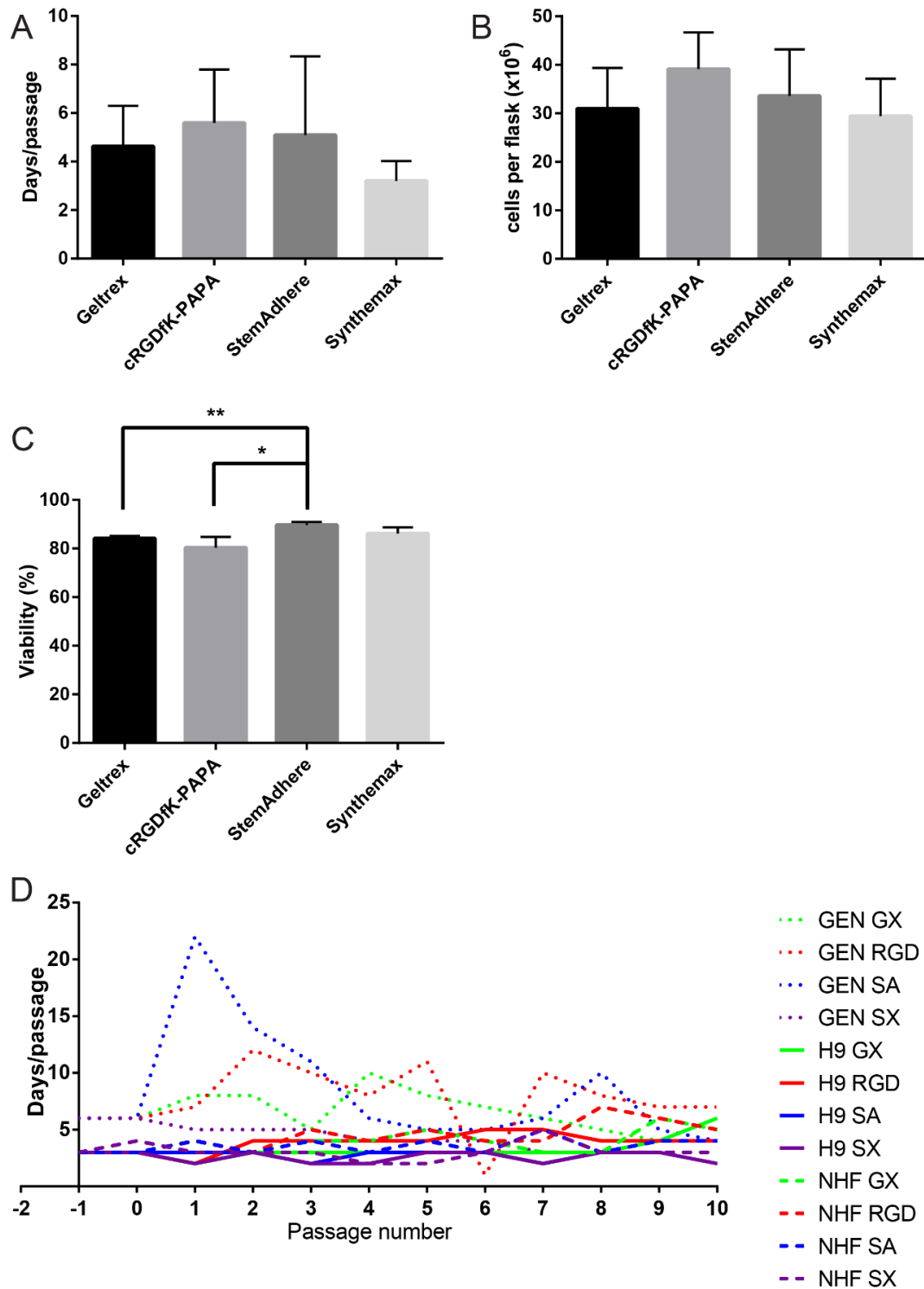


Figure 5.6: Growth dynamics of hPSC cultures maintained on different culture surfaces. (A) The number of days taken for cultures of H9, NHF-1-3 (NHF) and Genea-02 (GEN) hPSCs to reach passaging density on surfaces coated with Geltrex™ (GX), cRGDfK-PAPA (RGD), StemAdhere™ (SA) or Synthemax™ (SX) is presented alongside (B) the mean number of cells harvested at the end of each passage and (C) the viability of harvested cells, all grouped by surface-type. Mean \pm SD, $n = 30$ (10 passages for each of 3 cell lines). * $p \leq 0.05$, ** $p \leq 0.01$. (D) The number of days taken for each passage to reach harvesting confluence is also presented for every passage of each cell line on each surface.

The consistency of the proliferation data was affected by cell line variation; the passage durations of the Genea-02 cell line were highly variable, both between and within cultures maintained on different surfaces (Figure 5.6D). The first passage of Genea-02 cells on StemAdhere™-coated surfaces was the most obvious deviation from normal hPSC behaviour of any culture (Figures 5.6C and 5.7). When Genea-02 cells were initially seeded onto StemAdhere™-coated flasks, a typical number of single cells and small colonies were observed to adhere to the surface (Figure 5.7A). However, from day 4 many of these small colonies and single cells detached, reaching a nadir around day 7 (Figure 5.7B). As few as 10 colonies per flask were observed to remain bound at this point, but the colonies survived and continued to proliferate over the subsequent days and weeks. As the experiment progressed and the Genea-02 cell line continued to proliferate and be passaged between flasks coated with the other three surfaces, this initial adaptation of hPSCs maintained on Geltrex™ to culture on StemAdhere™ was repeated a further three times. A similar pattern was observed each time, with cells plating and then mostly detaching, and a low number of colonies surviving and proliferating for no fewer than 10 days before being ready to harvest. When the culture from the first adaptation of Genea-02 onto StemAdhere™ reached day 22 the colonies were very large, with dense centres surrounded by borders of morphologically normal hPSCs (Figure 5.7D), but were still only estimated to cover 5 % of the surface of the flask. The cells were harvested with EDTA and lifted as large clumps and single cells, which were all transferred to a single StemAdhere™-coated flask. This culture then took two weeks to recover from the second passage, and was observed to contain morphological differentiation that lingered for two passages before the culture finally behaved more typically and was ultimately maintained on StemAdhere™-coated surfaces for ten passages.

The incidence and degree of morphological differentiation (Figure 5.8A-D for representative images) was observed to vary between hPSC cultures maintained on different surfaces (Figure 5.8E) and also between individual cell lines (Figure 5.8F). Low or medium levels of morphological differentiation were occasionally observed in Geltrex™-coated flasks, particularly in the NHF-1-3 culture (in six of ten passages), whereas morphological differentiation was observed in at least 50 % of passages for each culture maintained in cRGDfK-PAPA-coated flasks. NHF-1-3 and Genea-02 cultures on cRGDfK-PAPA often contained high levels of differentiation, while the H9 culture only ever contained low levels (Figure 5.8F). When Genea-02 and NHF-1-3 cultures were seeded into cRGDfK-PAPA-coated flasks they often appeared to be entirely differentiated in the first few days, before tightly-packed colonies of morphologically normal hPSCs became visible and gradually took over the cultures, pushing the undifferentiated cells aside. Such cultures were harvested when the morphologically undifferentiated cells reached 60 % confluence, without considering the morphological differentiation which, at times, covered the rest of the culture surface. Differentiation was observed to lesser degrees and less often in cultures maintained on the commercially-available synthetic surfaces. Cultures maintained in Synthemax™-coated flasks were occasionally observed to contain only low levels of morphological differentiation, and aside from the second and third passages of the recovering Genea-02 culture, morphological differentiation was not observed in any hPSC cultures maintained in StemAdhere™-coated flasks (Figure 5.8F).

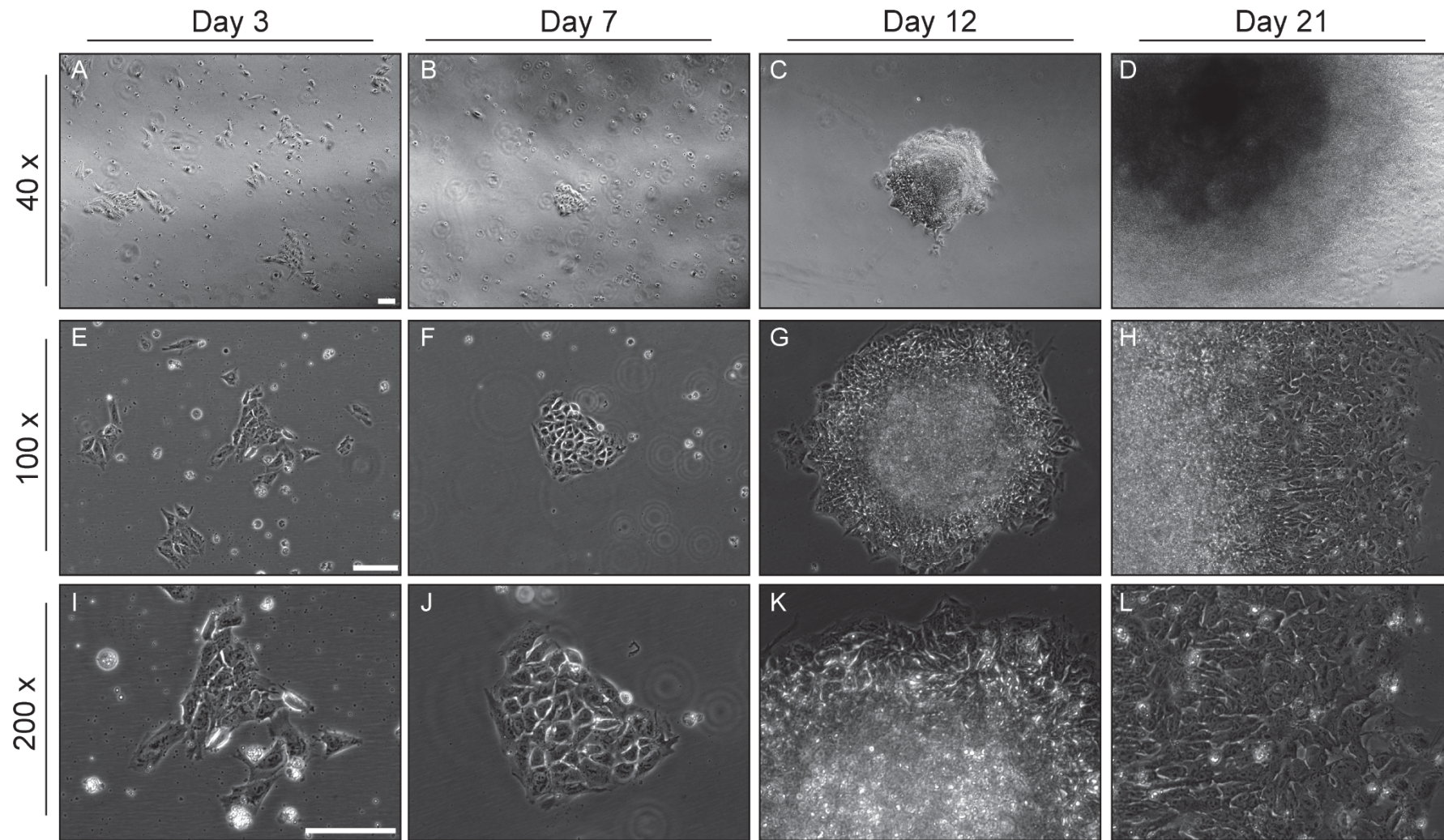


Figure 5.7: The gradual recovery of Genea-02 cells from the first passage on StemAdhere™-coated flasks. Representative images are presented from days 3, 7, 12 and 21 of culture, captured at 40x, 100x and 200x magnification. Scale bars represent 100 μ m and apply to every image in each row.

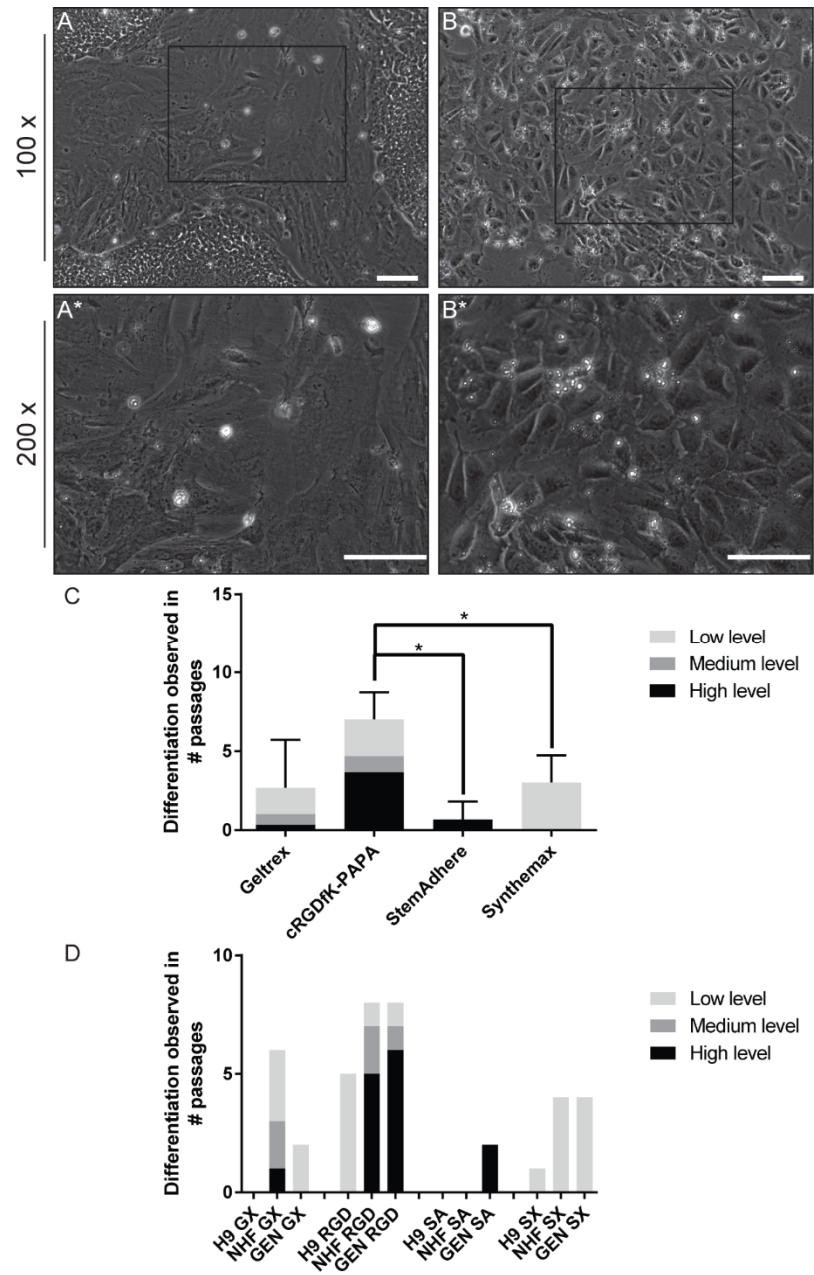


Figure 5.8: Observations of morphological differentiation in hPSC cultures on synthetic surfaces. (A-B*) The presented photomicrographs are representative of typical differentiation observed during the maintenance of hPSCs on surfaces coated with Geltrex™, cRGDfK-PAPA, StemAdhere™ and Synthemax™. Images A and A* were captured from the tenth passage of NHF-1-3 on cRGDfK-PAPA, and B and B* from the second passage of Genea-02 on Geltrex™. The outlines in A and B represent the fields of view of A* and B* respectively. Cells with undifferentiated morphology can be observed around the edge of image A. All scale bars represent 100 μ m. The degree of differentiation observed was arbitrarily categorised as low, medium or high based on the proportion of cells that appeared to be morphologically differentiated. The number of passages in which morphological differentiation was observed is plotted and arranged (C) by surface type and (D) by surface type and then by cell line. Means and standard deviations are presented for the total numbers of passages in which any level of differentiation was observed.

Although morphological differentiation was extremely uncommon in hPSC cultures maintained on StemAdhere™-coated flasks, other phenomena were occasionally observed in hPSC cultures maintained on this surface including large areas devoid of cells (Figure 5.9), and phase bright clumps of cells that were loosely tethered to the surface (Figure 5.10). The barren areas were roughly circular, possessed well-defined borders (Figure 5.9B) and were typically found near the base of the flask. Although the clumps were not quantified, there appeared to be more of them on the first day post-passage and fewer clumps as the days passed. It appeared that the clumps were either lifting off or settling gradually onto the surface (Figure 5.10B,D). These phenomena were not observed in cultures on other surfaces.

With regards to growth rate and morphology, hPSC cultures appeared to grow most consistently on Synthemax™-coated flasks (Figures 5.6A, 5.8F), with the exception of a “false start” for the NHF-1-3 culture. When NHF-1-3 cells were initially seeded on Synthemax™ at p29+14+13 they suffered massive, unexplained cell death, so cells from the Geltrex™-coated control flasks (p29+14+14) were used to start a fresh culture on Synthemax™, which was then maintained for the remainder of the experiment. This was the only occasion over the course of the experiment in which a culture was abandoned. All cell lines were also observed to recover from freeze-thaw cycles on all surfaces without any apparent morphological changes.

An inconvenient aspect of maintaining hPSC cultures on Synthemax™-coated surfaces was the inability of cells to lift from the surface without cell scraping. As described in Section 5.2.2, cell-surface molecular interactions were disrupted with EDTA treatment and then cells were removed from the surface using shear forces generated by pipetting fresh culture medium against the surface. When this was insufficient to remove cells from the surface they were physically removed with a cell scraper, and the proportion of cells that required scraping at each passage was estimated (Figure 5.11). A similar proportion of cells maintained on cRGDfK-PAPA and Geltrex™-coated surfaces required scraping, and cultures maintained on StemAdhere™ typically lifted very easily after a shorter incubation in EDTA than required for cultures maintained on other surfaces. Cell scraping was only required to lift cells from StemAdhere™-coated surfaces during the second and third passages of the recovering Genea-02 cell line. On the other hand hPSCs maintained on Synthemax™-coated surfaces were much more difficult to harvest, and an average of 80 % of cells had to be scraped from the surface (Figure 5.11A). Furthermore, cell scraping was required during TrypLE™ Express-mediated harvesting of some cultures in Synthemax™-coated flasks while preparing the cells for flow cytometry (Figure 5.11B). Of the flasks that were harvested with TrypLE™ Express for flow cytometric analysis, cell scraping was required to remove more than 80 % of the cells from five (5/6) Synthemax™-coated flasks except for one (NHF-1-3, passage 3). Roughly 40 % of cells had to be scraped from each of three (3/6) cRGDfK-coated flasks, and approximately 30 % from a single (1/8) Geltrex™-coated flask.

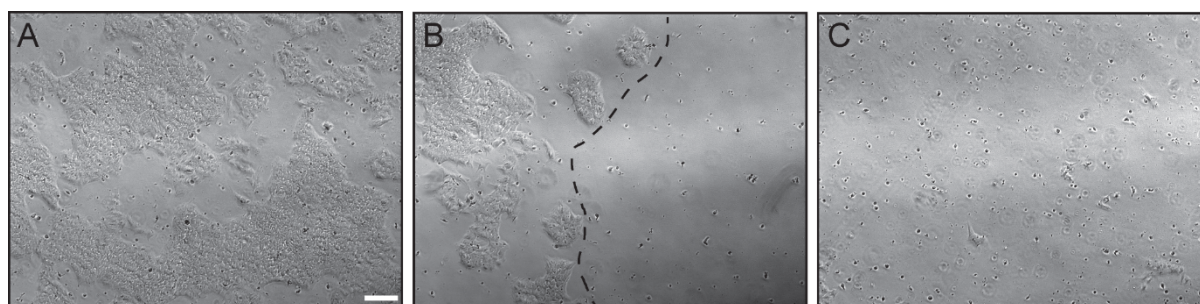


Figure 5.9: Large, cell-free regions were occasionally observed on StemAdhere™-coated flasks. (A) Otherwise typical hPSC cultures (B) halted abruptly (dotted line) and (C) gave way to large regions containing very few or no cell clumps. Representative images of a culture of the NHF-1-3 cell line are presented here at 3 days post-seeding on StemAdhere™. All three images were captured at the same time from the same flask. The scale bar represents 200 μm on all images. This phenomenon was observed in all cell lines cultured on StemAdhere™.

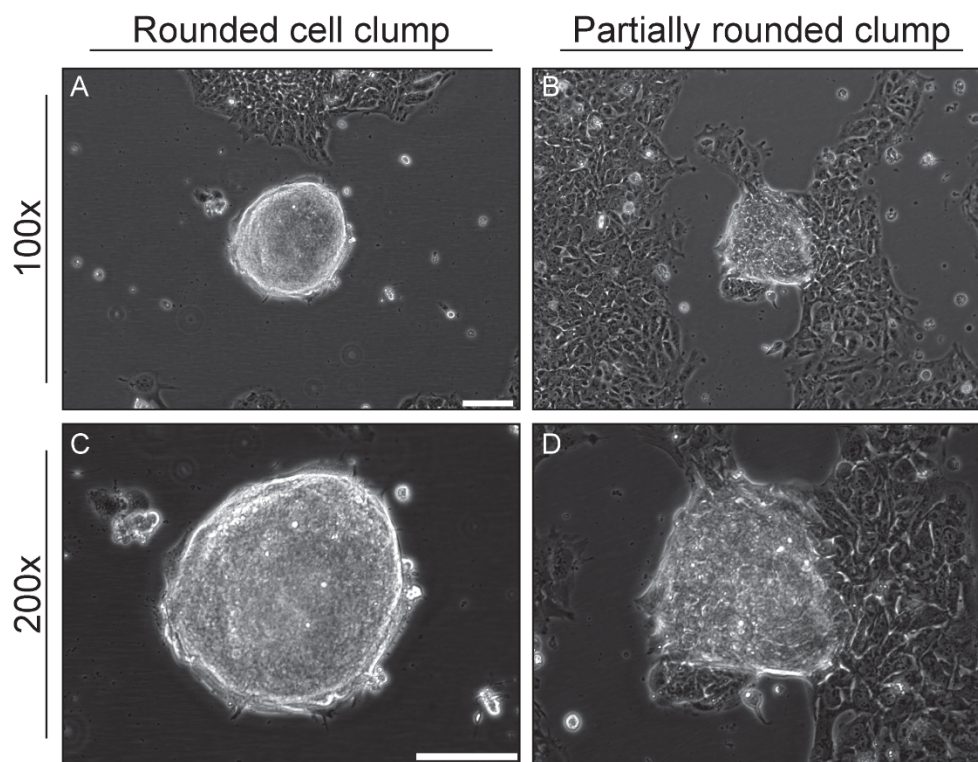


Figure 5.10: Rounded, phase bright clumps of cells were regularly observed alongside morphologically normal cells in StemAdhere™-coated flasks. (A,C) Clumps appeared to be bound to the surface by an underlying layer of adherent cells and (B,D) some clumps were observed in an intermediate stage of settle onto or lifting off the culture surface. Scale bars represent 100 μ m for both images in each row.

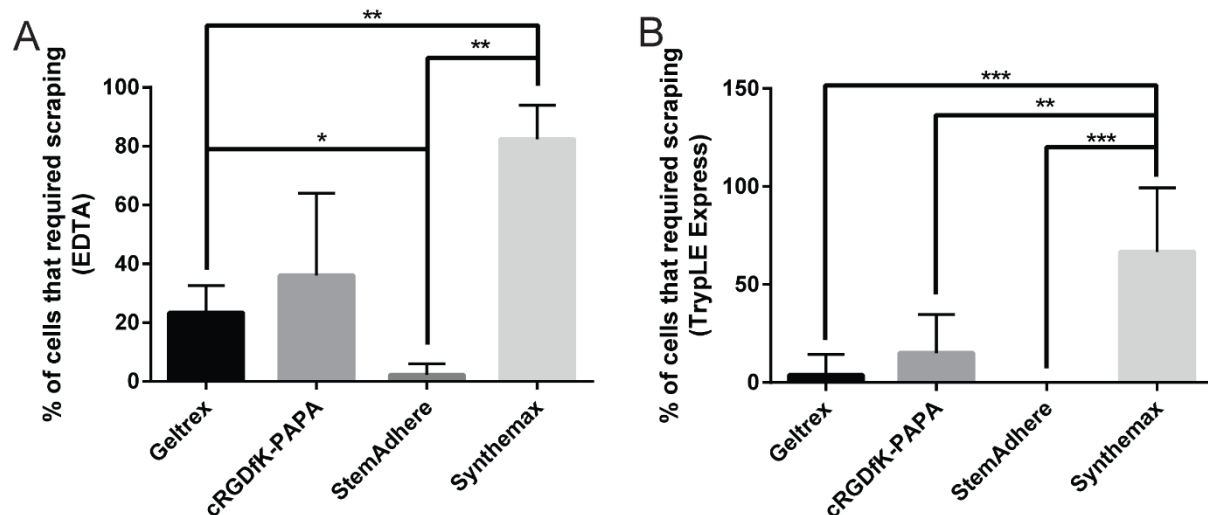


Figure 5.11: This figure presents the proportion of cells that required cell scraping during harvesting from each culture surface. Cultures of H9, NHF-1-3 and Genea-02 hPSCs were maintained in flasks coated with Geltrex™, cRGDFK-PAPA, StemAdhere™ or Synthemax™ for 10 passages. Cultures were harvested with EDTA for continuing culture, and occasionally harvested with TrypLE™ Express for flow cytometric analysis. After treatment with a dissociation agent and pipetting with media, cells that remained adherent were physically removed with a cell scraper. The proportion of cells that required scraping was estimated by visual assessment at each harvest and is presented for cultures treated with (A) EDTA ($n = 30$ harvests) or with (B) TrypLE™ Express ($n = 8$ harvests for Geltrex™ and $n = 6$ harvests for each of cRGDFK-PAPA, StemAdhere™ and Synthemax™). Means are presented with scale bars representing standard deviations. Data sets linked by an asterisk (*) are statistically significant according to unpaired two-tailed t-tests ($p \leq 0.05$). Multiple asterisks indicate higher levels of significance (** $p \leq 0.01$, *** $p \leq 0.001$).

5.3.3 Flow cytometric analysis of hPSC cultures maintained on defined culture surfaces

Aside from observations of colony morphology, maintenance of pluripotency over the culture period was also monitored by detecting the pluripotency marker OCT4 using immunocytochemistry and flow cytometric analysis, as described in Section 5.2.3.1. For each population of hPSCs that had been maintained for ten passages in flasks coated with cRGDfK-PAPA or with any of the control surfaces, at least 80 % of cells were detected as OCT4-positive compared to isotype controls (Figure 5.12).

5.3.4 Teratoma formation with hPSC cultures maintained on defined culture surfaces

To verify the pluripotency of the hPSC cultures following long-term culture on defined surfaces, they were subjected to a teratoma formation assay. Cells from each culture were harvested with EDTA and injected into the testis capsules of immunocompromised mice (Section 5.2.3.6). Following injection with the three hPSC cultures that had been maintained on cRGDfK-PAPA, tumours were observed to develop inside or proximal to the testis capsule, regardless of the culture surface on which the hPSCs had been cultured. Histological assessment of the tumours resulted in the identification of tissue types representative of all three embryonic germ layers (Figures 5.13). hPSC cultures maintained for ten passages in E8 medium on cRGDfK-PAPA-coated surfaces therefore passed the teratoma formation assay and can be considered to have retained pluripotency over the culture period. This result was also observed for all cell lines maintained on all control surfaces.

5.3.5 G-banding karyotyping of hPSC cultures maintained on defined culture surfaces

In order to determine whether or not the pluripotent cells that had been maintained for ten consecutive passages on cRGDfK-PAPA-coated flasks were genetically stable, G-banding chromosomal analysis was performed on all 12 cultures (Figure 5.14, Appendix 6.2). All hPSC cultures that had been maintained on cRGDfK-PAPA were observed to be karyotypically normal. In total nine out of twelve samples displayed normal karyotypes and no single surface consistently produced cells that were karyotypically abnormal. The most commonly observed abnormality was trisomy of chromosome 12, which was exclusively observed in cultures maintained on StemAdhere™ (Figure 5.14A). The +12 trisomy was detected at a moderate frequency in Genea-02 (11/20 cells) and H9 (7/20 cells) cultures maintained on StemAdhere™, but not in the NHF-1-3 culture (Figure 5.14B). Furthermore, the Genea-02 culture maintained on Geltrex™ was observed to contain several minor, low frequency abnormalities (2/20 cells 45,X; 2/20 cells 46,XY,add(20); 1/20 cells 47,XY,+mar] and one of the 30 cells scored out of the H9 culture on Synthemax™ was 46,XX,add(20)(p12). The karyotypic abnormalities identified in the culture of Genea-02 cells maintained in StemAdhere™-coated flasks may have arisen during the slow adaptation period, in which a high level of cell death was observed.

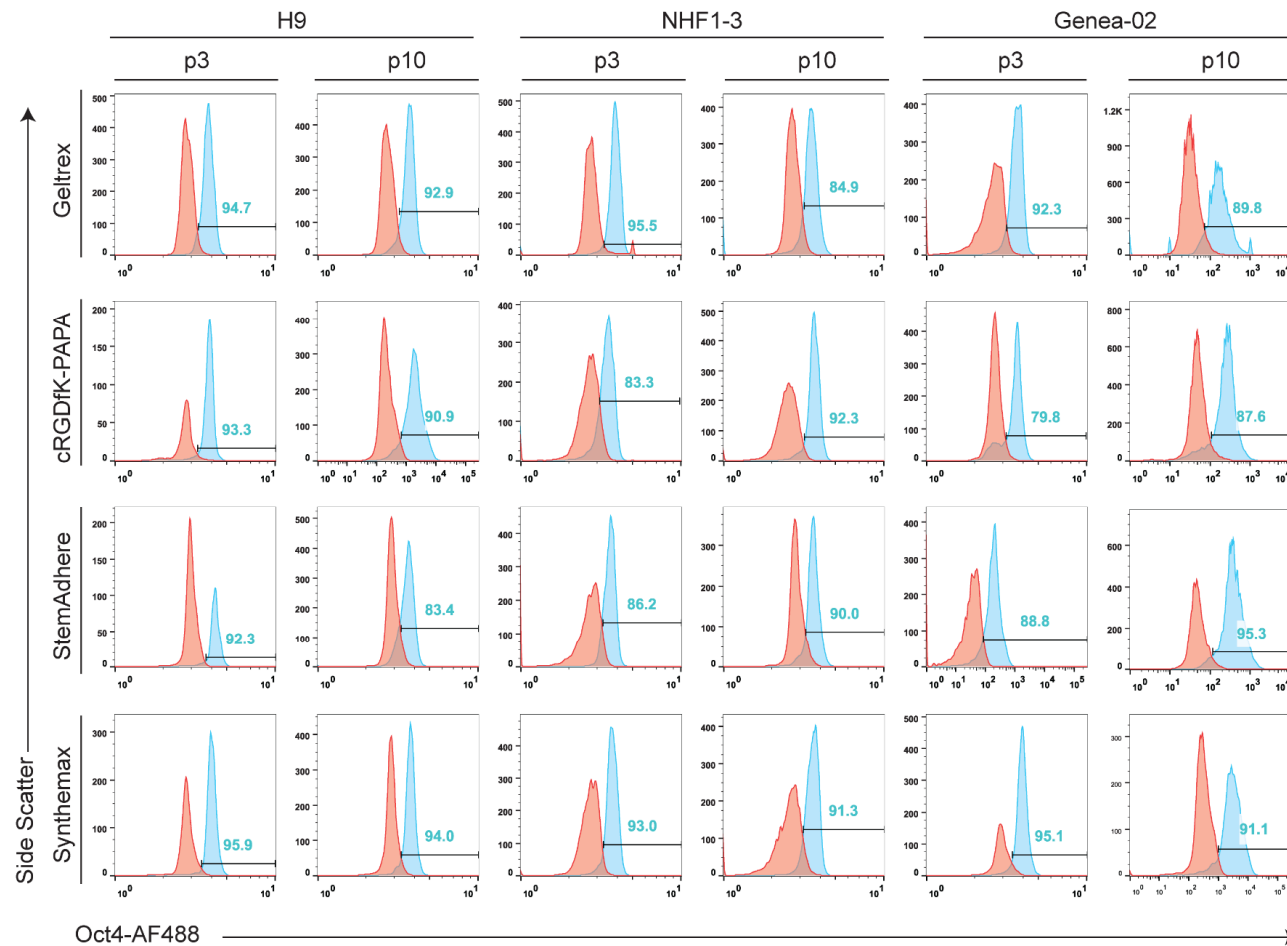


Figure 5.12 Histogram plots are presented of flow cytometric assessment of OCT4 protein detected in hPSCs cultured on test culture surfaces. After cultures of H9, NHF-1-3 and Genea-02 hPSCs had been maintained for 3 and 10 passages in E8 medium in flasks coated with Geltrex™, cRGDfK-PAPA, StemAdhere™ or Synthemax™, the cells were immunostained for OCT4 and assessed by flow cytometry. Gates for AF488-OCT4 were set against cells stained with the IgG1 isotype control antibody (red) and applied to samples that had been immunostained for OCT4 (blue). The percentage of OCT4-AF488-stained cells are displayed on each plot. The different axis scales are an artefact of samples being analysed on different flow cytometers.

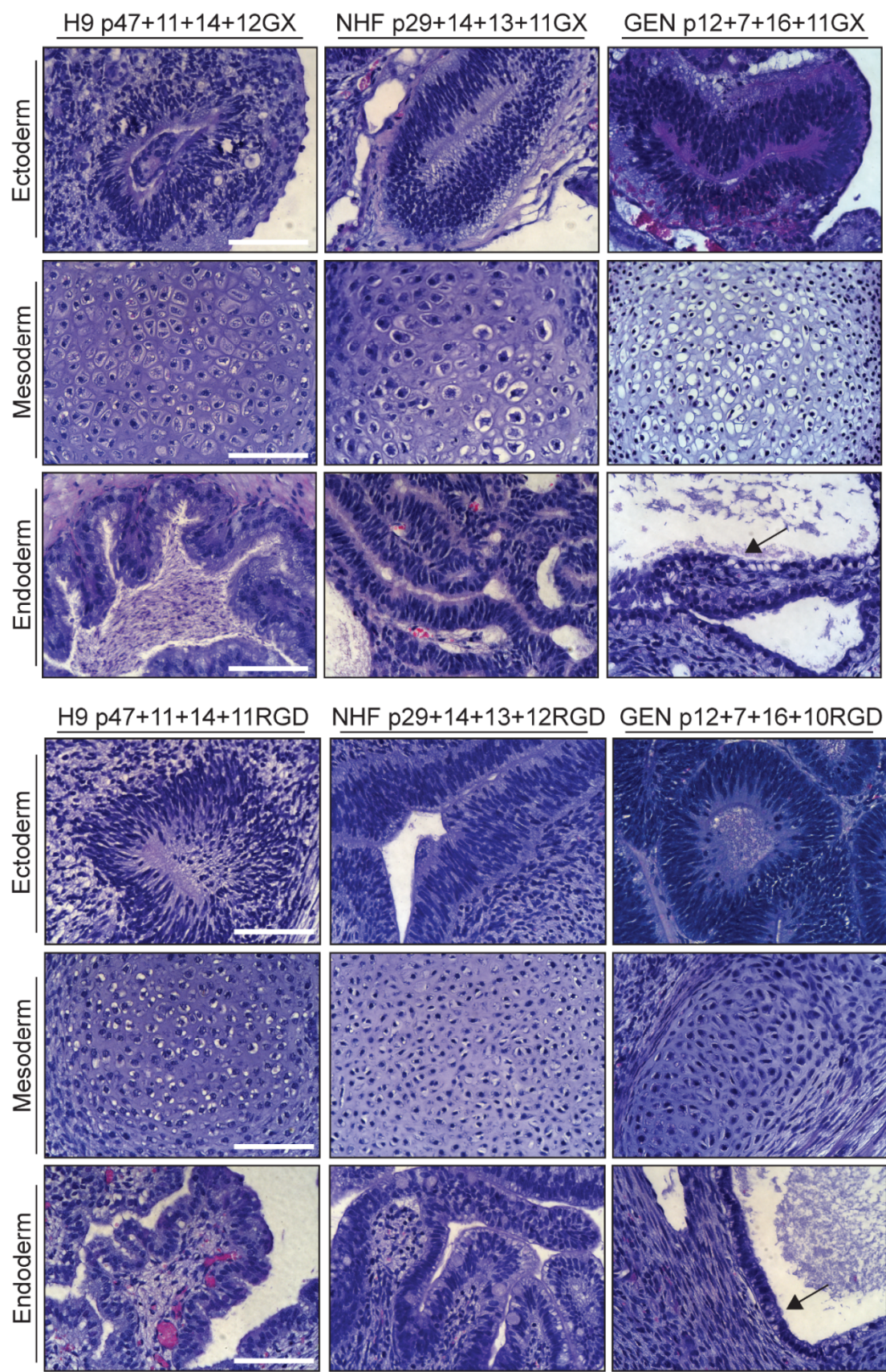


Figure 5.13 Caption is on the page after the following page.

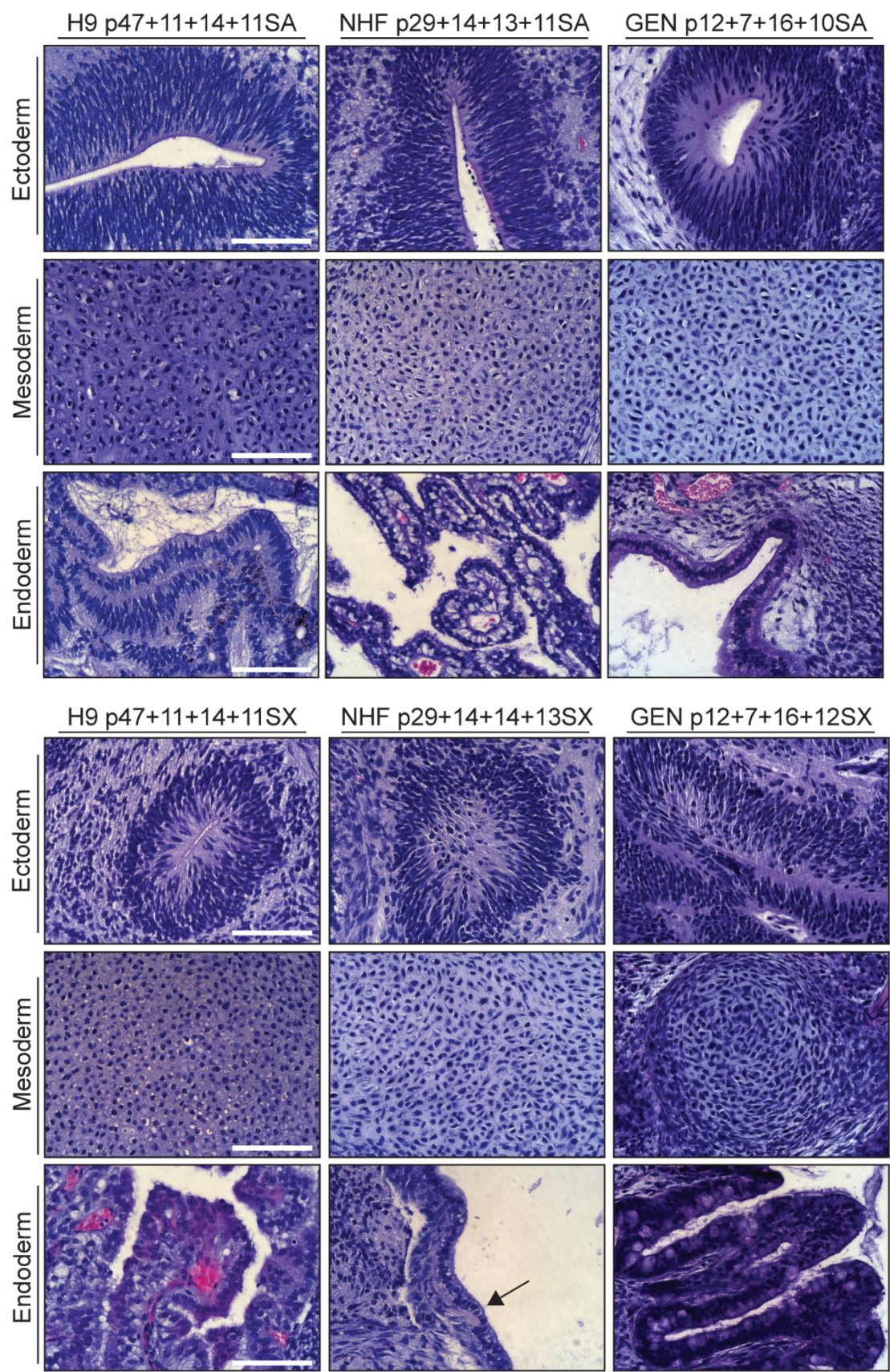


Figure 5.13 Caption is on the following page.

Figure 5.13 Figure is on the two previous pages. The results of a teratoma formation assay are presented for hPSCs following long-term maintenance on defined culture surfaces. H9, NHF-1-3 (NHF) and Genea-02 (GEN) cultures that had been maintained for at least 10 passages in flasks coated with Geltrex™ (GX), cRGDfK-PAPA (RGD), StemAdhere™ (SA) or Synthemax™ (SX) were injected into the testis capsules of immunocompromised mice and formed tumours. Representative images are presented of sections of those tumours which had been stained with haematoxylin and eosin, and scored for the presence of tissue types representative of the three germ layers including neural rosettes (ectoderm), cartilage (mesoderm) and secretory epithelial cells (endoderm, indicated by arrows in images I, R and AI). Scale bars represent 100 µm in all images.

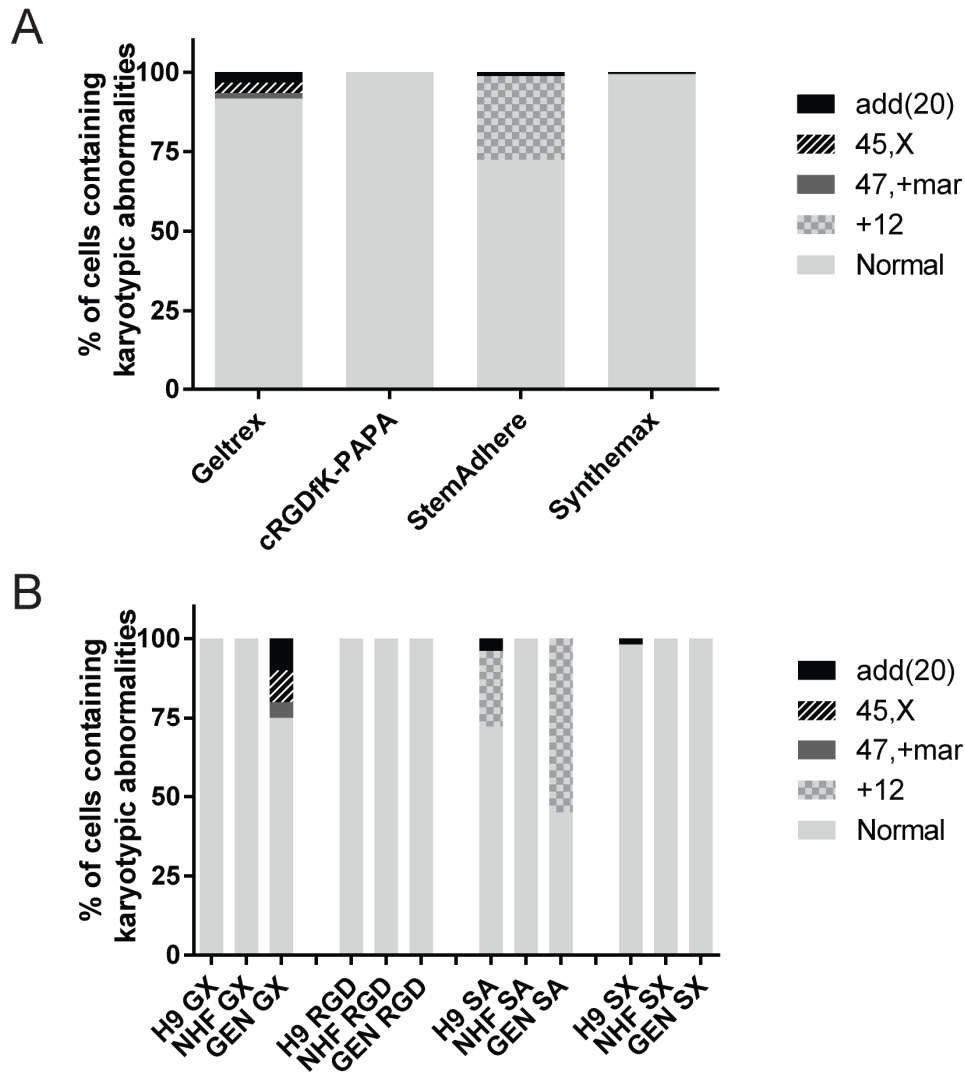


Figure 5.14 Summary of G-banding karyotyping assessment of hPSCs maintained on defined culture surfaces. The type and number of karyotypic abnormalities observed in H9, NHF-1-3 (NHF) and Genea-02 (GEN) hPSCs that had been maintained for at least 10 passages in flasks coated with Geltrex™ (GX), cRGDFK-PAPA(RGD), StemAdhere™ (SA) or Synthemax™ (SX) are plotted and arranged (A) by surface type and (B) by surface type and then by cell line.

5.3.6 PluriTest™ assessment of hPSC cultures maintained on defined culture surfaces

The PluriTest™ assay was employed to further validate the pluripotency of hPSCs maintained in cRGDfK-PAPA-coated flasks and also to assess global differences in gene expression patterns in hPSC cultures maintained on the various defined hPSC culture surfaces. To perform this microarray-based assay, total RNA was extracted from cell pellets that had been collected when all 12 cultures reached ten passages on the test surfaces. The extracted RNA passed nanodrop analysis with A260:260 values between 1.99 and 2.04 (Appendix 6.3) and generated RINs greater than 9.2 from the bioanalyser assay (Appendix 6.4). Furthermore, all microarray data that was uploaded to the PluriTest™ database displayed consistent mean probe intensities, which indicated that the microarray results were internally consistent, which technically validated the assay (Appendix 6.5).

All samples produced Novelty scores and Pluripotency scores typical of hPSC populations (Figure 5.15, Section 5.2.3.5 for details). However some samples, including all of the NHF-1-3 cultures, produced Pluripotency Scores slightly lower than the empirically set pluripotency threshold of 20 (Figure 5.15). These results were most likely not due to diminished pluripotency but were probably the result of a recently observed technical drift in the hybridisation chemistry of the Illumina HT 12V4 microarray platform, as well as an offset due to a new microarray scanner generation (iScan) that was used for these samples (Franz-Josef Müller, Zentrum für Integrative Psychiatrie Kiel, Germany, *pers. comm.*) (Müller et al., 2011).

Another output generated by the PluriTest™ assay was a phylogenetic tree, which determines relationships between data sets based on global gene expression levels (Figure 5.16). Cultures maintained on cRGDfK-PAPA were determined to be most closely related to the control cultures maintained on Geltrex™ for both the NHF-1-3 and Genea-02 cell lines. However, the H9 culture maintained on cRGDfK-PAPA was most closely related to the H9 Synthemax™ culture, and the matching Geltrex™ control culture was almost as closely related. Meanwhile cultures on StemAdhere™ and Synthemax™ paired together for Genea-02 and NHF-1-3 cultures.

The “transcriptional karyotype” is a new output of the PluriTest™ software that is still under development. A heat map (Figure 5.17) arranges gene expression levels by genetic locus and determines whether the genes located within each cytoband (the stripes on the G-banding chromosome spreads, Appendices 6.1 and 6.2) are up- or down-regulated on average compared to the hPSC reference data set. One of the most prominent features in the current data set was the horizontal red line at chromosome 12 of the Genea-02 cells maintained on StemAdhere™ (Figure 5.17, arrow), which represents the trisomy that was also identified by G-banding karyotyping (Figure 5.14). Other prominent features include the vertical red bands that can be seen at the N-terminus of chromosome 6 and in chromosome 19 among other places (Figure 5.17, arrowheads). These lines represent the loci of genes that were upregulated in all of the current cultures compared to the cultures that were included in the reference data set.

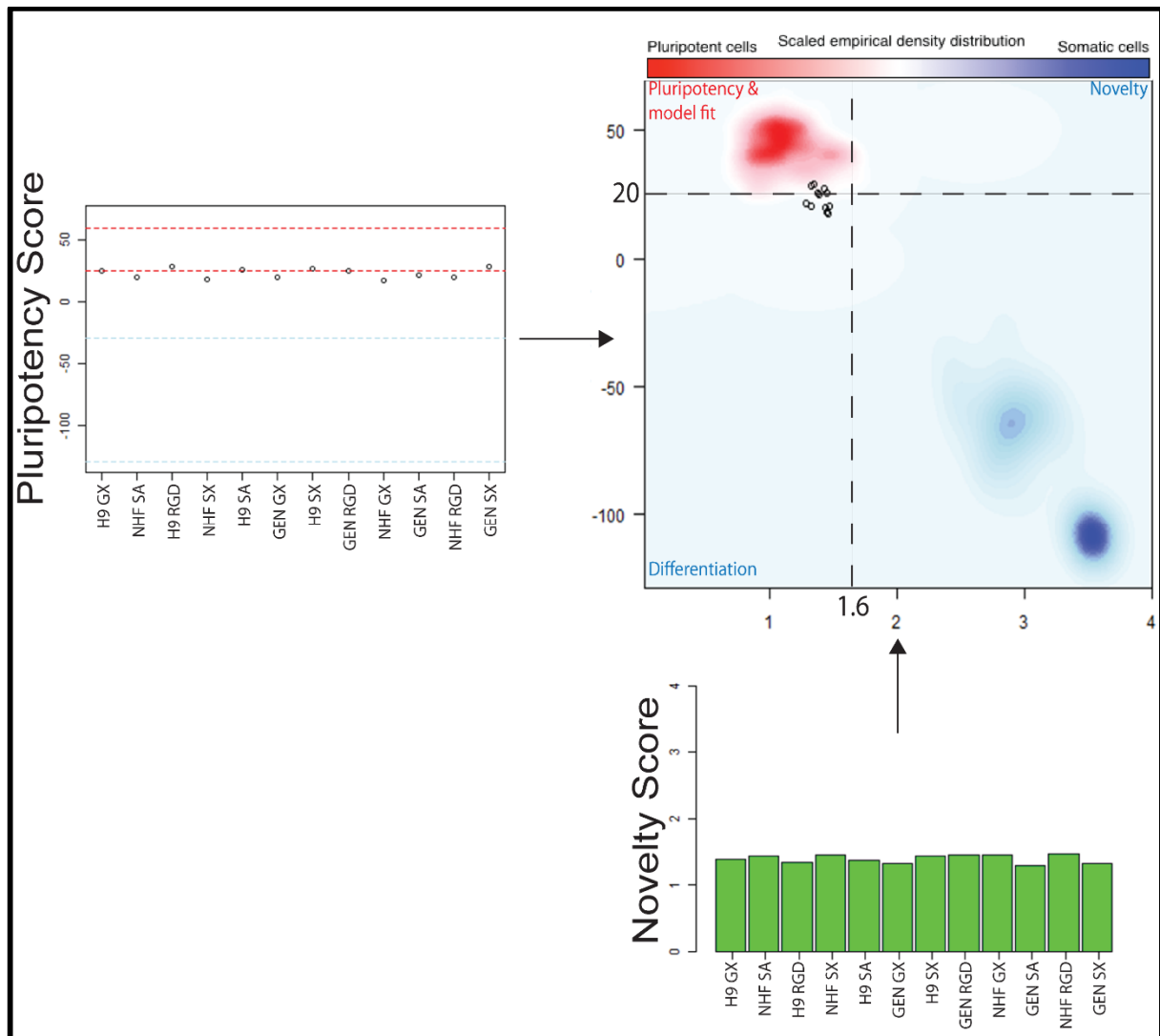


Figure 5.15 The pluripotency of hPSC cultures maintained on chemically defined surfaces was assessed by RNA microarray analysis using PluriTest™. The PluriTest™ assay was performed on RNA extracted from H9, NHF-1-3 (NHF) and Genea-02 (GEN) cultures that had been maintained for 10 passages in flasks coated with Geltrex™ (GX), cRGDfK-PAPA (RGD), StemAdhere™ (SA) or Synthamax™ (SX). The Pluripotency Scores of these samples are plotted (top-left) against 95 % confidence intervals for pluripotent (between the red lines) and non-pluripotent (between the blue line) populations. Novelty Scores are plotted (bottom right) and samples are colour-coded green (pluripotent), orange (uncertain) or red (not pluripotent) based on the probabilities given from the logistic regression model. Both scores are also represented together on a scatter plot (top-right). Here the samples (hollow circles) are compared to pluripotent reference data sets (red cloud, top-left quadrant) and differentiated and/or novel reference data sets (blue clouds, bottom-right quadrant).

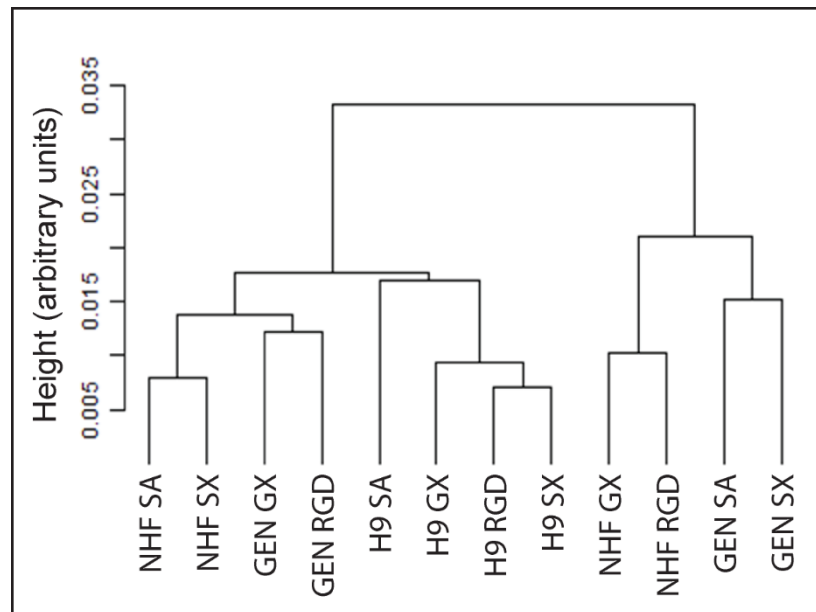


Figure 5.16 PluriTest™ phylogenetic tree. The PluriTest™ assay was performed on H9, NHF-1-3 (NHF) and Genea-02 (GEN) cultures that had been maintained for 10 passages in flasks coated with Geltrex (GX), cRGDfK-PAPA (RGD), StemAdhere™ (SA) or Synthamax™ (SX). After the samples were transformed with a variance stabilising transformation a phylogenetic tree was generated representing the relationships between data sets.

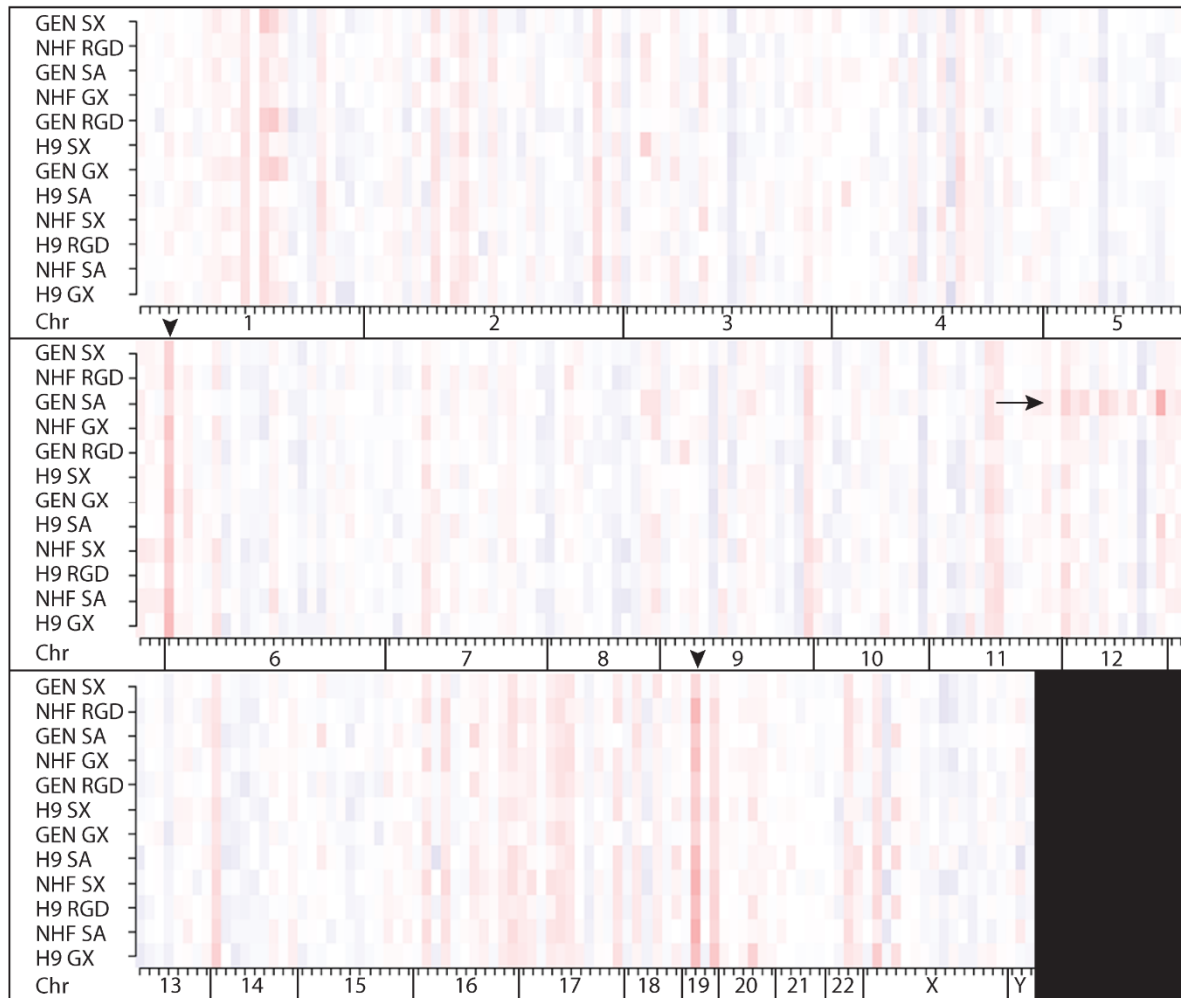


Figure 5.17 PluriTest™ transcriptional karyotype analysis of hPSC cultures after long-term maintenance culture on different surfaces. The PluriTest™ analysis was performed on RNA extracted from H9, NHF-1-3 (NHF) and Genea-02 (GEN) cultures that had been maintained in flasks coated with Geltrex™ (GX), cRGDfK-PAPA (RGD), StemAdhere™ (SA) or Synthamax™ (SX) for 10 passages. The transcriptional karyotype feature of the PluriTest™ assay compares the expression levels of groups of genes in sample data sets to homologous genes in the pluripotent reference data sets. A heat map is formed displaying cytobands in which overall gene expression levels are higher (red) or lower (blue) in samples than is predicted by the pluripotency model. Horizontal red lines (arrow) indicate upregulation of genes in each cytoband of an entire chromosome (Chr); vertical red lines (arrowheads) indicate examples of cytobands that are upregulated in all samples compared to the reference data set.

5.4 Discussion

The results presented in this chapter are based on a single experiment in which cultures of three independently-derived hPSC lines were maintained for ten passages in E8 medium in flasks coated with the novel cRGDFK-PAPA culture surface. Furthermore the results of these cultures were benchmarked against cultures maintained in parallel on the synthetic surfaces StemAdhere™ and Synthemax™, and against control hPSC cultures maintained on Geltrex™. All hPSC cultures maintained on cRGDFK-PAPA were observed to be morphologically (Figure 5.4) and karyotypically (Figure 5.13, Appendix 6.2) normal for at least ten passages. The resulting cells also passed assessments of pluripotency based on mRNA and protein levels, and *in vivo* differentiation (Figures 5.15, 5.12 and 5.14, respectively). All hPSC lines cultured on Geltrex™, StemAdhere™ or Synthemax™ also passed every assessment of pluripotency, however karyotypic abnormalities were observed in some of these cultures and other subtle differences were observed between cultures.

The clearest deviations from typical hPSC culture behaviour were observed in cultures of the Genea-02 cell line, which regularly took longer than H9 or NHF-1-3 cultures to reach confluence on Geltrex™, cRGDFK-PAPA and StemAdhere™-coated surfaces (Figures 5.6 and 5.7). The duration of recovery from each passage varied widely between Genea-02 cultures on each surface and also fluctuated over the course of the experiment, particularly for the Genea-02 culture maintained on StemAdhere™, which also produced unique results in other assays (Figures 5.8, 5.13, 5.17). The cause of this variation was unclear, but it could be due to a range of factors including those described below.

hPSC lines have long been observed to display variation in growth and metabolic profiles (Harvey et al., 2016, manuscript submitted to The Journal of Biological Chemistry), in transcriptional output, in differentiation potential (Di Giorgio et al., 2008, Osafune et al., 2008) and in the way they adapt to changing culture conditions. (Lam and Longaker, 2012, Meng et al., 2012). Such changes can be as blunt as using different culture media or surfaces or as subtle as being handled by different well-trained technicians (unpublished observations). Observations of variation in cell line behaviour have been variously attributed to the genome (Rouhani et al., 2014), epigenome (Bock et al., 2011), laboratory of origin (Bock et al., 2011, Newman and Cooper, 2010) and, for iPSCs, artefacts of reprogramming (Lister et al., 2011, Ohi et al., 2011, Meng et al., 2010). Since the PluriTest™ phylogenetic tree indicated that the variation in global gene expression between Genea-02 and the other two cell lines was no greater than the variation resulting from culture on different surfaces (Figure 5.16), genetic variation appears to be the most likely parameter responsible for the unique behaviour of the Genea-02 line in this study. This variation could either be in the form of normal diversity between the individuals from which the pluripotent cell lines were derived, or due to mutations. The karyotyping results for the cultures on Geltrex™ and StemAdhere™ indicate that genetic mutations may have contributed to cell line variation, and this data could be strengthened by using more sensitive measures of genomic integrity such as single-

nucleotide polymorphism (SNP) arrays. Nevertheless, the main aims of this study were to validate the cRGDFK-PAPA culture surface and the study was designed to identify differences between hPSCs that have been maintained on different synthetic surfaces, so reproducible variation observed across multiple cell lines was of more interest than cell line variation.

Evidence presented in this chapter indicates that the mean cell density of hPSC cultures was affected by certain culture surfaces on which they were maintained. Observations that hPSC cultures trended towards taking longer to recover from each passage on cRGDFK-PAPA-coated surfaces than on Synthemax™ (Figure 5.6A) were consistent with trends of cell yields per flask (Figure 5.6B). These trends suggest that proliferation rates were consistent across all surfaces and that there may have been some variation in cell density, either within each colony or in the distribution of colonies across a flask. However any such variation was not visually observed during culture. In fact the loosely-packed colonies of hPSCs maintained on StemAdhere™-coated flasks (Figure 5.4C,G,K) appeared to indicate a lower cell density on this coating, but this may have been offset by the regions of very high cell density (Figure 5.5).

Early studies of cells cultured on StemAdhere™ reported that murine ESCs scattered across the plate instead of forming typical defined colonies (Nagaoka et al., 2006). However hPSC cultures maintained on StemAdhere™ have been reported to be “morphologically indistinguishable” to control cultures on Matrigel™ (Nagaoka et al., 2010), which was unlike the observations in the present study. The looser or absent colony morphologies that have been observed in pluripotent cultures on StemAdhere™ may be due to the surface-based E-cadherin ligands interfering with early colony formation by competing with E-cadherin-mediated cell-cell adhesion. The looser colony morphology and flatter cells observed on StemAdhere™-coated surfaces in the current study are likely to be linked to the apparent reduction in mCherry brightness for the H9-OCT4-mCherry cells on StemAdhere™ (Figure 5.2G), since similar levels of OCT4 were detected by flow cytometry in cultures on StemAdhere™ as on other surfaces (Figure 5.12).

Despite the slightly atypical colony appearance, morphological differentiation was very rarely observed in cultures on StemAdhere™ (Figure 5.8). This was consistent with claims made by the manufacturers that down-regulation of E-cadherin expression during differentiation often results in differentiated cells dissociating from StemAdhere™-coated surfaces (Cai et al., 2008). On the other hand a high level of morphological differentiation was often observed in cultures maintained on the integrin-binding cRGDFK-PAPA-coated surfaces (Figure 5.8).

Although the small OCT4-negative populations observed in Genea-02 cultures on cRGDFK-PAPA at passages 3 and 10 (Figure 5.12) correlated with observations of “high” and “moderate” levels of morphological differentiation, a “high” level of morphological differentiation was also observed in the control Genea-02 culture after three passages on Geltrex™, and in the NHF-1-3 culture after 10 passages on cRGDFK-PAPA, yet neither of these samples were observed to contain clear OCT4-negative populations by flow cytometry. These results emphasise the requirement for more stringent analysis of hPSC cultures than simply assessing colony morphology.

The consistent maintenance of OCT4 protein over ten passages on cRGDfK-PAPA is inconsistent with an earlier report where hPSCs cultured on cRGDfK-presenting acrylamide-based polymer coatings were observed to lose OCT4 protein (77% or 43% of cells remained OCT4+) after only three passages (Klim et al., 2010). The results of this study were discussed in more detail in Section 4.4.

In any case, unlike genetic abnormalities large enough to be detectable by G-banding, observations of subtle changes in colony morphology or low levels of morphological differentiation have not been linked to changes in proliferation rates or differentiation potential and would not exclude cultures maintained on cRGDfK-PAPA from therapeutic applications (Tannenbaum et al., 2012). Although permissible mutation thresholds for cell therapy products have not been set, any mutations that affect cell survival or proliferative capacity would also be prohibitive due to the risk of cancer (Peterson and Loring, 2014).

The lack of gross karyotypic abnormalities in hPSC cultures on cRGDfK-PAPA in this study indicates that culture of hPSCs on this surface may improve genetic stability, although a far more comprehensive study would be required to assess this. Low frequencies of karyotypically abnormal cells as observed in the H9 culture on Synthemax™ (Figure 5.13B), indicated that the abnormalities either arose towards the end of the culture period or did not promote excessive proliferation. High frequencies of karyotypically abnormal cells were observed in the Genea-02 cultures on StemAdhere™ and Geltrex™, which also had two of the longest single passage durations (Figure 5.6D). With cultures seeded at consistent density, long periods of recovery to passaging density is indicative of either low proliferation rate or high levels of cell death, the latter of which selects for mutations that improve cellular survival. The high frequency of karyotypic abnormalities (trisomy of chromosome 12) observed in the Genea-02 culture maintained on StemAdhere™ was particularly unsurprising considering the high degree of cell death that had been observed in the first passage. That a matching mutation was observed in the H9 culture, which appeared not to adapt easily to culture on StemAdhere™, indicates that selection pressures that select for over-expression of genes on this chromosome may be exerted on hPSCs in culture on StemAdhere™. Most of the abnormalities detected in this study (Figure 5.14) were amplifications or duplications of chromosomes 12 and 20, which have been observed to be commonly amplified in hPSC cultures maintained in other culture systems (Laurent et al., 2011). Amplifications of these regions result in a selective advantage (Amps et al., 2011) for the mutated hPSCs due to the presence of key genes such as the pluripotency gene NANOG on chromosome 12 (Draper et al., 2004, Mitsui et al., 2003) and the tumour suppressor gene Bcl-xL on chromosome 20 (Nguyen et al., 2014, Avery et al., 2013). Abnormalities in chromosome 17 have also been regularly observed in hPSC cultures (Draper et al., 2004, Laurent et al., 2011, Garitaonandia et al., 2015) but were not detected in the current study.

The trisomy of chromosome 12 in the Genea-02 culture on StemAdhere™ (55 % of cells were abnormal by G-banding) was also detected by PluriTest™ transcriptional karyotype feature, which is still under development. However the transcriptional karyotype assay was unable to detect the same abnormality occurring at a lower frequency in the matching H9 culture (35 % cells were

abnormal by G-banding), or any other low-frequency abnormalities that had been detected with G-banding (Figure 5.13). The transcriptional karyotype therefore correlated with the G-banding result by indicating that the Genea-02 culture maintained on StemAdhere™ contained a greater proportion of cells with trisomy-12 than the H9 culture. These results suggest that the transcriptional karyotype feature seems suitable for identifying highly abnormal populations of cells, although it appears to be unsuitable for early detection of low-frequency abnormalities. The sensitivity of this feature clearly requires more comprehensive testing. It was also interesting to observe vertical red and blue lines, which represent genetic loci that are respectively up- or down-regulated in all of the current cultures compared to the reference data sets (Figure 5.17). This data set could be used to identify genes that are up-regulated in hPSCs during adaptation from culture in the conditions used to establish the reference data sets (KOSR-based medium on feeder cells) to culture in E8 medium on defined surfaces.

Overall, no clear surface-based variation was observed between hPSC cultures for OCT4 expression (Figure 5.12), karyotypic stability (Figure 5.13) gene expression (Figures 5.15-17) or *in vivo* differentiation potential (Figures 5.13) in the current study. Instead, the results presented here often represented greater cell line-based variation than surface-based variation, which shows that hPSC cultures maintained long-term on the cRGDfK-PAPA coating are comparable to cultures maintained on the commercially available culture surfaces. Aside from the quality of the cell product, factors such as cost, preparation, shelf life and challenges involved in passaging cells (e.g. the requirement for cell scraping) are worth considering when selecting a surface for maintaining and scaling up hPSC cultures. Each surface has been ranked for these parameters in Table 5.2. Cost was ranked according to a recently published comparison (Lambhead et al., 2013), preparation was ranked according to the number of steps involved in the coating procedures at the time of cell passaging (Section 5.2.1, cRGDfK-PAPA would be prepared as a complete coating onto which cells would be seeded directly), the shelf lives of commercially available surfaces were taken from their respective handbooks and were compared to the shelf life of cRGDfK-PAPA as assessed in Section 3.x, while the cell scraping rankings are a summary of the results presented in Figure 5.11. So far cRGDfK-PAPA has only been produced in relatively small scale (at CSIRO), although the production system is readily scalable. The actual commercial cost of cRGDfK-PAPA could therefore not be determined, although there are several reasons to assume that this surface will be less expensive to produce than Synthemax™. The peptide is the most expensive part of peptide-presenting polymer coatings. Since the input peptide concentration for Synthemax™ II-SC (Synthemax™) production is not disclosed, assumptions must be made from reports on the development of Synthemax™-R. Cell counts from day 5 hPSC cultures on Synthemax™-R coatings modified with solutions containing peptide concentrations greater than 500 µM were reported to be comparable to counts from control cultures maintained on Matrigel™ (Melkounian et al., 2010). While in the present study, hPSC cultures were maintained on cRGDfK-PAPA coatings modified with 36 µM peptide solutions and cultures were passaged approximately every 5 days and produced similar yields to control cells maintained on Geltrex™ for a similar amount of time (Figure 5.6A,B). While in the Synthemax™ paper, adherent cell numbers were observed to decrease when surfaces were modified with peptide concentrations below 500 µM. Surfaces were

modified with as little as 63 μM of peptide, at which point they supported one fifth (1/5) of the maximal cell numbers. On the other hand, day 2 cell counts from the optimisation of the cRGDfK-PAPA culture surface (Section 3.3.3) indicate surfaces modified with concentrations of peptide as low as 1 μM , could support numbers of hPSCs comparable to GeltrexTM-coated surfaces. This reflects a potential saving of peptide cost conservatively estimated at 15-fold, which could realistically extend to a 500-fold saving.

Table 5.3 GeltrexTM, cRGDfK-PAPA, StemAdhereTM and SynthemaxTM are ranked as hPSC culture surfaces from most (1) to least (4) preferred with regards to cost, preparation, shelf life and the requirement for scraping to harvest cells.

Surface	Cost	Preparation	Shelf life	Cell scraping
Geltrex TM	1	4	3	2
cRGDfK-PAPA	Unknown (cheaper than StemAdhere)	1	1	2
StemAdhere TM	2	3	4	1
Synthemax TM	3	2	2	4

The benefits of low-cost surfaces that require little preparation and have a long shelf life are self-evident. Although cell scraping is included in some hPSC passaging protocols (Wagner and Welch, 2010, Nagaoka et al., 2010, Beers et al., 2012), such manual harvesting is not easily scalable and could not be applied to multilayer flasks or three-dimensional cell culture systems like microcarriers and hydrogels (Nie et al., 2014). Attempts to minimise the requirement for cell scraping by extending exposure to dissociation reagents can result in the undesirable isolation of single cells and cell death (Beers et al., 2012). Enzyme-free, EDTA-based dissociation reagents like Versene (Thermo Fisher Scientific, Cat No: 15040-066) and ReLeSR (STEMCELL Technologies, Cat No: 05872) have been promoted as eliminating the need for cell scraping and the use of Versene to harvest hPSC cultures from SynthemaxTM coatings has been previously reported without any mention of cell scraping (Selekman et al., 2015, Laperle et al., 2015a). Use of a weaker calcium chelator, sodium citrate, as a dissociation reagent has also recently been reported to eliminate the need for cell scraping and to result in better control over the size of harvested cell clumps (Nie et al., 2014). Sodium citrate may therefore be a viable for harvesting hPSCs from SynthemaxTM-coated surfaces, although the need to scrape TrypLETM Express-treated cells in the present study (Figure 5.11B) indicates that this phenomenon is not strictly dissociation reagent specific. Aside from the logistical issues involved in large scale hPSC cultures, the use of cell scraping is also undesirable because the surface coating is more likely to be harvested along with the cells. The pharmacokinetics of any coating contaminants would therefore also need to be assessed prior to the application of cells cultured in these systems to cell therapies. Another interesting approach to simplify cell harvesting has been the development of thermosensitive coatings (Zhang et al., 2013b), although hPSCs were observed to take longer to reach confluence on these coatings than

control hPSCs cultured on Matrigel™, despite being seeded at a higher density. In the current study, hPSCs maintained in cRGDfK-PAPA-coated or Geltrex™-coated flasks were observed to require harvest by cell scraping significantly less often than cells cultures on Synthemax™-coated flasks. The surface that least required scraping for cell detachment was StemAdhere™ (Figure 5.11), which may be related to a lack of surface stability.

The ease of harvesting hPSCs from StemAdhere™-coated flasks and the associated improvement in viability (Figure 5.6D), the barren areas observed on these flasks (Figure 5.9) and the short shelf life compared to other coatings (Table 5.2) may reflect a reduced coating stability. Adsorption of a thin layer of the StemAdhere™ coating is thought to be mediated by hydrophobic interactions that form between the IgG1-Fc portion of the E-cadherin-IgG1-Fc fusion protein and non-tissue culture treated polystyrene flasks. The stability of StemAdhere™ coatings on polystyrene has not been reported, although the properties of coatings of human IgG on untreated polystyrene surfaces have been studied using ellipsometry (Svensson and Arnebrant, 2012). Uncontrolled adsorption of antibodies to polystyrene surfaces was found to result in inconsistent molecular orientation, which could affect the presentation of the Fab portion of the antibody (Svensson and Arnebrant, 2012), which has been replaced in StemAdhere™ with the E-cadherin ligand (Nagaoka et al., 2002). The antibody coatings were found to be stable when rinsed with water or when incubated in pure water or water containing 2.0 mg/mL BSA but incubations were only conducted over 20 minutes (Svensson and Arnebrant, 2012). In the present study the surface was incubated in a relatively complex medium containing settling hPSCs, dead cells and cellular debris for at least 24 hours before the bare patches were observed. Furthermore, the displacement of coated antibodies by serum in the Svensson study was restricted by a limitation of the ellipsometry approach, which quantifies protein adsorption but is unable to distinguish bound antibody from bound serum proteins. The barren areas observed on StemAdhere™-coated flasks (Figure 5.10) could also be a result of insufficient coverage of the flask with the coating solution, since antibody-coated surfaces showed a loss of surface density when the surface was nitrogen-dried and then rehydrated (Svensson and Arnebrant, 2012). Attempts were made to ensure that all coatings properly covered the underlying polystyrene at all times, but this was difficult in the case of StemAdhere™, since the non-tissue culture treated polystyrene surface was more hydrophobic and the coating solution was applied in smaller volumes than for Synthemax™, Geltrex™ or cRGDfK-PAPA.

5.5 Chapter Summary

In this chapter, production of the chemically defined and relatively affordable cRGDfK-PAPA coating that had been optimised for hPSC adhesion in Chapters 3 and 4 was scaled up. A sufficient number of flasks were generated to demonstrate that this novel cell culture substrate could maintain high quality hPSC cultures over the long-term. Cultures of three hPSC lines that were maintained in cRGDfK-PAPA-coated flasks remained comparable to control cultures maintained in parallel in Geltrex™-coated flasks in terms of growth rate and maintenance of pluripotency as assessed by cell morphology, gene expression and teratoma formation. Cultures maintained in parallel on the commercially available chemically defined surfaces StemAdhere™ and Synthemax™ were also observed to remain pluripotent. Detailed analysis of the proliferation rates were obscured by cell line-based variation, particularly in the Genea-02 cell line, for which variable growth rates were observed in individual cultures over the duration of the experiment. Although cultures maintained on cRGDfK-PAPA were observed to display higher levels of morphological differentiation than cultures on other surfaces, this was not reflected in any of the more stringent assessments of pluripotency and illustrates the limitations of gross morphological assessments. Furthermore, hPSC cultures maintained on cRGDfK-coated surfaces remained more karyotypically stable than cultures on other surfaces, including Geltrex™, although more detailed analysis would be required to support this observation. Trisomy of chromosome 12 arose frequently and only in hPSC cultures maintained on StemAdhere™-coated surfaces, indicating that this surface may predispose hPSC cultures to genetic instability. Cultures maintained on Synthemax™ in this study would not have been suitable for large scale production due to the need for physical harvesting of cells by cell scraping, although this may be ameliorated with novel dissociation reagents. The results from this chapter indicate that cRGDfK-PAPA has the potential to provide a viable commercial scale hPSC culture surface.

Chapter 6:

Conclusions and
future directions

6.1 Conclusions

The potential applications of hPSCs are diverse, and the research related to these applications is progressing rapidly. For many, the most exciting potential applications of hPSCs are cell replacement therapies, which will be facilitated by the maintenance of large numbers of hPSCs in chemically defined, xeno-free culture conditions. E8 medium represents an appropriate medium for maintaining clinical grade hPSCs that has been widely adopted by the stem cell community and that can be used in combination with a range of hPSC culture surfaces. However, the development of appropriate culture surfaces has lagged behind. At the commencement of this project, only two synthetic surfaces were commercially available: Synthemax™, a peptide acrylate surface that presents integrin-binding peptides which contain the RGD motif, and StemAdhere™, a fusion protein that adsorbs to TCPS and presents the E-cadherin binding site. StemAdhere™ and Synthemax™ specifically present different ligands that interact with different CAMs on the cell surface. hPSC culture surfaces have also been reported to present other ligands, which interact with a wide range of CAMs, yet the adhesion of hPSCs to synthetic surfaces that individually present many of the ligands reported to mediate cell adhesion has not been directly compared. Likewise, the results of long-term hPSC cultures on StemAdhere™, Synthemax™ have not been directly compared.

This thesis describes the optimisation, application to long-term hPSC culture and benchmarking of synthetic co-polymer brush coatings that are synthetic, chemically-defined, cheap to produce and easily scalable. Coating optimisation included comparing hPSC attachment efficiency to polymer coatings modified with the most comprehensive curated library of peptide ligands to date. hPSC cultures were maintained on the lead cRGDfK-PAPA surface for more than ten passages and were benchmarked against cultures maintained in parallel on Geltrex™, StemAdhere™ and Synthemax™. This was the first direct comparison of commercially available synthetic hPSC culture surfaces and both the quality of the resultant cells and the logistics of maintaining hPSC cultures on each surface were assessed.

Standard TCPS cultureware was chemically modified with PAAA and PAPA coatings by repeatedly exposing vessels that contained mixed monomer solutions to high intensity UV light. Chapter 3 of this thesis describes the optimisation and characterisation of PAAA and PAPA coatings that were used in the subsequent chapters to screen for appropriate peptide ligands and to maintain long-term hPSC cultures. At the commencement of this study, low numbers of hPSCs had previously been observed to bind to cRGDfK-PAAA coatings. Improved adhesion of mCherry-positive H9-OCT4-mCherry cells was observed on cRGDfK-PAAA coatings that contained an increased molar percentage of acrylic acid and that were modified with higher concentrations of peptide, both of which were expected to improve the peptide ligand density. It was also observed that reducing the number of UV exposures used in the synthesis of PAAA coatings resulted in an improvement in hPSC attachment. These results informed the optimisation of cRGDfK-PAPA culture surfaces, on which hPSC adhesion efficiency was consistent regardless of the number of UV exposures that had been used to synthesise the coatings and when coatings were modified using solutions containing as little as ~1 µM of peptide. This represents a ~300-fold reduction in input peptide concentration compared to other reports of peptide-modified polymer coatings, and resulted in deposition of ~3.6 pmol/cm² of peptide.

The chemical compositions of PAAA and PAPA coatings were observed to reflect the molar compositions of their respective monomer feed solutions according to XPS analysis. PAAA-25UV and PAPA-30UV coatings were each observed to be ~150-200 nm thick and to have a thin-film corrected elastic modulus of less than 250 Pa and ~500 Pa respectively. Increasing the number of UV exposures used in coating synthesis affected the two coating types differently. AFM assessment of PAAA-40UV coatings reported an increase in hydrated thickness to ~300 nm and an unchanged thin film-corrected elastic modulus of less than 250 Pa. Meanwhile the hydrated thickness of PAPA-60UV coatings were similar to PAPA-30UV coatings, but the thin film-corrected modulus was observed to increase to ~1000 Pa. It therefore appeared that UV exposure preferentially induced grafting of PAAA coatings from the surface, while inducing cross-linking in PAPA coatings. Cell-sensed stiffness was presumed to relate directly to intrinsic coating stiffness and inversely to coating thickness. The observed correlation between the perceived stiffness of PAAA coatings and hPSC adhesion efficiency was therefore consistent with previous reports.

A library of 36 peptides for which roles in cell adhesion had previously been reported, were individually used to modify PAAA and PAPA coatings. Peptide-modified coatings were then screened for adhesion of hPSCs. Of the peptide-modified polymer coatings, hPSCs were observed to adhere to surfaces modified with five peptides: 20, 31, 34, 35 and cRGDfK. Modification of both PAAA and PAPA coatings with the cRGDfK peptide resulted in surfaces to which larger numbers of hPSCs adhered than when coatings were modified with any other peptide. Low numbers of hPSC colonies were consistently observed to adhere to pep34-PAAA and pep35-PAAA surfaces. Increasing the reaction solution concentrations of peptides 34 and 35 from 200 μ M to 600 μ M failed to improve cell numbers equivalent to cRGDfK-PAAA surfaces modified with 200 μ M peptide solutions. Even fewer colonies of hPSCs were observed to adhere to PAPA coatings that had been modified with one of two HSPG-binding peptides (20 and 31), and hPSC adhesion to these surfaces was observed to be inconsistent and unstable. This result may have been due to insufficient surface peptide density or been related to the absence of Y-27632 media-supplementation.

Detailed characterisation of cultures of H9, NHF-1-3 and Genea-02 hPSCs was performed after each cell line had been adapted to culture on Geltrex™-coated surfaces in E8 medium for ten passages. Cultures of these adapted cell lines were then maintained in E8 medium on cRGDfK-PAPA coatings for ten passages, characterised again, and benchmarked against cultures maintained in parallel on StemAdhere™, Synthemax™ and Geltrex™. hPSC cultures maintained on cRGDfK-PAPA surfaces remained morphologically normal, OCT4-positive by flow cytometry, karyotypically normal, retained the ability to form teratomas and passed the microarray-based PluriTest™ assay. The results of these assays collectively demonstrated that the hPSC cultures maintained on cRGDfK were of high quality.

Parallel hPSC cultures maintained on the commercially available surfaces generally produced comparable assay results to cRGDfK-PAPA, except karyotypic abnormalities were observed in cultures maintained on each of the other surfaces. Abnormalities typically appeared at a low frequency, except for in some Genea-02 samples and especially in the sample from Genea-02 hPSCs maintained on StemAdhere™. There was no clear surface-based variation in proliferation rates or in the proportion of cells in which OCT4 was detected by flow cytometry. Furthermore, no clear variation in gene expression was identified by the PluriTest™ assay between cultures maintained on specific surfaces.

However genes in certain loci appeared to be upregulated in all samples in the present study compared to the reference data set, which may be related to the use of E8 medium.

It was observed that cultures maintained on Synthemax™-coated flasks regularly required cell scraping to remove large numbers of cells during harvesting. Cultures maintained on cRGDfK-PAPA and Geltrex™ required cell scraping less often, and it was very rarely required for removal of hPSCs from StemAdhere™-coated flasks. In fact there was evidence of incidental cell detachment from the StemAdhere™-coated flasks, which may have been related to the stability of the StemAdhere™ coating.

This thesis is the first report of long-term maintenance of hPSC cultures attached to a synthetic surface modified with cRGDfK peptide-alone. The screen presented in Chapter 4 indicated that hPSCs adhered more efficiently to surfaces modified with cRGDfK than any other peptide tested, and optimisation in Chapter 3 indicated that considerably less cRGDfK peptide was required to produce a surface to which hPSCs could adhere compared to other reported peptide-presenting surfaces. Following ten passages of maintenance on cRGDfK-PAPA coatings, hPSCs were observed to remain pluripotent and to be indistinguishable from cultures maintained on commercially available substrates by a wide range of measures.

6.2 Future directions

This thesis has described novel culture conditions for classical hPSCs. However not all pluripotent stem cells are the same, and cell culture conditions are informing recent investigations of the nature of pluripotency. A recent development in the study of pluripotent stem cell biology has been the identification of novel cell-types that fit the classical definition of hPSCs, yet can be further sub-categorised based on their culture conditions and contributions to developing embryos. Stem cell culture is an exercise in arresting the development of artefactual cells at a particular stage. PSCs are defined by their ability to self-renew and to differentiate into cell types from all three germ layers, yet there are subtypes of PSCs that are thought to represent distinct developmental stages. These cells all fit the definition of pluripotent stem cells, yet they have different levels of gene expression, vary in their contributions to developing embryos and are maintained by different culture conditions. mESCs and hESCs are both derived from the inner cell mass of pre-implantation embryos and were originally thought to represent that developmental stage. Many of the differences between mESCs and hESCs, including the ability to contribute to murine chimeras and differences in X chromosome inactivation, were attributed to species differences. This hypothesis was disrupted in 2007 by the derivation of mammalian epiblast-derived stem cells (EpiSCs), which more closely resembled hESCs (Brons et al., 2007). The existence of a “naïve” state of pluripotency, and the possibility of a human equivalent to mESCs was proposed in 2009 (Nichols and Smith, 2009).

More recently another sub-categorisation of PSCs has been identified in mice and primates (Wu et al., 2015). Region-selective pluripotent stem cells (rsPSCs) are proposed to represent a later epiblast stage, where cells retain the ability to differentiate into cells from all three germ layers, but gain specificity for the region of the developing embryo to which they will contribute. A similar stage has

not yet been isolated in humans but would be of interest because of the low risk of tumour formation that is predicted to be associated with rPSCs.

Several culture conditions have been developed for maintenance of naïve hPSCs, involving cocktails of growth factors and small molecule inhibitors. However reports of establishing and maintaining naïve hPSCs have mostly used MEFs as a substrate (Hanna et al., 2010, Theunissen et al., 2014), while one study also reported the maintenance of naïve hPSC cultures on TCPS coated with both vitronectin and gelatin (Gafni et al., 2013). Murine rPSCs were also derived and maintained on a layer of MEFs (Wu et al., 2015). The application of synthetic surfaces like PAAA and PAPA to investigating the optimal surface stiffness, ligand type and ligand density for maintaining these pluripotent sub-types would result in an interesting contribution to understanding the different stages of pluripotency. It would perhaps be unsurprising to discover that naïve pluripotent stem cells prefer softer substrates and that EpiSCs prefer stiffer substrates, considering the other observed similarities between hPSCs and EpiSCs. It would also be of interest to further characterise the hPSC cultures maintained for this project before and after 10 passages on each of the culture surfaces. Further characterisation of the cell cultures presented in this thesis could include additional assessment of cell markers in the undifferentiated populations, which may elucidate culture surface-based effects on specific mechanisms involved in the growth and differentiation potential of hPSC culture. Marker characterisation of the teratoma tissue would also strengthen evidence of differentiation and may be used to assess differentiation bias.

Although the sub-divisions of pluripotent phenotypes are academically interesting for investigating early development, the practical applications of these cell types are unclear (Davidson et al., 2015). Therapeutic applications of classical hPSCs will require the cost-effective generation of very large numbers of hPSCs and efficient differentiation into an efficacious and affordable cell-based product that can be safely implanted into patients. Maintenance of hPSC cultures in the chemically-defined, xeno-free E8/cRGDFK-PAPA culture system presented in this thesis meets many of these requirements. Reducing the concentration of peptide required to produce culture surfaces to which hPSCs will bind and the exclusion of xenogeneic components contribute to the cost-effectiveness of applying this culture system to the development of clinical applications.

Recommendation 3.1.2.3 of the draft 2015 ISSCR “Guidelines for Stem Cell Science and Clinical Translation” states that “Components of animal origin used in the culture or preservation of cells should be replaced with human or chemically defined components when possible”. Furthermore, according to the “Guidance for Industry: Source Animal, Product, Preclinical, and Clinical Issues Concerning the Use of Xenotransplantation Products in Humans” provided by the FDA, any cell product that has been exposed to culture conditions which contain components of animal origin must be classed as a xenotransplantation product and will be subject to additional precautions compared to autogeneic or allogeneic transplantations (FDA, 2003). The possible contamination of hPSCs with potentially immunogenic proteins (Hisamatsu-Sakamoto et al., 2008) or sugars (Martin et al., 2005) from xenogeneic culture conditions, indicates that hPSCs intended for clinical application must be derived and maintained in xeno-free culture conditions to minimise the need for post-transplantation immunosuppression, which is an added financial cost and a risk to the patient. The activity of endogenous retroviruses and transmissible spongiform encephalopathies (prions) also pose potential risks that cannot be easily mitigated.

Many reports claiming establishment “clinical grade” hPSC lines have maintained hPSC cultures on human feeder cells, which are a source of batch-to-batch variation and restrict the potential of these approaches to scale up (Crook et al., 2007, Tannenbaum et al., 2012, Wang et al., 2015). A recent study reported the development of the L7™ hPSC culture system a novel, xeno-free culture system for the derivation and maintenance of clinical grade hiPSCs developed by Lonza (Baghbaderani et al., 2015). The L7™ hPSC culture system includes a novel hPSC culture media and the proprietary culture surface “L7™ hPSC Matrix”. Unfortunately L7™ hPSC Matrix was released too late to be included in this study. It would have made an interesting inclusion to the comparative study reported in Chapter 5, and it also would have been interesting to assess the efficiency of the L7™ culture system using cRGDfK-PAPA in place of L7™ hPSC Matrix. The proprietary nature of L7™ hPSC Matrix prevents further discussion of this topic. The derivation of novel hPSC lines should be attempted in the E8/cRGDfK-PAPA culture system. Substituting any other peptide with the cRGDfK peptide and, if possible, introducing a CuAAC chemistry for peptide modification may also reduce the costs of large scale generation of other synthetic hPSC culture surfaces for clinical applications.

Following the generation of large numbers of clinically-relevant hPSCs, efficient differentiation protocols will be required to generate cell therapy products, and synthetic culture surfaces are contributing to the study of differentiation of hPSCs. It has been observed that the endogenous production of $\alpha 5$ laminins can promote hPSC self-renewal (Laperle et al., 2015a) and that changes to ECM production during early differentiation of hPSCs can contribute to driving differentiation (Pook et al., 2015). The underlying substrate used for hPSC maintenance has also been reported to influence both the expression of ECMPs and the differentiation bias of hPSCs (Laperle et al., 2015b). Furthermore, differentiation bias can be affected by the CAM-ligand interaction profile of surfaces used for differentiation assays (Wrighton et al., 2014) and the stiffness of the substrate on which differentiation occurs (Keung et al., 2012, Musah et al., 2014). It would be of interest to maintain hPSCs on PAAA and PAPA coatings of variable substrate stiffness and ligand type, and to assess the differentiation bias of the resultant hPSCs. However, meaningful assessment of differentiation bias is difficult to achieve, since there are typically a range of protocols available to direct differentiation of hPSCs to specific cell types and because increases in expression of intermediate markers may not necessarily translate to improved production efficiency of the desired cell type. Setting appropriate end points is therefore a challenge for assays of differentiation bias, yet the potential improvements to differentiation processes remain worth pursuing.

On the influence of the stiffness of culture surfaces on the cell state, several studies have reported that softer substrates are more suitable for differentiation of hPSCs to various cell types (Musah et al., 2014, Feaster et al., 2015) and also for the induction of reprogramming to pluripotency (Higuchi et al., 2014), while stiffer substrates have been linked to maintenance of hPSCs (as discussed in Section 3.4). Increasing the stiffness of cell culture surfaces is known to result in exertion of increased tension on the cultured cells through ligand-integrin interactions and in development of stress fibres in the actin-myosin cytoskeleton (reviewed by Crowder et al., 2016). A line of research has indicated that this increased stiffness is transferred through the cytoskeleton to the nucleus, which may result in physical inhibition of chromatin compaction and recruitment of epigenetic modifiers (Crowder et al., 2016). Softer surfaces may allow for the reorganisation of nuclear chromatin that is observed during differentiation and reprogramming. It is therefore possible that softer surfaces promote epigenetic

flux and therefore changes to cell state, although this is currently a contentious area, and the effects of surface stiffness on cell state are likely to be more complex.

Regardless of the mechanistic details of the effects of surface properties on hPSCs, cell therapy remains a major aim of pluripotent stem cell research. At the time of writing three companies are conducting or have conducted FDA-approved phase 1 clinical trials testing therapeutic applications of cells derived from hPSCs (summarised in Table 6.1).

Table 6.1: Ongoing clinical trials for cell therapy products derived from hPSCs. This table presents the company name, cell product, indication, hPSC culture surface, ClinicalTrials.gov Identifier code and a literature reference for each study.

Company name	Cell product	Indication	hPSC culture surface	ClinicalTrials.gov Identifier:	Reference
Asterias Biotherapeutics, Inc. (previously Geron, Inc.)	GRNOPC1 neurons	Spinal cord injury	Synthemax™	NCT01217008, 2010	(Lebkowski, 2011)
Ocata Therapeutics, Inc. (formerly Advanced Cells Technology, Inc.)	Retinal pigmented epithelial (RPE) cells	Macular degeneration and Stargardt disease	Mitomycin-C-treated MEFs	NCT01469832, 2011	(Schwartz et al., 2012)
Viacyte, Inc.	Pancreatic progenitor cells (PEC-01™)	Type one diabetes	N/A (hPSCs were maintained as free-floating clumps in the absence of microcarriers)	NCT02239354, 2015	(Schulz et al., 2012)

Of the studies conducted to date, only the hPSCs used in the spinal cord injury trial had been maintained on a chemically-derived synthetic surface, namely Synthemax™. In fact the development of Synthemax™ was pioneered by Geron, Inc. for use in clinical studies like this one (Melkounian et al., 2010). Nevertheless, the GRNOPC1 cell product is still treated as a xenotransplant because the relevant hPSC lines were originally derived and maintained on MEFs before switching to Synthemax™. This highlights the importance of finding conditions that can support the derivation of hPSC lines as well as maintain established lines in culture. For the study by Ocata Therapeutics, Inc., hPSCs were maintained on mitomycin-C-treated MEFs and the RPE cells would therefore also be classified as a xenotransplantation product (Schwartz et al., 2012). The hPSCs for the Viacyte study were scaled up as free-floating clumps (Schulz et al., 2012). Although this approach can produce high cell densities, control of clump size can be difficult to standardise due to clump aggregation and break up. Inconsistent clump size affects the diffusion of nutrients and concentration gradients of growth factors that direct differentiation (Fan et al., 2015). Approaches to prevent formation of necrotic centres in large clumps are still under development (Rostami et al., 2015). Alternatively, the use of microcarrier-based suspension culture systems prevents the formation of such large clumps and provides a high surface-to-volume ratio while exposing the cells more uniformly to the medium bulk concentrations of oxygen, nutrients and growth factors (Fan et al., 2015). The application of PAAA and PAPA coatings to microcarriers and other structures is under development at CSIRO (unpublished observations). The ability to control peptide density and ligand type, as well as the coating stiffness should allow these coatings to be optimised for adhesion of a range of cell types. The presence of shear forces in suspension culture systems can cause cells to detach when cultures are converted 2D to 3D (Fan et al., 2015). The stability of the polymer coatings described in this thesis, and the potential incorporation of high-affinity ligands like cRGDfK may result in more stable cell adhesion to coated microcarriers.

The development of a range of clinical applications for hPSC-derived cells is progressing rapidly. Less than 20 years after the original isolation of hESCs, the diverse range of hPSC culture conditions that have been developed is astonishing. Now, as hPSC-derived cell therapy products enter the clinic, the rush to optimise and standardise hPSC culture conditions appears to approach its zenith. At this stage, it is important to understand the different aspects that lead researchers and to choose certain hPSC culture conditions, and to learn as much as possible about how each candidate culture surface informs us of the properties of the cells. It is also important to develop culture conditions and differentiation protocols in process that remains as clinically-applicable as possible, to pave the way to the clinic. This project was undertaken to develop a synthetic culture surface that could maintain hPSC cultures using only the most chemically simple, including E8 medium and EDTA, with the understanding that these qualities are beneficial for translating to large scale production. The surface itself will also be eminently scalable with the design of more efficient laboratory and equipment layouts for exposing vessels that contain mixed monomer solutions to UV light. The optimisation of PAAA and PAPA coatings for hPSC culture has also reinforced the importance of surface stiffness for maintaining hPSC culture, and questions have

been raised about the relationship between approaches for assessing the stiffness of a surface and the stiffness as it is sensed by the cells. This project has also positioned the cRGDfK peptide as a strong candidate ligand that should be considered as a component of any developing peptide-presenting hPSC culture surfaces. Additionally, this was one of the first validations of the PluriTest™ assay with hPSCs cultures in E8 medium and has identified several cytobands that may contain genes that are differentially expressed between hPSCs maintained in E8 and in more complex media. Questions have also been raised about the differences between studies that report superior results using HSPG-binding or integrin-binding peptides, and the potential role of Y-27632 media supplementation. cRGDfK-PAPA is likely to represent a cost-effective and durable alternative hPSC culture surface that could also be used to optimise substrate conditions for culture of other cell types. A comparative study of hPSC cultures maintained on cRGDfK-PAPA, Geltrex™, StemAdhere™ or Synthemax™ identified few differences between the resultant cells and indicated that the appropriate synthetic culture surface should be selected based mainly on cost and logistical issues.

Bibliography

Bibliography

- ABBASALIZADEH, S., LARIJANI, M. R., SAMADIAN, A. & BAHARVAND, H. 2012. Bioprocess development for mass production of size-controlled human pluripotent stem cell aggregates in stirred suspension bioreactor. *Tissue Engineering - Part C: Methods*, 18, 831-851.
- ABRAHAM, S., RIGGS, M. J., NELSON, K., LEE, V. & RAO, R. R. 2010. Characterization of human fibroblast-derived extracellular matrix components for human pluripotent stem cell propagation. *Acta Biomaterialia*, 6, 4622-4633.
- ADEWUMI, O., AFLATOONIAN, B., AHRLUND-RICHTER, L., AMIT, M., ANDREWS, P. W., BEIGHTON, G., BELLO, P. A., BENVENISTY, N., BERRY, L. S., BEVAN, S., BLUM, B., BROOKING, J., CHEN, K. G., CHOO, A. B. H., CHURCHILL, G. A., CORBEL, M., DAMJANOV, I., DRAPER, J. S., DVORAK, P., EMANUELSSON, K., FLECK, R. A., FORD, A., GERTOW, K., GERTSENSTEIN, M., GOKHALE, P. J., HAMILTON, R. S., HAMPL, A., HEALY, L. E., HOVATTA, O., HYLLNER, J., IMREH, M. P., ITSKOVITZ-ELDOR, J., JACKSON, J., JOHNSON, J. L., JONES, M., KEE, K., KING, B. L., KNOWLES, B. B., LAKO, M., LEBRIN, F., MALLON, B. S., MANNING, D., MAYSHAR, Y., MCKAY, R. D. G., MICHALSKA, A. E., MIKKOLA, M., MILEIKOVSKY, M., MINGER, S. L., MOORE, H. D., MUMMERY, C. L., NAGY, A., NAKATSUJI, N., O'BRIEN, C. M., OH, S. K. W., OLSSON, C., OTONKOSKI, T., PARK, K. Y., PASSIER, R., PATEL, H., PATEL, M., PEDERSEN, R., PERA, M. F., PIEKARCZYK, M. S., PERA, R. A. R., REUBINOFF, B. E., ROBINS, A. J., ROSSANT, J., RUGG-GUNN, P., SCHULZ, T. C., SEMB, H., SHERRER, E. S., SIEMEN, H., STACEY, G. N., STOJKOVIC, M., SUEMORI, H., SZATKIEWICZ, J., TURETSKY, T., TUURI, T., VAN DEN BRINK, S., VINTERSTEN, K., VUORISTO, S., WARD, D., WEAVER, T. A., YOUNG, L. A. & ZHANG, W. 2007. Characterization of human embryonic stem cell lines by the International Stem Cell Initiative. *Nature Biotechnology*, 25, 803-816.
- ADJAYE, J., HUNTRISS, J., HERWIG, R., BENKAHLA, A., BRINK, T. C., WIERLING, C., HULTSCHIG, C., GROTH, D., YASPO, M. L., PICTON, H. M., GOSDEN, R. G. & LEHRACH, H. 2005. Primary differentiation in the human blastocyst: Comparative molecular portraits of inner cell mass and trophectoderm cells. *Stem Cells*, 23, 1514-1525.
- AKOPIAN, V., ANDREWS, P. W., BEIL, S., BENVENISTY, N., BREHM, J., CHRISTIE, M., FORD, A., FOX, V., GOKHALE, P. J., HEALY, L., HOLM, F., HOVATTA, O., KNOWLES, B. B., LUDWIG, T. E., MCKAY, R. D. G., MIYAZAKI, T., NAKATSUJI, N., OH, S. K. W., PERA, M. F., ROSSANT, J., STACEY, G. N. & SUEMORI, H. 2010. Comparison of defined culture systems for feeder cell free propagation of human embryonic stem cells. *In Vitro Cellular and Developmental Biology - Animal*, 46, 247-258.

- ALDERIGHI, M., IERARDI, V., FUSO, F., ALLEGRINI, M. & SOLARO, R. 2009. Size effects in nanoindentation of hard and soft surfaces. *Nanotechnology*, 20.
- AMERINGER, T., FRANSEN, P., BEAN, P., JOHNSON, G., PEREIRA, S., EVANS, R. A., THISSEN, H. & MEAGHER, L. 2012. Polymer coatings that display specific biological signals while preventing nonspecific interactions. *Journal of Biomedical Materials Research - Part A*, 100 A, 370-379.
- AMERINGER, T., MEAGHER, L., THISSEN, H., PASIC, P. & STYAN, K. 2014. Process for modifying a polymeric surface. Google Patents.
- AMPS, K., ANDREWS, P. W., ANYFANTIS, G., ARMSTRONG, L., AVERY, S., BAHARVAND, H., BAKER, J., BAKER, D., MUNOZ, M. B., BEIL, S., BENVENISTY, N., BEN-YOSEF, D., BIANCOTTI, J. C., BOSMAN, A., BRENA, R. M., BRISON, D., CAISANDER, G., CAMARASA, M. V., CHEN, J., CHIAO, E., CHOI, Y. M., CHOO, A. B. H., COLLINS, D., COLMAN, A., CROOK, J. M., DALEY, G. Q., DALTON, A., DE SOUSA, P. A., DENNING, C., DOWNIE, J., DVORAK, P., MONTGOMERY, K. D., FEKI, A., FORD, A., FOX, V., FRAGA, A. M., FRUMKIN, T., GE, L., GOKHALE, P. J., GOLAN-LEV, T., GOURABI, H., GROPP, M., GUANGXIU, L., HAMPL, A., HARRON, K., HEALY, L., HERATH, W., HOLM, F., HOVATTA, O., HYLLNER, J., INAMDAR, M. S., IRWANTO, A. K., ISHII, T., JACONI, M., JIN, Y., KIMBER, S., KISELEV, S., KNOWLES, B. B., KOPPER, O., KUKHARENKO, V., KULIEV, A., LAGARKOVA, M. A., LAIRD, P. W., LAKO, M., LASLETT, A. L., LAVON, N., LEE, D. R., LEE, J. E., LI, C., LIM, L. S., LUDWIG, T. E., MA, Y., MALTBY, E., MATEIZEL, I., MAYSHAR, Y., MILEIKOVSKY, M., MINGER, S. L., MIYAZAKI, T., MOON, S. Y., MOORE, H., MUMMERY, C., NAGY, A., NAKATSUJI, N., NARWANI, K., OH, S. K. W., OH, S. K., OLSON, C., OTONKOSKI, T., PAN, F., PARK, I. H., PELLIS, S., PERA, M. F., PEREIRA, L. V., QI, O., RAJ, G. S., REUBINOFF, B., ROBINS, A., ROBSON, P., ROSSANT, J., SALEKDEH, G. H., et al. 2011. Screening ethnically diverse human embryonic stem cells identifies a chromosome 20 minimal amplicon conferring growth advantage. *Nature Biotechnology*, 29, 1132-1144.
- ASPRER, J. S. T. & LAKSHMIPATHY, U. 2015. Current Methods and Challenges in the Comprehensive Characterization of Human Pluripotent Stem Cells. *Stem Cell Reviews and Reports*, 11, 357-372.
- AVERY, S., HIRST, A. J., BAKER, D., LIM, C. Y., ALAGARATNAM, S., SKOTHEIM, R. I., LOTHE, R. A., PERA, M. F., COLMAN, A., ROBSON, P., ANDREWS, P. W. & KNOWLES, B. B. 2013. BCL-XL mediates the strong selective advantage of a 20q11.21 amplification commonly found in human embryonic stem cell cultures. *Stem Cell Reports*, 1, 379-386.
- BAGHBADERANI, B. A., TIAN, X., NEO, B. H., BURKALL, A., DIMEZZO, T., SIERRA, G., ZENG, X., WARREN, K., KOVARCIK, D. P., FELLNER, T. & RAO, M. S. 2015. cGMP-Manufactured Human Induced Pluripotent Stem Cells Are Available for Pre-clinical and Clinical Applications. *Stem Cell Reports*, 5, 647-59.

- BAKER-ANDRESEN, D., RATNU, V. S. & BREDY, T. W. 2013. Dynamic DNA methylation: A prime candidate for genomic metaplasticity and behavioral adaptation. *Trends in Neurosciences*, 36, 3-13.
- BALLUT, L., SAPAY, N., CHAUTARD, É., IMBERTY, A. & RICARD-BLUM, S. 2013. Mapping of heparin/heparan sulfate binding sites on $\alpha v \beta 3$ integrin by molecular docking. *Journal of Molecular Recognition*, 26, 76-85.
- BARBEY, R., LAVANANT, L., PARIPOVIC, D., SCHÜWER, N., SUGNAUX, C., TUGULU, S. & KLOK, H. A. 2009. Polymer brushes via surface-initiated controlled radical polymerization: synthesis, characterization, properties, and applications. *Chemical Reviews*, 109, 5437-5527.
- BARCZYK, M., CARRACEDO, S. & GULLBERG, D. 2010. Integrins. *Cell and Tissue Research*, 339, 269-280.
- BARDY, J., CHEN, A. K., LIM, Y. M., WU, S., WEI, S., WEIPING, H., CHAN, K., REUVENY, S. & OH, S. K. W. 2013. Microcarrier suspension cultures for high-density expansion and differentiation of human pluripotent stem cells to neural progenitor cells. *Tissue Engineering - Part C: Methods*, 19, 166-180.
- BAXTER, M. A., CAMARASA, M. V., BATES, N., SMALL, F., MURRAY, P., EDGAR, D. & KIMBER, S. J. 2009. Analysis of the distinct functions of growth factors and tissue culture substrates necessary for the long-term self-renewal of human embryonic stem cell lines. *Stem Cell Research*, 3, 28-38.
- BEERS, J., GULBRANSON, D. R., GEORGE, N., SINISCALCHI, L. I., JONES, J., THOMSON, J. A. & CHEN, G. 2012. Passaging and colony expansion of human pluripotent stem cells by enzyme-free dissociation in chemically defined culture conditions. *Nature Protocols*, 7, 2029-2040.
- BIGDELI, N., ANDERSSON, M., STREHL, R., EMANUELSSON, K., KILMARE, E., HYLLNER, J. & LINDAHL, A. 2008. Adaptation of human embryonic stem cells to feeder-free and matrix-free culture conditions directly on plastic surfaces. *Journal of Biotechnology*, 133, 146-153.
- BINNIG, G., QUATE, C. F. & GERBER, C. 1986. Atomic force microscope. *Physical Review Letters*, 56, 930-933.
- BLASCHUK, O. W., SULLIVAN, R., DAVID, S. & POULIOT, Y. 1990. Identification of a cadherin cell adhesion recognition sequence. *Developmental Biology*, 139, 227-229.
- BOCK, C., KISKINIS, E., VERSTAPPEN, G., GU, H., BOULTING, G., SMITH, Z. D., ZILLER, M., CROFT, G. F., AMOROSO, M. W., OAKLEY, D. H., GNIRKE, A., EGGAN, K. & MEISSNER, A. 2011. Reference maps of human es and ips cell variation enable high-throughput characterization of pluripotent cell lines. *Cell*, 144, 439-452.
- BOYES, J. & BIRD, A. 1992. Repression of genes by DNA methylation depends on CpG density and promoter strength: Evidence for involvement of a methyl-CpG binding protein. *EMBO Journal*, 11, 327-333.
- BRAAM, S. R., ZEINSTRA, L., LITJENS, S., WARD-VAN OOSTWAARD, D., VAN DEN BRINK, S., VAN LAAKE, L., LEBRIN, F., KATS, P., HOCHSTENBACH, R., PASSIER, R., SONNENBERG, A. & MUMMERY,

- C. L. 2008. Recombinant vitronectin is a functionally defined substrate that supports human embryonic stem cell self-renewal via α 5 β 1 integrin. *Stem Cells*, 26, 2257-65.
- BRADLEY, C. K., CHAMI, O., PEURA, T. T., BOSMAN, A., DUMEVSKA, B., SCHMIDT, U. & STOJANOV, T. 2010. Derivation of three new human embryonic stem cell lines. *In Vitro Cellular and Developmental Biology - Animal*, 46, 294-299.
- BRAFMAN, D., SHAH, K., FELLNER, T., CHIEN, S. & WILLERT, K. 2009. Defining long-term maintenance conditions of human embryonic stem cells with arrayed cellular microenvironment technology. *Stem Cells Dev*, 18, 1141-54.
- BRAFMAN, D. A., CHANG, C. W., FERNANDEZ, A., WILLERT, K., VARGHESE, S. & CHIEN, S. 2010. Long-term human pluripotent stem cell self-renewal on synthetic polymer surfaces. *Biomaterials*, 31, 9135-9144.
- BRIGGS, J. A., SUN, J., SHEPHERD, J., OVCHINNIKOV, D. A., CHUNG, T. L., NAYLER, S. P., KAO, L. P., MORROW, C. A., THAKAR, N. Y., SOO, S. Y., PEURA, T., GRIMMOND, S. & WOLVETANG, E. J. 2013. Integration-free induced pluripotent stem cells model genetic and neural developmental features of down syndrome etiology. *Stem Cells*, 31, 467-478.
- BRONS, I. G. M., SMITHERS, L. E., TROTTER, M. W. B., RUGG-GUNN, P., SUN, B., CHUVA DE SOUSA LOPES, S. M., HOWLETT, S. K., CLARKSON, A., AHRlund-RICHTER, L., PEDERSEN, R. A. & VALLIER, L. 2007. Derivation of pluripotent epiblast stem cells from mammalian embryos. *Nature*, 448, 191-195.
- BUXBOIM, A., RAJAGOPAL, K., BROWN, A. E. X. & DISCHER, D. E. 2010. How deeply cells feel: Methods for thin gels. *Journal of Physics Condensed Matter*, 22.
- CAI, J., DELAFOREST, A., FISHER, J., URICK, A., WAGNER, T., TWAROSKI, K., CAYO, M., NAGAOKA, M. & DUNCAN, S. A. 2008. Protocol for directed differentiation of human pluripotent stem cells toward a hepatocyte fate. *StemBook*. Cambridge (MA): Harvard Stem Cell Institute
- Copyright: (c) 2012 Uri Ben-Davi and Nissim Benvenisty.
- CELIZ, A. D., SMITH, J. G. W., PATEL, A. K., HOOK, A. L., RAJAMOHAN, D., GEORGE, V. T., FLATT, L., PATEL, M. J., EPA, V. C., SINGH, T., LANGER, R., ANDERSON, D. G., ALLEN, N. D., HAY, D. C., WINKLER, D. A., BARRETT, D. A., DAVIES, M. C., YOUNG, L. E., DENNING, C. & ALEXANDER, M. R. 2015. Discovery of a Novel Polymer for Human Pluripotent Stem Cell Expansion and Multilineage Differentiation. *Advanced Materials*, 27, 4006-4012.
- CHADDAH, R., ARNTFIELD, M., RUNCIMAN, S., CLARKE, L. & VAN DER KOOY, D. 2012. Clonal neural stem cells from human embryonic stem cell colonies. *Journal of Neuroscience*, 32, 7771-7781.
- CHANG, C. W., HWANG, Y., BRAFMAN, D., HAGAN, T., PHUNG, C. & VARGHESE, S. 2013. Engineering cell-material interfaces for long-term expansion of human pluripotent stem cells. *Biomaterials*, 34, 912-921.

- CHEN, A. K. L., CHEN, X., CHOO, A. B. H., REUVENY, S. & OH, S. K. W. 2011a. Critical microcarrier properties affecting the expansion of undifferentiated human embryonic stem cells. *Stem Cell Research*, 7, 97-111.
- CHEN, G., GULBRANSON, D. R., HOU, Z., BOLIN, J. M., RUOTTI, V., PROBASCO, M. D., SMUGA-OTTO, K., HOWDEN, S. E., DIOL, N. R., PROPSON, N. E., WAGNER, R., LEE, G. O., ANTOSIEWICZ-BOURGET, J., TENG, J. M. C. & THOMSON, J. A. 2011b. Chemically defined conditions for human iPSC derivation and culture. *Nature Methods*, 8, 424-429.
- CHEN, W., VILLA-DIAZ, L. G., SUN, Y., WENG, S., KIM, J. K., LAM, R. H. W., HAN, L., FAN, R., KREBSBACH, P. H. & FU, J. 2012. Nanotopography influences adhesion, spreading, and self-renewal of Human embryonic stem cells. *ACS Nano*, 6, 4094-4103.
- CHOI, Y., KIM, E., LEE, Y., HAN, M. H. & KANG, I. C. 2010. Site-specific inhibition of integrin $\alpha\beta 3$ -vitronectin association by a ser-asp-val sequence through an Arg-Gly-Asp-binding site of the integrin. *Proteomics*, 10, 72-80.
- CHOWDHURY, F., LI, Y., POH, Y. C., YOKOHAMA-TAMAKI, T., WANG, N. & TANAKA, T. S. 2010a. Soft substrates promote homogeneous self-renewal of embryonic stem cells via downregulating cell-matrix tractions. *PLoS ONE*, 5.
- CHOWDHURY, F., NA, S., LI, D., POH, Y. C., TANAKA, T. S., WANG, F. & WANG, N. 2010b. Material properties of the cell dictate stress-induced spreading and differentiation in embryonic stemcells. *Nature Materials*, 9, 82-88.
- CLARK, A. T., RODRIGUEZ, R. T., BODNAR, M. S., ABEYTA, M. J., CEDARS, M. I., TUREK, P. J., FIRPO, M. T. & PERA, R. A. R. 2004. Human STELLAR, NANOG, and GDF3 Genes Are Expressed in Pluripotent Cells and Map to Chromosome 12p13, a Hotspot for Teratocarcinoma. *Stem Cells*, 22, 169-179.
- CLEVELAND, J. P., MANNE, S., BOCEK, D. & HANSMA, P. K. 1993. A nondestructive method for determining the spring constant of cantilevers for scanning force microscopy. *Review of Scientific Instruments*, 64, 403-405.
- COAD, B. R., LU, Y., GLATTAUER, V. & MEAGHER, L. 2012. Substrate-independent method for growing and modulating the density of polymer brushes from surfaces by atp. *ACS Applied Materials and Interfaces*, 4, 2811-2823.
- COLLINS, M. N. & BIRKINSHAW, C. 2012. Hyaluronic acid based scaffolds for tissue engineering-A review. *Carbohydrate Polymers*, 92, 1262-1279.
- CROOK, J. M., PEURA, T. T., KRAVETS, L., BOSMAN, A. G., BUZZARD, J. J., HORNE, R., HENTZE, H., DUNN, N. R., ZWEIGERDT, R., CHUA, F., UPSHALL, A. & COLMAN, A. 2007. The Generation of Six Clinical-Grade Human Embryonic Stem Cell Lines. *Cell Stem Cell*, 1, 490-494.
- CROWDER, S. W., LEONARDO, V., WHITTAKER, T., PAPATHANASIOU, P. & STEVENS, M. M. 2016. Material Cues as Potent Regulators of Epigenetics and Stem Cell Function. *Cell Stem Cell*, 18, 39-52.
- DAVIDSON, K. C., MASON, E. A. & PERA, M. F. 2015. The pluripotent state in mouse and human. *Development (Cambridge)*, 142, 3090-3099.

- DERDA, R., LI, L., ORNER, B. P., LEWIS, R. L., THOMSON, J. A. & KIESSLING, L. 2007. Defined substrates for human embryonic stem cell growth identified from surface arrays. *ACS Chemical Biology*, 2, 347-355.
- DERDA, R., MUSAH, S., ORNER, B. P., KLIM, J. R., LI, N. & KIESSLING, L. L. 2010. High-throughput discovery of synthetic surfaces that support proliferation of pluripotent cells. *Journal of the American Chemical Society*, 132, 1289-1295.
- DEUTZMANN, R., AUMAILLEY, M., WIEDEMANN, H., PYSNY, W., TIMPL, R. & EDGAR, D. 1990. Cell adhesion, spreading and neurite stimulation by laminin fragment E8 depends on maintenance of secondary and tertiary structure in its rod and globular domain. *European Journal of Biochemistry*, 191, 513-522.
- DI CIO, S. & GAUTROT, J. E. 2016. Cell sensing of physical properties at the nanoscale: Mechanisms and control of cell adhesion and phenotype. *Acta Biomaterialia*, 30, 26-48.
- DI GIORGIO, F. P., BOULTING, G. L., BOBROWICZ, S. & EGGAN, K. C. 2008. Human Embryonic Stem Cell-Derived Motor Neurons Are Sensitive to the Toxic Effect of Glial Cells Carrying an ALS-Causing Mutation. *Cell Stem Cell*, 3, 637-648.
- DIMITRIADIS, E. K., HORKAY, F., MARESCA, J., KACHAR, B. & CHADWICK, R. S. Method for determination of the elastic modulus of thin polymer gels using the atomic force microscope. 223rd ACS National Meeting, 2002 Orlando, FL. Polymer Preprints ACS, 436-437.
- DING, Y., YANG, H., YU, L., XU, C. L., ZENG, Y., QIU, Y. & LI, D. S. 2015. Feeder-free and xeno-free culture of human pluripotent stem cells using UCBS matrix. *Cell Biology International*, 39, 1111-1119.
- DOETSCHMAN, T. C., EISTETTER, H. & KATZ, M. 1985. The in vitro development of blastocyst-derived embryonic stem cell lines: Formation of visceral yolk sac, blood islands and myocardium. *Journal of Embryology and Experimental Morphology*, VOL. 87, 27-45.
- DOGRA, P., MARTIN, E. B., WILLIAMS, A., RICHARDSON, R. L., FOSTER, J. S., HACKENBACK, N., KENNEL, S. J., SPARER, T. E. & WALL, J. S. 2015. Novel heparan sulfate-binding peptides for blocking herpesvirus entry. *PLoS ONE*, 10.
- DOMOGATSKAYA, A., RODIN, S., BOUTAUD, A. & TRYGGVASON, K. 2008. Laminin-511 but Not-332,-111, or-411 Enables Mouse Embryonic Stem Cell Self-Renewal In Vitro. *Stem Cells*, 26, 2800-2809.
- DRAPER, J. S., MOORE, H. D., RUBAN, L. N., GOKHALE, P. J. & ANDREWS, P. W. 2004. Culture and characterization of human embryonic stem cells. *Stem Cells Dev*, 13, 325-36.
- DU, J., CHEN, X., LIANG, X., ZHANG, G., XU, J., HE, L., ZHAN, Q., FENG, X. Q., CHIEN, S. & YANG, C. 2011. Integrin activation and internalization on soft ECM as a mechanism of induction of stem cell differentiation by ECM elasticity. *Proceedings of the National Academy of Sciences of the United States of America*, 108, 9466-9471.

- EASTHAM, A. M., SPENCER, H., SONCIN, F., RITSON, S., MERRY, C. L. R., STERN, P. L. & WARD, C. M. 2007. Epithelial-mesenchymal transition events during human embryonic stem cell differentiation. *Cancer Research*, 67, 11254-11262.
- ENGLER, A., BACAKOVA, L., NEWMAN, C., HATEGAN, A., GRIFFIN, M. & DISCHER, D. 2004. Substrate Compliance versus Ligand Density in Cell on Gel Responses. *Biophysical Journal*, 86, 617-628.
- ENGLER, A. J., SEN, S., SWEENEY, H. L. & DISCHER, D. E. 2006. Matrix Elasticity Directs Stem Cell Lineage Specification. *Cell*, 126, 677-689.
- ENGLUND, E. A., WANG, D., FUJIGAKI, H., SAKAI, H., MICKLITSCH, C. M., GHIRLANDO, R., MARTIN-MANSO, G., PENDRAK, M. L., ROBERTS, D. D., DURELL, S. R. & APPELLA, D. H. 2012. Programmable multivalent display of receptor ligands using peptide nucleic acid nanoscaffolds. *Nature Communications*, 3.
- FADEEV, A. G., GEHMAN, J., MARTIN, A. W., MELKOUMIAN, Z., SHOGBON, C. B., WEBER, D. M. & ZHOU, Y. 2009. Swellable (meth)acrylate surfaces for culturing cells in chemically defined media. Google Patents.
- FAN, Y., WU, J., ASHOK, P., HSIUNG, M. & TZANAKAKIS, E. S. 2015. Production of Human Pluripotent Stem Cell Therapeutics under Defined Xeno-free Conditions: Progress and Challenges. *Stem Cell Reviews and Reports*, 11, 96-109.
- FDA 2003. Guidance for Industry: Source Animal, Product, Preclinical, and Clinical Issues Concerning the Use of Xenotransplantation Products in Humans.
- FEASTER, T. K., CADAR, A. G., WANG, L., WILLIAMS, C. H., CHUN, Y. W., HEMPEL, J., BLOODWORTH, N., MERRYMAN, W. D., LIM, C. C., WU, J. C., KNOLLMANN, B. C. & HONG, C. C. 2015. Matrigel Mattress: A Method for the Generation of Single Contracting Human-Induced Pluripotent Stem Cell-Derived Cardiomyocytes. *Circulation Research*.
- FINCH, B.W. & EPHRUSSI, B. W. 1967 Retention of multiple developmental potentialities by cells of a mouse testicular teratocarcinoma using prolonged culture *in vitro* and their extinction upon hybridization with cells of permanent lines. *Proceedings of the National Academy of Sciences of the United States of America*, 57(3), 615-621.
- FLETCHER, J. M., FERRIER, P. M., GARDNER, J. O., HARKNESS, L., DHANJAL, S., SERHAL, P., HARPER, J., DELHANTY, J., BROWNSTEIN, D. G., PRASAD, Y. R., LEBKOWSKI, J., MANDALAM, R., WILMUT, I. & DE SOUSA, P. A. 2006. Variations in humanized and defined culture conditions supporting derivation of new human embryonic stem cell lines. *Cloning and Stem Cells*, 8, 319-334.
- FLYNN, N. T., TRAN, T. N. T., CIMA, M. J. & LANGER, R. 2003. Long-term stability of self-assembled monolayers in biological media. *Langmuir*, 19, 10909-10915.
- FORD-PERRISS, M., GUIMOND, S. E., GREFERATH, U., KITA, M., GROBE, K., HABUCHI, H., KIMATA, K., ESKO, J. D., MURPHY, M. & TURNBULL, J. E. 2002. Variant heparan sulfates synthesized in developing mouse brain differentially regulate FGF signaling. *Glycobiology*, 12, 721-727.

- FU, J., WANG, Y. K., YANG, M. T., DESAI, R. A., YU, X., LIU, Z. & CHEN, C. S. 2010. Mechanical regulation of cell function with geometrically modulated elastomeric substrates. *Nature Methods*, 7, 733-736.
- FU, X., TOH, W. S., LIU, H., LU, K., LI, M. & CAO, T. 2011. Establishment of clinically compliant human embryonic stem cells in an autologous feeder-free system. *Tissue Engineering - Part C: Methods*, 17, 927-937.
- GAFNI, O., WEINBERGER, L., MANSOUR, A. A., MANOR, Y. S., CHOMSKY, E., BEN-YOSEF, D., KALMA, Y., VIUKOV, S., MAZA, I., ZVIRAN, A., RAIS, Y., SHIPONY, Z., MUKAMEL, Z., KRUPALNIK, V., ZERBIB, M., GEULA, S., CASPI, I., SCHNEIR, D., SHWARTZ, T., GILAD, S., AMANN-ZALCENSTEIN, D., BENJAMIN, S., AMIT, I., TANAY, A., MASSARWA, R., NOVERSHTERN, N. & HANNA, J. H. 2013. Derivation of novel human ground state naive pluripotent stem cells. *Nature*, 504, 282-286.
- GAO, S. Y., LEES, J. G., WONG, J. C. Y., CROLL, T. I., GEORGE, P., COOPER-WHITE, J. J. & TUCH, B. E. 2010. Modeling the adhesion of human embryonic stem cells to poly(lactic-co- glycolic acid) surfaces in a 3D environment. *Journal of Biomedical Materials Research - Part A*, 92, 683-692.
- GARITAONANDIA, I., AMIR, H., BOSCOLO, F. S., WAMBUA, G. K., SCHULTHEISZ, H. L., SABATINI, K., MOREY, R., WALTZ, S., WANG, Y. C., TRAN, H., LEONARDO, T. R., NAZOR, K., SLAVIN, I., LYNCH, C., LI, Y., COLEMAN, R., ROMERO, I. G., ALTUN, G., REYNOLDS, D., DALTON, S., PARAST, M., LORING, J. F. & LAURENT, L. C. 2015. Increased risk of genetic and epigenetic instability in human embryonic stem cells associated with specific culture conditions. *PLoS ONE*, 10.
- GASIMLI, L., LINHARDT, R. J. & DORDICK, J. S. 2012. Proteoglycans in stem cells. *Biotechnology and Applied Biochemistry*, 59, 65-76.
- GERECHT, S., BURDICK, J. A., FERREIRA, L. S., TOWNSEND, S. A., LANGER, R. & VUNJAK-NOVAKOVIC, G. 2007. Hyaluronic acid hydrogel for controlled self-renewal and differentiation of human embryonic stem cells. *Proceedings of the National Academy of Sciences of the United States of America*, 104, 11298-11303.
- GHARECHAH, J., PAKZAD, M., MIRSHAVALADI, S., SHARIFITABAR, M., BAHARVAND, H. & SALEKDEH, G. H. 2014. The effect of Rho-associated kinase inhibition on the proteome pattern of dissociated human embryonic stem cells. *Molecular BioSystems*, 10, 640-652.
- GRAF, J., IWAMOTO, Y., SASAKI, M., MARTIN, G. R., KLEINMAN, H. K., ROBEY, F. A. & YAMADA, Y. 1987. Identification of an amino acid sequence in laminin mediating cell attachment, chemotaxis, and receptor binding. *Cell*, 48, 989-996.
- GREENOW, K. & CLARKE, A. R. 2012. Controlling the stem cell compartment and regeneration in vivo: The role of pluripotency pathways. *Physiological Reviews*, 92, 75-99.
- GUAN, K., NAYERIA, K., MAIER, L. S., WAGNER, S., DRESSEL, R., LEE, J. H., NOLTE, J., WOLF, F., LI, M., ENGEL, W. & HASENFUSS, G. 2006.

- Pluripotency of spermatogonial stem cells from adult mouse testis. *Nature*, 440, 1199-1203.
- HAGAN, A. K. & ZUCHNER, T. 2011. Lanthanide-based time-resolved luminescence immunoassays. *Analytical and Bioanalytical Chemistry*, 400, 2847-2864.
- HAKALA, H., RAJALA, K., OJALA, M., PANULA, S., AREVA, S., KELLOMAKI, M., SUURONEN, R. & SKOTTMAN, H. 2009. Comparison of Biomaterials and Extracellular Matrices as a Culture Platform for Multiple, Independently Derived Human Embryonic Stem Cell Lines. *Tissue Engineering Part A*, 15, 1775-1785.
- HAMMERICK, K. E., HUANG, Z., SUN, N., LAM, M. T., PRINZ, F. B., WU, J. C., COMMONS, G. W. & LONGAKER, M. T. 2011. Elastic properties of induced pluripotent stem cells. *Tissue Engineering - Part A*, 17, 495-502.
- HANNA, J., CHENG, A. W., SAHA, K., KIM, J., LENGNER, C. J., SOLDNER, F., CASSADY, J. P., MUFFAT, J., CAREY, B. W. & JAENISCH, R. 2010. Human embryonic stem cells with biological and epigenetic characteristics similar to those of mouse ESCs. *Proceedings of the National Academy of Sciences of the United States of America*, 107, 9222-9227.
- HARB, N., ARCHER, T. K. & SATO, N. 2008. The Rho-Rock-Myosin signaling axis determines cell-cell integrity of self-renewing pluripotent stem cells. *PLoS ONE*, 3.
- HARRIS, D. T. & ROGERS, I. 2007. Umbilical cord blood: a unique source of pluripotent stem cells for regenerative medicine. *Current Stem Cell Research & Therapy*, 4, 301-309.
- HAUBNER, R., GRATIAS, R., DIEFENBACH, B., GOODMAN, S. L., JONCZYK, A. & KESSLER, H. 1996. Structural and Functional Aspects of RGD-Containing Cyclic Pentapeptides as Highly Potent and Selective Integrin $\alpha V\beta 3$ Antagonists. *Journal of the American Chemical Society*, 118, 7461-7472.
- HAUTANEN, A., GAILIT, J., MANN, D. M. & RUOSLAHTI, E. 1989. Effects of modifications of the RGD sequence and its context on recognition by the fibronectin receptor. *Journal of Biological Chemistry*, 264, 1437-1442.
- HEINO, J. 2007. The collagen family members as cell adhesion proteins. *Bioessays*, 29, 1001-1010.
- HENG, B. C., LI, J., CHEN, A. K. L., REUVENY, S., COOL, S. M., BIRCH, W. R. & OH, S. K. W. 2012. Translating human embryonic stem cells from 2-dimensional to 3-dimensional cultures in a defined medium on laminin- and vitronectin-coated surfaces. *Stem Cells and Development*, 21, 1701-1715.
- HIGUCHI, A., KAO, S. H., LING, Q. D., CHEN, Y. M., LI, H. F., ALARFAJ, A. A., MUNUSAMY, M. A., MURUGAN, K., CHANG, S. C., LEE, H. C., HSU, S. T., KUMAR, S. S. & UMEZAWA, A. 2015. Long-term xeno-free culture of human pluripotent stem cells on hydrogels with optimal elasticity. *Scientific Reports*, 5.
- HIGUCHI, S., WATANABE, T. M., KAWAUCHI, K., ICHIMURA, T. & FUJITA, H. 2014. Culturing of mouse and human cells on soft substrates promote the

- expression of stem cell markers. *Journal of Bioscience and Bioengineering*, 117, 749-755.
- HIRSCHFELD-WARNEKEN, V. C., ARNOLD, M., CAVALCANTI-ADAM, A., LÓPEZ-GARCÍA, M., KESSLER, H. & SPATZ, J. P. 2008. Cell adhesion and polarisation on molecularly defined spacing gradient surfaces of cyclic RGDfK peptide patches. *European Journal of Cell Biology*, 87, 743-750.
- HISAMATSU-SAKAMOTO, M., SAKAMOTO, N. & ROSENBERG, A. S. 2008. Embryonic stem cells cultured in serum-free medium acquire bovine apolipoprotein B-100 from feeder cell layers and serum replacement medium. *Stem Cells*, 26, 72-78.
- HOLLANDER, J. M. & JOLLY, W. L. 1970. X-ray photoelectron spectroscopy. *Accounts of Chemical Research*, 3, 193-200.
- HONG, V., PRESOLSKI, S. I., MA, C. & FINN, M. G. 2009. Analysis and optimization of copper-catalyzed azide-alkyne cycloaddition for bioconjugation. *Angewandte Chemie - International Edition*, 48, 9879-9883+9766.
- HONG, V., STEINMETZ, N. F., MANCHESTER, M. & FINN, M. G. 2010. Labeling live cells by copper-catalyzed alkyne-azide click chemistry. *Bioconjugate Chemistry*, 21, 1912-1916.
- HORÁK, V. & FLÉCHON, J. E. 1998. Immunocytochemical characterisation of rabbit and mouse embryonic fibroblasts. *Reproduction Nutrition Development*, 38, 683-695.
- HOUGH, S. R., LASLETT, A. L., GRIMMOND, S. B., KOLLE, G. & PERA, M. F. 2009. A continuum of cell states spans pluripotency and lineage commitment in human embryonic stem cells. *PLoS ONE*, 4, e7708.
- HOZUMI, K., AKIZUKI, T., YAMADA, Y., HARA, T., URUSHIBATA, S., KATAGIRI, F., KIKKAWA, Y. & NOMIZU, M. 2010. Cell adhesive peptide screening of the mouse laminin α 1 chain G domain. *Archives of Biochemistry and Biophysics*, 503, 213-222.
- HOZUMI, K., FUJIMORI, C., KATAGIRI, F., KIKKAWA, Y. & NOMIZU, M. 2015. Suppression of cell adhesion through specific integrin crosstalk on mixed peptide-polysaccharide matrices. *Biomaterials*, 37, 73-81.
- HU, P. & LUO, B. H. 2013. Integrin bi-directional signaling across the plasma membrane. *Journal of Cellular Physiology*, 228, 306-312.
- HUANG, B., NING, S., ZHUANG, L., JIANG, C., CUI, Y., FAN, G., QIN, L. & LIU, J. 2015. Ethanol inactivated mouse embryonic fibroblasts maintain the self-renew and proliferation of human embryonic stem cells. *PLoS ONE*, 10.
- HUANG, M. L., SMITH, R. A. A., TRIEGER, G. W. & GODULA, K. 2014. Glycocalyx remodeling with proteoglycan mimetics promotes neural specification in embryonic stem cells. *Journal of the American Chemical Society*, 136, 10565-10568.
- HUGHES, C. S., POSTOVIT, L. M. & LAJOIE, G. A. 2010. Matrigel: a complex protein mixture required for optimal growth of cell culture. *Proteomics*, 10, 1886-1890.

- HUGHES, C. S., RADAN, L., BETTS, D., POSTOVIT, L. M. & LAJOIE, G. A. 2011. Proteomic analysis of extracellular matrices used in stem cell culture. *Proteomics*, 11, 3983-3991.
- HYUN, I., LINDVALL, O., ÄHRLUND-RICHTER, L., CATTANEO, E., CAVAZZANA-CALVO, M., COSSU, G., DE LUCA, M., FOX, I. J., GERSTLE, C., GOLDSTEIN, R. A., HERMERÉN, G., HIGH, K. A., KIM, H. O., LEE, H. P., LEVY-LAHAD, E., LI, L., LO, B., MARSHAK, D. R., MCNAB, A., MUNSIE, M., NAKAUCHI, H., RAO, M., ROOKE, H. M., VALLES, C. S., SRIVASTAVA, A., SUGARMAN, J., TAYLOR, P. L., VEIGA, A., WONG, A. L., ZOLOTH, L. & DALEY, G. Q. 2008. New ISSCR Guidelines Underscore Major Principles for Responsible Translational Stem Cell Research. *Cell Stem Cell*, 3, 607-609.
- IBRAHIMI, O. A., ZHANG, F., HRSTKA, S. C. L., MOHAMMADI, M. & LINHARDT, R. J. 2004. Kinetic Model for FGF, FGFR, and Proteoglycan Signal Transduction Complex Assembly. *Biochemistry*, 43, 4724-4730.
- IRWIN, E. F., GUPTA, R., DASHTI, D. C. & HEALY, K. E. 2011. Engineered polymer-media interfaces for the long-term self-renewal of human embryonic stem cells. *Biomaterials*, 32, 6912-6919.
- ISO 2009. Biological evaluation of medical devices. *Part 5: Tests for in vitro cytotoxicity*. International Standards Organization.
- JANG, M., LEE, S. T., KIM, J. W., YANG, J. H., YOON, J. K., PARK, J. C., RYOO, H. M., VAN DER VLIES, A. J., AHN, J. Y., HUBBELL, J. A., SONG, Y. S., LEE, G. & LIM, J. M. 2013. A feeder-free, defined three-dimensional polyethylene glycol-based extracellular matrix niche for culture of human embryonic stem cells. *Biomaterials*, 34, 3571-3580.
- JESCHKE, B., MEYER, J., JONCZYK, A., KESSLER, H., ADAMIETZ, P., MEENEN, N. M., KANTLEHNER, M., GOEPFERT, C. & NIES, B. 2002. RGD-peptides for tissue engineering of articular cartilage. *Biomaterials*, 23, 3455-3463.
- JIN, S., YAO, H., WEBER, J. L., MELKOUMIAN, Z. K. & YE, K. 2012. A Synthetic, Xeno-Free Peptide Surface for Expansion and Directed Differentiation of Human Induced Pluripotent Stem Cells. *PLoS ONE*, 7.
- JING, D., PARIKH, A., CANTY JR, J. M. & TZANAKAKIS, E. S. 2008. Stem cells for heart cell therapies. *Tissue Engineering - Part B: Reviews*, 14, 393-406.
- JODDAR, B., NISHIOKA, C., TAKAHASHI, E. & ITO, Y. 2015. Chemically fixed autologous feeder cell-derived niche for human induced pluripotent stem cell culture. *Journal of Materials Chemistry B*, 3, 2301-2307.
- JONAS, S. J., ALVA, J. A., RICHARDSON, W., SHERMAN, S. P., GALIC, Z., PYLE, A. D. & DUNN, B. 2013. A spatially and chemically defined platform for the uniform growth of human pluripotent stem cells. *Materials Science and Engineering C*, 33, 234-241.
- JONES-VILLENEUVE, E. M. V., MCBURNEY, M. W., ROGERS, K. A. & KALNINS, V. I. 1982. Retinoic acid induces embryonal carcinoma cells to differentiate into neurons and glial cells. *Journal of Cell Biology*, 94, 253-262.

- JONES, M. B., CHU, C. H., PENDLETON, J. C., BETENBAUGH, M. J., SHILOACH, J., BALJINNYAM, B., RUBIN, J. S. & SHAMBLOTT, M. J. 2010. Proliferation and pluripotency of human embryonic stem cells maintained on type i collagen. *Stem Cells Dev*, 19, 1923-1935.
- JURCHENKO, C., CHANG, Y., NARUI, Y., ZHANG, Y. & SALAITA, K. S. 2014. Integrin-generated forces lead to streptavidin-biotin unbinding in cellular adhesions. *Biophysical Journal*, 106, 1436-1446.
- JURCHENKO, C. & SALAITA, K. S. 2015. Lighting up the force: Investigating mechanisms of mechanotransduction using fluorescent tension probes. *Molecular and Cellular Biology*, 35, 2570-2582.
- KADLER, K. E., HILL, A. & CANTY-LAIRD, E. G. 2008. Collagen fibrillogenesis: fibronectin, integrins, and minor collagens as organizers and nucleators. *Current Opinion in Cell Biology*, 20, 495-501.
- KALASKAR, D. M., DOWNES, J. E., MURRAY, P., EDGAR, D. H. & WILLIAMS, R. L. 2013. Characterization of the interface between adsorbed fibronectin and human embryonic stem cells. *J R Soc Interface*, 10, 20130139.
- KANTLEHNER, M., SCHAFFNER, P., FINSINGER, D., MEYER, J., JONCZYK, A., DIEFENBACH, B., NIES, B., HÖLZEMANN, G., GOODMAN, S. L. & KESSLER, H. 2000. Surface coating with cyclic RGD peptides stimulates osteoblast adhesion and proliferation as well as bone formation. *Chembiochem : a European journal of chemical biology*, 1, 107-114.
- KELLER, G. M. 1995. In vitro differentiation of embryonic stem cells. *Current Opinion in Cell Biology*, 7, 862-869.
- KESKI OJA, J. 1976. Polymerization of a major surface associated glycoprotein, fibronectin, in cultured fibroblasts. *FEBS Letters*, 71, 325-329.
- KEUNG, A. J., ASURI, P., KUMAR, S. & SCHAFFER, D. V. 2012. Soft microenvironments promote the early neurogenic differentiation but not self-renewal of human pluripotent stem cells. *Integrative Biology*, 4, 1049-1058.
- KIM, H. T., LEE, K. I., KIM, D. W. & HWANG, D. Y. 2013. An ECM-based culture system for the generation and maintenance of xeno-free human iPS cells. *Biomaterials*, 34, 1041-1050.
- KIM, S. H., TURNBULL, J. & GUIMOND, S. 2011. Extracellular matrix and cell signalling: The dynamic cooperation of integrin, proteoglycan and growth factor receptor. *Journal of Endocrinology*, 209, 139-151.
- KLEINSMITH, L. J. & PIERCE, G. B., JR. 1964. Multipotentiality of Single Embryonal Carcinoma Cells. *Cancer Res*, 24, 1544-51.
- KLIM, J. R., FOWLER, A. J., COURTNEY, A. H., WRIGHTON, P. J., SHERIDAN, R. T. C., WONG, M. L. & KIESSLING, L. L. 2012. Small-molecule-modified surfaces engage cells through the α v β 3 integrin. *ACS Chemical Biology*, 7, 518-525.
- KLIM, J. R., LI, L., WRIGHTON, P. J., PIEKARCZYK, M. S. & KIESSLING, L. L. 2010. A defined glycosaminoglycan-binding substratum for human pluripotent stem cells. *Nature Methods*, 7, 989-994.
- KOLHAR, P., KOTAMRAJU, V. R., HIKITA, S. T., CLEGG, D. O. & RUOSLAHTI, E. 2010. Synthetic surfaces for human embryonic stem cell culture. *Journal of Biotechnology*, 146, 143-146.

- KOLLE, G., HO, M., ZHOU, Q., CHY, H. S., KRISHNAN, K., CLOONAN, N., BERTONCELLO, I., LASLETT, A. L. & GRIMMOND, S. M. 2009. Identification of human embryonic stem cell surface markers by combined membrane-polysome translation state array analysis and immunotranscriptional profiling. *Stem Cells*, 27, 2446-2456.
- KRAUSHAAR, D. C., YAMAGUCHI, Y. & WANG, L. 2010. Heparan sulfate is required for embryonic stem cells to exit from self-renewal. *Journal of Biological Chemistry*, 285, 5907-5916.
- KRAWETZ, R. J., LI, X. & RANCOURT, D. E. 2009. Human embryonic stem cells: Caught between a ROCK inhibitor and a hard place. *BioEssays*, 31, 336-343.
- LAI, D., WANG, Y., SUN, J., CHEN, Y., LI, T., WU, Y., GUO, L. & WEI, C. 2015. Derivation and characterization of human embryonic stem cells on human amnion epithelial cells. *Scientific Reports*, 5.
- LAM, A. T. L., LI, J., CHEN, A. K. L., REUVENY, S., OH, S. K. W. & BIRCH, W. R. 2014. Cationic surface charge combined with either vitronectin or laminin dictates the evolution of human embryonic stem cells/microcarrier aggregates and cell growth in agitated cultures. *Stem Cells and Development*, 23, 1688-1703.
- LAM, M. T. & LONGAKER, M. T. 2012. Comparison of several attachment methods for human iPS, embryonic and adipose-derived stem cells for tissue engineering. *Journal of Tissue Engineering and Regenerative Medicine*, 6, s80-s86.
- LAMBSHEAD, J., MEAGHER, L., O'BRIEN, C. & LASLETT, A. L. 2013. Defining synthetic surfaces for human pluripotent stem cell culture. *Cell Regeneration*, 2.
- LAPERLE, A., HSIAO, C., LAMPE, M., MORTIER, J., SAHA, K., PALECEK, S. M. & MASTERS, K. S. 2015a. α -5 Laminin Synthesized by Human Pluripotent Stem Cells Promotes Self-Renewal. *Stem Cell Reports*.
- LAPERLE, A., MASTERS, K. S. & PALECEK, S. P. 2015b. Influence of substrate composition on human embryonic stem cell differentiation and extracellular matrix production in embryoid bodies. *Biotechnology Progress*, 31, 212-219.
- LAURENT, L. C., ULITSKY, I., SLAVIN, I., TRAN, H., SCHORK, A., MOREY, R., LYNCH, C., HARNESS, J. V., LEE, S., BARRERO, M. J., KU, S., MARTYNOVA, M., SEMECHKIN, R., GALAT, V., GOTTESFELD, J., BELMONTE, J. C. I., MURRY, C., KEIRSTEAD, H. S., PARK, H. S., SCHMIDT, U., LASLETT, A. L., MULLER, F. J., NIEVERGELT, C. M., SHAMIR, R. & LORING, J. F. 2011. Dynamic changes in the copy number of pluripotency and cell proliferation genes in human ESCs and iPSCs during reprogramming and time in culture. *Cell Stem Cell*, 8, 106-118.
- LEBKOWSKI, J. 2011. GRNOPC1: the world's first embryonic stem cell-derived therapy. Interview with Jane Lebkowski. *Regenerative medicine*, 6, 11-13.
- LEE, S. T., JANG, M., LEE, G. & MOOK LIM, J. 2013. Development of three dimensional culture and expression of integrin heterodimers in human embryonic stem cells. *Organogenesis*, 9, 143-148.

- LEVENSTEIN, M. E., LUDWIG, T. E., XU, R. H., LLANAS, R. A., VANDENHEUVEL-KRAMER, K., MANNING, D. & THOMSON, J. A. 2006. Basic fibroblast growth factor support of human embryonic stem cell self-renewal. *Stem Cells*, 24, 568-574.
- LI, L., BENNETT, S. A. L. & WANG, L. 2012. Role of E-cadherin and other cell adhesion molecules in survival and differentiation of human pluripotent stem cells. *Cell Adhesion and Migration*, 6, 59-70.
- LI, Y., POWELL, S., BRUNETTE, E., LEBKOWSKI, J. & MANDALAM, R. 2005. Expansion of human embryonic stem cells in defined serum-free medium devoid of animal-derived products. *Biotechnology and Bioengineering*, 91, 688-698.
- LI, Y. J., CHUNG, E. H., RODRIGUEZ, R. T., FIRPO, M. T. & HEALY, K. E. 2006. Hydrogels as artificial matrices for human embryonic stem cell self-renewal. *Journal of Biomedical Materials Research - Part A*, 79, 1-5.
- LIB, J., BARDY, J., YAP, L. Y. W., CHEN, A., NURCOMBE, V., COOL, S. M., OH, S. K. W. & BIRCH, W. R. 2010. Impact of vitronectin concentration and surface properties on the stable propagation of human embryonic stem cells. *Biointerphases*, 5, 132-142.
- LISTER, R., PELIZZOLA, M., KIDA, Y. S., HAWKINS, R. D., NERY, J. R., HON, G., ANTOSIEWICZ-BOURGET, J., OGMALLEY, R., CASTANON, R., KLUGMAN, S., DOWNES, M., YU, R., STEWART, R., REN, B., THOMSON, J. A., EVANS, R. M. & ECKER, J. R. 2011. Hotspots of aberrant epigenomic reprogramming in human induced pluripotent stem cells. *Nature*, 471, 68-73.
- LIU, S., SMITH, S. E., JULIAN, J., ROHDE, L. H., KARIN, N. J. & CARSON, D. D. 1996. cDNA cloning and expression of HIP, a novel cell surface heparan sulfate/heparin-binding protein of human uterine epithelial cells and cell lines. *Journal of Biological Chemistry*, 271, 11817-11823.
- LIU, Y., CHARLES, L. F., ZAREMBINSKI, T. I., JOHNSON, K. I., ATZET, S. K., WESSELSCHMIDT, R. L., WIGHT, M. E. & KUHN, L. T. 2012. Modified Hyaluronan Hydrogels Support the Maintenance of Mouse Embryonic Stem Cells and Human Induced Pluripotent Stem Cells. *Macromolecular Bioscience*, 12, 1034-1042.
- LOVE, J. C., ESTROFF, L. A., KRIEBEL, J. K., NUZZO, R. G. & WHITESIDES, G. M. 2005. Self-assembled monolayers of thiolates on metals as a form of nanotechnology. *Chemical Reviews*, 105, 1103-1169.
- LU, H. F., NARAYANAN, K., LIM, S. X., GAO, S., LEONG, M. F. & WAN, A. C. A. 2012. A 3D microfibrillar scaffold for long-term human pluripotent stem cell self-renewal under chemically defined conditions. *Biomaterials*, 33, 2419-2430.
- LU, J., HOU, R., BOOTH, C. J., YANG, S. H. & SNYDER, M. 2006. Defined culture conditions of human embryonic stem cells. *Proc Natl Acad Sci U S A*, 103, 5688-93.
- LUDWIG, T. E., BERGENDAHL, V., LEVENSTEIN, M. E., YU, J., PROBASCO, M. D. & THOMSON, J. A. 2006a. Feeder-independent culture of human embryonic stem cells. *Nat Methods*, 3, 637-46.

- LUDWIG, T. E., LEVENSTEIN, M. E., JONES, J. M., BERGGREN, W. T., MITCHEN, E. R., FRANE, J. L., CRANDALL, L. J., DAIGH, C. A., CONARD, K. R., PIEKARCZYK, M. S., LLANAS, R. A. & THOMSON, J. A. 2006b. Derivation of human embryonic stem cells in defined conditions. *Nat Biotechnol*, 24, 185-7.
- MAHLSTEDT, M. M., ANDERSON, D., SHARP, J. S., MCGILVRAY, R., BARBADILLO MUÑOZ, M. D., BUTTERY, L. D., ALEXANDER, M. R., ROSE, F. R. A. J. & DENNING, C. 2010. Maintenance of pluripotency in human embryonic stem cells cultured on a synthetic substrate in conditioned medium. *Biotechnology and Bioengineering*, 105, 130-140.
- MALKOCH, M., THIBAUT, R. J., DROCKENMULLER, E., MESSERSCHMIDT, M., VOIT, B., RUSSELL, T. P. & HAWKER, C. J. 2005. Orthogonal approaches to the simultaneous and cascade functionalization of macromolecules using click chemistry. *Journal of the American Chemical Society*, 127, 14942-14949.
- MANTON, K. J., RICHARDS, S., VAN LONKHUYZEN, D., CORMACK, L., LEAVESLEY, D. & UPTON, Z. 2010. A chimeric vitronectin: IGF-I protein supports feeder-cell-free and serum-free culture of human embryonic stem cells. *Stem Cells Dev*, 19, 1297-1305.
- MARTIN, G. R. & EVANS, M. J. 1975. Differentiation of clonal lines of teratocarcinoma cells: formation of embryoid bodies in vitro. *Proc Natl Acad Sci U S A*, 72, 1441-5.
- MARTIN, M. J., MUOTRI, A., GAGE, F. & VARKI, A. 2005. Human embryonic stem cells express an immunogenic nonhuman sialic acid. *Nature Medicine*, 11, 228-232.
- MARTIN, Y., WILLIAMS, C. C. & WICKRAMASINGHE, H. K. 1987. Atomic force microscope-force mapping and profiling on a sub 100-Å scale. *Journal of Applied Physics*, 61, 4723-4729.
- MEI, Y., SAHA, K., BOGATYREV, S. R., YANG, J., HOOK, A. L., KALCIOGLU, Z. I., CHO, S. W., MITALIPOVA, M., PYZOGHA, N., ROJAS, F., VAN VLIET, K. J., DAVIES, M. C., ALEXANDER, M. R., LANGER, R., JAENISCH, R. & ANDERSON, D. G. 2010. Combinatorial development of biomaterials for clonal growth of human pluripotent stem cells. *Nature Materials*, 9, 768-778.
- MELDAL, M. 2008. Polymer "clicking" by CuAAC reactions. *Macromolecular Rapid Communications*, 29, 1016-1051.
- MELKOUMIAN, Z. & BRANDENBERGER, R. 2011. Feeder-free, xeno-free culture of hESCs. *Genetic Engineering and Biotechnology News*, 31.
- MELKOUMIAN, Z., WEBER, J. L., WEBER, D. M., FADEEV, A. G., ZHOU, Y., DOLLEY-SONNEVILLE, P., YANG, J., QIU, L., PRIEST, C. A., SHOGBON, C., MARTIN, A. W., NELSON, J., WEST, P., BELTZER, J. P., PAL, S. & BRANDENBERGER, R. 2010. Synthetic peptide-acrylate surfaces for long-term self-renewal and cardiomyocyte differentiation of human embryonic stem cells. *Nature Biotechnology*, 28, 606-610.
- MENG, G., LIU, S. & RANCOURT, D. E. 2012. Synergistic effect of medium, matrix, and exogenous factors on the adhesion and growth of human

- pluripotent stem cells under defined, xeno-free conditions. *Stem Cells Dev*, 21, 2036-2048.
- MENG, Y., ESHGHI, S., LI, Y. J., SCHMIDT, R., SCHAFFER, D. V. & HEALY, K. E. 2010. Characterization of integrin engagement during defined human embryonic stem cell culture. *FASEB Journal*, 24, 1056-1065.
- MITSUI, K., TOKUZAWA, Y., ITOH, H., SEGAWA, K., MURAKAMI, M., TAKAHASHI, K., MARUYAMA, M., MAEDA, M. & YAMANAKA, S. 2003. The homeoprotein nanog is required for maintenance of pluripotency in mouse epiblast and ES cells. *Cell*, 113, 631-642.
- MIYAZAKI, T., FUTAKI, S., HASEGAWA, K., KAWASAKI, M., SANZEN, N., HAYASHI, M., KAWASE, E., SEKIGUCHI, K., NAKATSUJI, N. & SUEMORI, H. 2008. Recombinant human laminin isoforms can support the undifferentiated growth of human embryonic stem cells. *Biochemical and Biophysical Research Communications*, 375, 27-32.
- MIYAZAKI, T., FUTAKI, S., SUEMORI, H., TANIGUCHI, Y., YAMADA, M., KAWASAKI, M., HAYASHI, M., KUMAGAI, H., NAKATSUJI, N., SEKIGUCHI, K. & KAWASE, E. 2012. Laminin E8 fragments support efficient adhesion and expansion of dissociated human pluripotent stem cells. *Nature Communications*, 3.
- MONDAL, G., BARUI, S. & CHAUDHURI, A. 2013. The relationship between the cyclic-RGDfK ligand and $\alpha v \beta 3$ integrin receptor. *Biomaterials*, 34, 6249-6260.
- MORIMATSU, M., MEKHDJIAN, A. H., CHANG, A. C., TAN, S. J. & DUNN, A. R. 2015. Visualizing the Interior Architecture of Focal Adhesions with High-Resolution Traction Maps. *Nano Letters*, 15, 2220-2228.
- MÜLLER, F. J., LAURENT, L. C., KOSTKA, D., ULITSKY, I., WILLIAMS, R., LU, C., PARK, I. H., RAO, M. S., SHAMIR, R., SCHWARTZ, P. H., SCHMIDT, N. O. & LORING, J. F. 2008. Regulatory networks define phenotypic classes of human stem cell lines. *Nature*, 455, 401-405.
- MÜLLER, F. J., SCHULDT, B. M., WILLIAMS, R., MASON, D., ALTUN, G., PAPAPETROU, E. P., DANNER, S., GOLDMANN, J. E., HERBST, A., SCHMIDT, N. O., ALDENHOFF, J. B., LAURENT, L. C. & LORING, J. F. 2011. A bioinformatic assay for pluripotency in human cells. *Nature Methods*, 8, 315-317.
- MURPHY, W. L., MCDEVITT, T. C. & ENGLER, A. J. 2014. Materials as stem cell regulators. *Nature Materials*, 13, 547-557.
- MUSAH, S., MORIN, S. A., WRIGHTON, P. J., ZWICK, D. B., JIN, S. & KIESSLING, L. L. 2012. Glycosaminoglycan-binding hydrogels enable mechanical control of human pluripotent stem cell self-renewal. *ACS Nano*, 6, 10168-10177.
- MUSAH, S., WRIGHTON, P. J., ZALTSMAN, Y., ZHONG, X., ZORN, S., PARLATO, M. B., HSIAO, C., PALECEK, S. P., CHANG, Q., MURPHY, W. L. & KIESSLING, L. L. 2014. Substratum-induced differentiation of human pluripotent stem cells reveals the coactivator YAP is a potent regulator of neuronal specification. *Proceedings of the National Academy of Sciences of the United States of America*, 111, 13805-13810.

- NAGAOKA, M., ISE, H. & AKAIKE, T. 2002. Immobilized E-cadherin model can enhance cell attachment and differentiation of primary hepatocytes but not proliferation. *Biotechnology Letters*, 24, 1857-1862.
- NAGAOKA, M., KOSHIMIZU, U., YUASA, S., HATTORI, F., CHEN, H., TANAKA, T., OKABE, M., FUKUDA, K. & AKAIKE, T. 2006. E-cadherin-coated plates maintain pluripotent ES cells without colony formation. *PLoS ONE*, 1.
- NAGAOKA, M., SI-TAYEB, K., AKAIKE, T. & DUNCAN, S. A. 2010. Culture of human pluripotent stem cells using completely defined conditions on a recombinant E-cadherin substratum. *BMC Developmental Biology*, 10.
- NANDIVADA, H., VILLA-DIAZ, L. G., O'SHEA, K. S., SMITH, G. D., KREBSBACH, P. H. & LAHANN, J. 2011. Fabrication of synthetic polymer coatings and their use in feeder-free culture of human embryonic stem cells. *Nature Protocols*, 6, 1037-1043.
- NAUMKIN, A. V., KRAUT-VASS, A., GAARENSTROOM, S. W. & POWELL, C. J. 2016. *NIST X-ray Photoelectron Spectroscopy Database* [Online]. Available: <http://srdata.nist.gov/xps/Default.aspx> [Accessed 2 Feb 2016].
- NEWMAN, A. M. & COOPER, J. B. 2010. Lab-specific gene expression signatures in pluripotent stem cells. *Cell Stem Cell*, 7, 258-262.
- NGUYEN, H. T., GEENS, M., MERTZANIDOU, A., JACOBS, K., HEIRMAN, C., BRECKPOT, K. & SPITS, C. 2014. Gain of 20q11.21 in human embryonic stem cells improves cell survival by increased expression of Bcl-xL. *Molecular Human Reproduction*, 20, 168-177.
- NICHOLS, J. & SMITH, A. 2009. Naive and Primed Pluripotent States. *Cell Stem Cell*, 4, 487-492.
- NICHOLS, J., ZEVIK, B., ANASTASSIADIS, K., NIWA, H., KLEWE-NEBENIUS, D., CHAMBERS, I., SCHÖLER, H. & SMITH, A. 1998. Formation of pluripotent stem cells in the mammalian embryo depends on the POU transcription factor Oct4. *Cell*, 95, 379-391.
- NIE, Y., WALSH, P., CLARKE, D. L., ROWLEY, J. A. & FELLNER, T. 2014. Scalable passaging of adherent human pluripotent stem cells. *PLoS ONE*, 9.
- NOMIZU, M., KURATOMI, Y., SONG, S. Y., PONCE, M. L., HOFFMAN, M. P., POWELL, S. K., MIYOSHI, K., OTAKA, A., KLEINMAN, H. K. & YAMADA, Y. 1997. Identification of cell binding sequences in mouse laminin chain by systematic peptide screening. *Journal of Biological Chemistry*, 272, 32198-32205.
- O'BRIEN, C. & LASLETT, A. L. 2012. Suspended in culture - Human pluripotent cells for scalable technologies. *Stem Cell Research*, 9, 167-170.
- OHI, Y., QIN, H., HONG, C., BLOUIN, L., POLO, J. M., GUO, T., QI, Z., DOWNEY, S. L., MANOS, P. D., ROSSI, D. J., YU, J., HEBROK, M., HOCHEDLINGER, K., COSTELLO, J. F., SONG, J. S. & RAMALHO-SANTOS, M. 2011. Incomplete DNA methylation underlies a transcriptional memory of somatic cells in human iPS cells. *Nature Cell Biology*.
- OLDBERG, A., FRANZEN, A., HEINEGARD, D., PIERSCHBACHER, M. & RUOSLAHTI, E. 1988. Identification of a bone sialoprotein receptor in osteosarcoma cells. *Journal of Biological Chemistry*, 263, 19433-19436.

- ORAL, I., GUZEL, H. & AHMETLI, G. 2011. Measuring the Young's modulus of polystyrene-based composites by tensile test and pulse-echo method. *Polymer Bulletin*, 67, 1893-1906.
- OSAFUNE, K., CARON, L., BOROWIAK, M., MARTINEZ, R. J., FITZ-GERALD, C. S., SATO, Y., COWAN, C. A., CHIEN, K. R. & MELTON, D. A. 2008. Marked differences in differentiation propensity among human embryonic stem cell lines. *Nature Biotechnology*, 26, 313-315.
- PARK, H. J., YANG, K., KIM, M. J., JANG, J., LEE, M., KIM, D. W., LEE, H. & CHO, S. W. 2015. Bio-inspired oligovitronection-grafted surface for enhanced self-renewal and long-term maintenance of human pluripotent stem cells under feeder-free conditions. *Biomaterials*, 50, 127-139.
- PETERSON, S. E. & LORING, J. F. 2014. Genomic instability in pluripotent stem cells: Implications for clinical applications. *Journal of Biological Chemistry*, 289, 4578-4584.
- PIERSCHBACHER, M. D. & RUOSLAHTI, E. 1984. Cell attachment activity of fibronectin can be duplicated by small synthetic fragments of the molecule. *Nature*, 309, 30-33.
- PIERSCHBACHER, M. D. & RUOSLAHTI, E. 1987. Influence of stereochemistry of the sequence Arg-Gly-Asp-Xaa on binding specificity in cell adhesion. *Journal of Biological Chemistry*, 262, 17294-17298.
- POOK, M., TEINO, I., KALLAS, A., MAIMETS, T., INGERPUU, S. & JAKS, V. 2015. Changes in laminin expression pattern during early differentiation of human embryonic stem cells. *PLoS ONE*, 10.
- PRATHALINGAM, N., FERGUSON, L., YOUNG, L., LIETZ, G., OLDERSHAW, R., HEALY, L., CRAIG, A., LISTER, H., BINAYKIA, R., SHETH, R., MURDOCH, A. & HERBERT, M. 2012. Production and validation of a good manufacturing practice grade human fibroblast line for supporting human embryonic stem cell derivation and culture. *Stem Cell Research and Therapy*, 3.
- PRZYBORSKI S. A., CHRISTIE, M. W., HAYMAN, R., STEWART, R. & HORROCKS, G. M. 2004. Human embryonal carcinoma stem cells: Models of embryonic development in humans. *Stem Cells and Development*, 13, 400-408.
- PRICE, P. J., GOLDSBOROUGH, M. D. & TILKINS, M. L. 1998. Embryonic stem cell serum replacement. Google Patents.
- PROWSE, A. B. J., DORAN, M. R., COOPER-WHITE, J. J., CHONG, F., MUNRO, T. P., FITZPATRICK, J., CHUNG, T. L., HAYLOCK, D. N., GRAY, P. P. & WOLVETANG, E. J. 2010. Long term culture of human embryonic stem cells on recombinant vitronectin in ascorbate free media. *Biomaterials*, 31, 8281-8288.
- RAMOS-MEJIA, V., BUENO, C., ROLDAN, M., SANCHEZ, L., LIGERO, G., MENENDEZ, P. & MARTIN, M. 2012. The adaptation of human embryonic stem cells to different feeder-free culture conditions is accompanied by a mitochondrial response. *Stem Cells Dev*, 21, 1145-1155.
- RENAUD-YOUNG, M. & GALLIN, W. J. 2002. In the first extracellular domain of E-cadherin, heterophilic interactions, but not the conserved His-Ala-Val

- motif, are required for adhesion. *Journal of Biological Chemistry*, 277, 39609-39616.
- RODIN, S., ANTONSSON, L., NIAUDET, C., SIMONSON, O. E., SALMELA, E., HANSSON, E. M., DOMOGATSKAYA, A., XIAO, Z., DAMDIMOPOULOU, P., SHEIKHI, M., INZUNZA, J., NILSSON, A. S., BAKER, D., KUIPER, R., SUN, Y., BLENNOW, E., NORDENSKJÖLD, M., GRINNEMO, K. H., KERE, J., BETSHOLTZ, C., HOVATTA, O. & TRYGGVASON, K. 2014. Clonal culturing of human embryonic stem cells on laminin-521/E-cadherin matrix in defined and xeno-free environment. *Nature Communications*, 5.
- RODIN, S., DOMOGATSKAYA, A., STRÖM, S., HANSSON, E. M., CHIEN, K. R., INZUNZA, J., HOVATTA, O. & TRYGGVASON, K. 2010. Long-term self-renewal of human pluripotent stem cells on human recombinant laminin-511. *Nature Biotechnology*, 28, 611-615.
- ROSS, A. M., NANDIVADA, H., RYAN, A. L. & LAHANN, J. 2012. Synthetic substrates for long-term stem cell culture. *Polymer (United Kingdom)*, 53, 2533-2539.
- ROSTAMI, M. R., WU, J. & TZANAKAKIS, E. S. 2015. Inverse problem analysis of pluripotent stem cell aggregation dynamics in stirred-suspension cultures. *Journal of Biotechnology*, 208, 70-79.
- ROUHANI, F., KUMASAKA, N., DE BRITO, M. C., BRADLEY, A., VALLIER, L. & GAFFNEY, D. 2014. Genetic Background Drives Transcriptional Variation in Human Induced Pluripotent Stem Cells. *PLoS Genetics*, 10.
- RUOSLAHTI, E. 1996. RGD and other recognition sequences for integrins. *Annual Review of Cell and Developmental Biology*.
- SAHA, K., MEI, Y., REISTERER, C. M., PYZOSHA, N. K., YANG, J., MUFFAT, J., DAVIES, M. C., ALEXANDER, M. R., LANGER, R., ANDERSON, D. G. & JAENISCH, R. 2011. Surface-engineered substrates for improved human pluripotent stem cell culture under fully defined conditions. *Proceedings of the National Academy of Sciences*, 108, 18714-18719.
- SCHULZ, T. C., YOUNG, H. Y., AGULNICK, A. D., BABIN, M. J., BAETGE, E. E., BANG, A. G., BHOUMIK, A., CEPAS, I., CESARIO, R. M., HAAKMEESTER, C., KADOYA, K., KELLY, J. R., KERR, J., MARTINSON, L. A., MCLEAN, A. B., MOORMAN, M. A., PAYNE, J. K., RICHARDSON, M., ROSS, K. G., SHERRE, E. S., SONG, X., WILSON, A. Z., BRANDON, E. P., GREEN, C. E., KROON, E. J., KELLY, O. G., D'AMOUR, K. A. & ROBINS, A. J. 2012. A scalable system for production of functional pancreatic progenitors from human embryonic stem cells. *PLoS ONE*, 7.
- SCHVARTZ, I., SEGER, D. & SHALTIEL, S. 1999. Vitronectin. *International Journal of Biochemistry and Cell Biology*, 31, 539-544.
- SCHWARTZ, S. D., HUBSCHMAN, J. P., HEILWELL, G., FRANCO-CARDENAS, V., PAN, C. K., OSTRICK, R. M., MICKUNAS, E., GAY, R., KLIMANSKAYA, I. & LANZA, R. 2012. Embryonic stem cell trials for macular degeneration: A preliminary report. *The Lancet*, 379, 713-720.
- SELEKMAN, J. A., LIAN, X. & PALECEK, S. P. 2015. Generation of epithelial cell populations from human pluripotent stem cells using a small-molecule

- inhibitor of Src family kinases. *Methods in Molecular Biology*. Humana Press Inc.
- SERRA, M., BRITO, C., CORREIA, C. & ALVES, P. M. 2012. Process engineering of human pluripotent stem cells for clinical application. *Trends in Biotechnology*, 30, 350-359.
- SHEN, B., DELANEY, M. K. & DU, X. 2012. Inside-out, outside-in, and inside-outside-in: G protein signaling in integrin-mediated cell adhesion, spreading, and retraction. *Current Opinion in Cell Biology*, 24, 600-606.
- SINGH, P., CARRAHER, C. & SCHWARZBAUER, J. E. 2010. Assembly of fibronectin extracellular matrix. *Annual Review of Cell and Developmental Biology*, 26, 397-419.
- SOLTER, D. & KNOWLES, B. B. 1978. Monoclonal antibody defining a stage-specific mouse embryonic antigen (SSEA-1). *Proceedings of the National Academy of Sciences of the United States of America*, 75, 5565-5569.
- SPENCER, H., KERAMARI, M. & WARD, C. M. 2011. Using cadherin to assess spontaneous differentiation of embryonic stem cells. *Methods in Molecular Biology*, 690, 81-94.
- STEPHENSON, E., JACQUET, L., MIERE, C., WOOD, V., KADEVA, N., CORNWELL, G., CODOGNOTTO, S., DAJANI, Y., BRAUDE, P. & ILIC, D. 2012. Derivation and propagation of human embryonic stem cell lines from frozen embryos in an animal product-free environment. *Nature Protocols*, 7, 1366-1381.
- SUN, Y., VILLA-DIAZ, L. G., LAM, R. H. W., CHEN, W., KREBSBACH, P. H. & FU, J. 2012. Mechanics regulates fate decisions of human embryonic stem cells. *PLoS ONE*, 7.
- SUZUKI, S., OLDBERG, A., HAYMAN, E. G., PIERSCHBACHER, M. D. & RUOSLAHTI, E. 1985. Complete amino acid sequence of human vitronectin deduced from cDNA. Similarity of cell attachment sites in vitronectin and fibronectin. *EMBO Journal*, 4, 2519-2524.
- SVENSSON, O. & ARNEBRANT, T. 2012. Antibody-antigen interaction on polystyrene: An in situ ellipsometric study. *Journal of Colloid and Interface Science*, 368, 533-539.
- TAKAHASHI, K., TANABE, K., OHNUKI, M., NARITA, M., ICHISAKA, T., TOMODA, K. & YAMANAKA, S. 2007. Induction of pluripotent stem cells from adult human fibroblasts by defined factors. *Cell*, 131, 861-72.
- TAMADA, Y. & IKADA, Y. 1993. Effect of Preadsorbed Proteins on Cell Adhesion to Polymer Surfaces. *Journal of Colloid and Interface Science*, 155, 334-339.
- TANNENBAUM, S. E., TURETSKY, T., SINGER, O., AIZENMAN, E., KIRSHBERG, S., ILOUZ, N., GIL, Y., BERMAN-ZAKEN, Y., PERLMAN, T. S., GEVA, N., LEVY, O., ARBELL, D., SIMON, A., BEN-MEIR, A., SHUFARO, Y., LAUFER, N. & REUBINOFF, B. E. 2012. Derivation of xeno-free and gmp-grade human embryonic stem cells - platforms for future clinical applications. *PLoS ONE*, 7.
- TANUMA, S., POWELL, C. J. & PENN, D. R. 1993. Calculations of electron inelastic mean free paths (IMFPs) IV. Evaluation of calculated IMFPs and

- of the predictive IMFP formula TPP-2 for electron energies between 50 and 2000 eV. *Surface and Interface Analysis*, 20, 77-89.
- THEUNISSEN, T., POWELL, B., WANG, H., MITALIPOVA, M., FADDAH, D., REDDY, J., FAN, Z., MAETZEL, D., GANZ, K., SHI, L., LUNGJANGWA, T., IMSOONTHORNRUKSA, S., STELZER, Y., RANGARAJAN, S., D'ALESSIO, A., ZHANG, J., GAO, Q., DAWLATY, M., YOUNG, R., GRAY, N. & JAENISCH, R. 2014. Systematic Identification of Culture Conditions for Induction and Maintenance of Naive Human Pluripotency (DOI:10.1016/j.stem.2014.07.002). *Cell Stem Cell*.
- THOMSON, J. A., ITSKOVITZ-ELDOR, J., SHAPIRO, S. S., WAKNITZ, M. A., SWIERGIEL, J. J., MARSHALL, V. S. & JONES, J. M. 1998. Embryonic stem cell lines derived from human blastocysts. *Science*, 282, 1145-7.
- TIELSCH, B. J. & FULGHUM, J. E. 1994. Application of angle-resolved XPS algorithms to overlayers and concentration gradients. *Surface and Interface Analysis*, 21, 621-630.
- TOMPKINS, J. D., HALL, C., CHEN, V. C. Y., LI, A. X., WU, X., HSU, D., COUTURE, L. A. & RIGGS, A. D. 2012. Epigenetic stability, adaptability, and reversibility in human embryonic stem cells. *Proceedings of the National Academy of Sciences of the United States of America*, 109, 12544-12549.
- TRAPPMANN, B. & CHEN, C. S. 2013. How cells sense extracellular matrix stiffness: A material's perspective. *Current Opinion in Biotechnology*, 24, 948-953.
- TSUTSUI, H., VALAMEHR, B., HINDOYAN, A., QIAO, R., DING, X., GUO, S., WITTE, O. N., LIU, X., HO, C.-M. & WU, H. 2011. An optimized small molecule inhibitor cocktail supports long-term maintenance of human embryonic stem cells. *Nat Commun*, 2, 167.
- VILLA-DIAZ, L. G., BROWN, S. E., LIU, Y., ROSS, A. M., LAHANN, J., PARENT, J. M. & KREBSBACH, P. H. 2012. Derivation of mesenchymal stem cells from human induced pluripotent stem cells cultured on synthetic substrates. *Stem Cells*, 30, 1174-1181.
- VILLA-DIAZ, L. G., NANDIVADA, H., DING, J., NOGUEIRA-DE-SOUZA, N. C., KREBSBACH, P. H., O'SHEA, K. S., LAHANN, J. & SMITH, G. D. 2010. Synthetic polymer coatings for long-term growth of human embryonic stem cells. *Nature Biotechnology*, 28, 581-583.
- VINCKIER, A. & SEMENZA, G. 1998. Measuring elasticity of biological materials by atomic force microscopy. *FEBS Letters*, 430, 12-16.
- VOGEL, B. E., LEE, S. J., HILDEBRAND, A., CRAIG, W., PIERSCHBACHER, M. D., WONG-STAAAL, F. & RUOSLAHTI, E. 1993. A novel integrin specificity exemplified by binding of the $\alpha(v)\beta 5$ integrin to the basic domain of the HIV Tat protein and vitronectin. *Journal of Cell Biology*, 121, 461-468.
- VUORISTO, S., TOIVONEN, S., WELTNER, J., MIKKOLA, M., USTINOV, J., TROKOVIC, R., PALGI, J., LUND, R., TUURI, T. & OTONKOSKI, T. 2013. A Novel Feeder-Free Culture System for Human Pluripotent Stem Cell Culture and Induced Pluripotent Stem Cell Derivation. *PLoS ONE*, 8.

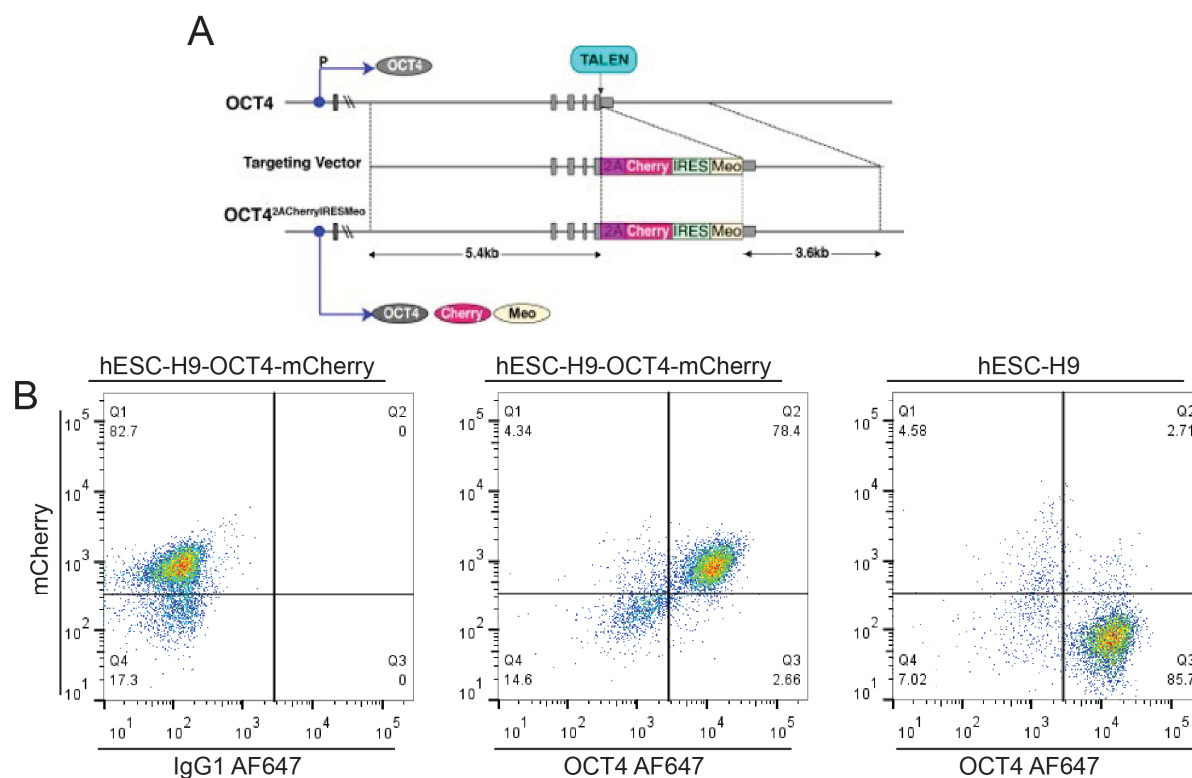
- WAGNER, K. & WELCH, D. 2010. Feeder-free adaptation, culture and passaging of human IPS cells using complete Knockout Serum Replacement feeder-free medium. *Journal of visualized experiments : JoVE*.
- WANG, C., YAN, Q., LIU, H. B., ZHOU, X. H. & XIAO, S. J. 2011. Different EDC/NHS activation mechanisms between PAA and PMAA brushes and the following amidation reactions. *Langmuir*, 27, 12058-12068.
- WANG, J., HAO, J., BAI, D., GU, Q., HAN, W., WANG, L., TAN, Y., LI, X., XUE, K., HAN, P., LIU, Z., JIA, Y., WU, J., LIU, L., WANG, L., LI, W., LIU, Z. & ZHOU, Q. 2015. Generation of clinical-grade human induced pluripotent stem cells in Xeno-free conditions. *Stem Cell Research and Therapy*, 6.
- WANG, Q., MOU, X., CAO, H., MENG, Q., MA, Y., HAN, P., JIANG, J. & ZHANG, H. 2012. A novel xeno-free and feeder-cell-free system for human pluripotent stem cell culture. *Protein and Cell*, 3, 51-59.
- WANT, A. J., NIENOW, A. W., HEWITT, C. J. & COOPMAN, K. 2012. Large-scale expansion and exploitation of pluripotent stem cells for regenerative medicine purposes: Beyond the T flask. *Regenerative Medicine*, 7, 71-84.
- WONG, J., CHILKOTI, A. & MOY, V. T. 1999. Direct force measurements of the streptavidin-biotin interaction. *Biomolecular Engineering*, 16, 45-55.
- WRIGHTON, P. J., KLIM, J. R., HERNANDEZ, B. A., KOONCE, C. H., KAMP, T. J. & KIESSLING, L. L. 2014. Signals from the surface modulate differentiation of human pluripotent stem cells through glycosaminoglycans and integrins. *Proceedings of the National Academy of Sciences of the United States of America*, 111, 18126-18131.
- WU, J., OKAMURA, D., LI, M., SUZUKI, K., LUO, C., MA, L., HE, Y., LI, Z., BENNER, C., TAMURA, I., KRAUSE, M. N., NERY, J. R., DU, T., ZHANG, Z., HISHIDA, T., TAKAHASHI, Y., AIZAWA, E., KIM, N. Y., LAJARA, J., GUILLEN, P., CAMPISTOL, J. M., ESTEBAN, C. R., ROSS, P. J., SAGHATELIAN, A., REN, B., ECKER, J. R. & BELMONTE, J. C. I. 2015. An alternative pluripotent state confers interspecies chimaeric competency. *Nature*, 521, 316-321.
- XIONG, J. P., STEHLE, T., ZHANG, R., JOACHIMIAK, A., FRECH, M., GOODMAN, S. L. & ARNAOUT, M. A. 2002. Crystal structure of the extracellular segment of integrin $\alpha V\beta 3$ in complex with an Arg-Gly-Asp ligand. *Science*, 296, 151-155.
- XU, C., INOKUMA, M. S., DENHAM, J., GOLDS, K., KUNDU, P., GOLD, J. D. & CARPENTER, M. K. 2001. Feeder-free growth of undifferentiated human embryonic stem cells. *Nat Biotechnol*, 19, 971-4.
- XU, R. H., PECK, R. M., LI, D. S., FENG, X., LUDWIG, T. & THOMSON, J. A. 2005. Basic FGF and suppression of BMP signaling sustain undifferentiated proliferation of human ES cells. *Nature Methods*, 2, 185-190.
- XU, Y., ZHU, X., HAHM, H. S., WEI, W., HAO, E., HAYEK, A. & DING, S. 2010. Revealing a core signaling regulatory mechanism for pluripotent stem cell survival and self-renewal by small molecules. *Proceedings of the National Academy of Sciences of the United States of America*, 107, 8129-8134.
- YAP, L. Y. W., LI, J., PHANG, I. Y., ONG, L. T., OW, J. Z. E., GOH, J. C. H., NURCOMBE, V., HOBLEY, J., CHOO, A. B. H., OH, S. K. W., COOL, S. M.

- & BIRCH, W. R. 2011. Defining a threshold surface density of vitronectin for the stable expansion of human embryonic stem cells. *Tissue Engineering - Part C: Methods*, 17, 193-207.
- YUE, X. S., FUJISHIRO, M., NISHIOKA, C., ARAI, T., TAKAHASHI, E., GONG, J. S., AKAIKE, T. & ITO, Y. 2012. Feeder cells support the culture of induced pluripotent stem cells even after chemical fixation. *PLoS ONE*, 7.
- ZABA, C., RITZ, S., TAN, C. W. D., ZAYNI, S., MÜLLER, M., REUNING, U. & SINNER, E. K. 2015. Functional Cell Adhesion Receptors (Integrins) in Polymeric Architectures. *ChemBioChem*, 16, 1740-1743.
- ZHANG, L., CAO, Z., BAI, T., CARR, L., ELLA-MENYE, J. R., IRVIN, C., RATNER, B. D. & JIANG, S. 2013a. Zwitterionic hydrogels implanted in mice resist the foreign-body reaction. *Nat Biotechnol*.
- ZHANG, R., MJOSENG, H. K., HOEVE, M. A., BAUER, N. G., PELLIS, S., BESSELING, R., VELUGOTLA, S., TOURNIAIRE, G., KISHEN, R. E. B., TSENKINA, Y., ARMIT, C., DUFFY, C. R. E., HELFEN, M., EDENHOFER, F., DE SOUSA, P. A. & BRADLEY, M. 2013b. A thermoresponsive and chemically defined hydrogel for long-term culture of human embryonic stem cells. *Nature Communications*, 4.
- ZHANG, X., ZHOU, P., ZHAO, Y., WANG, M. & WEI, S. 2016. Peptide-conjugated hyaluronic acid surface for the culture of human induced pluripotent stem cells under defined conditions. *Carbohydrate Polymers*, 136, 1061-1064.

Appendices

Appendix 1: Validation of the H9-OCT4-mCherry reporter cell line

Appendix 1.1: Genetics and validation of the H9-OCT4-mCherry reporter cell line. (A) A schematic is presented of the vector with which the H9-OCT4-mCherry cell line was transformed. (B) Flow cytometric validation of the H9-OCT4-mCherry cell line compares (centre) a population of H9-OCT4-mCherry cells that had been immunostained for OCT4 AF647 to (left) a population of H9-OCT4-mCherry cells stained with an isotype control antibody and (right) a population of untransformed H9 cells that had been immunostained for OCT4 AF647.



Appendix 2: Common laboratory reagents

Appendix 2.1: DPBS- was prepared by diluting the reagents listed in the table below into MQ H₂O at the concentrations provided. The final solution was adjusted to a pH of 7.4 and an osmolality of 256-288 mOsm/kg.

Reagent (Supplier details)	Concentration
KCl (Univar, Ingleburn, Australia, Cat No: A383)	2.7 mM
KH ₂ PO ₄ (Merck Millipore, Cat No: 1.04873)	1.5 mM
Na ₂ HPO ₄ (Merck Millipore, Cat No: 1.06586)	8.1 mM
NaCl (Merck Millipore, Cat No: 1.06404)	137 mM

Appendix 2.2: Composition of the 10x stock solution of Tris Buffered Saline Azide that was used for tagging cRGDFK peptide with DELFIA Eu-N1-Amino chelate. The pH was adjusted to 8.0.

Tris Buffered Saline Azide (10x stock)	Concentration
Tris(hydroxymethyl)aminomethane (Sigma Aldrich, Cat No: 252859)	40 mM
NaCl (Merck Millipore, Cat No: 106404)	150 mM
KCl (Merck Millipore, Cat No: 104936)	3mM
Sodium Azide (Sigma Aldrich, Cat No: 438456)	0.2 mg/mL

Appendix 2.3: Composition of Gel Filtration Chromatography Buffer. The pH was adjusted to pH 7.5.

Gel Filtration Chromatography Buffer	Concentration
HEPES (Sigma Aldrich, Cat No: H0887)	10 mM
NaCl (Merck Millipore, Cat No: 106404)	150 mM

Appendix 2.4: The components of L929 fibroblast medium are listed along with the volumes required to prepare 500 mL of medium.

<u>L929 fibroblast culture medium</u>	<u>500 mL</u>
MEM-Glutamax™ (Life Technologies, Cat No: 41090)	450 mL
FBS (heat inactivated) (SAFC Biosciences, Lenexa, KS, Cat No: 1200#C-500 mL, Lot #: 9N0075)	50 mL
Non-essential amino acids (Life Technologies, Cat No: 11140)	5 mL
Antibiotic-antimycotic (Life Technologies, Cat No: 15240)	5 mL

Appendix 2.5: Components of buffers and fixative used in the teratoma assay.

<u>0.2 M Sorenson's phosphate buffer (pH 7.4)</u>	<u>500 mL</u>
0.2 M Na ₂ HPO ₄ (Merck Millipore, Cat No: 1.06586.0500)	0.2 M
0.2 M KH ₂ PO ₄ (Merck Millipore, Cat No: 1.04873.0500)	0.2 M
Sucrose (Merck Millipore, Cat No: 1.07687.0250)	100 mg/ml

<u>0.1 M Sorenson's phosphate buffer (pH 7.4)</u>	<u>500 mL</u>
0.2 M Sorenson's phosphate buffer (pH 7.4)	250 mL
MQ H ₂ O	250 mL

<u>Animal tissue fixative (pH 7.0)</u>	<u>40 mL</u>
0.2 M Sorenson's buffer	20 mL
MQ H ₂ O	10 mL
Paraformaldehyde (16 %; Electron Microscopy Sciences, Hatfield, PA Cat No: 15710)	10 mL
Glutaraldehyde (25 %; Electron Microscopy Sciences, Cat No: 16020)	160 µL

Appendix 3: Peptide library characterisation details

Appendix 3.1: Information about the peptides used in this thesis is presented. The peptide code # and sequence are given along with the supplier, the purity as determined by the HPLC analyses of each peptide (presented in full in Appendix 3.2), the theoretical molecular mass, and experimental molecular mass as determined by mass spectrometry and presented in full in Appendix 3.2. The types of cells to which peptides have been reported to bind are also presented alongside relevant references.

#	Sequence	Supplier	Purity	Theoretical molecular mass	Experimental molecular mass	Cell type	Literature reference
1	K(N3)GTTVKYIFR	Mimotopes	96	1280.49	1280.7	hESCs HT-1080 human fibrosarcoma and B16-F10 mouse melanoma cells	(Derda et al., 2007, Nomizu et al., 1997)
2	K(N3)GRNIAEIIKDI	Mimotopes	96	1437.66	1437.8	Murine embryonic neurons	(Liesi et al., 1989)
3	Ac-KGRYVVLPR	Genscript	99.5	1129.36	565.7	Murine fibrosarcoma cells	(Skubitz et al., 1990)
4	K(N3)LTTAPKLPKVTR	CSIRO	95	1520.818	1520.43	hESCs	(Derda et al., 2010)
5	K(N3)TVKHRPDALHPQ	CSIRO	97	1594.776	1595.20	hESCs	(Derda et al., 2010)
6	Ac-KPHSRN	Genscript	98.3	779.85	390.95	3T3 fibroblasts	(Feng and Mrksich, 2004)
7	Ac-KYIGSR	Genscript	97.9	928.05	928.55	Microvascular endothelial cells, human vascular smooth muscle cells	(Fittkau et al., 2005, Freitas et al., 2007, Maeda et al., 1994, Caniggia et al., 1996)
8	Ac-KGACRRETAWACGA	Genscript	98.6	1519.72	760.55	Various cell lines presenting α5, α5β1, αvβ5 or αvβ3 integrins	(Koivunen et al., 1994)

#	Sequence	Supplier	Purity	Theoretical molecular mass	Experimental molecular mass	Cell type	Literature reference
9	Ac-KGCWLDVCGY	Genscript	98.8	1183.36	1883.7	MO7e leukaemia cells	(Gunawan et al., 2007)
10	Ac-KSVVYGLR	Genscript	99.3	963.14	963.65	hMSCs	(Egusa et al., 2009)
11	Ac-KVDTYDGRGDSVVYGLR	Genscript	97.7	1942.10	971.82	hMSCs	(Egusa et al., 2009)
12	Ac-KYGYGDALR	Genscript	95.1	1247.36	624.7	Endothelial cells	(Underwood et al., 1995)
13	Ac-KFYFDLR	Genscript	99	1030.18	1030.7	Endothelial cells	(Underwood et al., 1995)
14	K(N3)-IKVAV	CSIRO	95.0	838.92	838.45	HeLa derivative HSG cells HT-1080 human fibrosarcoma plus others	(Freitas et al., 2007, Tashiro et al., 1989, Nomizu et al., 1998, Maeda et al., 1994, Caniggia et al., 1996)
15	Ac-KDGEA	Genscript	96.1	560.56	561.35	Platelets, breast adenocarcinoma cells	(Staatz et al., 1991)
16	K(N3)GDITYVRLKF	Mimotopes	95	1407.64	1407.6	hESCs HT-1080 human fibrosarcoma and B16-F10 mouse melanoma cells	(Derda et al., 2007, Nomizu et al., 1997)
17	Ac-KGDIRVTLNRL	Genscript	98.4	1326.55	664.25	hESCs HT-1080 human fibrosarcoma and B16-F10 mouse melanoma cells	(Derda et al., 2007, Nomizu et al., 1997, Meng et al., 2010)
18	K(N3)GFQVAYIIKA	Mimotopes	63.00	1418.7	1414.6	HT-1080 human fibrosarcoma	(Nomizu et al., 1998)
19	Ac-KGSIYITRF	Genscript	98.20	1126.31	1126.8	HT-1080 human fibrosarcoma	(Hozumi et al., 2010)
20	K(N3)GLSIELVRGRVKV	Mimotopes	98.00	1621.95	1621.6	HT-1080 human fibrosarcoma	(Hozumi et al., 2010)

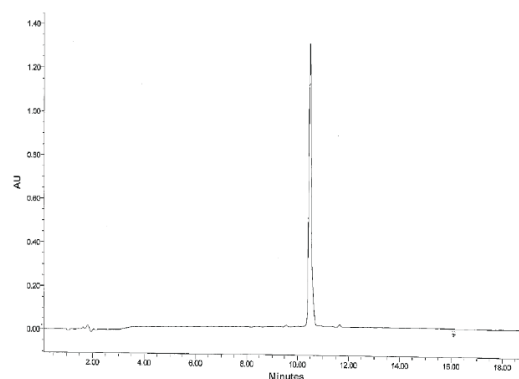
#	Sequence	Supplier	Purity	Theoretical molecular mass	Experimental molecular mass	Cell type	Literature reference
21	Ac-KGLOVQLSIR	Genscript	95.40	1183.41	1183.8	HT-1080 human fibrosarcoma	(Hozumi et al., 2010)
22	Ac-KGHQNQMDYATLQLQ	Genscript	95.00	1817.00	909.45	HT-1080 human fibrosarcoma	(Hozumi et al., 2010)
23	K(N3)GSYNGIIFFLK	Mimotopes	92.00	1454.69	1454.6	HT-1080 human fibrosarcoma	(Makino et al., 2002)
24	Ac-KGHQMNGSVNVSVG	Genscript	96.80	1455.60	1456.8	HT-1080 human fibrosarcoma	(Makino et al., 2002)
25	Ac-KGSYLQFVGI	Genscript	98.20	1153.33	1153.7	HT-1080 human fibrosarcoma	(Makino et al., 2002)
26	Ac-KGAPVNVNTASVQIQ	Genscript	93.70	1453.65	1454.15	HT-1080 human fibrosarcoma	(Makino et al., 2002)
27	Ac-KGAFGVLALWGTR	Genscript	96.60	1417.66	1417.9	HT-1080 human fibrosarcoma and B16-F10 mouse melanoma cells	(Nomizu et al., 2000)
28	K(N3)GDSITKYFQMSL	Mimotopes	92.00	1585.8	1585.7	HT-1080 human fibrosarcoma and B16-F10 mouse melanoma cells	(Nomizu et al., 2000)
29	Ac-KGILQOSAADIAR	Genscript	98.00	1412.60	707.35	HT-1080 human fibrosarcoma and B16-F10 mouse melanoma cells	(Nomizu et al., 2000)
30	K(N3)GTSIKIRGTYS	Mimotopes	97.00	1378.55	1378.4	hESCs HT-1080 human fibrosarcoma and B16-F10 mouse melanoma cells	(Derda et al., 2007, Nomizu et al., 1997)

#	Sequence	Supplier	Purity	Theoretical molecular mass	Experimental molecular mass	Cell type	Literature reference
31	K(N3)GGKKQFRHRNRKG	CSIRO	95.00	1921.20	1920.2	hESCs	(Vogel et al., 1993, Klim et al., 2012)
32	K(N3)GFHRIKA	CSIRO	96.00	1180.37	1179.68	hESCs	(Rezania and Healy, 1999, Harbers and Healy, 2005)
33	Ac-KGGWQPPRARI	Genscript	95.10	1307.51	1308.7	hESCs	(Klim et al., 2010)
34	Ac-KGGNGEPRGDTYRAY	Genscript	96.40	1682.76	842.3	hESCs	(Oldberg et al., 1988, Melkounian et al., 2010)
35	Ac-KGGPQVTRGDVFTM-OH	CSIRO	98.00	1631.85	1632.84	hESCs	(Melkounian et al., 2010, Suzuki et al., 1985)
36	cRGDfK	Peptides International	98.4	603.30	603.41	hPSCs, osteoblasts, chondrocytes	(Klim et al., 2010, Hirschfeld-Warneken et al., 2008, Kantlehner et al., 2000)
36	cRGDfK-N3	Peptides International	99.7	629.3	629.29	hPSCs, osteoblasts, chondrocytes	(Klim et al., 2010, Hirschfeld-Warneken et al., 2008, Kantlehner et al., 2000)
N/A	cRADfK	Peptides International	99.7	617.33	617.39	None	(Kok et al., 2002)

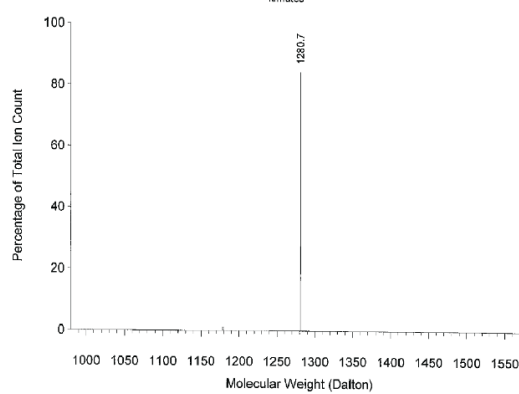
Appendix 3.2: Characterisation of the molecular mass and purity for the peptides used in this thesis. All peptides were characterised for identity by HPLC analysis and mass spectrometry. The molecular masses and purities determined from these analysis are summarized in Appendix 3.1.

Peptide 1

HPLC chromatogram

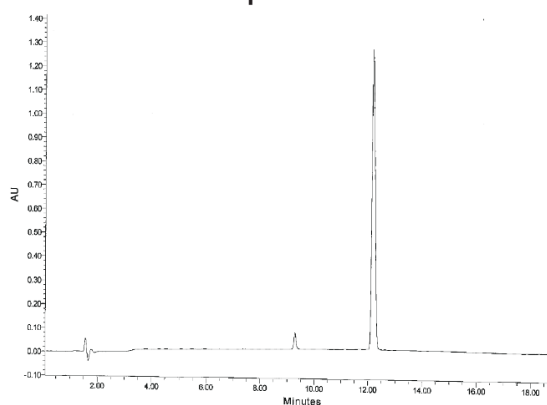


Mass spectrum

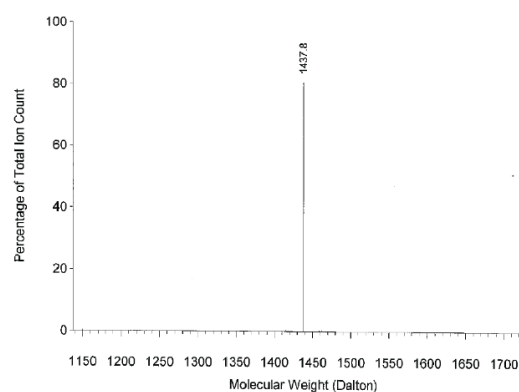


Peptide 2

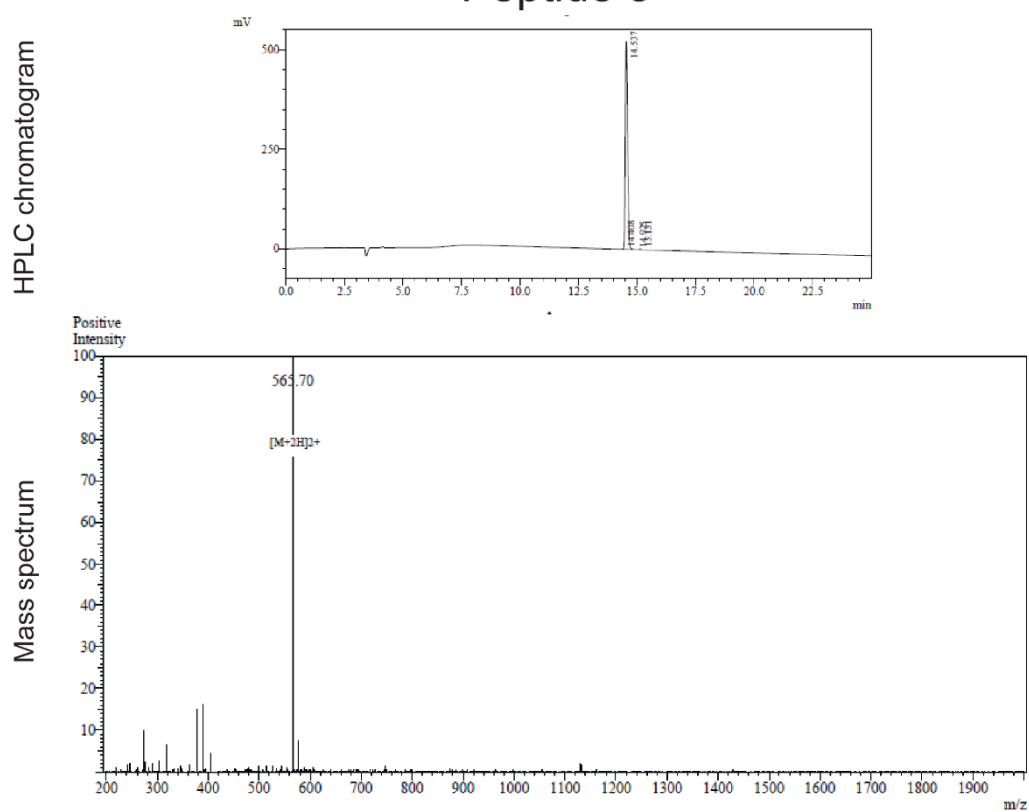
HPLC chromatogram



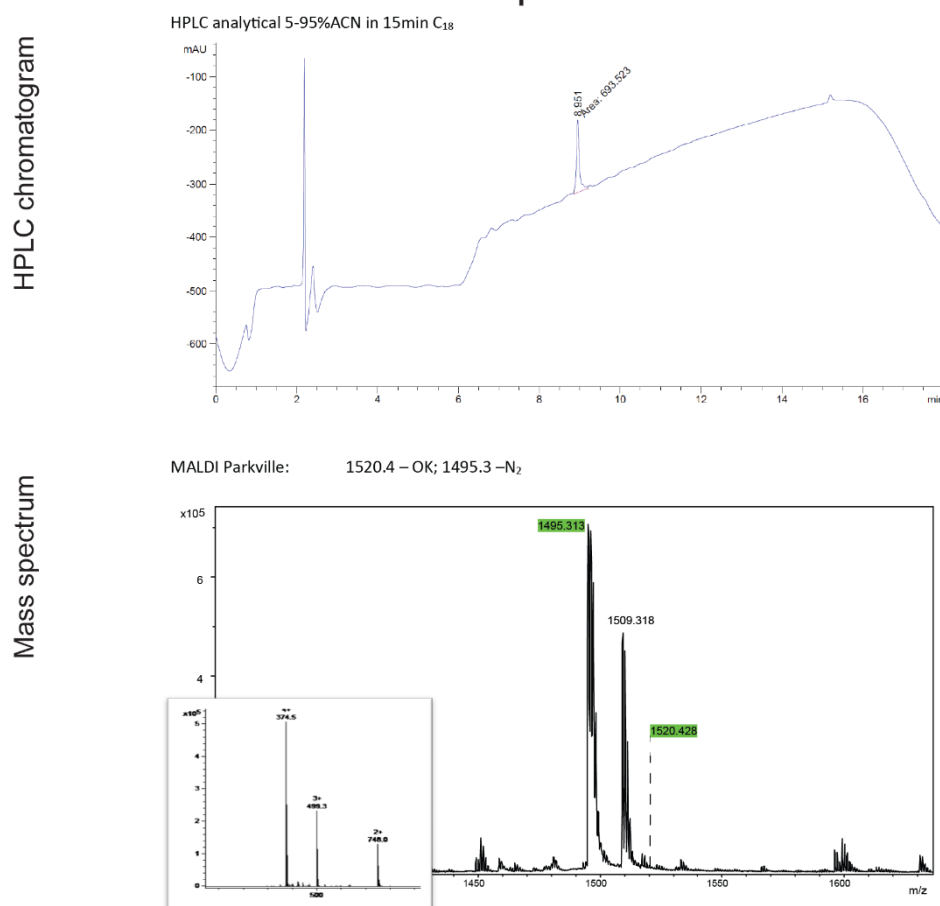
Mass spectrum



Peptide 3

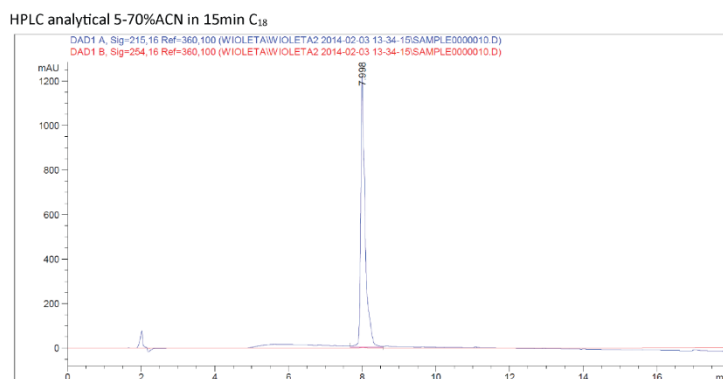


Peptide 4

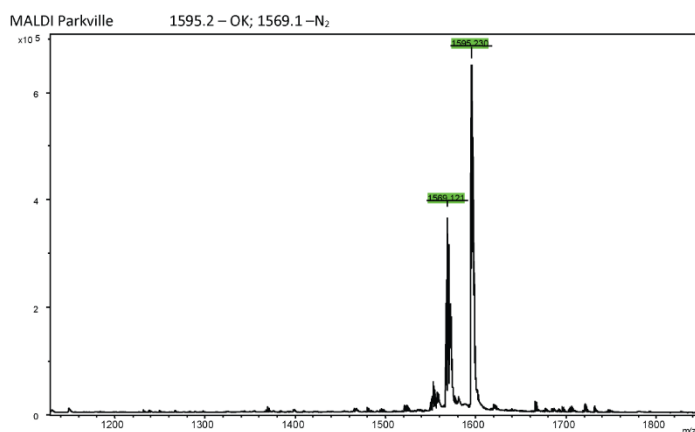


Peptide 5

HPLC chromatogram

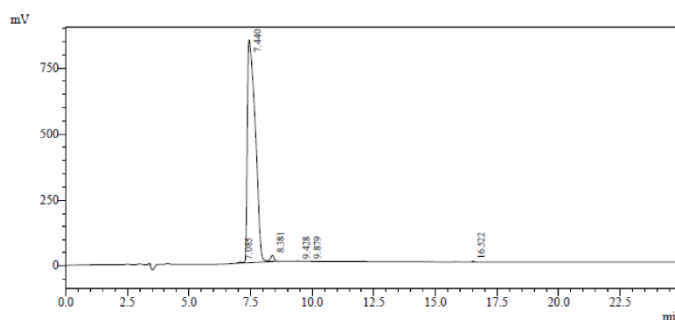


Mass spectrum

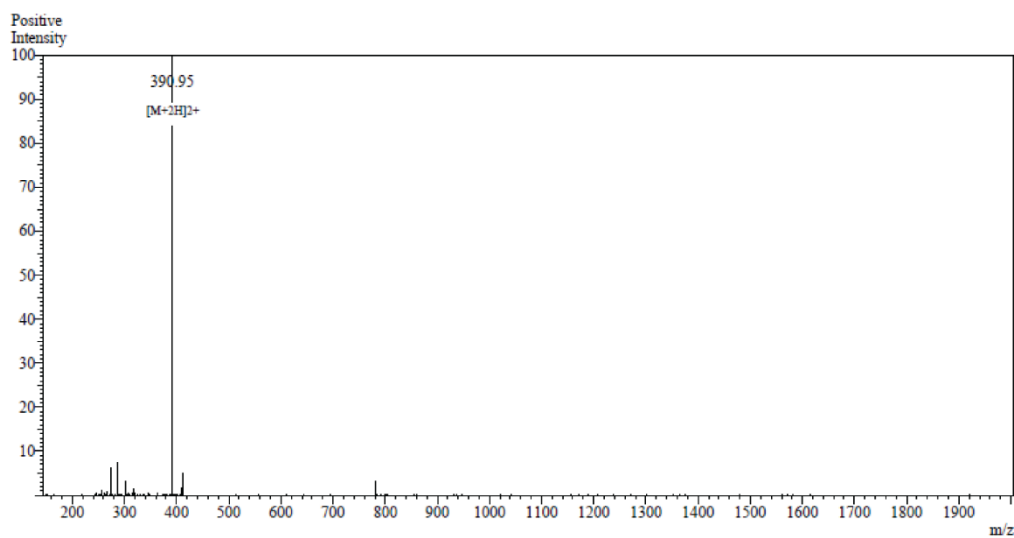


Peptide 6

HPLC chromatogram

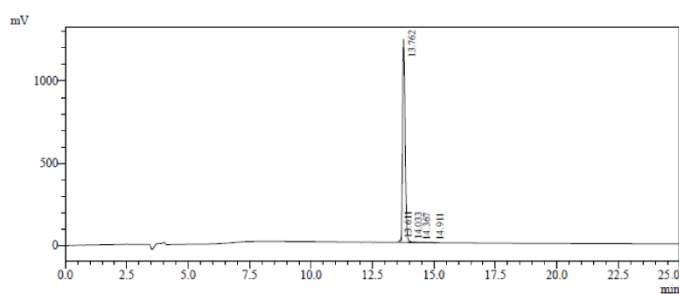


Mass spectrum

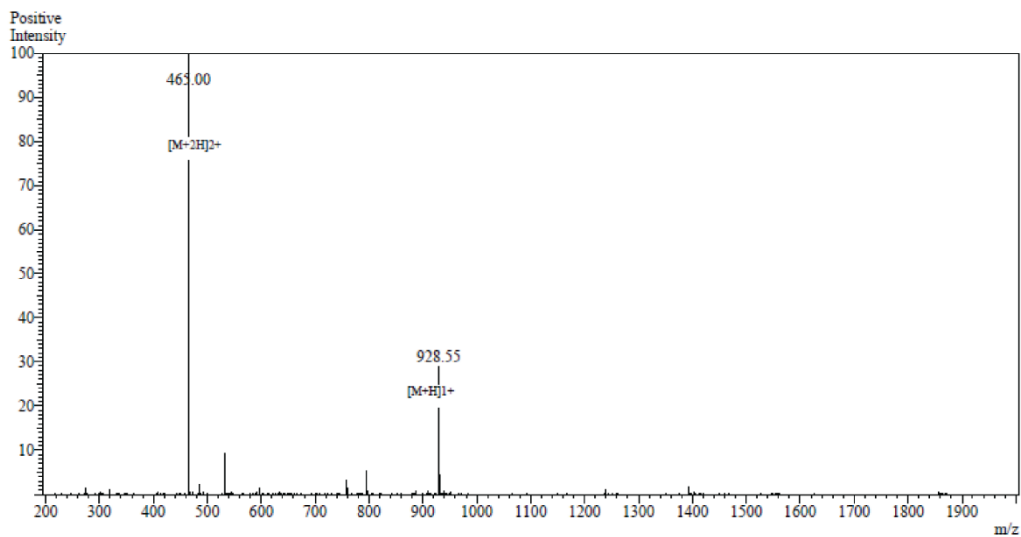


Peptide 7

HPLC chromatogram

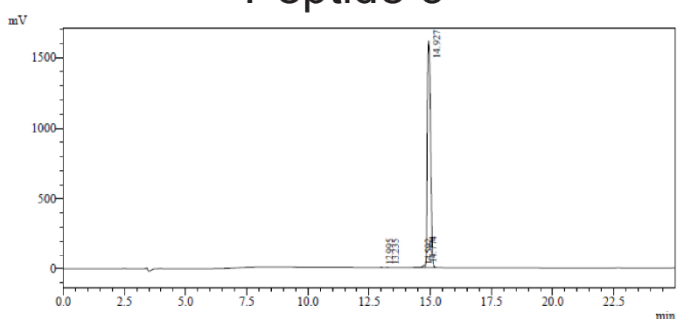


Mass spectrum

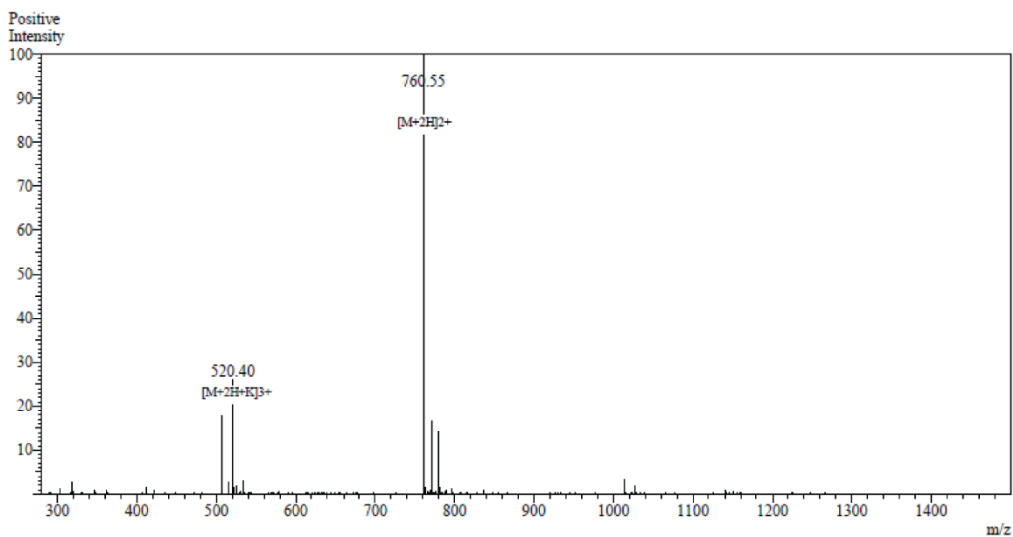


Peptide 8

HPLC chromatogram

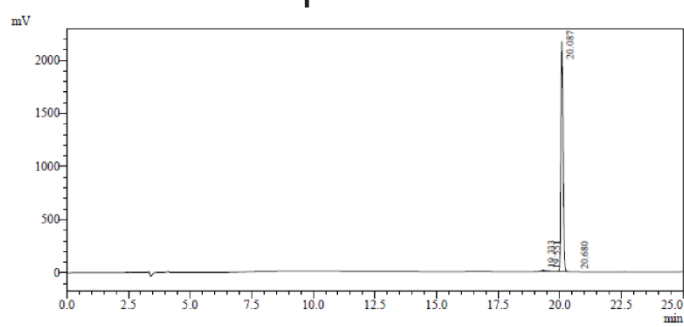


Mass spectrum

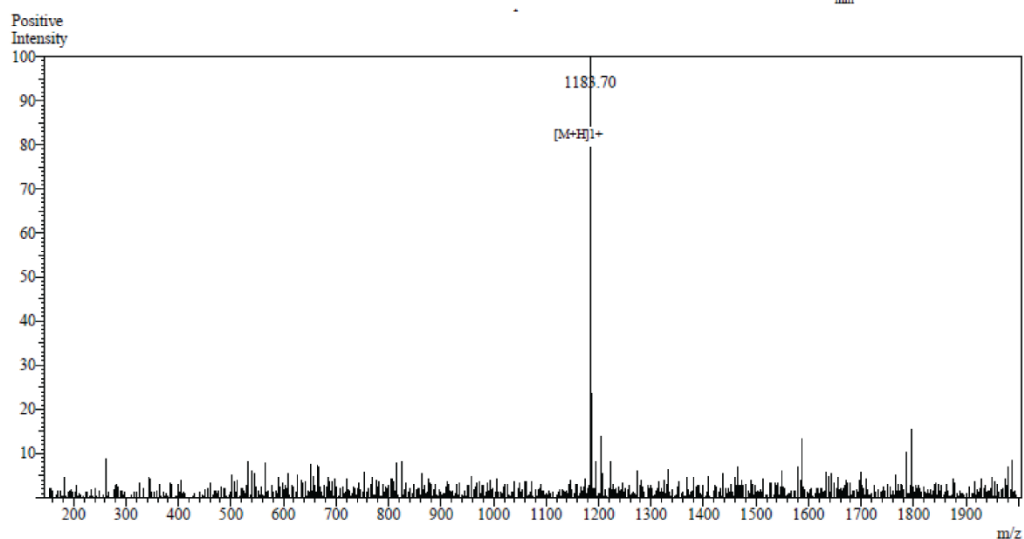


Peptide 9

HPLC chromatogram

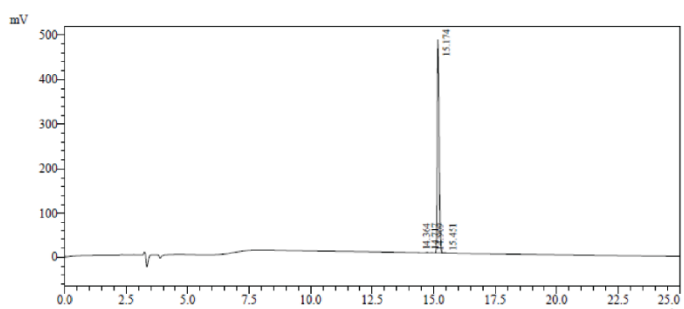


Mass spectrum

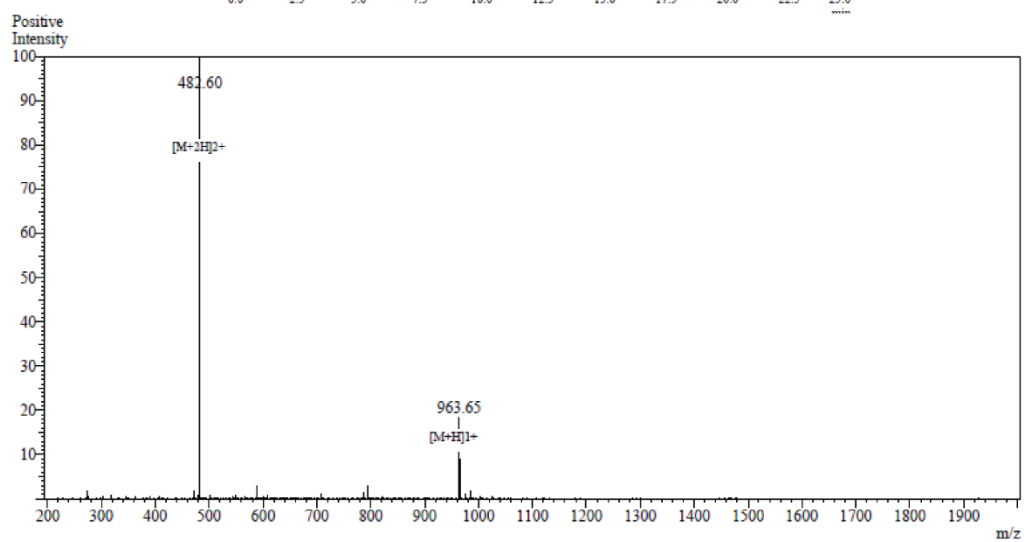


Peptide 10

HPLC chromatogram

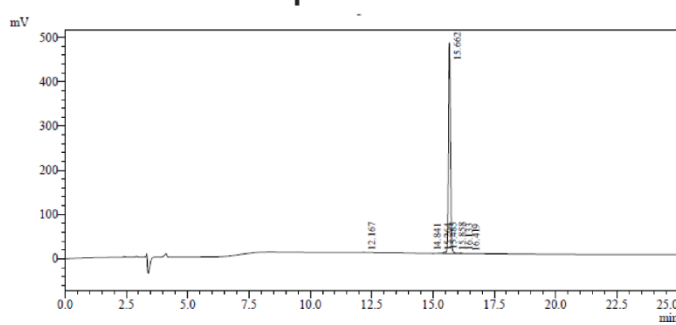


Mass spectrum

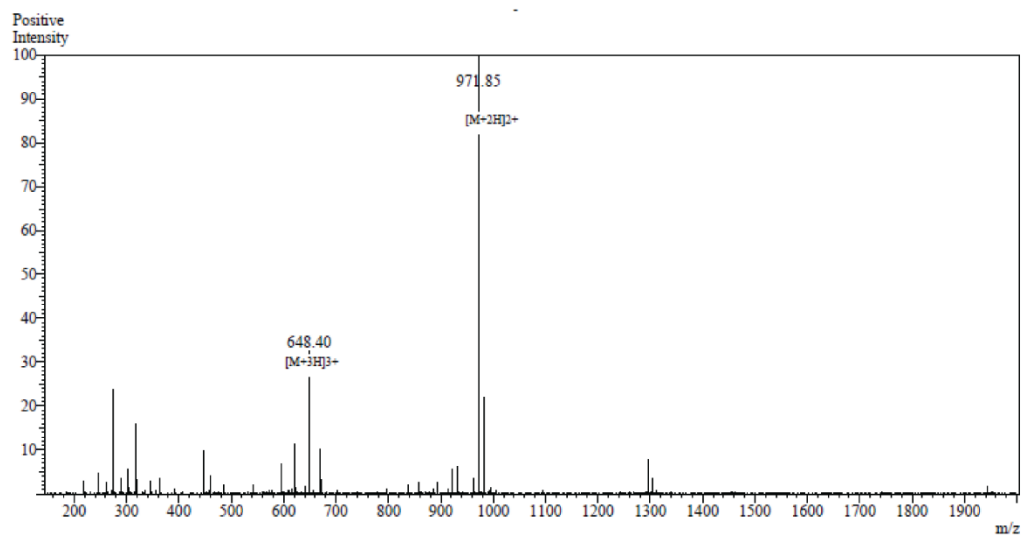


Peptide 11

HPLC chromatogram

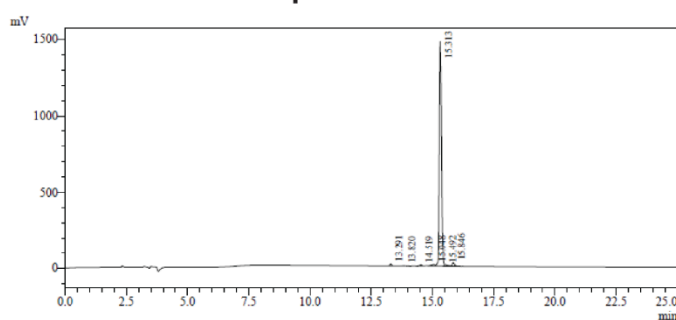


Mass spectrum

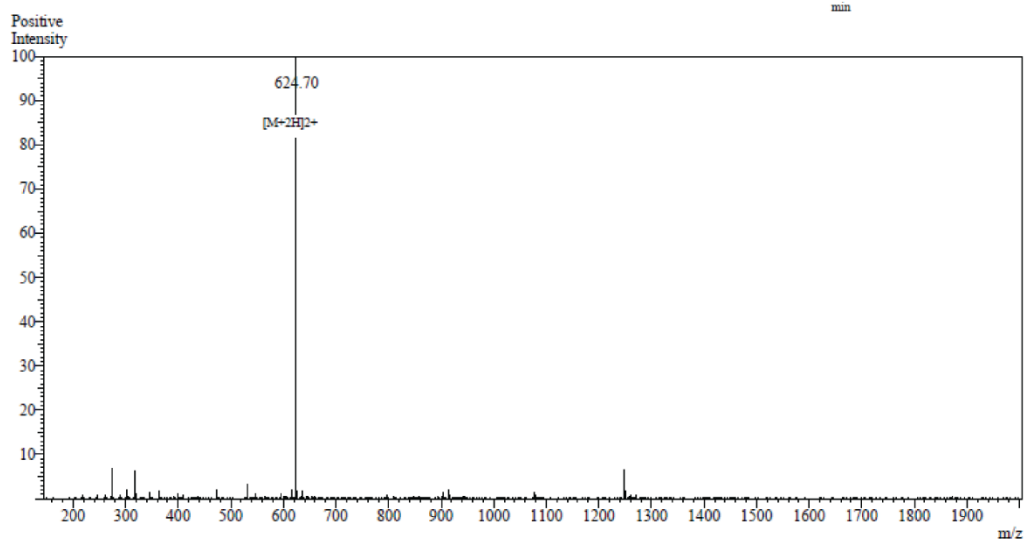


Peptide 12

HPLC chromatogram

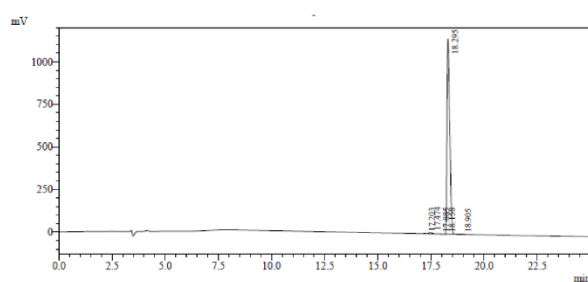


Mass spectrum

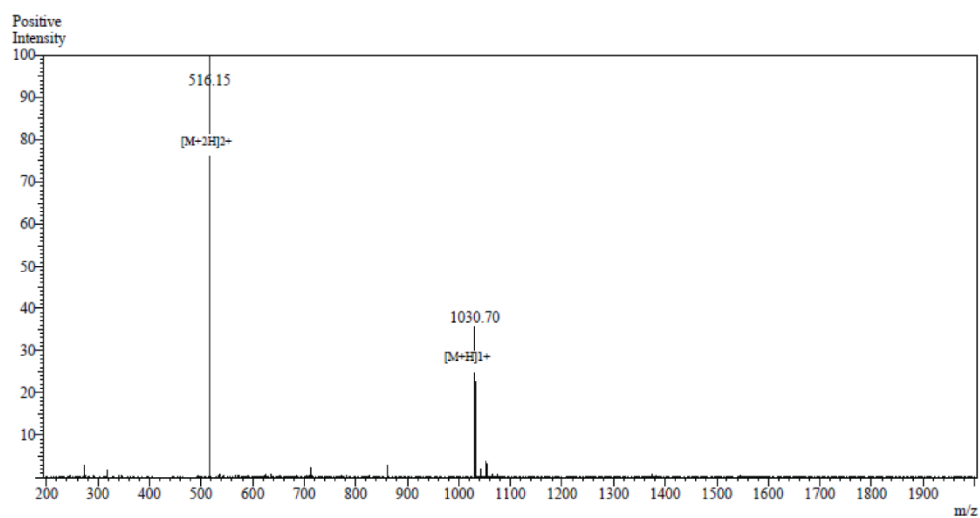


Peptide 13

HPLC chromatogram

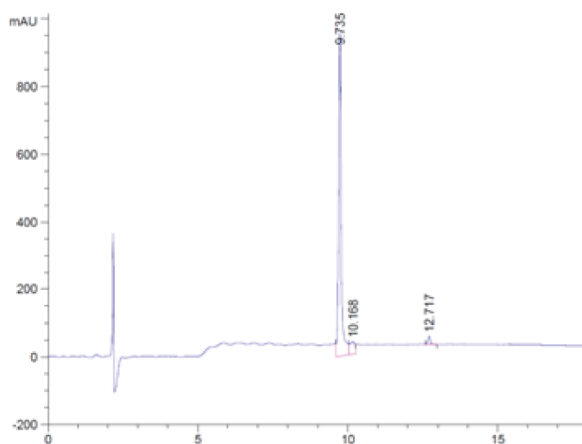


Mass spectrum

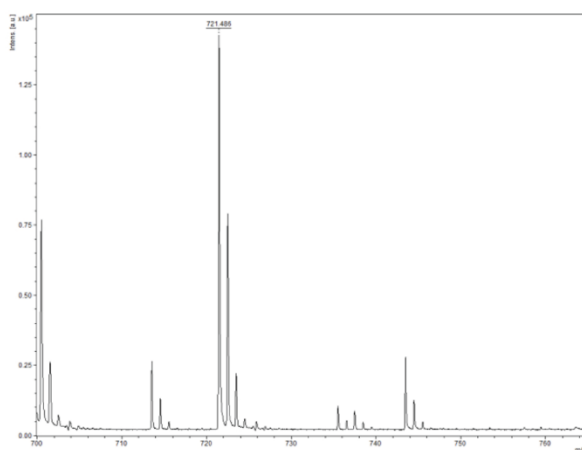


Peptide 14

HPLC chromatogram

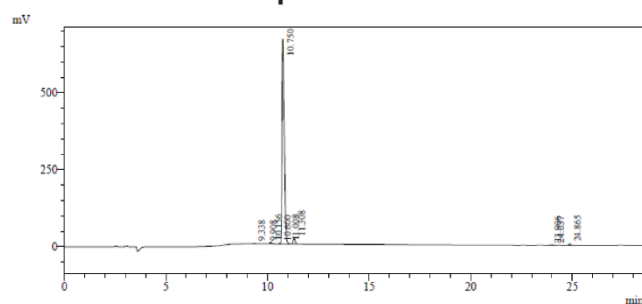


Mass spectrum

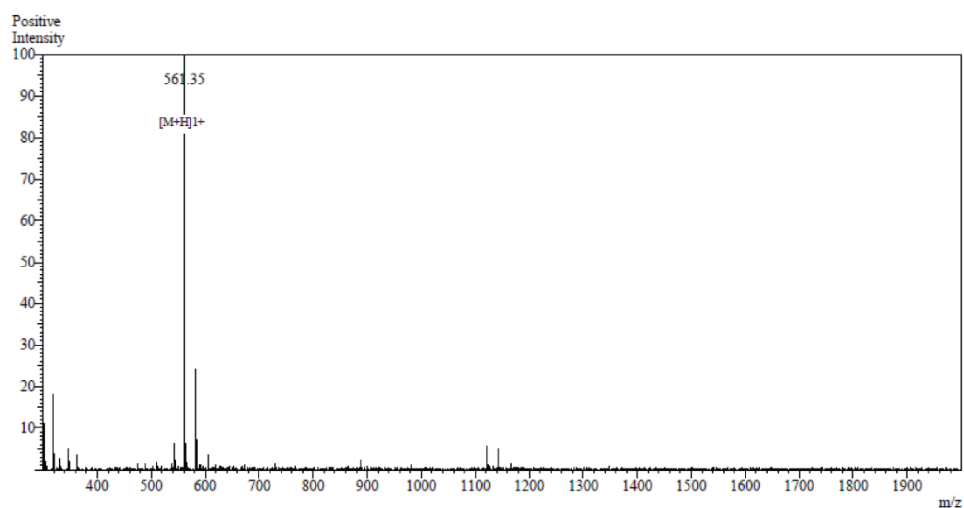


Peptide 15

HPLC chromatogram

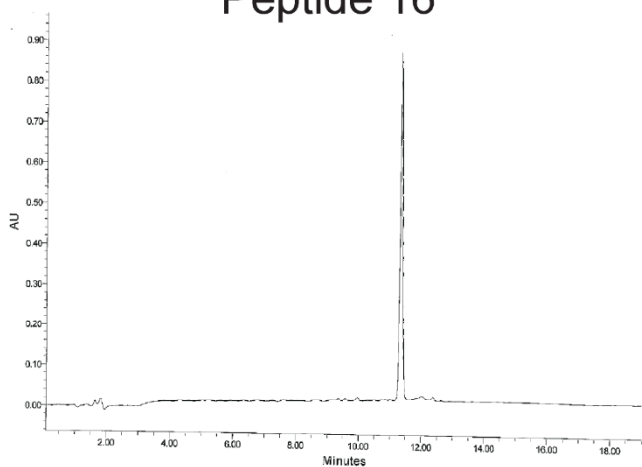


Mass spectrum

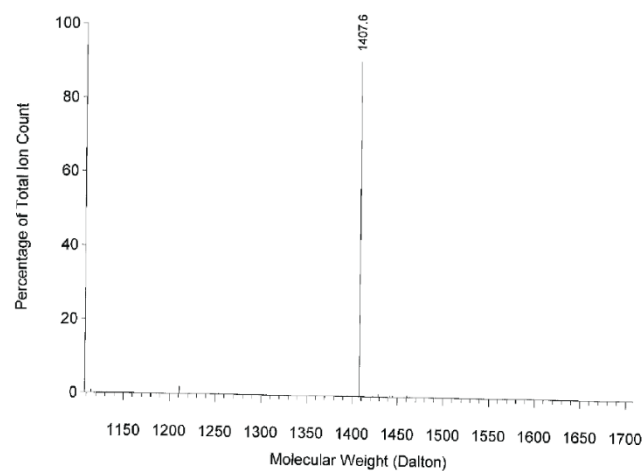


Peptide 16

HPLC chromatogram

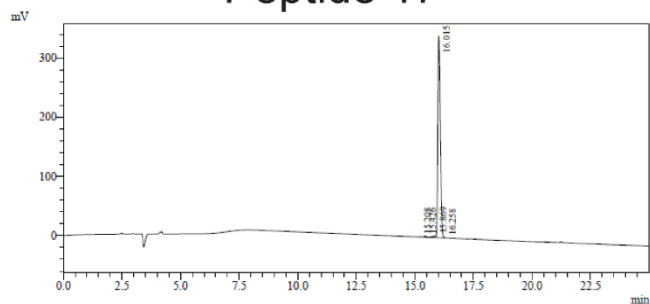


Mass spectrum

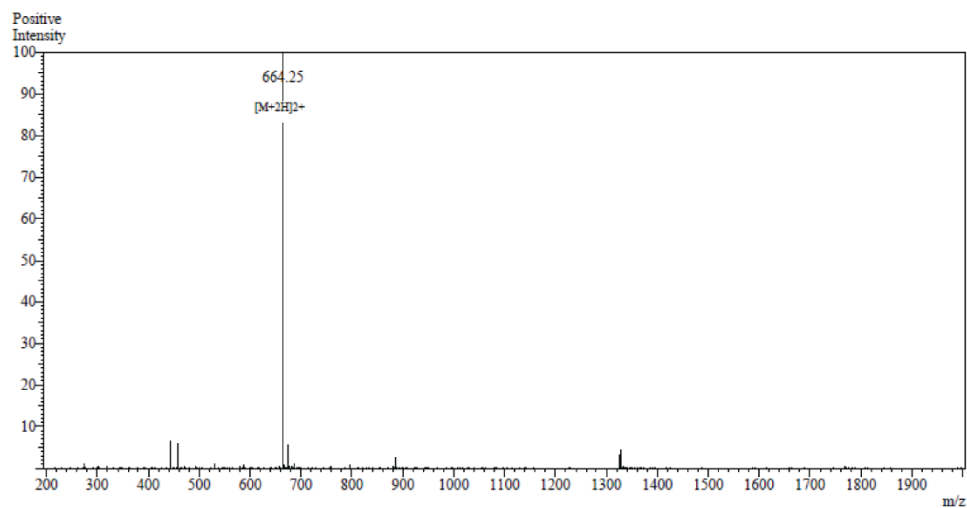


Peptide 17

HPLC chromatogram

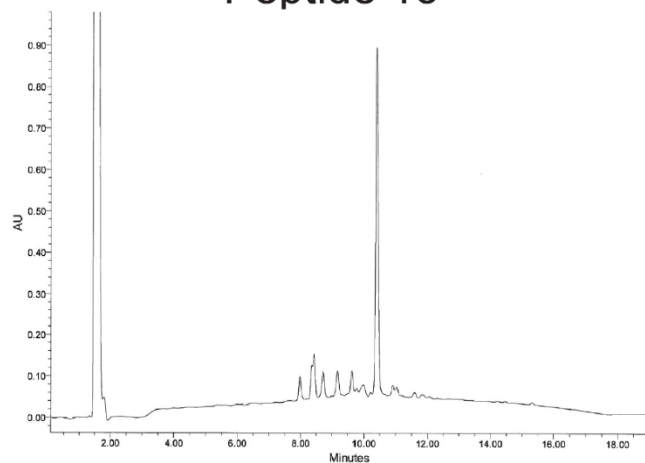


Mass spectrum

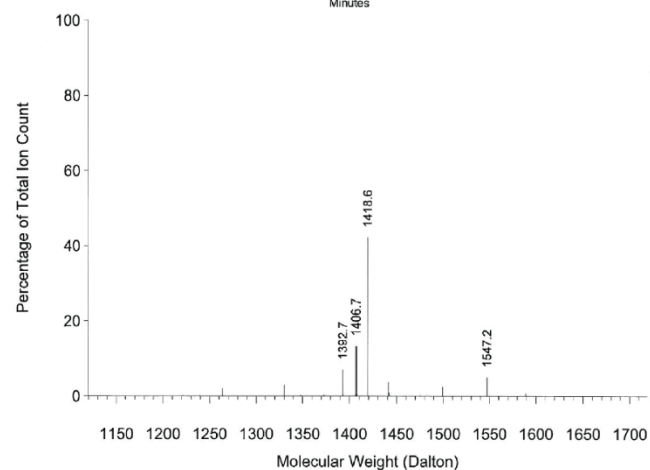


Peptide 18

HPLC chromatogram

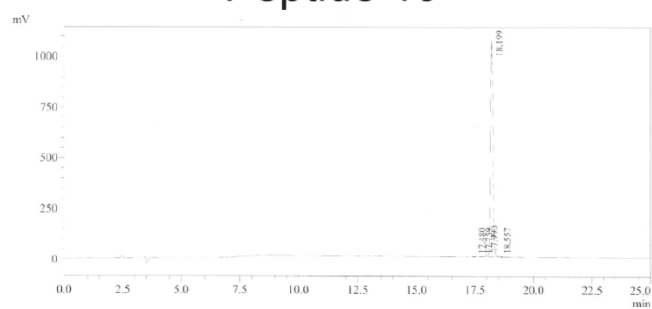


Mass spectrum

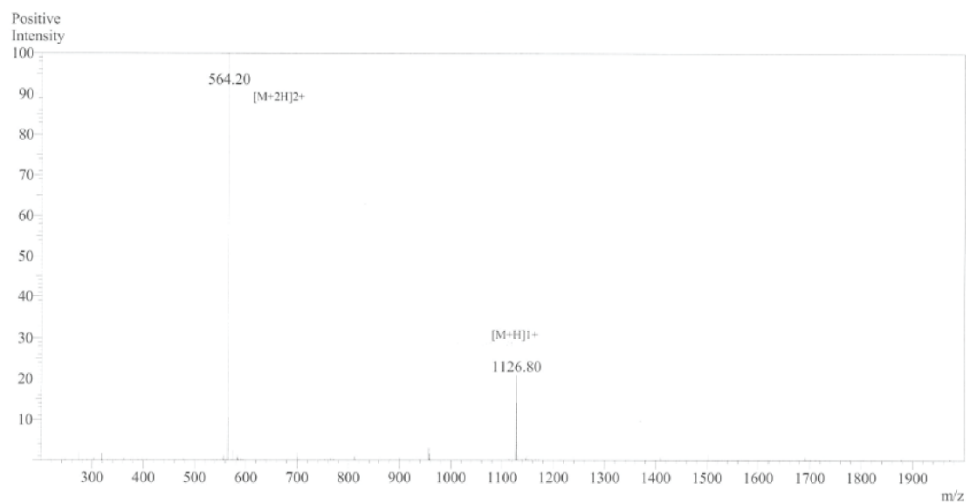


Peptide 19

HPLC chromatogram

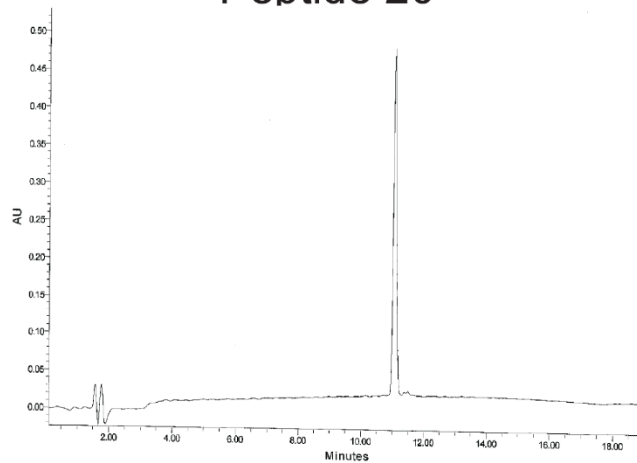


Mass spectrum

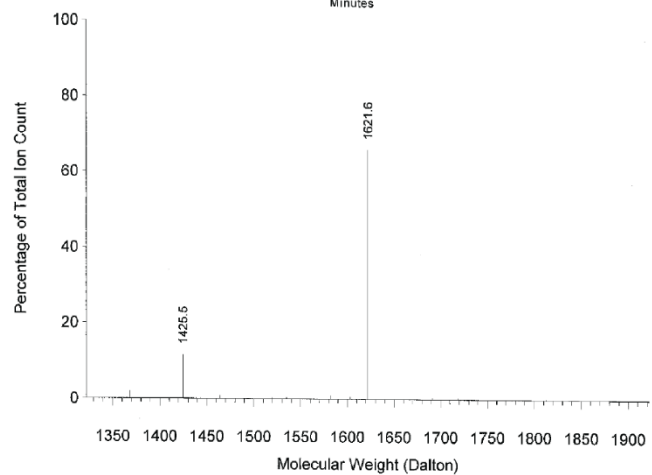


Peptide 20

HPLC chromatogram

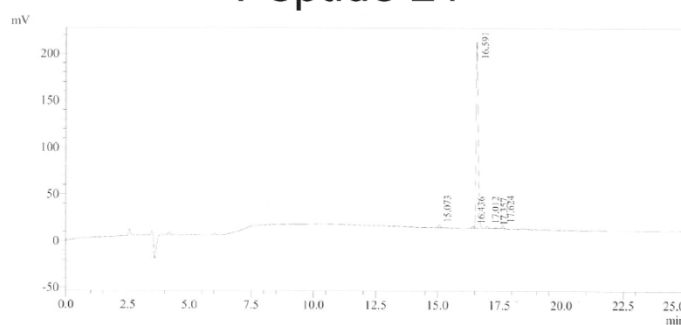


Mass spectrum

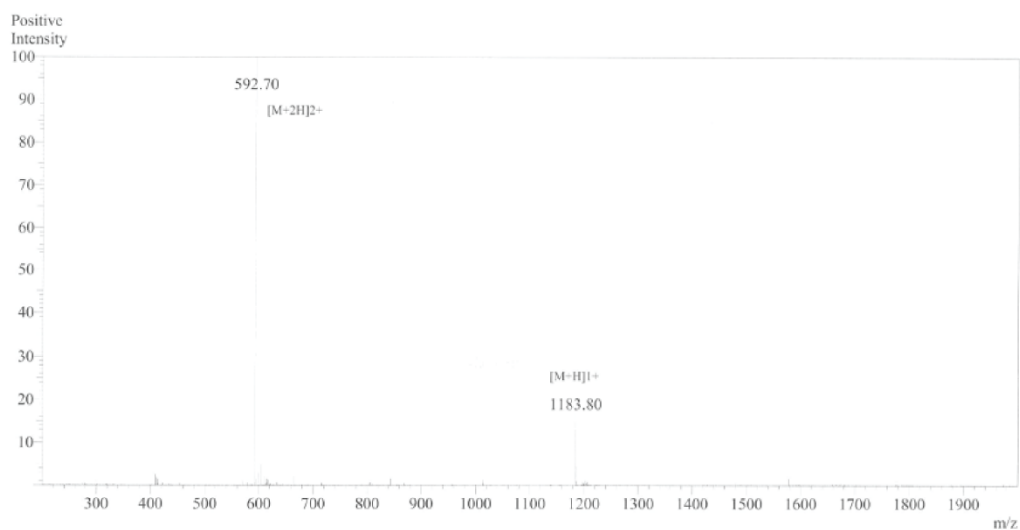


Peptide 21

HPLC chromatogram

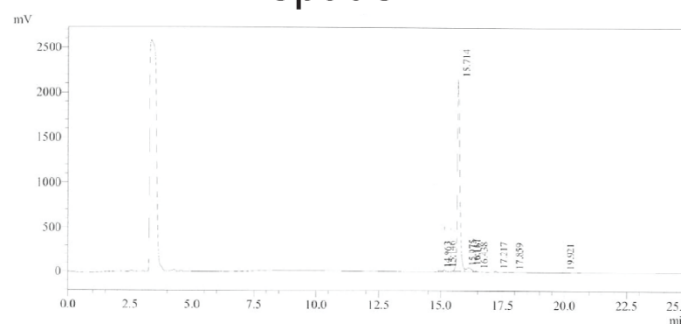


Mass spectrum

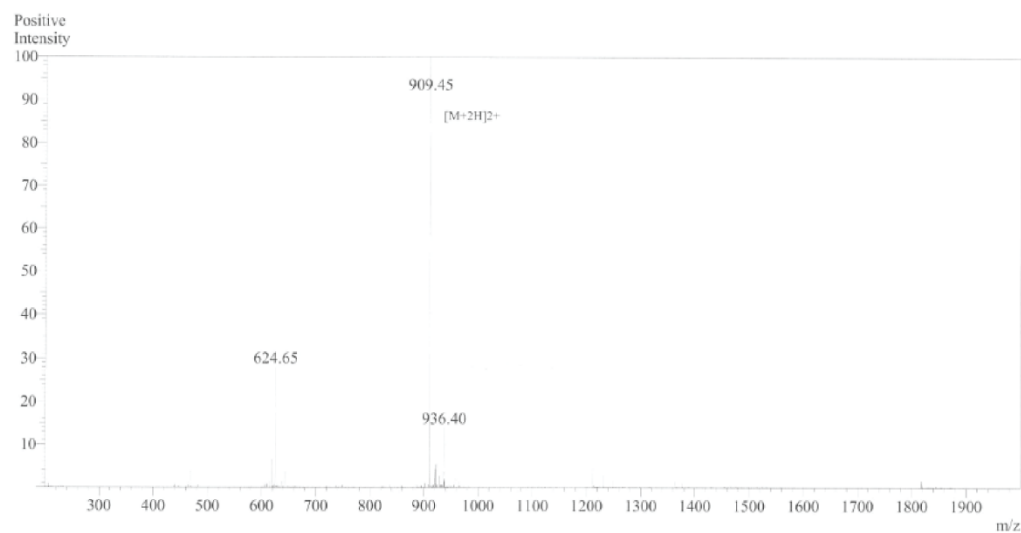


Peptide 22

HPLC chromatogram

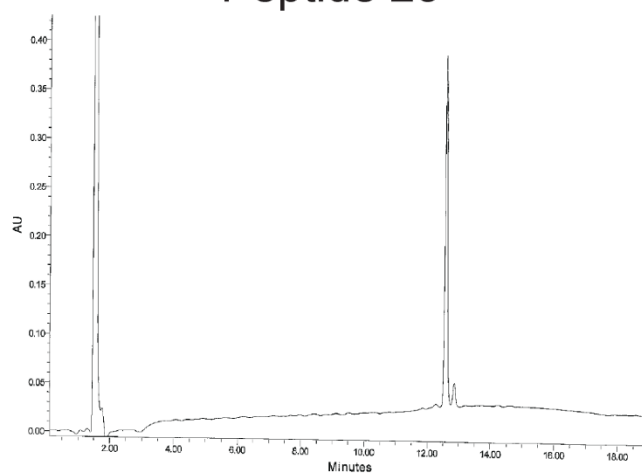


Mass spectrum

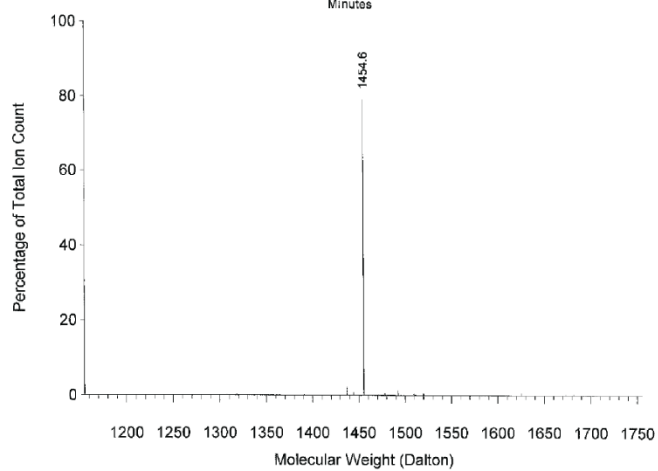


Peptide 23

HPLC chromatogram

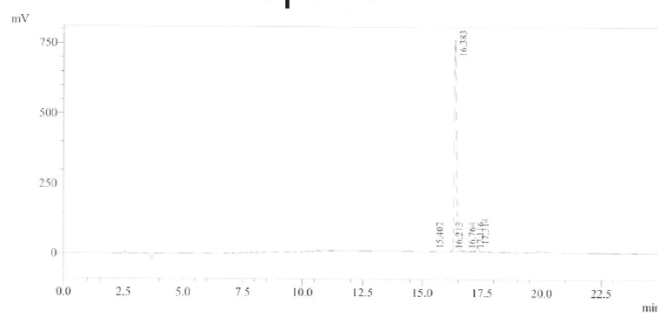


Mass spectrum

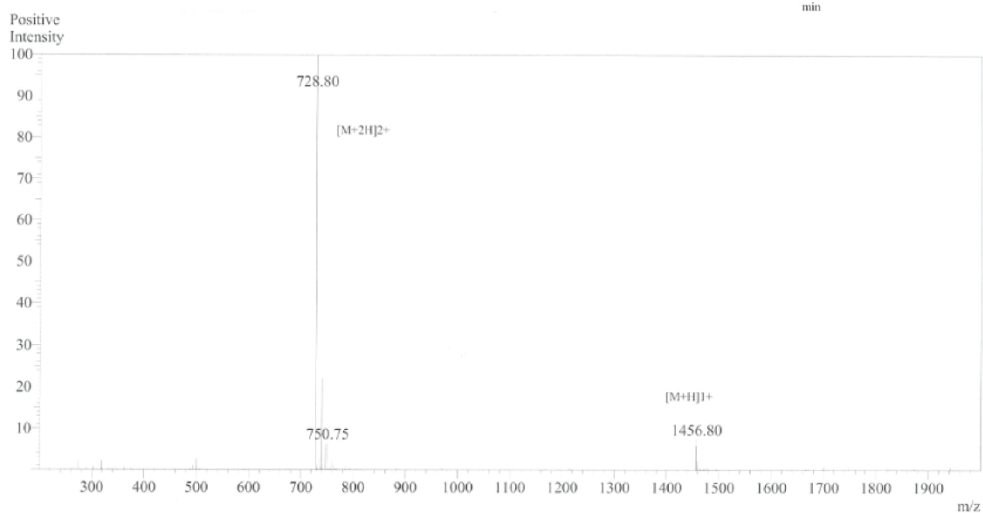


Peptide 24

HPLC chromatogram

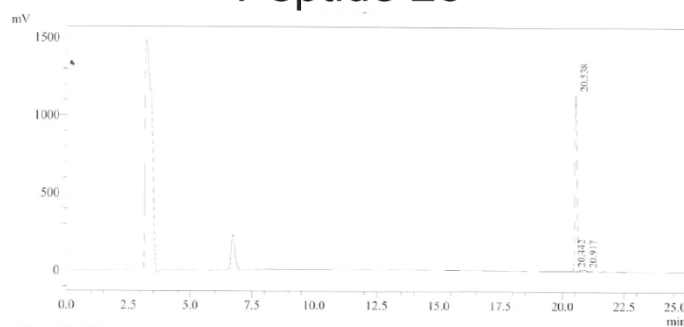


Mass spectrum

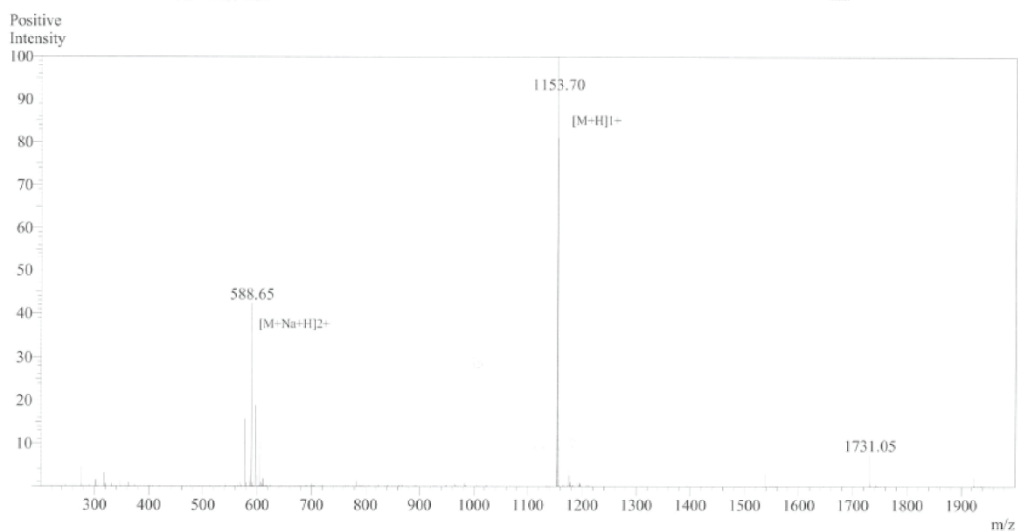


Peptide 25

HPLC chromatogram

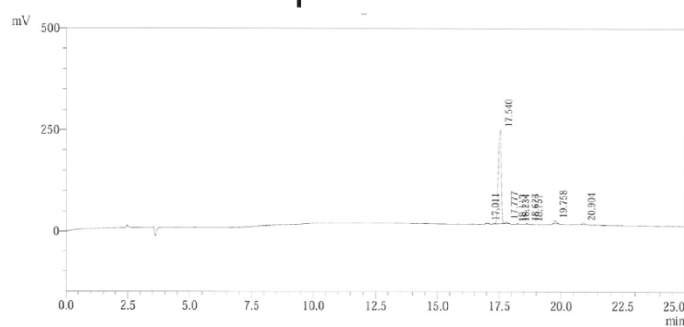


Mass spectrum

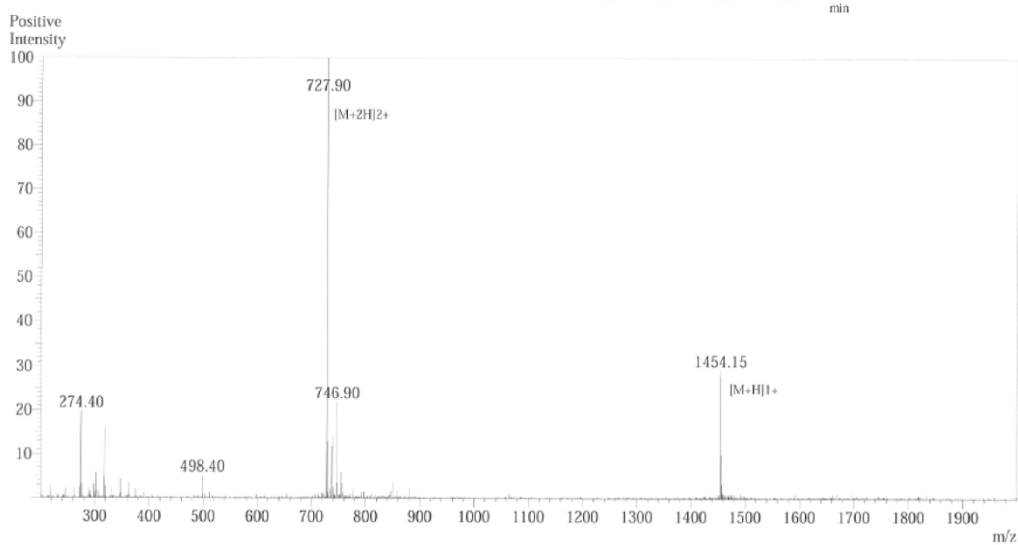


Peptide 26

HPLC chromatogram

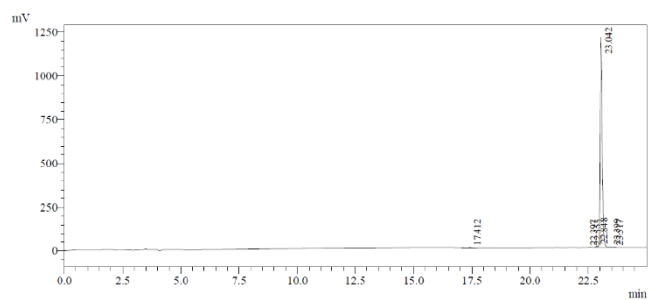


Mass spectrum

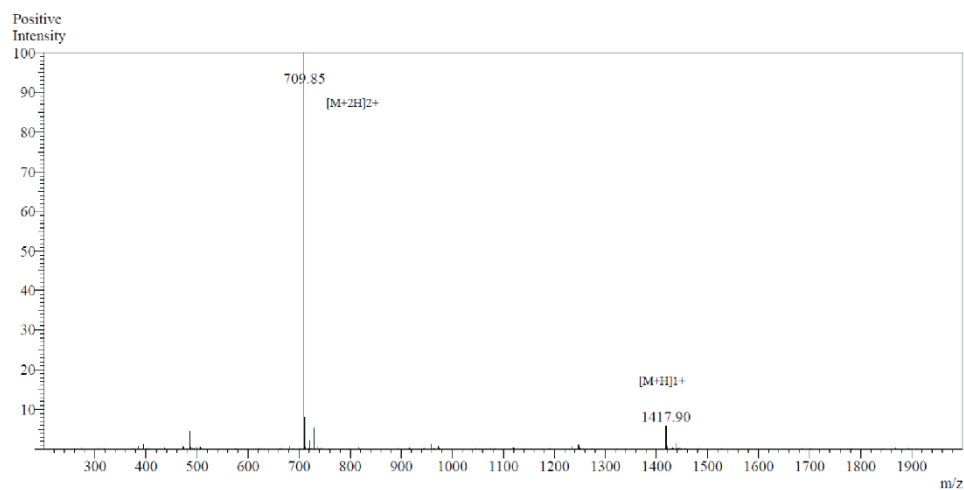


Peptide 27

HPLC plot

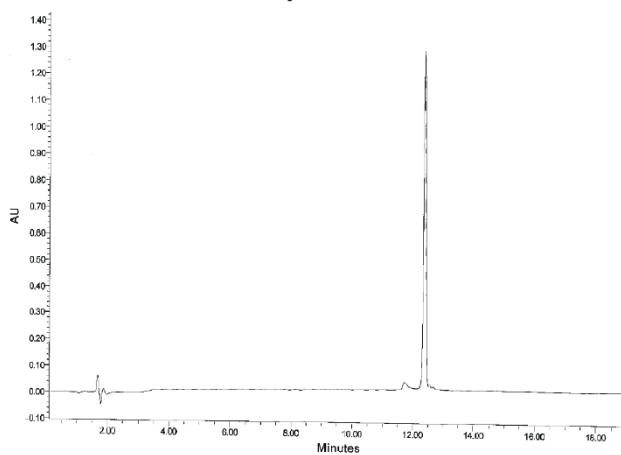


Mass spec plot

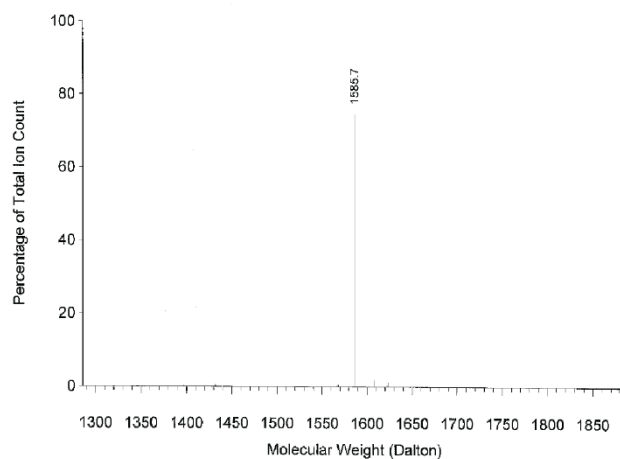


Peptide 28

HPLC plot

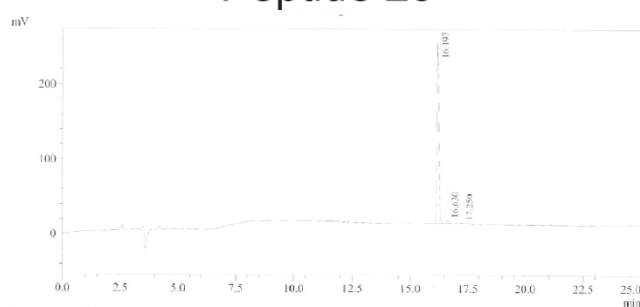


Mass spec plot

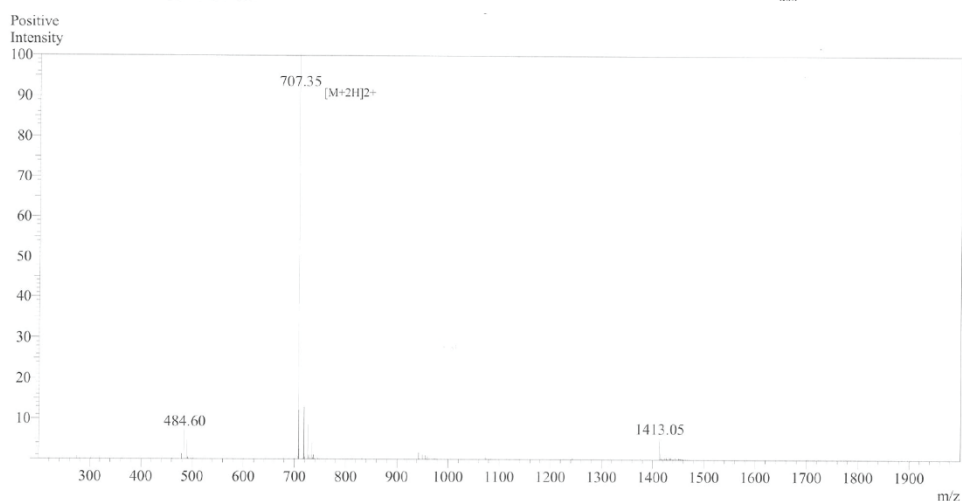


Peptide 29

HPLC chromatogram

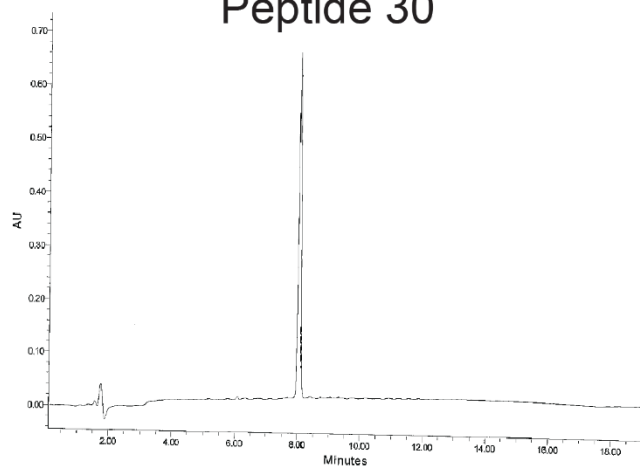


Mass spectrum

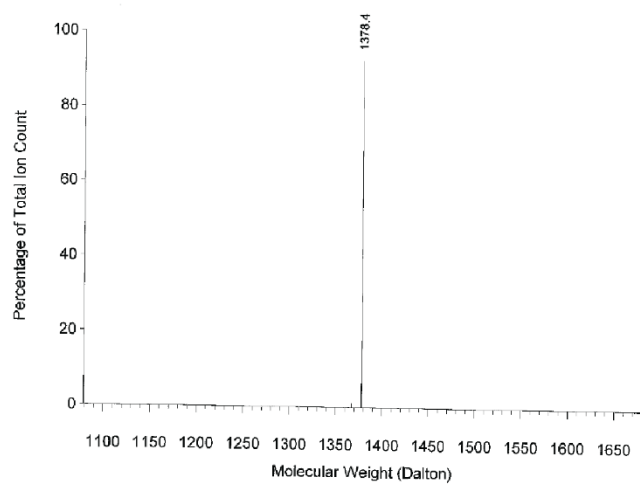


Peptide 30

HPLC chromatogram



Mass spectrum



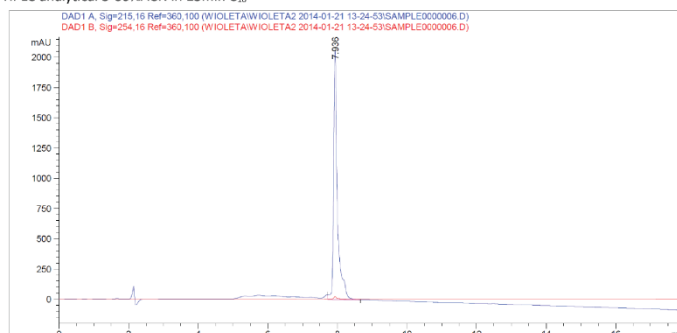
Peptide 31

Chemical Formula: $C_{80}H_{137}N_{37}O_{19}$ Exact Mass: 1920.0891 Molecular Weight: 1921.1803

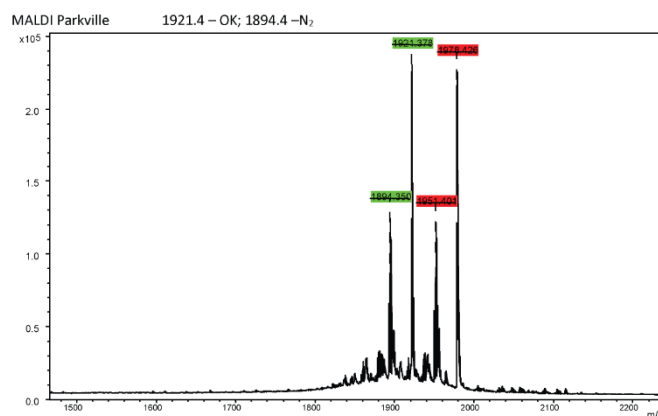
m = 24 mg

HPLC analytical 5-60%ACN in 15min C_{18}

HPLC chromatogram



Mass spectrum



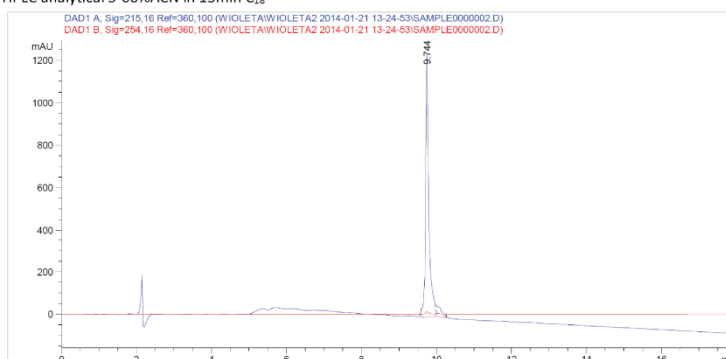
Peptide 32

Chemical Formula: $C_{52}H_{85}N_{21}O_{11}$ Exact Mass: 1179.6737 Molecular Weight: 1180.3654

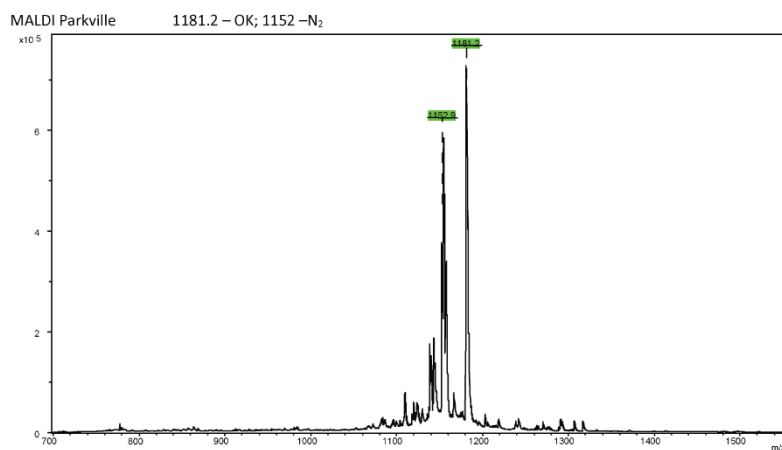
m = 5mg

HPLC analytical 5-60%ACN in 15min C_{18}

HPLC chromatogram

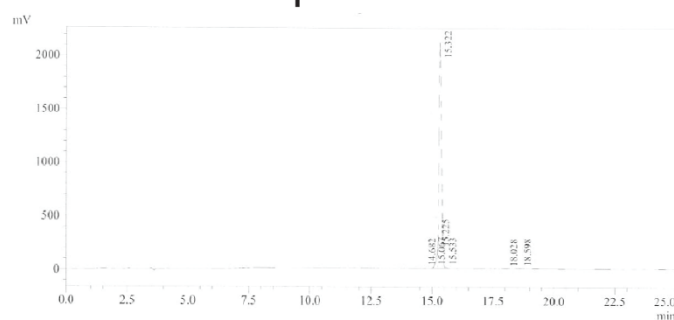


Mass spectrum

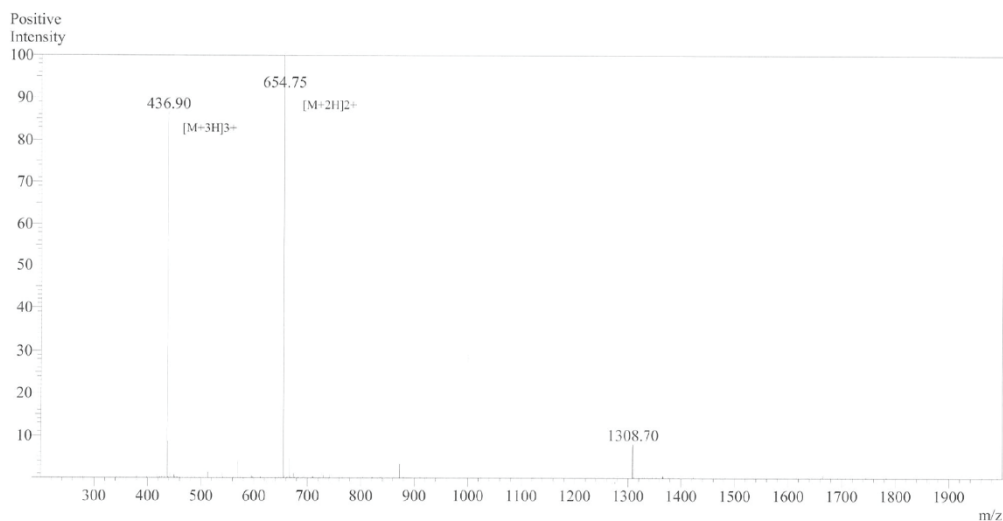


Peptide 33

HPLC chromatogram

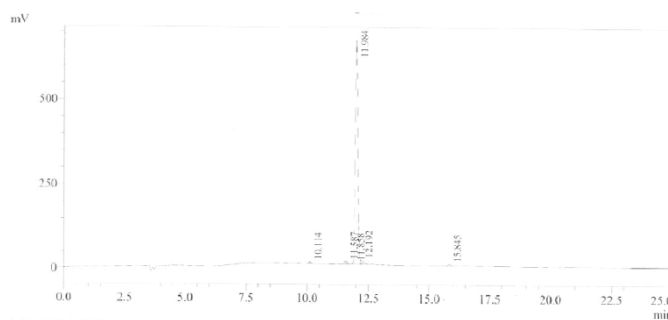


Mass spectrum

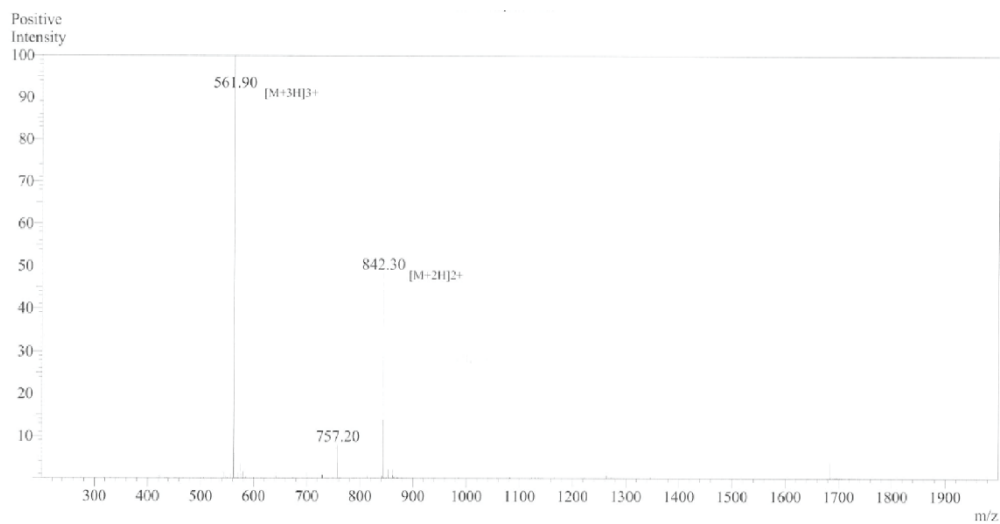


Peptide 34

HPLC chromatogram

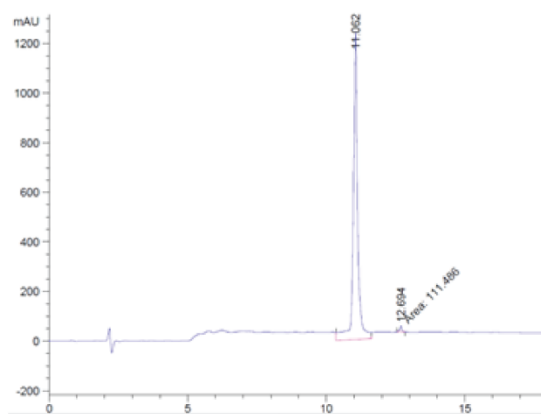


Mass spectrum

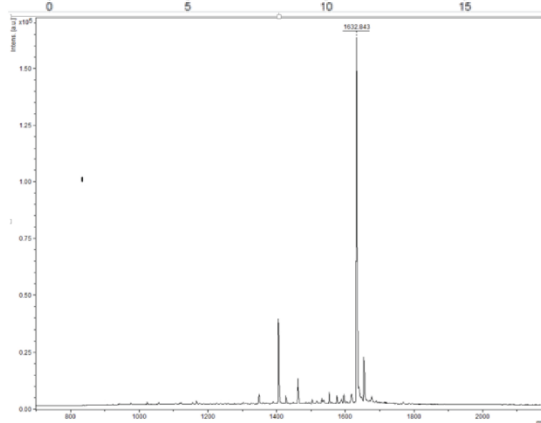


Peptide 35

HPLC chromatogram

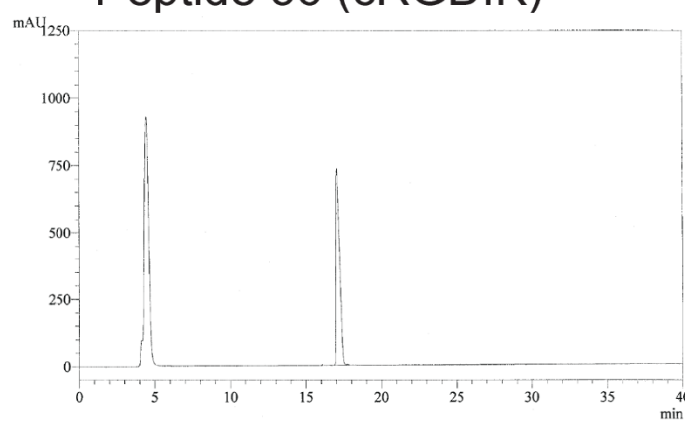


Mass spectrum



Peptide 36 (cRGDfK)

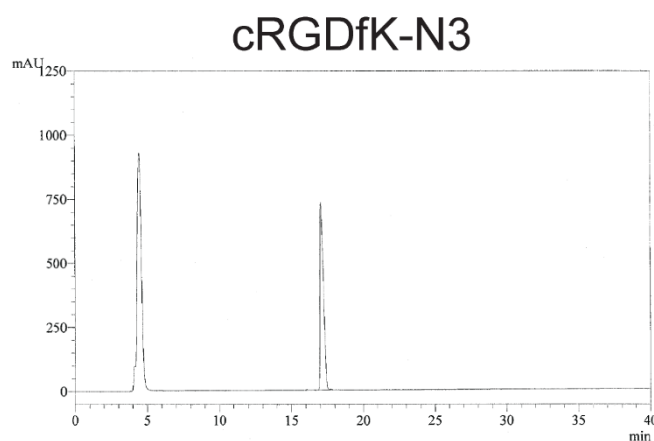
HPLC chromatogram



Mass spectrum

A molecular weight of 603.41 was reported.
The mass spectrum plot was not provided

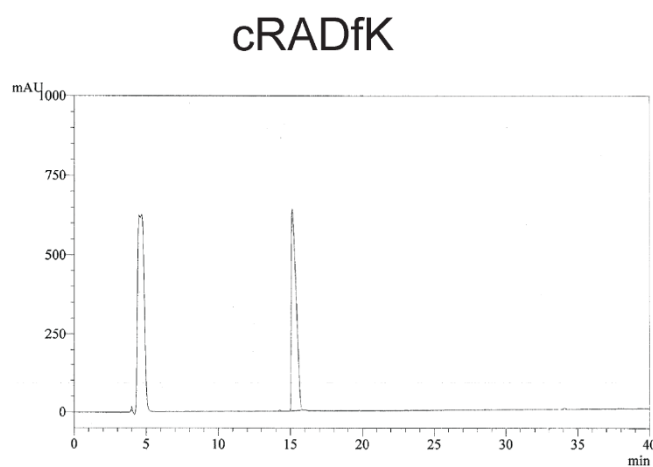
HPLC chromatogram



Mass spectrum

A molecular weight of 629.29 was reported.
The mass spectrum plot was not provided

HPLC chromatogram



Mass spectrum

A molecular weight of 617.39 was reported.
The mass spectrum plot was not provided

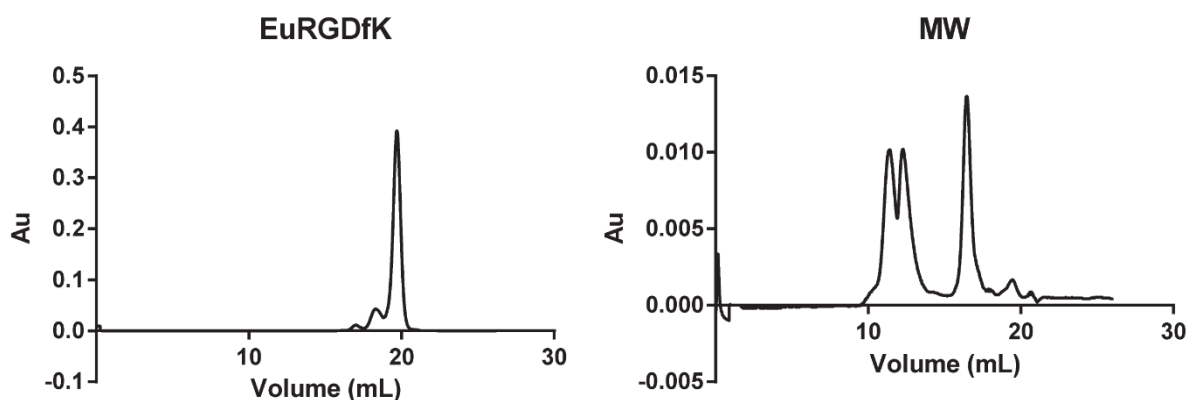
Appendix 4: Inelastic mean free paths for interpretation of XPS results

Appendix 4.1: Attenuation lengths are presented for the photoelectrons of elements relevant to the XPS analysis of polymer coatings on TCPS performed in this study.

Selected Peaks	Tanuma/ Powell/ Penn (nm)
O 1s	2.91
N 1s	3.25
C 1s	3.52

Appendix 5: Information about Eu-tagged peptides

Appendix 5.1: Characterisation of Eu-tagged cRGDfK peptide. Results from fast protein liquid chromatography (FPLC) of Eu-tagged cRGDfK peptide (left) is presented and compared to analysis of low molecular weight standards (right). Amino acid analysis (bottom) is also presented.



AMINO ACID ANALYSIS REPORT

High Sensitivity Amino Acid Analysis- Results

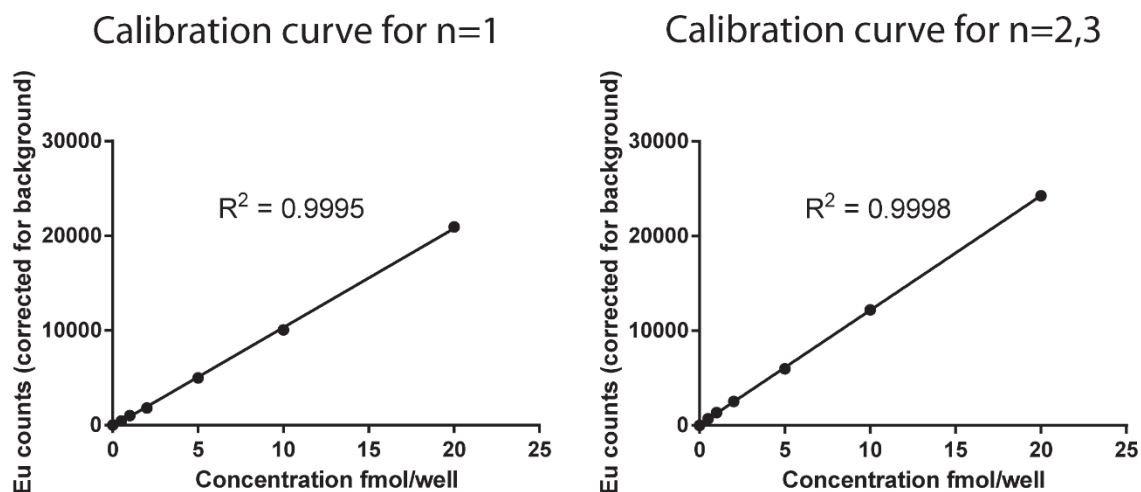
Sample ID: Vial 1

Name	Amino Acid (-H ₂ O)* (ng / sample)	pmol / sample	Mole%
Serine	2.1	24	2.3
Arginine	37.2	238	22.9
Glycine	15.2	266	25.7
Aspartic acid	28.1	244	23.5
Lysine	4.6	36	3.5
Phenylalanine	33.7	229	22.1
Total	120.8	1036	100.0

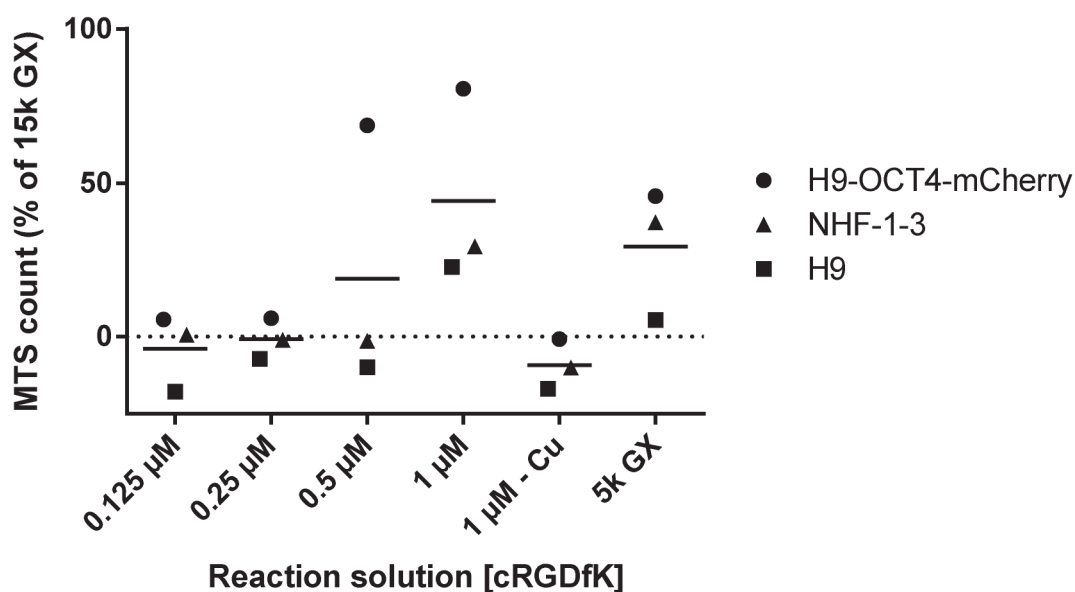
* Calculation based on amino acid residue mass in protein (molecular weight minus H₂O).

Nb. Amino acid analysis was unable to detect the azide-functionalised lysine residue. The detection of Serine was a contaminant that arose due to the presence of Tris buffer.

Appendix 5.2: Eu standard calibration curves are presented. The curves were constructed from an Eu standard diluted to 0.2 nM, 0.1 nM, 0.05 nM, 0.02 nM, 0.01 nM and 0.005 nM and were included in each plate to allow quantification of Eu-containing solutions liberated from wells that had been modified with Eu-tagged cRGDfK peptide.

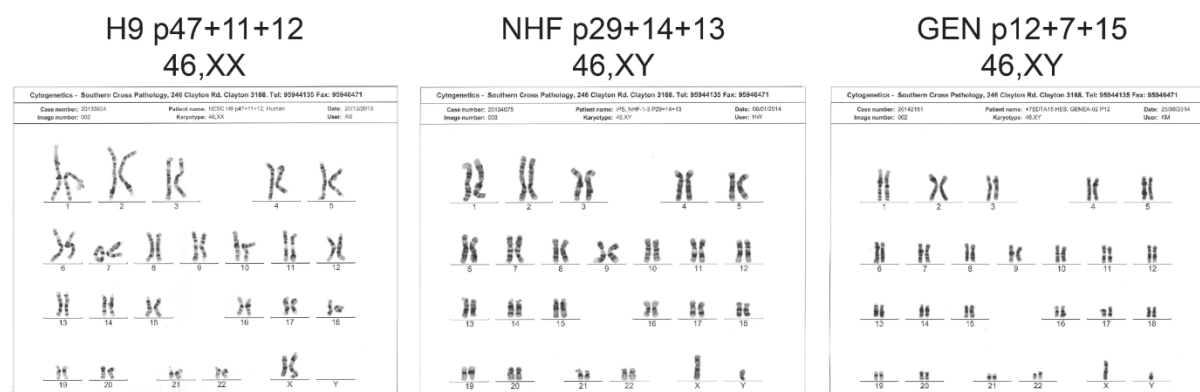


Appendix 5.3: Results from the hPSC-binding control wells included in the Eu-cRGDfK assay. Individual data points are presented from MTS cell proliferation assays. Results were normalised against the mean MTS values from wells seeded at 15 000 cells/cm² on Geltrex™, following subtraction of mean MTS values from plates modified with peptide-free reaction solutions.

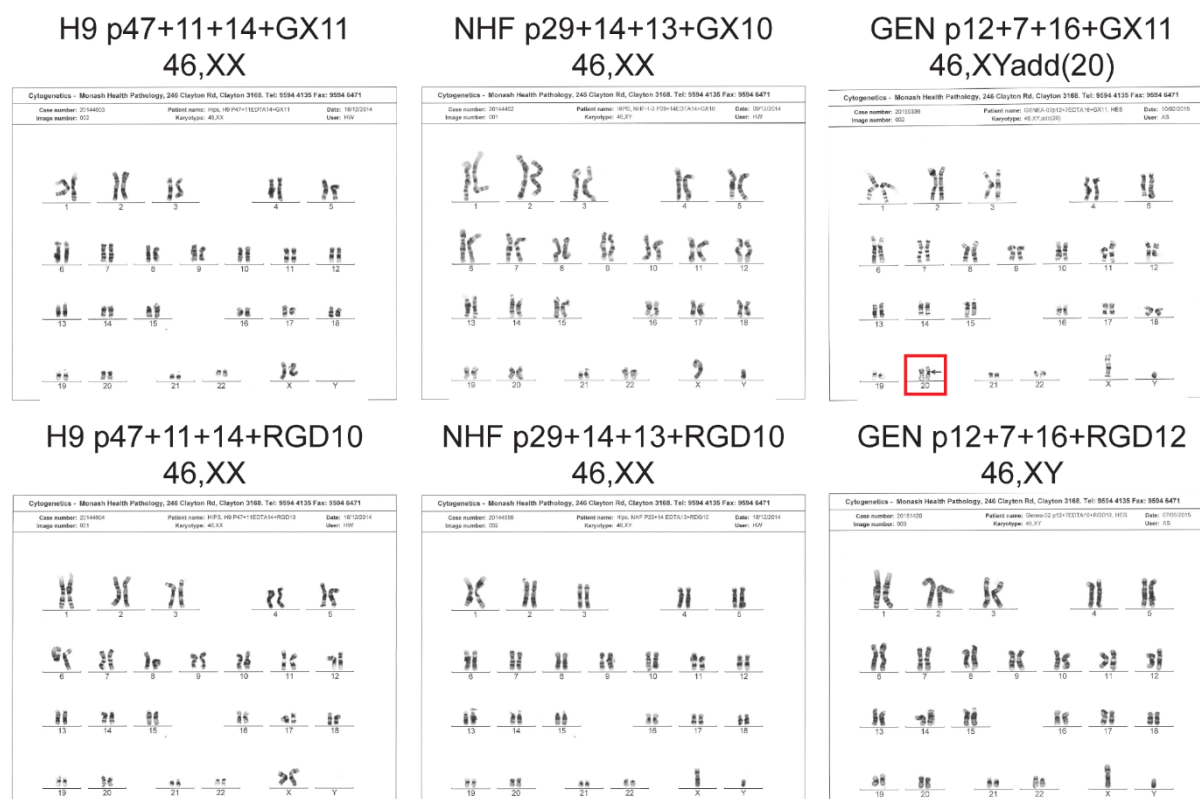


Appendix 6: hPSC characterisation results

Appendix 6.1: Karyograms are presented from G-banding karyotype analyses of H9, NHF-1-3 (NHF) and Genea-02 (GEN) hPSCs that had been adapted to culture on Geltrex™-coated surfaces in E8 medium for 12, 13 and 15 passages, respectively.



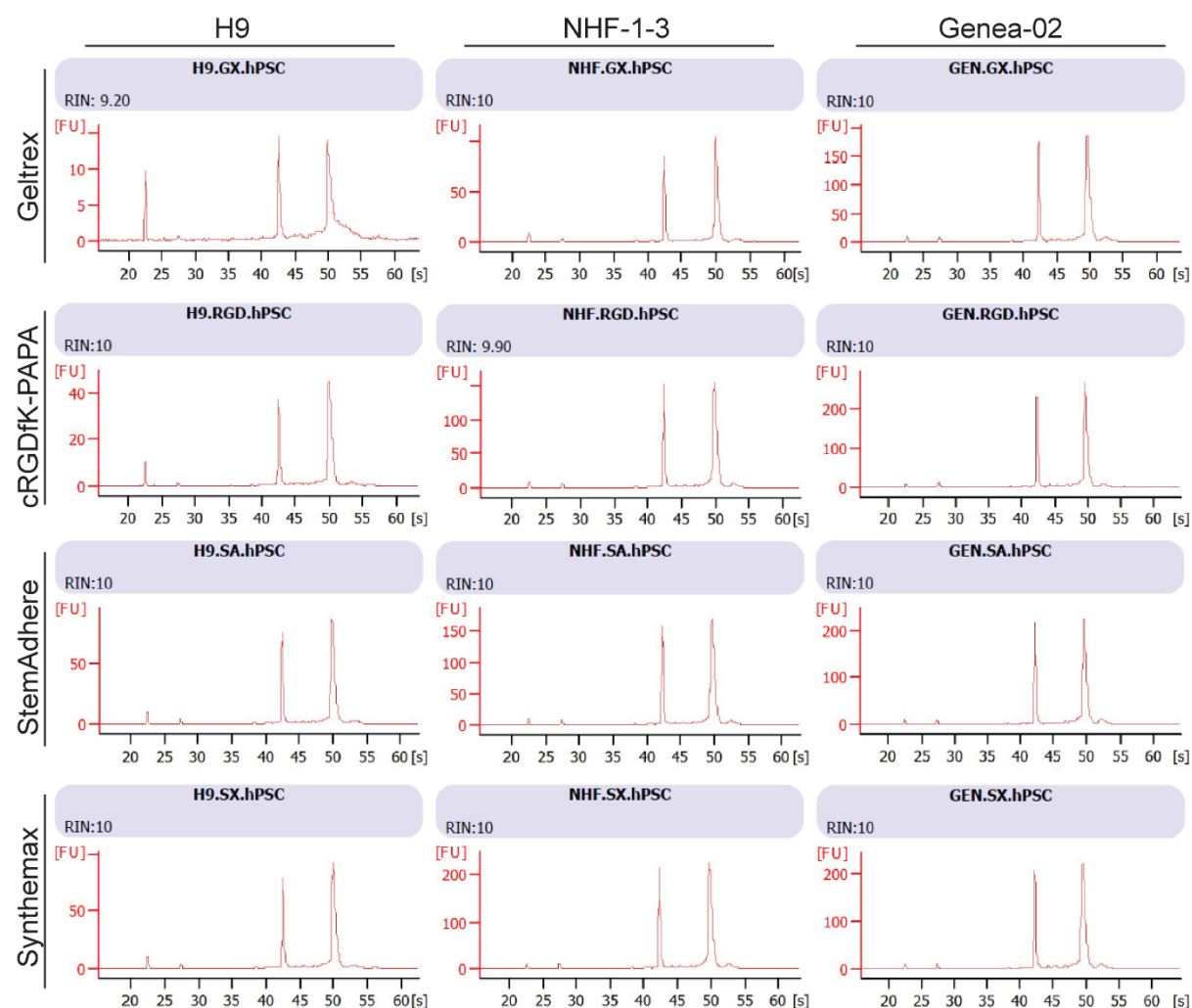
Appendix 6.2: This appendix presents the results of G-banding karyotyping assessment of hPSC cultures maintained on defined culture surfaces. Karyograms are presented from cultures of H9 (left column), NHF-1-3 (NHF, central column) and Genea-02 (GEN, right column) hPSCs that had been maintained for at least 10 passages in flasks coated with Geltrex™ (GX), cRGDFK-PAPA (RGD), StemAdhere™ (SA) or Synthemax™ (SX). Red boxes highlight karyotypic abnormalities.



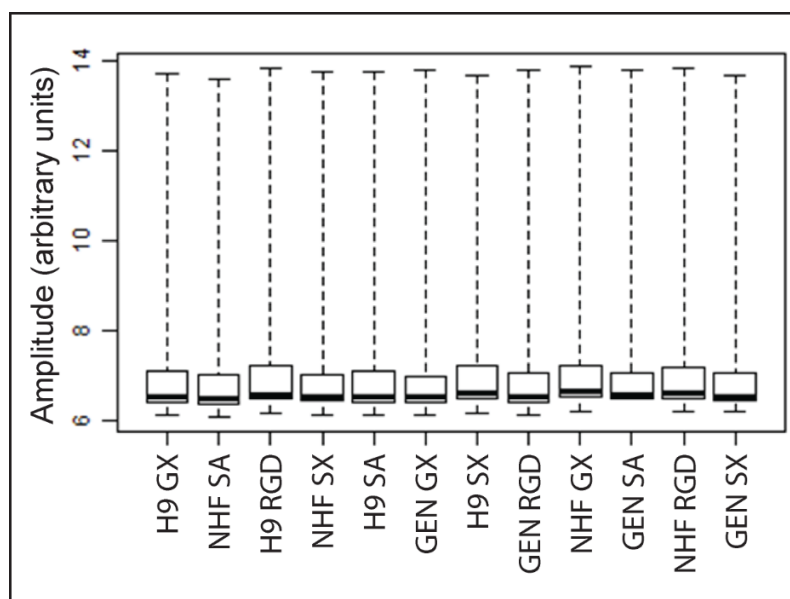
Appendix 6.3 Nanodrop analysis of RNA extracted from hPSCs maintained on defined culture surfaces. Total RNA was isolated from H9, NHF-1-3 and Genea-02 cultures after for 10 passages in flasks coated with Geltrex™ (GX), cRGDfK-PAPA (RGD), StemAdhere™ (SA) or Synthemax™ (SX). Absorbance of light at 260nm (A260) and 280nm (A280) is presented from nanodrop analysis of these samples along with the A260/280 ratio and the total RNA concentration determined for each sample.

Sample	A260	A280	A260/280	Concentration (ng/μl)
H9 GX	0.988	0.487	2.03	49.40
H9 RGD	2.084	1.042	2.00	104.19
H9 SA	3.874	1.922	2.02	193.69
H9 SX	3.936	1.943	2.03	196.81
NHF-1-3 GX	3.847	1.924	2.00	192.34
NHF-1-3 RGD	7.873	3.927	2.00	393.66
NHF-1-3 SA	7.941	3.925	2.02	397.03
NHF-1-3 SX	10.114	5.058	2.00	505.72
Genea-02 GX	7.492	3.750	2.00	374.59
Genea-02 RGD	9.952	4.928	2.02	497.59
Genea-02 SA	9.481	4.652	2.04	474.06
Genea-02 SX	8.017	4.024	1.99	400.83

Appendix 6.4 Bioanalysis of RNA extracted from hPSCs maintained on defined culture surfaces. Total RNA was isolated from H9, NHF-1-3 and Genea-02 cultures after 10 passages in flasks coated with Geltrex™ (GX), cRGDfK-PAPA (RGD), StemAdhere™ (SA) or Synthemax™ (SX). (A) Plots of electropherogram summaries of the isolated RNA are presented alongside RNA integrity numbers (RIN), which are derived from the electrophoretic trace and score RNA integrity out of ten. Fluorescence units (FU) are plotted over time; [s], seconds.



Appendix 6.5 PluriTest™ quality control results. The PluriTest™ assay was performed on H9, NHF-1-3 (NHF) and Genea-02 (GEN) cultures that had been maintained for 10 passages in flasks coated with Geltrex™ (GX), cRGDFK-PAPA (RGD), StemAdhere™ (SA) or Synthemax™ (SX). After samples were transformed with a variance stabilizing transformation, a probe intensity plot was generated to allow detection of outlier samples with inappropriate expression levels.



Reference list for appendices

- CANIGGIA, I., LIU, J., HAN, R., WANG, J., TANSWELL, A. K., LAURIE, G. & POST, M. 1996. Identification of receptors binding fibronectin and laminin on fetal rat lung cells. *American Journal of Physiology - Lung Cellular and Molecular Physiology*, 270, L459-L468.
- DERDA, R., LI, L., ORNER, B. P., LEWIS, R. L., THOMSON, J. A. & KIESSLING, L. 2007. Defined substrates for human embryonic stem cell growth identified from surface arrays. *ACS Chemical Biology*, 2, 347-355.
- DERDA, R., MUSAHA, S., ORNER, B. P., KLIM, J. R., LI, N. & KIESSLING, L. L. 2010. High-throughput discovery of synthetic surfaces that support proliferation of pluripotent cells. *Journal of the American Chemical Society*, 132, 1289-1295.
- EGUSA, H., KANEDA, Y., AKASHI, Y., HAMADA, Y., MATSUMOTO, T., SAEKI, M., THAKOR, D. K., TABATA, Y., MATSUURA, N. & YATANI, H. 2009. Enhanced bone regeneration via multimodal actions of synthetic peptide SVVYGLR on osteoprogenitors and osteoclasts. *Biomaterials*, 30, 4676-4686.
- FENG, Y. & MRKSICH, M. 2004. The synergy peptide PHSRN and the adhesion peptide RGD mediate cell adhesion through a common mechanism. *Biochemistry*, 43, 15811-15821.
- FITTKAU, M. H., ZILLA, P., BEZUIDENHOUT, D., LUTOLF, M. P., HUMAN, P., HUBBELL, J. A. & DAVIES, N. 2005. The selective modulation of endothelial cell mobility on RGD peptide containing surfaces by YIGSR peptides. *Biomaterials*, 26, 167-174.
- FREITAS, V. M., VILAS-BOAS, V. F., PIMENTA, D. C., LOUREIRO, V., JULIANO, M. A., CARVALHO, M. R., PINHEIRO, J. J. V., CAMARGO, A. C. M., MORISCOT, A. S., HOFFMAN, M. P. & JAEGER, R. G. 2007. SIKVAV, a laminin α 1-derived peptide, interacts with integrins and increases protease activity of a human salivary gland adenoid cystic carcinoma cell line through the ERK 1/2 signaling pathway. *American Journal of Pathology*, 171, 124-138.
- GUNAWAN, R. C., KING, J. A., LEE, B. P., MESSERSMITH, P. B. & MILLER, W. M. 2007. Surface presentation of bioactive ligands in a nonadhesive background using DOPA-tethered biotinylated poly(ethylene glycol). *Langmuir*, 23, 10635-10643.
- HARBERS, G. M. & HEALY, K. E. 2005. The effect of ligand type and density on osteoblast adhesion, proliferation, and matrix mineralization. *Journal of Biomedical Materials Research - Part A*, 75, 855-869.
- HIRSCHFELD-WARNEKEN, V. C., ARNOLD, M., CAVALCANTI-ADAM, A., LÓPEZ-GARCÍA, M., KESSLER, H. & SPATZ, J. P. 2008. Cell adhesion and polarisation on molecularly defined spacing gradient surfaces of cyclic RGDfK peptide patches. *European Journal of Cell Biology*, 87, 743-750.
- HOZUMI, K., AKIZUKI, T., YAMADA, Y., HARA, T., URUSHIBATA, S., KATAGIRI, F., KIKKAWA, Y. & NOMIZU, M. 2010. Cell adhesive peptide screening of

- the mouse laminin $\alpha 1$ chain G domain. *Archives of Biochemistry and Biophysics*, 503, 213-222.
- KANTLEHNER, M., SCHAFFNER, P., FINSINGER, D., MEYER, J., JONCZYK, A., DIEFENBACH, B., NIES, B., HÖLZEMANN, G., GOODMAN, S. L. & KESSLER, H. 2000. Surface coating with cyclic RGD peptides stimulates osteoblast adhesion and proliferation as well as bone formation. *Chembiochem : a European journal of chemical biology*, 1, 107-114.
- KLIM, J. R., FOWLER, A. J., COURTNEY, A. H., WRIGHTON, P. J., SHERIDAN, R. T. C., WONG, M. L. & KIESSLING, L. L. 2012. Small-molecule-modified surfaces engage cells through the $\alpha v\beta 3$ integrin. *ACS Chemical Biology*, 7, 518-525.
- KLIM, J. R., LI, L., WRIGHTON, P. J., PIEKARCZYK, M. S. & KIESSLING, L. L. 2010. A defined glycosaminoglycan-binding substratum for human pluripotent stem cells. *Nature Methods*, 7, 989-994.
- KOIVUNEN, E., WANG, B. & RUOSLAHTI, E. 1994. Isolation of a highly specific ligand for the $\alpha 5\beta 1$ integrin from a phage display library. *Journal of Cell Biology*, 124, 373-380.
- KOK, R. J., SCHRAA, A. J., BOS, E. J., MOORLAG, H. E., ÁSGEIRSDÓTTIR, S. A., EVERTS, M., MEIJER, D. K. F. & MOLEMA, G. 2002. Preparation and functional evaluation of RGD-modified proteins as $\alpha v\beta 3$ integrin directed therapeutics. *Bioconjugate Chemistry*, 13, 128-135.
- LIESI, P., NARVANEN, A., SOOS, J., SARIOLA, H. & SNOUNOU, G. 1989. Identification of a neurite outgrowth-promoting domain of laminin using synthetic peptides. *FEBS Letters*, 244, 141-148.
- MAEDA, T., TITANI, K. & SEKIGUCHI, K. 1994. Cell-adhesive activity and receptor-binding specificity of the laminin-derived YIGSR sequence grafted onto Staphylococcal protein A. *Journal of Biochemistry*, 115, 182-189.
- MAKINO, M., OKAZAKI, I., KASAI, S., NISHI, N., BOUGAEVA, M., WEEKS, B. S., OTAKA, A., NIELSEN, P. K., YAMADA, Y. & NOMIZU, M. 2002. Identification of cell binding sites in the laminin $\alpha 5$ -chain G domain. *Experimental Cell Research*, 277, 95-106.
- MELKOUMIAN, Z., WEBER, J. L., WEBER, D. M., FADEEV, A. G., ZHOU, Y., DOLLEY-SONNEVILLE, P., YANG, J., QIU, L., PRIEST, C. A., SHOGBON, C., MARTIN, A. W., NELSON, J., WEST, P., BELTZER, J. P., PAL, S. & BRANDENBERGER, R. 2010. Synthetic peptide-acrylate surfaces for long-term self-renewal and cardiomyocyte differentiation of human embryonic stem cells. *Nature Biotechnology*, 28, 606-610.
- MENG, Y., ESHGHI, S., LI, Y. J., SCHMIDT, R., SCHAFFER, D. V. & HEALY, K. E. 2010. Characterization of integrin engagement during defined human embryonic stem cell culture. *FASEB Journal*, 24, 1056-1065.
- NOMIZU, M., KURATOMI, Y., MALINDA, K. M., SONG, S. Y., MIYOSHI, K., OTAKA, A., POWELL, S. K., HOFFMAN, M. P., KLEINMAN, H. K. & YAMADA, Y. 1998. Cell binding sequences in mouse laminin $\alpha 1$ chain. *Journal of Biological Chemistry*, 273, 32491-32499.
- NOMIZU, M., KURATOMI, Y., PONCE, M. L., SONG, S. Y., MIYOSHI, K., OTAKA, A., POWELL, S. K., HOFFMAN, M. P., KLEINMAN, H. K. & YAMADA, Y.

2000. Cell adhesive sequences in mouse laminin $\beta 1$ chain. *Archives of Biochemistry and Biophysics*, 378, 311-320.
- NOMIZU, M., KURATOMI, Y., SONG, S. Y., PONCE, M. L., HOFFMAN, M. P., POWELL, S. K., MIYOSHI, K., OTAKA, A., KLEINMAN, H. K. & YAMADA, Y. 1997. Identification of cell binding sequences in mouse laminin chain by systematic peptide screening. *Journal of Biological Chemistry*, 272, 32198-32205.
- OLDBERG, A., FRANZEN, A., HEINEGARD, D., PIERSCHBACHER, M. & RUOSLAHTI, E. 1988. Identification of a bone sialoprotein receptor in osteosarcoma cells. *Journal of Biological Chemistry*, 263, 19433-19436.
- REZANIA, A. & HEALY, K. E. 1999. Biomimetic peptide surfaces that regulate adhesion, spreading, cytoskeletal organization, and mineralization of the matrix deposited by osteoblast-like cells. *Biotechnology Progress*, 15, 19-32.
- SKUBITZ, A. P. N., MCCARTHY, J. B., ZHAO, Q., YI, X. Y. & FURCHT, L. T. 1990. Definition of a sequence RYVVLPR, within laminin peptide F-9 that mediates metastatic fibrosarcoma cell adhesion and spreading. *Cancer Research*, 50, 7612-7622.
- STAATZ, W. D., FOK, K. F., ZUTTER, M. M., ADAMS, S. P., RODRIGUEZ, B. A. & SANTORO, S. A. 1991. Identification of a tetrapeptide recognition sequence for the $\alpha 2\beta 1$ integrin in collagen. *Journal of Biological Chemistry*, 266, 7363-7367.
- SUZUKI, S., OLDBERG, A., HAYMAN, E. G., PIERSCHBACHER, M. D. & RUOSLAHTI, E. 1985. Complete amino acid sequence of human vitronectin deduced from cDNA. Similarity of cell attachment sites in vitronectin and fibronectin. *EMBO Journal*, 4, 2519-2524.
- TASHIRO, K., SEPHEL, G. C., WEEKS, B., SASAKI, M., MARTIN, G. R., KLEINMAN, H. K. & YAMADA, Y. 1989. A synthetic peptide containing the IKVAV sequence from the A chain of laminin mediates cell attachment, migration, and neurite outgrowth. *Journal of Biological Chemistry*, 264, 16174-16182.
- UNDERWOOD, P. A., BENNETT, F. A., KIRKPATRICK, A., BEAN, P. A. & MOSS, B. A. 1995. Evidence for the location of a binding sequence for the $\alpha 2\beta 1$ integrin of endothelial cells, in the B1 subunit of laminin. *Biochemical Journal*, 309, 765-771.
- VOGEL, B. E., LEE, S. J., HILDEBRAND, A., CRAIG, W., PIERSCHBACHER, M. D., WONG-STAL, F. & RUOSLAHTI, E. 1993. A novel integrin specificity exemplified by binding of the $\alpha(v)\beta 5$ integrin to the basic domain of the HIV Tat protein and vitronectin. *Journal of Cell Biology*, 121, 461-468.